Ph.D. Thesis

Factorization of Seiberg-Witten Curves and Black Holes on a Circle

Peter Browne Rønne

Niels Bohr Institute
Faculty of Science
University of Copenhagen

Ph.D. Advisor: Niels Obers

September 4, 2007

Contents

Acknowledgements

First and foremost I would like to thank my advisor Niels Obers for his help and support throughout my studies. Also, I would like to thank my collaborators Troels Harmark, Kristján Kristjánsson and Romuald Janik for our many discussions.

For the choice of literature on Riemann surfaces I thank Bergfinnur Durhuus and Hidenori Sonoda for suggestions.

In general, thanks to the professors, postdocs, students and secretaries at the Niels Bohr Institute for helpfulness and discussions, and to the Institute itself with its historically inspiring environment.

Last, but not least, I would like to thank Wiebke for her support during the writing of this thesis.

Niels Bohr Institutet, September 4, 2007,

Peter Browne Rønne

List of publications

Chapter 6, except the conclusions in section 6.7, is a modified version of [1] (see also [2] for a brief review). Also appendices C, D and E are taken from [1].

Sections 4.4 and 4.5 are modified versions of section 5 and section 6 in reference [3]. Also appendices A and B are taken from [3].

Chapter 1

Introduction

Theoretical high energy physics is a broad field ranging from the study of field theories over string theory to black holes. This thesis falls into two parts that each examines their end of this field.

1.1 Abstract

In the first part we will consider the factorization of Seiberg-Witten curves. The Seiberg-Witten curve captures the low energy (i.e. strong coupling) quantum dynamics of $\mathcal{N}=2$ super Yang-Mills theory where we consider a $U(N_c)$ gauge group, and we will also allow fundamental matter in the theory. The factorization of these curves corresponds to examining the vacua of $\mathcal{N}=1$ supersymmetric theories obtained by softly breaking the $\mathcal{N}=2$ supersymmetry by a tree-level superpotential. This gives the classical gauge group breaking pattern $U(N_c) \mapsto \prod_{i=1}^{g+1} U(N_i)$. We examine the action of the $\mathrm{PGL}(2,\mathbb{C})$ group on the factorization problem and find equivalence relations among same genus factorizations. In order to solve the factorization problem we use a method where we work on the Jacobian of the hyperelliptic Seiberg-Witten curve. We rederive the solution for the complete factorization case and present the solution of the genus one case with $U(N_c) \mapsto U(N_1) \times U(N_2)$ [3]. Further, we give an explicit proposal for the $g-1$ equations of motion for the period matrix of the factorized curve, for arbitrary genus g, in terms of zeroes of hyperelliptic theta functions. This proposal, for sure, holds in the genus two case $U(N_c) \mapsto U(N_1) \times U(N_2) \times U(N_3)$. We then show how the solution of the factorization problem should be obtained, and briefly discuss the implications for the global structure of $\mathcal{N}=1$ vacua. We also give thorough reviews of Seiberg-Witten curves and Riemann surfaces.

In the second part we construct five-dimensional three-charge black holes with a circle in their transverse space for which the charges are carried by a F1-D0-D4

brane configuration [1, 2]. These solutions are obtained by an explicit mapping of neutral and static Kaluza-Klein black holes in five dimensions which we review. We also show how to take a near-extremal limit of these non-extremal three-charge black holes which reveals new physical behaviour – most importantly that the relative tension is constant. This turns out to be a consequence of the fact that extremal black holes which are localised on the circle have a finite entropy $2\pi\sqrt{N_1 N_4 N_0}$ where N_i are the number of branes/fundamental strings. We obtain the correction to this formula as a function of the energy above extremality to next-to-leading correction. Partial near-extremal limits are also investigated and for the case with two extremal charges and one finite, we check that the entropy formula to leading order can be obtained via the microscopic model by taking into account that the number of branes shifts due to the presence of the circle. In general, we study the rich phase structure of the non- and near-extremal black holes and their two-charge analogs both analytically and numerically, and new phases with the black holes non-uniformly distributed on the circle are found. The thermodynamic stability is investigated and especially for the two-charge case this can have interesting consequences for the dual CFT_2.

Before introducing each part in detail we will see how they can be seen in the bigger picture of string theory and share important features such as supersymmetry and open/closed string duality.

1.2 String Theory, Open/Closed String Duality and Supersymmetry

We will now introduce and motivate the research directions of this thesis in a broader context.

String theory solutions

The three-charge solutions with a transverse circle that we present in this thesis (published in [1, 2]) are directly low energy solutions of Type IIA/B string theory. We create these solutions by a method that is an extension of the one used in reference [4] (see also [5, 6]). There, a map was created, following the procedure of [7], that takes any Kaluza-Klein black hole (i.e. black holes on a space with a compact circle, see [8, 9] and chapter 5 for reviews) in $d+1$ dimensions ($4 \leq d \leq 9$) into a brane solution of Type IIA/IIB String Theory and M-theory. These brane solutions are thermal excitations of extremal 1/2-BPS branes in String/M-theory with transverse space $\mathbb{R}^{d-1} \times S^1$ (i.e. a transverse circle). The full knowledge of the phases of Kaluza-Klein black holes can then simply be mapped to phases of the brane. This is especially interesting in the near-extremal limit where the thermodynamics of the brane was obtained and related to the non-gravitational theories dual to the near-extremal brane.

Our three-charge solutions with a circle in the transverse space are obtained from any five-dimensional Kaluza-Klein black hole using a generalisation of the above map. The solutions are three-charge brane configurations in Type IIA/IIB String Theory and M-theory. The charges are carried by the F1-D0-D4 brane system or a dual thereof e.g. P-D1-D5, and the three-charge solutions are thus thermal excitations of the corresponding extremal 1/8-BPS brane system. We can compactify on the world-volume of the system to obtain three-charge black holes in five-dimensional supergravity.

So the three-charge black holes are low energy string solutions, but, as we will see below, the low-energy superpotential of the $\mathcal{N} = 1$ supersymmetric theories that we investigate in this thesis are also obtainable via string theory methods.

Supersymmetry

Supersymmetry is not only fascinating as a theoretical tool, but may be manifest in nature for the description of the fundamental interactions at sufficiently high energies. A question that might be answered in the near future by LHC.

In string theory one has to introduce supersymmetry to avoid the tachyon of the bosonic string. Also in general, outside string theory, supersymmetry is extremely useful. Quantum corrections are much more restricted in supersymmetric theories since we have cancellations between the bosonic and fermionic loops. This gives rise to non-renormalisation theorems and we can sometimes even make non-perturbative calculations. Using also e.g. holomorphicity the supersymmetry gives so strong constraints that the low-energy effective action is often determined exactly. However, perhaps most important physically is the fact that in the supersymmetric theories we can investigate confinement and make calculations for confining vacua.

We will consider the minimal four-dimensional supersymmetric gauge theory that is "closest" to nature: $\mathcal{N} = 1$ supersymmetric $U(N_c)$ gauge theory with N_f fundamental flavours. The fundamental matter is important since it, at low energies, describes strongly coupled quarks.

The aim is to understand the vacua of this (pseudo-confining) theory which, in general, is very hard since this involves an infinite series of non-perturbative fractional instanton corrections. Here the low-energy (glueball) superpotential is important since it determines the structure of the vacua. Importantly, this can be determined via string theory, as we will see below, and with the Dijkgraaf-Vafa conjecture a systematic way of computing it via a large-N matrix model was found.

However, the route we take in this thesis is different. We start by instead considering the extended supersymmetric case of $\mathcal{N} = 2$ super Yang-Mills – also with fundamental flavours allowed. As shown in the seminal work of Seiberg and Witten [10, 11] the strongly coupled low-energy dynamics of this theory is beautifully encoded in the properties of an associated hyperelliptic Riemann surface, the Seiberg-Witten curve.

We can then break $\mathcal{N} = 2$ to $\mathcal{N} = 1$ supersymmetry in a controlled way by adding a tree-level superpotential for the adjoint chiral field. The addition of the superpotential means that the gauge group is classically broken into $g + 1$ factors: $U(N_c) \mapsto \prod_{i=1}^{g+1} U(N_i)$. The point is that the vacuum data of the $\mathcal{N} = 1$ theory can be calculated via the $\mathcal{N} = 2$ Seiberg-Witten curve that factorizes into a genus g reduced hyperelliptic curve. This factorization problem is highly non-linear, but we will nevertheless pursue a solution.

We also saw above that the three-charge black holes are supergravity solutions and they can be seen in ten dimensions as the excitations of extremal 1/8-BPS states. The supersymmetry is thus also important for the black holes and, as we will see below, the BPS property is important for the microscopic model that we use to explain the entropy as a degeneracy of states. The possibility of taking the near-extremal limit that we will define for the three-charge black holes is actually a main motivation for considering such charged solutions.

Open/closed string duality

The open/closed string duality is the basis of many remarkable conjectures in string theory. It arises by considering the interaction between static D-branes. These can interact by exchange of closed strings and the tree-level diagram is the familiar cylinder extended between the two branes. But this diagram can dually be seen as a pair of open strings, extending between the branes, that are created and later annihilated in a virtual loop. Thus the interaction of the D-branes is in one picture the exchange of the closed string modes: Graviton, dilaton, Ramond-Ramond fields, etc. and in the other picture a Casimir-like modification of the vacuum energy. In general, the endpoints of the open strings that are confined to the branes give rise to the world-volume gauge theory on the brane, whereas the low-energy modes of the closed string gives the bulk supergravity theory. Thus the duality will often relate gauge and gravity theories.

This open/closed string duality plays an important role both for the three-charge black holes and the supersymmetric vacua, as we will now see.

AdS/CFT

The AdS/CFT conjecture [12, 13, 14, 15] is the most prominent example of open/closed string duality. By considering the near-horizon limit of, say, N D3-branes which has the geometry $AdS_5 \times S^5$, the type IIB strings propagating on this background can equivalently be seen as the four-dimensional world-volume $U(N)$ gauge theory with $\mathcal{N} = 4$ supersymmetry, but it is a strong/weak coupling duality. However, more relevant for us is the $\mathrm{AdS}_3/\mathrm{CFT}_2$ correspondence where one instead considers the near-horizon limit of coincident D1-D5 branes.

This is one of the reasons why adding charges to the neutral Kaluza-Klein black holes is so important to consider – it allows us to study the near-extremal limit of solutions that might be dual to a CFT. Importantly, in the two-charge subcase of our three-charge black holes the localised phase is T-dual to the D1-D5 system, but with a circle in the transverse space. We can then make predictions for the thermodynamics of the dual CFT by investigating the thermodynamics on the gravity side.

One might wonder whether the AdS/CFT duality also applies to the $\mathcal{N} = 1$ supersymmetric theories that we consider. However, it turns out that it is very difficult to extend to this class of theories. But, as we will see below, these theories are conjectured by Vafa to have a dual description in terms of special geometry relations on a Calabi-Yau three-fold. A conjecture that also arises from an open/closed string duality.

The AdS/CFT conjecture is an example of the holographic principle introduced by 't Hooft and Susskind. The idea builds on the entropy of a black hole being proportional to its horizon area, not the volume as would be expected in a local field theory. Thus gravity in D dimensions should be described by a boundary local field theory in $D-1$ dimensions. The microscopic understanding of the black hole entropy for the three-charge black holes with a transverse circle is one of the highlights of this thesis.

Microscopic understanding of entropy

One of the great achievements of string theory is the microscopic explanation of the Bekenstein-Hawking entropy of five-dimensional three-charge black holes [16, 17, 18, 19, 20]. The reason to focus on three-charge black holes is that we here have a macroscopic horizon and hence finite entropy. This entropy turns out to be $2\pi\sqrt{N_1 N_4 N_0}$ where N_i are the number of branes (or fundamental strings etc.) in the configuration. For instance in the two-charge case we only get an effective horizon at the Plank scale. The only other case with finite entropy is the four-charge black hole in four dimensions [21, 22].

The extremal three-charge black holes are constructed, as in our case with a circle, as D-brane configurations in ten-dimensional string theory where the calculation can be done, and in the end one can compactify to the five-dimensional black holes.

The original calculation [16] illustrates the power of the open/closed string duality. In the weak curvature limit we can see the object as a black hole in gravity and use the area law to obtain the entropy. However, to do the calculation of degeneracy of states we have to take the string coupling small (smaller than the inverse number of branes) such that we have an effective weak coupling. Here the system is described by D-branes wrapping supersymmetric cycles and we can count the degeneracy of the world-volume gauge theory living on the branes given by the open string endpoints. However, the string length is here larger than the Schwarzschild radius and description in terms of a black hole suffers stringy corrections.

As one might guess correctly from this description, the calculation can also be seen via the AdS/CFT correspondence even though it historically was discovered later.

The supersymmetry is essential in this calculation. It ensures that the BPS degeneracy of states is a topological quantity that does not change as we go to strong coupling in order to compare with the black hole picture.

For non-BPS states the degeneracy is not topologically protected and we could have strong coupling effects when extrapolating from the weak coupling calculation. It is therefore interesting to consider non- and near-extremal black holes. Here it was found [20, 23] that the entropy calculation also matches (see also the recent developments [24, 25, 26] for calculations on neutral solutions). The calculation can be done in the "dilute gas" regime where two charges are taken to be much bigger than the third. It was found that the entropy takes the form

$$S = 2\pi\sqrt{N_1 N_4}\left[\sqrt{N_0} + \sqrt{N_{\bar{0}}}\right], \tag{1.1}$$

where $N_{\bar{0}}$ is the number of added anti-D0-branes in the non-extremal case. That the comparison of entropy is not accidental here was shown in [27]: The CFT description holds true because multiple wound strings lead to a very low energy gap.

Even though the counting works in the non-extremal case there is a benefit in adding charges since the microscopic description in this case also explains the low-energy Hawking radiation [28, 29, 30] and thus also captures the dynamics of the system.

So we see that the three-charge black holes have a very prominent role (see also reviews [31, 32]). One of the main aims in this thesis is to extend the considerations of the entropy to our situation where the three-charge configuration has a circle in the transverse space i.e. asymptotes to Minkowski space times a circle, $\mathcal{M}^4 \times S^1$. Note that we can not consider the four charge black holes in four dimensions that also had a macroscopic horizon since the compact circle means, that the asymptotics does not work in this case.

For our case the entropy of the extremal (vanishing energy above extremality) black hole that is localised on the circle fits with the non-compact case. This is because considering the covering space of the circle we get an infinite array of black holes, but these are not interacting since they are BPS. Thus the entropy is again $2\pi\sqrt{N_1 N_4 N_0}$ where we remember that we chose the charges to be carried by a F1-D0-D4 brane system. Moving away from extremality we get corrections to this formula and in our case we also get corrections from the interactions across the circle. We find that the entropy including next-to-leading order corrections in the energy above extremality (i.e. small mass or large radius of the compact circle) is

$$S = 2\pi\sqrt{N_1 N_4 N_0}\left(1 + \sqrt{\frac{\epsilon}{8}} + \frac{\epsilon}{16} + \mathcal{O}(\epsilon^{3/2})\right). \tag{1.2}$$

Here ϵ is the energy above extremality rescaled to be dimensionless.

We also consider the partial extremal dilute gas limit, mentioned above, where two of the charges are sent to infinity, while one is kept finite. Here we find that the first correction to the energy is in agreement with the microscopic entropy (1.1) when we take into consideration that the number of D0 and anti-D0 branes will shift due to the interactions across the circle [33]. Thus we confirm that the microscopic model works for the three-charge black holes with a circle in the transverse space.

Thus by considering boosted (and U-dualised) solutions of the neutral and static black holes – which is merely a kinematic change in the gravity solution – we are able to take the near-extremal limit and compare with the microscopic side.

Geometric transition and the Dijkgraaf-Vafa conjecture

Let us end this section by briefly reviewing that the low-energy dynamics of the four-dimensional $\mathcal{N} = 1$ supersymmetric gauge theory that we consider actually is encoded in the closed string superpotential on a Calabi-Yau [34]. Hence there is again an open/closed string duality at work.

The first step is to realise that the $\mathcal{N} = 1$ supersymmetric gauge theory can be geometrically engineered by considering a Calabi-Yau where we wrap N D5-branes on S^2 cycles (see [35, 36, 37, 38]). The non-compact directions of the D5-branes gives the four dimensions for our gauge theory. The tree-level superpotential for the adjoint chiral superfield that breaks $\mathcal{N} = 2$ to $\mathcal{N} = 1$ is taken into account in the geometry, and the N branes should wrap cycles located at the minima of the superpotential. The number of branes on the ith cycle is N_i giving the gauge group breaking pattern $U(N_c) \mapsto \prod_{i=1}^{g+1} U(N_i)$ mentioned above.

The next step is to go from this open string description to closed strings propagating in the background of the D-branes. The conjecture is that this involves a geometric transition that changes the topology [34, 39, 40, 37] (important here is the topological duality [41, 42]). For the dual Calabi-Yau we have S^3-cycles instead of the S^2 cycles and N_i, which before was the number of D5-branes on a given cycle, is now the units of flux through the corresponding S^3 cycle. On the Calabi-Yau there is a unique holomorphic three-form Ω whose α-periods S_i on the cycles fixes the moduli and β_j-period gives $\partial\mathcal{F}(S_i)/\partial S_j$ where $\mathcal{F}$ fixes the geometry of the Calabi-Yau. One can also construct a superpotential via Ω and the flux through the cycles (see section 2.3). The conjecture is that this closed string superpotential is the glueball superpotential of the $\mathcal{N}=1$ supersymmetric gauge theory with the S_is being the glueball superfields. This superpotential determines the low-energy dynamics of the confining theory.

Importantly, all the S^3-cycles can be seen as fibrations of S^2 over an interval. The integrals over S^2 are trivial and we are left with the integrals over the intervals that can be seen as cuts of a Riemann surface, and Ω reduces to a one-form on the surface. This Riemann surface is exactly the reduced hyperelliptic curve of the factorized Seiberg-Witten curve, and Ω is the Seiberg-Witten one-form.

It is the aim of the first part of this thesis to obtain a solution for these hyperelliptic curves. For the genus zero and genus one case we present the solution [3]. For the higher genus cases we propose that the period matrix of the curve (which determines the curve up to $\mathrm{PGL}(2,\mathbb{C})$ transformations) has $g-1$ equations of motion written in terms of zeroes of hyperelliptic theta functions. In the genus two case this indeed holds true. We also show explicitly how the solution is constructed when the period matrix is determined. This analysis of the higher genus cases is an unpublished result.

Let us also note that the setup was used by Dijkgraaf and Vafa to show that the superpotential is determined by the planar contribution to the free energy of an auxiliary large-N matrix model [43, 44, 45]. This was later understood purely within field theory [46, 47, 48, 49] (pedagogical introductions can be found in [50, 51, 52, 53, 54, 55]). The relation of the Dijkgraaf-Vafa conjecture and the factorized Seiberg-Witten curves were studied in e.g. [56, 46, 57, 58, 59, 60, 61].

We will now go on to describe the contents of the thesis for each of the two parts.

1.3 Factorized Seiberg-Witten Curves

For the factorized Seiberg-Witten curves we will start by giving a review of the curves in chapter 2. In section 2.1 we will introduce the $\mathcal{N}=2$ supersymmetric QCD with $U(N_c)$ gauge group that we consider, and which can be broken to $\mathcal{N}=1$ with a tree-level superpotential for the adjoint chiral superfield

$$W_{tree} = \sum_{p\in\mathbb{N}} \frac{g_p}{p} \operatorname{Tr} \Phi^p. \tag{1.3}$$

We also present the form of the low-energy effective action. In section 2.2 we will show how examining the monodromies for going around singular points on the vacuum moduli space will give the Seiberg-Witten curves. We will then consider what happens when we add the tree-level superpotential to break the theory to $\mathcal{N} = 1$ in section 2.3. This means that we are localised at points in the vacuum moduli space where we have massless dyons which in turn means that the curve factorizes. We also discuss the low-energy potential and how it is obtained by the geometric engineering and transition that we saw above.

Since we are going to need a lot of Riemann surface technology we will give an introduction to these in chapter 3. After introducing the surfaces we will present the analytical structure in section 3.2 including concepts like modular transformations, meromorphic one-forms and divisors that all will be important for us. In section 3.3 we will introduce the concept of the Jacobian associated to the Riemann surface. This will be central in our efforts to solve the factorization problem. Since the Seiberg-Witten curves are hyperelliptic, we will devote a section to these before turning to the theta functions and their properties in section 3.5.

The main part is chapter 4. Here we will try to solve the factorization problem for general genus. This is an important problem to solve e.g. since it was found in [62, 63, 64] that we have a very complex structure of $\mathcal{N} = 1$ vacua with connected components that allows multiple dual descriptions of the same physics, but with different classical gauge group breaking patterns. However, the structure of vacua had to be examined for low N_c and case by case, since only the complete factorization problem corresponding to unbroken gauge group had been solved [65]. But in reference [66] an exact solution of the genus one factorization problem corresponding to $U(N_c) \mapsto U(N_1) \times U(N_2)$ was found. This works for general $N_c = N_1 + N_2$ and using the solution it was possible to determine precisely the equivalent descriptions of the same vacua (see also [67]).

This was, however, for the case without fundamental flavours. For the important case with flavours a lot of work has been done, too. The complete factorization case was solved in reference [68] using the matrix model we saw above in the Dijkgraaf-Vafa conjecture. The relation between Seiberg-Witten curves and the matrix model in the presence of fundamental matter has also been investigated in references [69, 70, 71, 72, 73, 74, 75, 76] and the structure of $\mathcal{N} = 1$ vacua was investigated in [77, 78, 79, 80, 81], but again for low N_c and low number of flavours.

This called for an exact solution in the case with fundamental flavours, and in reference [3] the solution of the factorization problem was found in the genus one case i.e. $U(N_c) \mapsto U(N_1) \times U(N_2)$ with the number of flavours N_f in the range $0 \leq N_f < 2N_c$ and general $N_c = N_1 + N_2$ thus extending the method in [66]. We present this result in section 4.5. Also, in section 4.4 we present the simple rederivation of the original solution for complete factorization [68] that was also found in [3]. Further, we present the two appendices of [3]: Appendix A where we show that the

Seiberg-Witten curve factorizes if and only if there exists a meromorphic one-form with prescribed poles and integral periods, and appendix B where it is shown that the solution includes the flavourless case [66] by decoupling flavours.

But all of this are only special cases of the general genus factorization (notice here also the work of [82, 83] where a microscopic superpotential is found that captures all vacua – independent of the genus). In section 4.1 we explain the setup for solving the factorization problem which follows the idea in [66] that builds on the observation of [48, 77] that a certain one-form has integral periods (the α-periods of which are the N_is in the gauge group breaking) for the factorized curve. This one-form is essential in constructing the solution. We further examine the action of $\mathrm{PGL}(2, \mathbb{C})$ on the factorized Seiberg-Witten curves which gives us equivalences between the factorization problems for different specifications of the holomorphic scale Λ and quark masses m_i, but importantly also between different numbers of flavours. Let us also stress that we here consider an arbitrary number of flavours, also the special case $N_f = 2N_c$. In the main section 4.2 we will use the Jacobian associated to the reduced hyperelliptic curve of the factorization problem to try to solve the problem. The genus one case directly reduces to the solution we already have obtained. In the higher genus g cases the period matrix of the curve is shown to be constrained and we make a proposal for $g - 1$ explicit equations of motion written in terms of the zeroes of hyperelliptic theta functions. This indeed works for the genus two case. We then show how the problem should be solved once the period matrix is determined. This is then used in section 4.3 to investigate the global structure of vacua for general N_c and N_f. These are all unpublished results. We will conclude and discuss further research directions in section 4.6.

1.4 Three-Charge Black Holes on a Circle

For the black hole part of the thesis we will start by reviewing the neutral and static Kaluza-Klein black holes in chapter 5. We keep the discussion general to $D = d + 1$ dimensions. We will start by introducing the asymptotic quantities that we can measure in section 5.1, namely the mass and the tension that arises due to the compact circle. Many of the Kaluza-Klein black holes have a $SO(d - 1)$ symmetry and these can be written in an ansatz introduced in [84] (and proven in [85, 86]) that we review in section 5.2. The thermodynamics of the black holes are then discussed in section 5.3. In section 5.4 we describe the different phases of Kaluza-Klein black holes. We have a branch with bubble-black hole sequences [87, 88, 89] that involves Kaluza-Klein bubbles which provide a repelling force between black holes giving a static equilibrium. We will not focus on this branch here but rather the remaining that fits into the mentioned ansatz. The first of these is the localised black hole branch which in the limit of zero mass, or large radius of the compact circle, approaches the D-dimensional Schwarzschild black hole and it thus has horizon topology S^{d-1}. This has been studied analytically in the small mass limit [90, 91, 92, 93, 94] and the thermodynamics is known to second order, and the metric to first order.[1] Numerically, however, the phase was obtained in [95, 96, 97]. Further, we have a uniform phase which is the black string obtained by the d-dimensional Schwarzschild black hole times a circle. This is unstable for masses below the Gregory-Laflamme mass [98, 99]. At the Gregory-Laflamme point it is marginally unstable, and from this point the non-uniform phase emerges. This has the same horizon topology as the uniform string, namely $S^{d-2} \times S^1$, but is non-uniform along the circle. This phase has been studied in [100, 101, 102], and in [103] the entire phase for $d = 4$ was computed numerically. All of these phases can be plotted numerically in a two-dimensional mass vs. relative tension-phase diagram [104, 105, 86].

In chapter 6 we will then use these five-dimensional (i.e. $d = 4$) Kaluza-Klein black holes to create three-charge solutions. We start in section 6.1 by generating the map from these five-dimensional "seeding" solutions to ten-dimensional three-charge configurations by a combination of boosts and U-dualities. We find the physical quantities (masses, tensions, charges and thermodynamics) of these in terms of the seeding solution and the boost parameters. Three appendices are related to the calculations done in this section: In appendix C we give the details on the boosts and U-dualities used in section 6.1. Appendix D gives the precise relation between the asymptotics of the seeding solution and that of the three-charge solution. Finally, appendix E provides some further details on our definition of electric masses and tensions and also an analysis of what this means for the tensions in the near-extremal limit.

The map constructed in section 6.1 is used in section 6.2 on the ansatz of [84] to create an ansatz for three-charge black holes. This is then used on the three phases of seeding solutions mentioned above that falls into this ansatz. This leads to a uniform, a non-uniform and a localised phase of non-extremal three-charge black holes.

In section 6.3 we define how to take the near-extremal limit of the non-extremal three-charge black holes. This is the limit that we have seen above which is very interesting for the microscopic model of entropy and the dual CFT descriptions of the brane systems. As for the one-charge case [4] the map here simplifies, but we find new and interesting physics in this five-dimensional three-charge case, e.g. that the

[1] Actually, in the case of $d = 4$ the corrections to the metric are also known [93]. However, for simplicity we will only use the first order corrected metric, but still go to second order in the thermodynamics.

tension along the transverse circle is proportional to the energy above extremality. That this is a very special case might not be surprising taking our considerations of entropy in section 1.2 into account, and indeed we show in generality that the proportionality of tension and energy above extremality always happens in a system which involves a finite entropy in the extremal limit – as is the case here.

The near-extremal limit obtained in section 6.3 is then in section 6.4 applied to the non-extremal phases of three-charge black holes found in section 6.2 thus giving three new near-extremal phases. We examine each of these phases in detail both analytically and numerically and especially present diagrams of their thermodynamics. Particularly interesting is the localised phase where we have finite entropy in the near extremal limit and we find the corrections to this entropy for small energy above extremality as mentioned above in equation (1.2). However, also the non-uniform case is interesting in its own right as a new P-D1-D5 brane system non-uniformly distributed on the transverse circle.

In section 6.5 we consider other near-extremal limits, i.e. where we keep one or two of the charges finite. For these two cases the corrections to the thermodynamics of the small localised black holes are found, especially the entropy. We also consider the two-charge case obtained by setting one of the three charges to zero. Here the corresponding map from seeding solutions to non-extremal two-charge black holes with a transverse circle is found and the near-extremal limit is considered. We choose to consider the D0-D4 system, and again we apply the map to the three phases and present the phase diagrams and thermodynamics. The situation here is more analogous to the one-charge case [4] (see [106] for a very short review) than the three-charge case. But this system is also interesting, in particular note that the T-dual is a D1-D5 system and the localised phase is thus relevant for the dual CFT_2, but where we here have a transverse circle. The thermodynamics of the localised phase is thus found and it is confirmed that, in the canonical ensemble, the free energy has the conformal behaviour $F \propto T^2$ and we find the small temperature corrections. Considering the non-uniform branch as seeding solutions we get a new phase of D1-D5 branes non-uniformly distributed on the transverse circle. For the uniform branch, which is dual to a D2-D6 system, we find a Hagedorn behaviour. The thermodynamic behaviour that we find for the near-extremal two-charge case is actually analogous to that of the near-extremal NS5-brane considered in reference [107].

Finally, in section 6.6 we do the microstate counting that we mentioned above in section 1.2. This is done for the small localised black hole in the dilute gas limit where we keep one charge finite and send two to infinity. Following reference [33] we find the first correction to the entropy in the microscopic model using (1.1) and the fact that the number of branes are shifted due to the interaction across the circle for fixed total energy. This reproduces the leading order correction of the entropy obtained in section 6.5.

We end with conclusions and outlook (updated compared to [1]) in section 6.7.

Chapter 2

Seiberg-Witten Curves

In this chapter we will introduce the Seiberg-Witten curves. We will specify the gauge theories that we consider, show how the low-energy effective theory beautifully is captured by the Seiberg-Witten curves [10, 11] (for reviews see [108, 109, 110, 55]) and explain the significance of their factorization. This factorization problem is an intriguingly simply posed mathematical problem: Find the coefficients for the polynomial $P_N(x)$ such that

$$P_N(x)^2 - C = F_n(x) H_m(x)^2, \tag{2.1}$$

where C is a constant (or more generally a polynomial) and F_n and H_m are polynomials. However, the solutions have significant physical applications.

2.1 Gauge Theory Setup

Our main goal is to investigate low energy supersymmetric QCD. To be more specific, we will at first consider $\mathcal{N} = 2$ supersymmetric gauge theory with a $U(N_c)$ gauge group, and later also $\mathcal{N} = 1$ supersymmetric theories – all in four dimensions. We have two possible representations of the $\mathcal{N} = 2$ supersymmetry algebra, the $\mathcal{N} = 2$ gauge supermultiplet and the $\mathcal{N} = 2$ hypermultiplet. The gauge multiplet transforms in the adjoint of the gauge group and in the language of $\mathcal{N} = 1$ superfields it consists of a vector superfield V and a chiral superfield Φ. The hypermultiplet consists of a $\mathcal{N} = 1$ chiral superfield Q and an anti-chiral superfield $\widetilde{Q}^\dagger$. If we include this matter in the theory we will assume it transforms in the fundamental of $U(N_c)$ (i.e. $\widetilde{Q}$ is anti-fundamental), and consider N_f copies indexed by the flavour index i, Q_i.

2.1.1 Lagrangian

The (renormalisable) $\mathcal{N}=2$ Lagrangian for the gauge multiplet written in terms of the $\mathcal{N}=1$ superfields takes the form (for a simple gauge group)

$$\mathcal{L}_{\mathcal{N}=2} = \frac{\tau}{16\pi i C(\mathbf{r})} \operatorname{Tr}_{\mathbf{r}} \left(\int \mathrm{d}^2\theta \mathcal{W}^\alpha \mathcal{W}_\alpha + 2 \int \mathrm{d}^4\theta \Phi^\dagger e^{-2V} \Phi \right) + \text{c.c.}, \tag{2.2}$$

where $\mathcal{W}^\alpha$ is the supersymmetric gauge field strength and $\mathbf{r}$ is the representation that we use for the generators of the gauge group, i.e. $\Phi = \Phi^a T_a^{(\mathbf{r})}$, while $C(\mathbf{r})$ is the corresponding quadratic invariant. τ is the complex gauge coupling, $\tau = \vartheta/2\pi + i4\pi/g^2$.

If we include N_f multiples of fundamental matter, the renormalisable Lagrangian will be proportional to (denoting gauge indices by capital letters, but suppressing them in the first part of the equation)

$$\begin{aligned}\mathcal{L}_{matter} = &\int \mathrm{d}\theta^4 \left(Q_i^\dagger e^{-2V} Q^i + \widetilde{Q}_i e^{-2V} \widetilde{Q}^{\dagger i} \right) \\ &+ \int \mathrm{d}\theta^2 \left(\sqrt{2} \widetilde{Q}_i^A \Phi_A^B Q_B^i + \sqrt{2} \widetilde{Q}_i^A m^i{}_j Q_A^j \right) + \text{c.c.},\end{aligned} \tag{2.3}$$

where $m^i{}_j$ is the quark mass matrix. This matrix can be diagonalised by a rotation in flavour space since the matrix must fulfill $[m, m^\dagger] = 0$ due to the $\mathcal{N}=2$ supersymmetry, and we denote the corresponding masses m_i. We could also have considered a general polynomial $m^i{}_j(\Phi)$ such that the superpotential term takes the form $\sqrt{2}\widetilde{Q}_i m^i{}_j(\Phi) Q^j$. This generically breaks the $\mathcal{N}=2$ supersymmetry to $\mathcal{N}=1$, however, in the end many results will only depend on $B(x) = \det m(x)$ which in our case takes the form:

$$B(x) = \prod_{i=1}^{N_f} (x + m_i). \tag{2.4}$$

Finally, we will also consider $\mathcal{N}=1$ SYM where we softly break the above $\mathcal{N}=2$ theory by a superpotential

$$W_{tree} = \sum_{p \in \mathbb{N}} \frac{g_p}{p} \operatorname{Tr} \Phi^p. \tag{2.5}$$

2.1.2 Symmetries

Let us now examine the symmetries of our Lagrangian. Classically, we have, besides the gauge symmetry, the following global symmetries: A $U(1)_B \times SU(N_f)$ flavour symmetry and a $U(1)_R \times SU(2)_R$ chiral R-symmetry. The $SU(2)_R$ symmetry is not manifest in our $\mathcal{N}=1$ superfield notation, however, a $U(1)_J$ subgroup that acts on Q and $\widetilde{Q}$ is manifest. In general, the R-symmetry rotates the spinors of the gauge multiplet while it rotates the scalar part of the hypermultiplet. In order to

	$SU(N_c)$	$SU(N_f)$	$U(1)_B$	$U(1)_R$	$U(1)_J$
Q	$\mathbf{N_c}$	$\mathbf{N_f}$	1	0	1
$\widetilde{Q}$	$\overline{\mathbf{N}}_\mathbf{c}$	$\overline{\mathbf{N}}_\mathbf{f}$	-1	0	1
Φ	**adj**	**1**	0	2	0
m_A	**1**	**adj**	0	2	0
m_S	**1**	**1**	0	2	0
$\Lambda^{2N_c-N_f}$	**1**	**1**	0	$2(2N_c - N_f)$	0
g_k	**1**	**1**	0	$2-2k$	2

Table 2.1: The classical symmetries of the $\mathcal{N}=2$ SQCD.

preserve the flavour symmetry in the massive case, the traceless part of the mass, m_A, must transform in the adjoint while the trace of the mass, m_S, is a singlet. Also for the $U(1)_R$ symmetry the masses have to be charged. Table 2.1 gives the representations and charges for the scalar part of the superfields and the masses. Please note that here and in the following we will denote the complex scalar part of the chiral superfields Φ, Q and $\widetilde{Q}$ by the same symbol.

In the table we have also included the charges of the holomorphic scale, Λ. We have written Λ as the usual instanton factor Λ^b, where

$$b = 3C(\mathbf{adj}) - \sum_n C(\mathbf{r}_n) = 2N_c - N_f, \tag{2.6}$$

and the sum is over the representations of the chiral field. We have one chiral field with $C(\mathbf{adj}) = N_c$ and $2N_f$ with $C(\mathbf{fund}) = 1/2$. The chiral anomaly of $U(1)_R$ gives a transformation of the ϑ-angle and hence a charge to Λ^b. The charge is given by

$$2\sum_i q_i C(\mathbf{r}_i) = 2(2N_c - N_f), \tag{2.7}$$

where the sum is over the representations of the Weyl fermions and q_i their respective charges ($+1$ for the fermions in the gauge multiplet and -1 for the fermions in the hypermultiplet). This chiral anomaly also means that $U(1)_R$ is broken down to $\mathbb{Z}_{2(2N_c-N_f)}$ in the quantum case. Please note that this analysis is for $N_f < 2N_c$, where the theory is asymptotically free. For $N_f = 2N_c$ we have a scale-invariant theory (for zero masses) and thus no holomorphic scale Λ.

Note that the polynomial in (2.4) is given by $B(x) = \det(x\mathbf{1}+m_i)$, and especially all its coefficients, are invariant under the residual flavour symmetry which acts as permutations of m_i and we expect to find expressions in terms of these permutation invariant coefficients.

2.1.3 Classical vacuum moduli space

The moduli space of the theory was studied in [111]. Classically, we have flat directions given by the D- and F-term equations. The D-term equations are:

$$0 = [\Phi, \Phi^\dagger], \tag{2.8}$$
$$0 = Q^i_A Q^{\dagger B}_i - \widetilde{Q}^{\dagger i}_A \widetilde{Q}^B_i, \tag{2.9}$$

and the F-term equations are:

$$0 = W'(\Phi)^A_B + \sqrt{2}\widetilde{Q}^A_i Q^i_B, \tag{2.10}$$
$$0 = m^i{}_j Q^j_A + \Phi^B_A Q^i_B, \tag{2.11}$$
$$0 = \widetilde{Q}^A_j m^j{}_i + \widetilde{Q}^B_i \Phi^A_B. \tag{2.12}$$

The first D-term equation (2.8) means that we can diagonalise Φ

$$\Phi = \begin{pmatrix} \phi_1 & & \\ & \ddots & \\ & & \phi_{N_c} \end{pmatrix}. \tag{2.13}$$

In the case of a $SU(N_c)$ gauge group we should impose $\sum_A \phi_A = 0$.

We should now distinguish between two types of branches of the vacuum moduli space: The Coulomb branch and the Higgs branches. In the Coulomb branch the quarks have zero expectation value $\langle Q \rangle = \langle \widetilde{Q} \rangle = 0$. This is the branch that we will investigate in this thesis. For the Higgs branch the quarks have non-zero expectation value.

Let us first examine the Coulomb branch. In the $\mathcal{N} = 2$ case without any superpotential W_{tree} the eigenvalues are generically all different and the gauge group is broken to $U(N_c) \mapsto U(1)^{N_c}$ – hence the name Coulomb branch. In the $\mathcal{N} = 1$ case where we turn on W_{tree} we will, however, also have to obey (2.10), which tells us that the eigenvalues have to lie in the minima of W_{tree}. Let us denote the degree of W'_{tree} by n and write $W'_{tree}(\Phi) = (\Phi - \phi_1) \cdots (\Phi - \phi_n)$. Thus $\Phi = \mathrm{diag}(\phi_1 \mathbf{1}_{N_1}, \ldots, \phi_n \mathbf{1}_{N_n})$ and the gauge group breaks into n parts as

$$U(N_c) \mapsto \prod_{i=1}^{n} U(N_i), \tag{2.14}$$

where $\sum_i N_i = N_c$ and we should rather be talking about pseudo-confining vacua. In both of the above cases we should remember that we have residual gauge symmetry, and we should parameterise the vacuum moduli space in terms of parameters which are invariant under the Weyl group that permutes the ϕ_As. These are given by the coefficients of

$$P_{N_c}(x) = \det(x\mathbf{1} - \Phi). \tag{2.15}$$

However, it is customary to use that these coefficients can instead be written in terms of the Weyl invariants (the relation will be given in the next section)

$$u_k = \frac{1}{k}\langle Tr\Phi^k\rangle, \quad k = 1, \ldots, N_c, \tag{2.16}$$

where we have taken the expectation value to anticipate the quantum case. The u_ks will be used to parameterise the vacuum moduli space. Again for a $SU(N_c)$ gauge group we have to impose $u_1 = 0$.

Let us consider the Higgs branches briefly for completeness. Examining the Lagrangian we see that the squarks of Q^i_A and $\widetilde{Q}^A_i$ have mass $\phi_A + m_i$. From the F-flatness equations (2.11) and (2.12) we see that when this mass is zero the quarks can have non-zero expectation value. Thus the Higgs branch emanates from the Coulomb branch at points where the squarks become massless. Also note that on this *root* of the Higgs branch $W'_{tree}(-m_i) = 0$ by (2.10). The Higgs branches are separated into baryonic and non-baryonic branches. The baryonic branches exist for $N_F \geq N_c$ and breaks the gauge group completely. The non-baryonic branches are labelled by an integer $r \geq \min\{[N_f/2], N_c - 2\}$ depending on the size of the non-zero part of the matrix Q^i_A (in principle we have one such integer for each m_i).

Let us now consider what happens in the quantum case.

2.1.4 Low-energy effective action

Here we consider the $\mathcal{N} = 2$ low-energy effective theory for the Coulomb branch. In section 2.3 we will take into account W_{tree}. We saw above that the gauge group generically was broken as $SU(N_c) \mapsto U(1)^{N_c-1}$ – where we now do not take into consideration the trivial overall $U(1)$ of the $U(N_c)$ gauge group. So the field content should be $N_c - 1$ copies of $\mathcal{N} = 2$ $U(1)$ gauge multiplets which we write in terms of the chiral $\mathcal{N} = 1$ superfields A_i and $\mathcal{W}_i$ where i labels the generators of the Cartan subalgebra.[1] The point is that the Coulomb branch is not lifted by quantum corrections [10, 11] i.e. that this is really the low energy field content. Of course, this is for generic points where e.g. none of the ϕ_A coincide to give a larger gauge group.

The Wilsonian effective Lagrangian is by (super)symmetries constrained to be determined by a prepotential $\mathcal{F}(A_k)$ such that

$$\mathcal{L}_{\mathit{eff}} = \frac{1}{8\pi i}\int \mathrm{d}^4\theta A^i_D \bar{A}_i + \frac{1}{16\pi i}\int \mathrm{d}^2\theta \tau_{ij}\mathcal{W}_i\mathcal{W}_j + \text{c.c.}, \tag{2.17}$$

[1] This is an abuse of the index i since it was already used for labelling the $U(N_F)$ index. However, there ought to be no confusion.

where

$$A_D^i = \frac{\partial \mathcal{F}(A_k)}{\partial A_i}, \tag{2.18}$$

$$\tau_{ij} = \frac{\partial^2 \mathcal{F}(A_k)}{\partial A_i \partial A_j}. \tag{2.19}$$

Classically, the prepotential is simply $\mathcal{F}(A_k) = \frac{\tau}{2}\sum_{i=1}^{N_c-1} A_i^2$. Perturbatively, it will only receive one-loop corrections due to non-renormalisation theorems. However, we will also have non-perturbative instanton corrections proportional to powers of $\Lambda^{2N_c-N_f}$ as discussed above. The quantum prepotential then takes the form (see e.g. [112] for the case with flavour)

$$\begin{aligned}\mathcal{F}(A_k) = \;& \frac{\tau}{2}\sum_{i=1}^{N_c-1} A_i^2 \\ & -\frac{1}{8\pi i}\left(\sum_{k,l}^{N_c-1}(A_k - A_l)^2 \ln\frac{(A_k-A_l)^2}{\Lambda^2} - \sum_i^{N_f}\sum_k^{N_c-1}(A_k+m_i)^2\ln\frac{(A_k+m_i)^2}{\Lambda^2}\right) \\ & +\sum_{l=1}^{\infty}\mathcal{F}_l(A_k)\Lambda^{l(2N_c-N_f)}.\end{aligned} \tag{2.20}$$

The properties of the effective action will be discussed in the next section.

2.2 The Seiberg-Witten Curves

In the last section we saw how the low-energy effective theory was determined by a prepotential. In this section we will see how the properties of this prepotential enables us to construct the Seiberg-Witten curves that determines the prepotential exactly.

2.2.1 Properties of the prepotential

Expanding the action using (2.20) shows that $\tau_{ij}(a_i)$ is the effective complex coupling and $\operatorname{Im}\tau_{ij}(a_i)$ is the metric on the moduli space, where a_i is the complex scalar part of A_i. The relation between a_i and the parameters of the moduli space u_k will be given later (2.30). The metric has to be positive to ensure unitarity. However, $\operatorname{Im}\tau_{ij}$ is a harmonic function in the a_is and hence can not have a minimum. Here and in the following we consider the case of a $SU(2)$ gauge group with just one a_i and thus classically by (2.16) $u_2 = a^2/2$ (and $u_1 = 0$), but we will quote the general $U(N_c)$ results. The conclusion for $\tau(a)$ is that it is only locally defined and we need different descriptions of the theory on the full quantum moduli space. Also, we see from the logarithms in the one-loop terms that the prepotential is actually a multi-valued function.

The dual description of the same physics is the strong-weak electric-magnetic duality sending $\tau \mapsto -1/\tau$. Further we also have the symmetry $\tau \mapsto \tau + 1$. Combining these two, the full duality group becomes $SL(2,\mathbb{Z})$ whereas in the general case we get a $Sp(2(N_c-1),\mathbb{Z})$ duality group transforming τ_{ij} as

$$\tau' = (C + D\tau)(A + B\tau)^{-1}, \qquad \begin{pmatrix} A & B \\ C & D \end{pmatrix} \in Sp(2(N_c-1),\mathbb{Z}). \tag{2.21}$$

This is the same formula as for the modular transformations of period matrices of Riemann surfaces that we will meet in the next chapter, so this suggests an intimate relation to these. One immediate advantage is that period matrices always have positive definite imaginary part ensuring unitarity.

2.2.2 Monodromies

The above duality transformation of $\tau \mapsto -1/\tau$ is by (2.18) and (2.19) realised by $A \mapsto A_D$ and $A_D \mapsto -A$ hence the reason for the index D for dual. For the full duality group we get for $U(N_C)$ but without matter

$$\begin{pmatrix} A_D^i \\ A_j \end{pmatrix} \mapsto \mathcal{M} \begin{pmatrix} A_D^i \\ A_j \end{pmatrix} \tag{2.22}$$

where $\mathcal{M} \in Sp(2(N_c-1),\mathbb{Z})$. Actually, one could add a constant vector on the right hand side, but this would not leave the BPS formula for the mass invariant. However, when we have fundamental matter in the theory we get an extra term in the formula for the central charge, Z, that gives the mass of the BPS multiplet $M^2 = |Z|^2$. Consider a state with electric charge $n_e \in \mathbb{Z}^{N_c-1}$, magnetic charge $n_m \in \mathbb{Z}^{N_c-1}$, and quark number charge $q \in \mathbb{Z}^{N_f}$ which comes from the $U(N_f)$ flavour symmetry broken to $U(1)^{N_f}$ when all masses are different (as discussed in the previous section where we preserved the symmetry by letting the masses transform). The central charge is then

$$Z = a \cdot n_e + a_D \cdot n_m + m \cdot q, \tag{2.23}$$

where a_D is the scalar part of A_D and $m = (m_i)$. The extra term here means that for fundamental matter we can and do have in (2.22) an extra vector with integers times the bare masses m_i. In this way the central charge is preserved under the duality transformation by letting the charges (n_e, n_m, q) transform properly.

The point is now that $(a_D^i(u_k), a_i(u_k))$ is a section of a $Sp(2(N_c-1),\mathbb{Z})$ bundle over the moduli space parameterised by the u_ks. The metric on the moduli space can be expressed as the pullback of

$$\frac{i}{2}(da_i \wedge d\bar{a}_D^i - da_D^i \wedge d\bar{a}_i). \tag{2.24}$$

If we go around a closed loop on the moduli space encircling a singular submanifold $(a_D^i(u_k), a_i(u_k))$ will be transformed by an element of the monodromy group as in (2.22), and the monodromy group is a subgroup of $Sp(2(N_c-1), \mathbb{Z})$.

The main point is then to associate to each point of the vacuum moduli space a genus N_c Riemann surface. The monodromy group for going around a closed loop is then reflected by modular transformations in the Riemann surface which, as we will see in the next section, just corresponds to a change of homology basis. This was suggested by the transformations of τ_{ij} above, which will be identified with the period matrix of the Riemann surface. The family of Riemann surfaces is called the Seiberg-Witten curve.

The exact form of the Seiberg-Witten curve is determined by examining the monodromies in details. We will not go into details here, but let us briefly consider the $SU(2)$ gauge group without matter. We can immediately see one singularity around which we have monodromy. This is for a very large, i.e. large energy, where the theory is asymptotically free (and here $u_2 = a^2/2$ holds). At this weak coupling we can trust the perturbation theory and thus the one-loop part of the prepotential (2.20). Let us circle $u_2 = \infty$ such that $\ln u_2 \mapsto \ln u_2 + 2\pi i$ i.e. $a \mapsto -a$. By (2.20) the logarithmic part of $a_D = \partial\mathcal{F}/\partial a$ is $\frac{2ia}{\pi} \ln \frac{a}{\Lambda}$ and thus $a_D \mapsto -a_D + 2a$. We have thus determined the monodromy around $u_2 = \infty$. For consistency there has to be more singularities than the one at ∞. Such singularities arise at points where we have accidentally integrated out massless fields. One might think this happens at $u_2 = 0$ where the gauge bosons become massless, but the analysis of Seiberg-Witten showed that this was not the case. The only remaining possibility is that the singularities correspond to monopoles or dyons becoming massless. These fields, which are described by hypermultiplets, can not be coupled locally to our theory. However, they can be described in the dual picture (2.22), where they become the elementary weakly coupled objects. This allows one to calculate that we have two more singular points corresponding to respectively a monopole and a dyon becoming massless.

The Seiberg-Witten curves presented in the next section should then solve this monodromy problem as well as have the right $U(1)_R$ charge assignments. Further, for larger gauge groups and hypermultiplets one should have the right decoupling limits. This allows one to determine the Seiberg-Witten curves.

2.2.3 Seiberg-Witten curves

The Seiberg-Witten curve solving the above monodromy problem is given as a genus $N_c - 1$ hyperelliptic curve Σ (see section 3.4) depending on u_k, the parameters of the vacuum moduli space (2.16), and given by (here in the case of a $U(N_c)$ gauge group and no matter found in [113, 114]):

$$\Sigma : y^2 = P_{N_c}(x, u_k)^2 - 4\Lambda^{2N_c}, \tag{2.25}$$

where the polynomial P_{N_c} is given as in (2.15):

$$P_{N_c}(x, u_k) = \langle \det(x\mathbf{I} - \Phi) \rangle = x^{N_c} + \sum_{i=1}^{N_c} s_i x^{N_c - i}. \tag{2.26}$$

Here the coefficients s_i are polynomials in the u_ks determined by Newton's formula

$$is_i + \sum_{k=1}^{i} k s_{i-k} u_k = 0, \;\; i = 0, \dots, N_c, \tag{2.27}$$

with the definition $s_0 \equiv 1$. This can be derived from:

$$\begin{aligned} \det(x\mathbf{I} - \Phi) &= x^{N_c} \det\left(\mathbf{I} - \frac{\Phi}{x}\right) = x^{N_c} e^{\operatorname{Tr}\ln\left(\mathbf{I} - \frac{\Phi}{x}\right)} = x^{N_c} \exp\left(-\sum_{n=1}^{\infty} \frac{\operatorname{Tr}(\Phi^n)}{n x^n}\right) \\ &= x^{N_c} - \operatorname{Tr}\Phi\, x^{N_c - 1} - \frac{1}{2}\left(\operatorname{Tr}\left(\Phi^2\right) - \operatorname{Tr}(\Phi)\operatorname{Tr}(\Phi)\right) x^{N_c - 2} - \dots \end{aligned} \tag{2.28}$$

The relation to the low-energy effective action determined by a_i and a_D^i is given in terms of the Seiberg-Witten one-form (see next chapter for definition of Riemann surface concepts) given by:

$$\lambda_{SW} = \frac{1}{2\pi i} x\, d\ln(y + P_{N_c}(x, u_k)). \tag{2.29}$$

Given the canonical homology basis (α_i, β_j) for Σ, the relation to a_i and a_D^i is given by:

$$a_i = \oint_{\alpha_i} \lambda_{SW}, \qquad a_D^i = \oint_{\beta_i} \lambda_{SW}. \tag{2.30}$$

This gives the relation between u_k and a_i. Remembering that a_D is given in terms of the prepotential as (2.18) and the gauge coupling τ_{ij} is given by the derivative of a_D^i we get $\tau_{ij}(a_i) = \oint_{\beta_i} \frac{\partial \lambda_{SW}}{\partial a_j}$ or

$$\tau = \frac{\partial a_D}{\partial u} \left(\frac{\partial a}{\partial u}\right)^{-1}, \tag{2.31}$$

where

$$\frac{\partial a_i}{\partial u_j} = \oint_{\alpha_i} \frac{\partial \lambda_{SW}}{\partial u_j} \qquad \frac{\partial a_D^i}{\partial u_j} = \oint_{\beta_i} \frac{\partial \lambda_{SW}}{\partial u_j}. \tag{2.32}$$

As we will see in the next chapter this is exactly the period matrix of the hyperelliptic surface for $\partial\lambda_{SW}/\partial u_j$ a basis of holomorphic one-forms.

The curve for a $SU(N_c)$ gauge group is the same as above but with constraint $u_1 = 0$. Thus for $SU(2)$ we get

$$y^2 = (x^2 - u_2)^2 - 4\Lambda^{2N_c} = (x^2 - u_2 - 2\Lambda^{N_c})(x^2 - u_2 + 2\Lambda^{N_c}). \tag{2.33}$$

Thus if $u_2 = \pm 2\Lambda^{N_c}, \infty$ we got double roots and the curve degenerates. These are the singular points on the vacuum moduli space around which we have monodromies. The monodromy corresponds to the modular transformation that arises from the change in homology basis as we let u_2 circle one of these points corresponding to vanishing cycles.

For other gauge groups the curves were found in [115, 116, 117]. Let us here just quote the $SO(N)$ result (see e.g. [59])

$$\Sigma : y^2 = P_N(x, v_p)^2 - 4x^{2q}\Lambda^{2\tilde{h}}, \quad P_N(x) = \prod_{k=1}^{r}(x^2 - e_k^2) \tag{2.34}$$

Here $v_p = \frac{1}{2p} \operatorname{Tr} \Phi^{2p}$ (only even powers of Φ contribute), $\tilde{h}$ is the dual Coxeter number which for $SO(N)$ is $\tilde{h} = N-2$. Given the rank, $r = [N/2]$, of $SO(N)$ then $q = 2r - \tilde{h}$ which is $q = 2$ for $SO(2N)$ and $q = 1$ for $SO(2N+1)$. Finally, $v_p = \frac{1}{p}\sum_{k=1}^{r} e_k^{2p}$.

Let us now consider the Seiberg-Witten curves with fundamental matter. Here the curve for a $U(N_c)$ gauge group takes the form (found in [118, 119], see [120, 121] for other gauge groups)

$$\Sigma : y^2 = P_{N_c}(x, u_k)^2 - 4\Lambda^{2N_c - N_f}\prod_{i=1}^{N_f}(x + m_i), \tag{2.35}$$

where we assume $N_f < 2N_c$.

Importantly, we get quantum corrections to the Newton formula (2.27) for $N_c \leq N_f < 2N_c$ and we have to replace (2.26) by [77] (see also derivation in section 4.1)

$$P_{N_c}(x, u_k) = \langle \det(x\mathbf{I} - \Phi)\rangle + \left[\Lambda^{2N_c - N_f}\frac{B(x)}{x^{N_c}}\exp\left(\sum_{i=1}^{\infty}\frac{u_i}{x^i}\right)\right]_+, \tag{2.36}$$

where the subscript "+" stands for the polynomial part and $B(x) = \prod_{i=1}^{N_f}(x + m_i)$ was defined in (2.4).

The curve for the case $N_c = 2N_f$ can also be found [118]. Here we do not have a holomorphic scale Λ since the β function vanishes, but the curve will depend on the bare coupling τ through $h(\tau) = 2\theta_1^4/(\theta_2^4 - \theta_1^4)$ (the definition of the theta functions is given in section 3.5). The curve then takes the form

$$\Sigma : y^2 = P_{N_c}(x, u_k)^2 - h(h+2)\prod_{i=1}^{N_f}(x + m_i + hm_S), \tag{2.37}$$

where $m_S = \sum_i m_i/N_f$ is the trace of the mass matrix defined above in section 2.1.

The curves for $N_f < 2N_c$ can be obtained from this solution by decoupling flavours. To lower the value of N_f by one unit we integrate out the ith flavour by taking the limit $m_i \to \infty$ while taking $\Lambda \to 0$ ($q = e^{i\pi t} \to 0$ for $N_f = 2N_c$), but keeping $\Lambda^{2N_c-N_f}m_i \equiv \Lambda_{new}^{2N_c-(N_f-1)}$ constant ($16qm_i \equiv \Lambda_{new}$ constant). This removes the ith flavour and the new scale Λ_{new} is exactly given by the scale matching condition. Using this procedure one can ultimately obtain the curve without fundamental matter. Actually, the curve for $N_f > 2N_c$ can also be deduced using this method [111], however, these are not asymptotically free theories. The curves are the same as in (2.35).

Finally, we note that curves for the Higgs branch roots also exist. E.g. for the rth non-baryonic branch root we have (see e.g. [111, 122])

$$\Sigma : y^2 = x^{2r}\left(P_{N_c-r}(x,u_k)^2 - 4\Lambda^{2N_c-N_f}x^{N_f-2r}\right), \tag{2.38}$$

where we are in the massless case, and P is only of degree $N_c - r$ since we only have $N_c - r$ non-zero eigenvalues of Φ.

So we see that the complete dynamics of the low energy theory of $\mathcal{N} = 2$ supersymmetric gauge theory is completely determined by the geometry of the Seiberg-Witten curve. In the next section we will consider the $\mathcal{N} = 1$ theory.

2.3 Factorisation of Seiberg-Witten Curves

Let us now consider what happens when we add the tree-level superpotential (2.5), W_{tree}, breaking the $\mathcal{N} = 2$ theory to $\mathcal{N} = 1$. The analysis we will do here is without matter, but for the Coulomb branch where the quarks have zero expectation value the analysis with matter is the same.

2.3.1 Massless dyons and the low-energy effective theory

The lore of the low energy theory is that it has a mass gap and confinement. The term $m\,\mathrm{Tr}(\Phi^2)$ in W_{tree} gives mass to Φ, but we still need to give the gauge fields A_i mass. This could happen either by having light gauge fields giving strong coupling effects or light charged fields giving mass by the Higgs mechanism. As mentioned above Seiberg and Witten argued that the second option is the correct one and we have massless dyons at certain submanifolds of the vacuum moduli space. These dyons (here we take them to be monopoles) can be described by $\mathcal{N} = 1$ chiral superfields M_i, $\widetilde{M}^i$ where $i = 1,\ldots,N_c-1$. Since we are at strong coupling, these monopoles should couple to the dual of A_i, i.e. A_D^i from (2.22). So in the vicinity of a point with massless monopoles the effective superpotential should be (equivalent to (2.3)):

$$W_{eff} = \sum_{i=1}^{N_c-1} \widetilde{M}^i M_i A_D^i \tag{2.39}$$

Taking into account W_{tree} we simply get

$$W_{\mathit{eff}} = \sum_{i=1}^{N_c-1} \widetilde{M}^i M_i A_D^i + \sum_p g_p U_p, \tag{2.40}$$

where the U_ps are the chiral fields representing $\frac{1}{p}\operatorname{Tr}\Phi^p$ at low energies. Here we have used the ILS linearity principle [123] saying that the low-energy effective potential should be linear in g_p. If we do not allow any singularity as $g_p \to 0$ we could also argue for this simply using the $U(1)_R$ symmetry from table 2.1.

Let us now consider the vacua determined from this low-energy action. The D-flatness equations are

$$|m_i| = |\widetilde{m_i}|, \tag{2.41}$$

where m_i ($\widetilde{m}^i$) is the scalar part of M_i ($\widetilde{M}^i$). The F-flatness equations are[2]

$$g_p + \sum_{i=1}^{N_c-1} \frac{\partial a_D^i(u_p,\Lambda)}{\partial u_p} \widetilde{m}^i m_i = 0, \quad p = 1,\ldots,N_c, \tag{2.42}$$

$$a_D^i m_i = a_D^i \widetilde{m}^i = 0, \quad i = 1,\ldots,N_c-1. \tag{2.43}$$

From (2.42) we see that if any g_p is different from zero we must have some $\widetilde{m}^i m_i \neq 0$ for $i = 1,\ldots,l$ and thus by (2.43) we must have the corresponding $a_D^i = 0$. However, as we see from (2.40), this is the mass term for the monopoles so we have, say l, massless monopoles (see also the mass formula (2.23)). So we conclude that the $\mathcal{N} = 1$ superpotential lifts the Coulomb branch except for submanifolds where l (mutually local) monopoles become massless:

$$a_D^i(u_p,\Lambda) = 0, \quad i = 1,\ldots,l, \tag{2.44}$$

$$m_i = \widetilde{m}^i = 0, \quad i = l+1,\ldots,N_c-1. \tag{2.45}$$

Of course, we should still remember equation (2.42) as determining whether a given W_{tree} really gives a $\mathcal{N} = 1$ vacuum, and it determines the expectation values of the monopoles (or more generally, dyons). Equation (2.44) gives l constraints and thus these submanifolds should be of dimension $N_c - l$, i.e. the solution is parameterised by c_i where $i = 1,\ldots,N_c - l$.

For the l massless monopoles we have non-zero expectation values and condensation. By the lore of gauge theory this induces confinement of the corresponding electric charges (the dual Meissner effect). Thus the low energy gauge group is $U(1)^{N_c-l-1} \times U(1)$ where the last $U(1)$ is the overall $U(1)$ from $U(N_c)$. Each of these $U(1)$ can be thought of as a $U(1) \subseteq U(N_i)$ of the classic gauge group breaking pattern $U(N_c) \mapsto \prod_{i=1}^{N_c-l} U(N_i)$ that we saw in (2.14). Each of the $SU(N_i)$ gauge groups confines, has a mass gap and gaugino condensation determined by a corresponding scale Λ_i thus leaving us with $U(1)^{N_c-l}$.

[2]For simplicity we take W_{tree} to have maximal degree N_c since we only consider the U_ks up to $k = N_c$ as being independent.

2.3.2 Factorization

The submanifolds of the Coulomb branch where we have massless monopoles and possibility of $\mathcal{N} = 1$ vacua are determined by factorized curves. This is seen from (2.30) for the massless monopoles:

$$a_D^i(u_k^{(fact)}, \Lambda) = \oint_{\beta_i} \lambda_{SW} = 0. \tag{2.46}$$

This means that the β_i-cycles shrink to zero size and the genus $N_c - 1$ Riemann surface is reduced to a genus $N_c - l - 1$ curve. The shrinking of cycles means that some of the cuts become single points and hence that we have l double roots in the curve. I.e. the Seiberg-Witten curve takes the form

$$y^2 = P_{N_c}(x, u_k^{(fact)})^2 - 4\Lambda^{2N_c} = F_{2(N_c-l)}(x) H_l(x)^2 \tag{2.47}$$

where $F_{2(N_c-l)}(x)$ and $H_l(x)$ are polynomials of degree $2(N_c - l)$ and l, respectively. We will generally assume that we have no multiple roots in $F_{2(N_c-l)}$ and H_l and that they have no common roots. This means that we have no roots of order higher than two in the curve. The submanifold should, as we also saw above, have dimension $N_c - l$ since we constrain the N_c independent u_ks by imposing the condition of l double roots. We can immediately see that one of these parameters is realised by translation invariance of the above problem. However, this is not the case when we include matter – since this would translate the masses:

$$y^2 = P_{N_c}(x, u_k^{(fact)})^2 - 4\Lambda^{2N_c - N_f} \prod_{i=1}^{N_f} (x + m_i) = F_{2(N_c-l)}(x) H_l(x)^2. \tag{2.48}$$

However, the solution is still invariant under translation and simultaneous translation of the masses so the translation parameter will also be found in this case. Further we should expect some discrete parameters labeling the branches, especially one corresponding to the different vacua that appear when $\mathbb{Z}_{2(2N_c - N_f)} \subset U(1)_J$ breaks further down at low energies. See e.g. [122] for a brane picture of the factorization.

2.3.3 Low energy potential

The value of the low energy potential is then simply by (2.40), (2.44) and (2.45)

$$W_{\mathit{eff}}(\Lambda, g_p, c_i) = \sum_p g_p u_p^{(fact)}(c_i), \tag{2.49}$$

where the c_is are the $N_c - l$ parameters of the submanifold with l mutually local massless monopoles.

Let us now assume, for simplicity, that W_{tree} is of order $n+1$ where $n = N_c - l$:[3]

$$W_{tree} = \sum_{p=2}^{n+1} \frac{g_p}{p} \operatorname{Tr} \Phi^p. \tag{2.50}$$

We thus see that (2.42) gives $N_c - l = n$ equations after solving for the expectation values of the monopoles $\widetilde{m}^i m_i$ for $i = 1, \ldots, l$ – the rest being zero by (2.45). Thus we get n equations relating the n g_ps and the n c_is. Solving for the g_ps and inserting in (2.50) gives the low energy potential W_{low}

$$W_{low}(\Lambda, g_p) = \sum_{p=2}^{n+1} g_p u_p^{(fact)}(\Lambda, g_p). \tag{2.51}$$

This is equivalent to extremising W_{eff} over the submanifold and solving for the c_is. This can be seen since the $\widetilde{m}^i m_i$ simply act as Lagrange multipliers in (2.40).

2.3.4 Geometric engineering

The effective superpotential can also be found by geometrical engineering [37, 56, 124, 45], as we reviewed in the introduction. Here it was shown that there is an equivalence between the $\mathcal{N} = 1$ theory studied above and the type IIB superstring on Calabi-Yau threefold geometries with fluxes. Dijkgraaf and Vafa showed that the effective superpotential can be obtained simply by solving a related matrix model.

The point is here that integrals over the Calabi-Yau threefold reduces to integrals over the genus $n-1$ Riemann surface (the matrix model curve in the Dijkgraaf-Vafa conjecture)

$$y^2 = W'_{tree}(x)^2 + f_{n-1}(x), \tag{2.52}$$

where f_{n-1} is a polynomial of degree $n-1$ whose coefficients we will parameterise by S_i given by the α-periods of the one-form of (2.52)

$$\Omega = y\, dx = \sqrt{W'_{tree}(x)^2 + f_{n-1}(x)}\, dx, \tag{2.53}$$

i.e.

$$S_i = \int_{\alpha_i} \Omega. \tag{2.54}$$

These S_i are representing the glueball superfields given by the expectation values of the gauge field strengths for the broken gauge group factors $U(N_c) \mapsto \prod_{i=1}^{n} U(N_i)$

$$S_i = -\frac{1}{16\pi^2} \operatorname{Tr}\left(\mathcal{W}_{(i)}^{\alpha} \mathcal{W}_{(i)\alpha}\right). \tag{2.55}$$

[3] g_1 can trivially be removed.

We can think of S_i as being dual of Λ_i, the scale corresponding to the broken factor $U(N_i)$ that we saw above. The β-periods of Ω are

$$\frac{\partial \mathcal{F}_0}{\partial S_i} = \int_{\beta_i} \Omega, \tag{2.56}$$

where $\mathcal{F}_0$ is the prepotential of the Calabi-Yau geometry. Here the periods are thought of as non-compact, but with some large distance cut-off Λ_0. There is another one-form H with α-periods N_i and β-periods τ_i, where the τ_is are the gauge couplings (we will see more to this one-form later). The effective glueball superpotential is then given by (this is $SU(N_c)$ case):

$$W_{\mathit{eff}}(S_i) = \int \Omega \wedge H = \sum_i \left(N_i \frac{\partial \mathcal{F}_0}{\partial S_i} + \tau_i S_i \right). \tag{2.57}$$

The relation to the above factorization of the Seiberg-Witten curves with $l = N_c - n$ massless monopoles (2.47) turns out to simply be that the curve is given by the reduced curve for the factorization:

$$g_{n+1}^2 F_{2n}(x) = W'_{\mathit{tree}}(x)^2 + f_{n-1}(x). \tag{2.58}$$

But please note that the β-curves in (2.56) are not the same as the ones used on the Seiberg-Witten curve. The curves in (2.56) start on the lower sheet at Λ_0, continue through one of the cuts, and end on Λ_0 on the upper sheet. Thus for n cuts we have n β-curves. We can also make an nth α-curve encircling the last cut giving us n α-curves and thus n S_i. The matrix $\frac{\partial^2 \mathcal{F}_0}{\partial S_i \partial S_j}$ can, in an appropriate basis (also taking τ_i all equal to $\tau(\Lambda_0)$ which as noted depends on Λ_0), be written [56] such that $\tau_{in} = 0$, $\tau_{nn} = \tau(\Lambda_0)$ and τ_{ij} with $i, j = 1, \ldots, n-1$ is the period matrix of the factorized Seiberg-Witten curve. Further it was shown that [37]

$$W_{\mathit{eff}}(\langle S_i \rangle) = W_{\mathit{low}}(g_i, \Lambda), \tag{2.59}$$

where by $\langle S_i \rangle$ we mean that the expectation value have been found extremising $W_{\mathit{eff}}(S_i)$ (integrating out S_i). This has been used to test the conjecture especially for the complete factorization corresponding to an unbroken gauge group, which we will discuss later in section 4.4.

2.3.5 Solutions

Please note that it is easy to give solutions for the factorization problem (2.47). Consider the classical solution corresponding to $U(N_c) \mapsto U(1)^{N_c - 2r} \times U(2)^r$ where $\Phi = \mathrm{diag}(a_1, a_1, \ldots, a_r, a_r, b_1, \ldots, b_{N_c - 2r})$. This means that the polynomial $P_{\mathit{clas.}}(x, u_k) = \langle \det(x\mathbf{I} - \Phi) \rangle$ has double zeroes in a_1 to a_r i.e. that $P_{\mathit{clas.}}(a_i) = P'_{\mathit{clas.}}(a_i) = 0$. But this in turn shows that $P_{N_c} = P_{\mathit{clas.}} \pm 2\Lambda^{N_c}$ solves the factorization problem as:

$$P_{N_c}(x, u_k)^2 - 4\Lambda^{2N_c} = H_{2N_c - 2r}(x) \prod (x - a_i)^2. \tag{2.60}$$

This is the generalisation of the solution found in [125] for one $U(2)$-factor simply by obtaining the low-energy effective potential by integrating out matter and imposing confinement and gaugino condensation.

However, how to find all solutions and analyse how these are continuously connected is the question in the next chapters. In order to do our analysis we will use Riemann surfaces, and the next chapter will be devoted to an introduction to these.

Chapter 3

Riemann Surfaces

In this chapter we will give an introduction to Riemann surfaces. Readers familiar with the topic can skip to next chapter. A pedagogical review can be found in [126] and much of this chapter is based on [127] and [128, 129]. Other references are [130, 131, 132, 133, 134].

3.1 Riemann Surfaces

3.1.1 Definition

An n-dimensional *complex manifold* is defined exactly as a standard real manifold where we simply replace the coordinates into $\mathbb{R}^n$ with coordinates into $\mathbb{C}^n$ and demand that the transition functions (coordinate change maps) should be holomorphic. It is easily proven that complex manifolds are always orientable.

Here we will be concerned with *Riemann surfaces* which are connected one-dimensional complex manifolds. These can, of course, be seen as ordinary real two-dimensional manifolds and it can be shown that real two-dimensional differentiable manifolds, which are orientable and compact, admit complex structure and thus can be seen as equivalent to compact Riemann surfaces. We will generally assume our surfaces to be compact. It turns out that these are always triangulable.

From real surfaces we now know that we can topologically classify the (compact) Riemann surfaces according to their *genus* $g \in \mathbb{N}_0$ (i.e. the number of handles on the surface). However, we only consider two surfaces as being equivalent if they are analytically isomorphic, i.e. related by a bijective function f for which both f and f^{-1} are holomorphic. It turns out that there is a continuity of analytic equivalence classes for each genus – table 3.1 gives, for each genus, the number of continuous complex parameters (*moduli*) parameterising the analytic classes.[1] In the table

[1] Note the difference from diffeomorphic equivalence in the real case. Here we only have one unique diffeomorphy type for each genus since the diffeomorphies are not constrained by the com-

Genus	Moduli	Hyperelliptic moduli
0	0	-
1	1	1
$g > 1$	$3g - 3$	$2g - 1$

Table 3.1: The number of moduli for each genus, both for general Riemann surfaces and hyperelliptic surfaces.

we have included the moduli for the hyperelliptic curves that will be discussed in section 3.4. For $g = 0$ we only have one Riemann surface which is the Riemann sphere, $\mathbb{C} \cup \{\infty\} = \mathbb{P}^1$, and we have no hyperelliptic curves.

3.1.2 Simplicial homology group

For a given Riemann surface we now define the *simplicial homology*. To this end think of a triangulation of the surface. We then define the 0-, 1- and 2-simplices as respectively the vertices, the edges and the faces of the triangulation.[2] Let us denote the set of 0-simplices (i.e. points on the surface) as $\{P_1, \ldots, P_l\}$. Since our surface is orientable we can give our triangles (2-simplices) and edges (1-simplices) an orientation. With this orientation we can write the 1-simplices as $\langle P_i, P_j \rangle$ for the edge from P_i to P_j and similarly the 2-simplices as $\langle P_i, P_j, P_k \rangle$ for the triangle with vertices P_i, P_j and P_k taken in the direction of the orientation. In this notation we can give the simplices a sign for opposite orientation so we identify $\langle P_i, P_j \rangle \equiv -\langle P_j, P_i \rangle$ and $\langle P_i, P_j, P_k \rangle \equiv -\langle P_k, P_j, P_i \rangle$.

Let now C_n define the free abelian group over the n-simplices (i.e. we can freely add and subtract a finite number of n-simplices). The elements of C_n are called n-chains. We can define the boundary operator, δ, by its action on the n-simplices in the following natural way:

$$\delta \langle P \rangle = 0, \qquad \delta \langle P_i, P_j \rangle = P_j - P_i, \tag{3.1}$$

$$\delta \langle P_i, P_j, P_k \rangle = \langle P_i, P_j \rangle + \langle P_j, P_k \rangle + \langle P_k, P_i \rangle, \tag{3.2}$$

where $\delta : C_n \mapsto C_{n-1}$. This allows us to define the *n-cycles*, Z_n, as the closed n-chains i.e. the n-chains $a \in C_n$ for which $\delta a = 0$. Finally, we define the n^{th} *simplicial homology group* as the n-cycles modulo the boundaries $B_n = \delta(C_{n+1})$:

$$H_n = \frac{Z_n}{B_n}, \tag{3.3}$$

which is well-defined since $\delta^2 = 0$.

plex structure.

[2]For higher dimensional complex manifolds we of course need higher n-simplices as well.

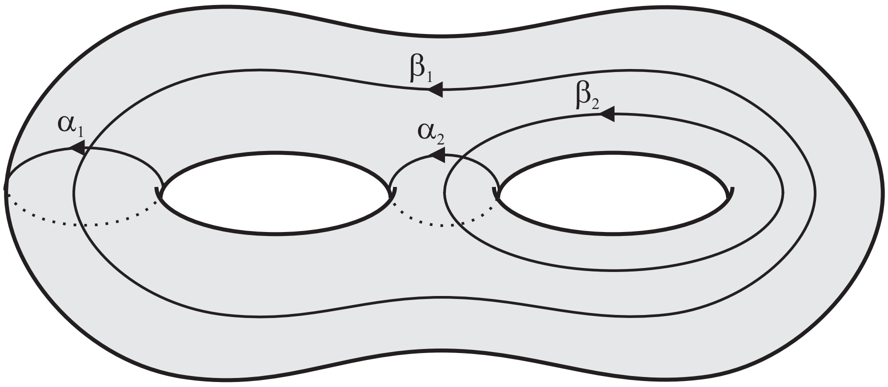

Figure 3.1: The figure shows a canonical homology basis (seen as continuous curves) in the case of a genus-2 torus.

Now it is easy to see that H_0 and H_2 are simply isomorphic to $\mathbb{Z}$ (for a compact surface). However, H_1 is interesting for us. These are, of course, 1-cycles modulo boundaries. The number of generators of this abelian group is called the first Betti number β_1. Actually, the group is independent of the triangulation that we have used, and it is not surprising that it is isomorphic to the abelianisation of the fundamental group (first homotopy group). It turns out that the Betti number is $2g$ where g is the genus of the surface.

3.1.3 Canonical homology basis

We choose to denote the basis for H_1 as $\{\alpha_i, \beta_i\}$ with $i = 1, \dots, g$. The generators can be seen as closed continuous curves by the above mentioned relation to the fundamental group. It is possible to define the *intersection number* which is an antisymmetric bilinear form on H_1 that essentially counts the number of times two 1-cycles intersect each other. We will always choose the generators such that α_i intersects only β_i and this only once (and vice versa), i.e. if the intersection bilinear form is denoted by a dot:

$$\alpha_i \cdot \beta_j = -\beta_j \cdot \alpha_i = \delta_{ij}, \tag{3.4}$$

or in other words: The intersection matrix for the basis is the $2g \times 2g$ symplectic matrix J. Such a basis is then called a *canonical homology basis*. An example can be seen in figure 3.1.

3.2 Analytical Structure

Let us now consider the analytic structure of the Riemann surface. The holomorphic functions are defined, as usual, using the coordinate maps. Likewise we define a meromorphic function as being holomorphic up to a set of isolated points (poles) where it diverges. In the usual way we define the multiplicity of zeroes and poles. Naturally, we can also see the meromorphic functions as holomorphic functions into $\mathbb{P}^1$. One can quickly see that for a compact Riemann surface the only (global) holomorphic functions are the constant ones.

3.2.1 One-forms

Let z denote a local complex coordinate map on our Riemann surface. A one-form, ω, is then defined by locally having the form:

$$\omega = f(z)dz + g(z)d\bar{z}, \tag{3.5}$$

and it should transform covariantly under coordinate transformations. A *holomorphic one-form* has locally the form $f(z)dz$ with $f(z)$ holomorphic on the coordinate patch. Note that since this is defined patchwise, we are not constrained by the fact that we only have constant global holomorphic functions. Instead, the space of (global) holomorphic one-forms, $\mathscr{H}^1$, has dimension g. Given a canonical homology basis $\{\alpha_i, \beta_i\}$ one can find a unique basis, $\{\sigma_1, \ldots, \sigma_g\}$, for $\mathscr{H}^1$ which obeys:

$$\int_{\alpha_j} \sigma_i = \delta_{ij}. \tag{3.6}$$

3.2.2 Period matrix

Thus, given the canonical homology basis, we can uniquely define the period matrix for the surface:

$$\tau_{ij} = \int_{\beta_j} \sigma_i. \tag{3.7}$$

τ is a symmetric $g \times g$ matrix and the imaginary part is positive definite, i.e. it belongs to the Siegel upper half space $\mathscr{H}_g = \{\tau \in \mathrm{Mat}(g) \mid \tau_{ij} = \tau_{ji}, \mathrm{Im}\,\tau > 0\}$. This can be shown by the Riemann bilinear relations, e.g. the symmetry follows from:

$$\sum_{i=1}^{g} \left(\int_{\alpha_i} \omega \int_{\beta_i} \rho - \int_{\alpha_i} \rho \int_{\beta_i} \omega \right) = 0, \tag{3.8}$$

where ω and ρ are holomorphic one-forms. The period matrix will be essential for us.

3.2.3 Modular transformations

With a given canonical homology basis $\{\alpha_i, \beta_i\}$ we found the corresponding unique basis for the holomorphic one-forms $\{\sigma_i\}$. The *full period matrix*, Ω, is a $g \times 2g$ matrix of the form $\Omega = (\mathbf{I}, \tau)$ where the first matrix gives the periods with respect to the α_i cycles, and the second the periods with respect to the β_i cycles. However, suppose that we have chosen another canonical homology basis $\{\alpha'_i, \beta'_i\}$. This basis will be related to the old basis by an invertible linear transformation represented by an invertible matrix, $N \in \mathrm{Sl}(2g, \mathbb{Z})$, with integer entries[3] – in vector notation:

$$\begin{pmatrix} \alpha' \\ \beta' \end{pmatrix} = N \begin{pmatrix} \alpha \\ \beta \end{pmatrix} \equiv \begin{pmatrix} A & B \\ C & D \end{pmatrix} \begin{pmatrix} \alpha \\ \beta \end{pmatrix}, \tag{3.9}$$

where N is split into $g \times g$ matrices as shown. However, for $\{\alpha'_i, \beta'_i\}$ to be a canonical homology basis we must preserve the symplectic intersection matrix J. This exactly means that N is an element in the symplectic group $\mathrm{Sp}(2g, \mathbb{Z})$ (and all elements in this group are possible and generate all canonical homology bases). With respect to the new canonical homology basis the full period matrix, Ω, for the σ_i's is no longer in the standard form:

$$\Omega = (\int_{\alpha'} \sigma, \int_{\beta'} \sigma) = (A^T + \tau B^T, C^T + \tau D^T). \tag{3.10}$$

In order to obtain the period matrix we must change the basis of the holomorphic one-forms, $\{\sigma_i\}$, to $\{\sigma'_i\}$ that turns the first part of the full period matrix into the identity, i.e. $\sigma' = (A^T + \tau B^T)^{-1}\sigma$ and then we see that the new period matrix becomes:

$$\tau' = (C + D\tau)(A + B\tau)^{-1}, \qquad \begin{pmatrix} A & B \\ C & D \end{pmatrix} \in \mathrm{Sp}(2g, \mathbb{Z}). \tag{3.11}$$

Thus a change in the canonical homology basis just gives a transformation of the period matrix by the symplectic modular group. This is the same transformation that we found for the monodromy on the vacuum moduli space (2.21).

3.2.4 Meromorphic one-forms

Also important for us is the existence of *meromorphic one-forms*. These are just one-forms which are holomorphic except at finitely many points $\{P_1, \ldots, P_k\}$, and such that locally the coordinate function is meromorphic. This means that for z a local coordinate around a point P with $z(P) = 0$, the meromorphic one-form, ω, takes the form $f(z)dz$ where $f(z)$ has the Laurent expansion $f(z) = \sum_{i=m}^{\infty} f_i z^i$ with

[3] The determinant is ± 1 since the inverse matrix (with inverse determinant) must also have integer entries (and thus integer determinant).

$m \in \mathbb{Z}$ and $f_m \neq 0$. Invariant of the chosen coordinate we can then define the order and the residue of ω at P as:

$$\operatorname{ord}_P \omega = m, \qquad \operatorname{res}_P \omega = f_{-1}. \tag{3.12}$$

Integrating around all the 2-simplices in an triangulation of a compact Riemann surface immediately gives:

Theorem. *If ω is a meromorphic one-form on a compact Riemann surface, Σ, then:*

$$\sum_{P \in \Sigma} \operatorname{res}_P \omega = 0. \tag{3.13}$$

Now, there exist meromorphic one-forms with just a single pole. These must have residue zero by this theorem and hence the pole must be of order higher than one: $\operatorname{ord}_{P_i} \omega < -1$ (meromorphic one-forms with zero residues are called abelian differentials of the second kind). It turns out that there also exist meromorphic one-forms with non-zero residues and by the theorem they must have two or more poles (they are called abelian differentials of the third kind).[4] To obtain some uniqueness let us consider meromorphic one-forms with only simple poles ($\operatorname{ord}_{P_i} \omega = -1$). However, we still have the possibility to add an arbitrary holomorphic one-form. But we can fix this redundancy by determining the α-periods of ω in the canonical homology basis – since determining these periods of a holomorphic one-form uniquely determines its coefficients in the basis for the holomorphic one-forms (3.6). This gives rise to the following existence and uniqueness theorem for a compact Riemann surface Σ:

Theorem. *Let $\{P_1, \ldots, P_n\}$ be a set of distinct points in Σ with $n \geq 2$. Let $r_1, \ldots, r_n \in \mathbb{C} \setminus \{0\}$ be given such that $\sum_i r_i = 0$ and let also $a_1, \ldots, a_g \in \mathbb{C}$ be given. Then there exists a unique meromorphic one-form, ω, which is holomorphic on $\Sigma \setminus \{P_1, \ldots, P_n\}$, has simple poles in $P_1, \ldots, P_n$, and fulfills:*

$$\operatorname{res}_{P_i} \omega = r_i, \qquad \int_{\alpha_i} \omega = a_i. \tag{3.14}$$

In the last equation we think of α_is as specific curves, not homology classes, since meromorphic one-forms integrated over homology classes are only defined modulo $2\pi i r_1 \mathbb{Z} + \ldots + 2\pi i r_n \mathbb{Z}$. This is because the α_is otherwise are equivalence classes modulo boundaries that can encircle the poles, thus giving an integral linear combination of ($2\pi i$ times) the residues. This would spoil the uniqueness.

Especially we see that given to distinct point P and Q we have a unique meromorphic one-form ω_{PQ} with simple poles at P and Q, and residues $+1$ and -1 respectively, and zero α-periods. Any meromorphic one-form in the theorem can then

[4] Abelian differentials of the first kind are just the holomorphic differentials.

be written using these meromorphic one-forms and the holomorphic one-forms, σ_i. A useful formula is (can be proven using the Riemann bilinear relations):

$$\int_{\beta_i} \omega_{PQ} = 2\pi i \int_Q^P \sigma_i. \tag{3.15}$$

3.2.5 Divisors

The last concept we will introduce in this subsection is *divisors*. The group of divisors on our Riemann surface Σ, $\mathrm{Div}(\Sigma)$, is simply the free abelian group generated by the points of Σ. Thus a divisor can be written as:[5]

$$D = \sum_{P \in \Sigma} n(P) P, \tag{3.16}$$

where the sum is over all points P on Σ and $n(P) \in \mathbb{Z}$, but where there are only finitely many points P with $n(P)$ non-zero. Given two divisors $D = \sum n(P)P$ and $D' = \sum m(P)P$ we define $D \geq D'$ if and only if $n(P) \geq m(P)$ for all points P.

An important example of divisors are the *principal divisors*: Given a meromorphic function $f \neq 0$ the corresponding principal divisor (f) is given by

$$(f) = \sum_{P \in \Sigma} \mathrm{ord}_P f \, P, \tag{3.17}$$

where $\mathrm{ord}_P f$ depends on whether there is a pole or a zero or neither in P: It is the multiplicity of a zero in P, minus the multiplicity of a pole, and zero if there is neither a zero nor a pole. If f is identically zero the order is infinity. We can also define the divisors of zeroes (respectively the polar divisor) where we simply set all negative (positive) orders to zero in (3.17). Note that under $f \mapsto (f)$ multiplication is mapped into addition. We can now define two divisors to be linearly equivalent if their difference is a principal divisor. Letting $\mathscr{K}(\Sigma)$ denote the field of meromorphic functions on Σ, we can also define a vector space, $L(D)$, corresponding to a general divisor D as:[6]

$$L(D) = \{f \in \mathscr{K}(\Sigma) \mid (f) \geq D\}. \tag{3.18}$$

The corresponding dimension of the vector space is denoted $r(D)$.

We also define the degree of a divisor, $D = \sum_i n_i P_i$, as:

$$\deg D = \sum_i n_i, \tag{3.19}$$

which is a homomorphism, $\deg : \mathrm{Div}(\Sigma) \to \mathbb{Z}$. A subgroup is the divisors of degree 0, $\mathrm{Div}^0(\Sigma)$, and a further subgroup hereof is the group of principal divisors. This is

[5] Sometimes this is written in factor-notation where the $n(P)$s are then the powers of the Ps.

[6] Here we have chosen to follow the notation of [127], however, it is common in the literature to have a minus on the D in this definition.

because any meromorphic function must have the same number of zeroes and poles counted with multiplicity, as can be seen from (3.13) used on $d\log f$. Using this, we can define the Picard group, $\mathrm{Pic}(\Sigma)$, as the quotient of the divisors by the principal divisors, and the restricted Picard group, $\mathrm{Pic}^0(\Sigma)$, as the quotient of $\mathrm{Div}^0(\Sigma)$ by the principal divisors.

Consider an abelian differential, i.e. a holomorphic or meromorphic one-form, ω. We can then define the corresponding *canonical* divisor, (ω), exactly as in (3.17) using (3.12). Since the quotient of two abelian differentials is a meromorphic function, all canonical divisors are linearly equivalent.

Given a divisor D we define the index of speciality $i(D)$ as the dimension of the vector space

$$\Omega(D) = \{\omega \mid \omega \text{ is an abelian differential with } (\omega) \geq D\}. \tag{3.20}$$

Both $r(D)$ and $i(D)$ only depend on the linear equivalence class. And one can show that for $\omega \neq 0$ any abelian differential we have $i(D) = r(D - (\omega))$. We can now state the very useful Riemann-Roch theorem.

Theorem (Riemann-Roch). *For D an integral divisor (i.e. $\deg D \geq 0$) on the compact genus g Riemann surface Σ we have*

$$r(-D) = \deg D - g + 1 + i(D), \tag{3.21}$$

where $r(-D)$ is dimension of the space $L(-D)$ defined by (3.18) *and $i(D)$ is the dimension of the space in* (3.20).

The divisors gives a way to compactly write and prove theorems for Riemann surfaces. But let us now continue on to introduce the concept of Jacobians.

3.3 Jacobians

In this and the following sections we will only consider Riemann surfaces, Σ, with genus $g > 0$. The reason is that we then have a non-trivial canonical homology basis $\{\alpha_i, \beta_i\}$ and corresponding basis of holomorphic one-forms $\{\sigma_i\}$. This allows us to define the Jacobian, $Jac(\Sigma)$, which has many advantages e.g. it is easier to obtain the moduli space, and we will see that using the Jacobian we can construct explicit functions and differentials on the surface.

To define the Jacobian remember that we have the full period matrix $\Omega = (\mathbf{I}, \tau)$. Let then L be the lattice over $\mathbb{Z}$ generated by the columns of Ω, i.e. $L = \mathbf{I}\cdot\mathbb{Z}^g \oplus \tau\cdot\mathbb{Z}^g$. The columns are linearly independent over $\mathbb{R}$ since $\mathrm{Im}\,\tau > 0$. The Jacobian is then simply:

$$Jac(\Sigma) = \frac{\mathbb{C}^g}{L}, \tag{3.22}$$

along with the symplectic intersection matrix J from above. This pair makes up a so called *principally polarised torus*.

The point is that we have Torelli's theorem which states that two Riemann surfaces are equivalent if and only if their Jacobians are equivalent. Here we, of course, have to remember the modular transformations which preserves the symplectic intersection matrix.

3.3.1 Abel-Jacobi map

We can embed the Riemann surface Σ in the Jacobian using the Abel-Jacobi map:

$$P \in \Sigma \mapsto \vec{z}(P) \in Jac(\Sigma), \qquad z_i(P) = \int_{Q_0}^{P} \sigma_i. \tag{3.23}$$

Here Q_0 is just some arbitrary base-point. Choosing another base-point will just give an overall translation of the embedding. In principle, the integrals are not well-defined since they depend on the chosen path. However, other choices of paths will only give a change which is in the lattice L. This means that we have a well-defined embedding (as it can be proven to be) of our surface into the Jacobian. We will, however, also think of the map as being into $\mathbb{C}^g$, but we will then specify how to choose the path.

Actually, using the divisors introduced in the last section we can expand on this in the following way: Consider a divisor of degree zero, i.e. $D \in \mathrm{Div}^0$. This we can split as $D = A - B$ where $A = \sum_{i=1}^n p_i$ and $B = \sum_{i=1}^n q_i$ are both integral divisors (there can be repetitions in the p_is and q_is). We can then define the Abel-Jacobi map on the divisors of degree zero similarly:

$$D \in \mathrm{Div}^0(\Sigma) \mapsto \vec{z}(D) \in Jac(\Sigma), \qquad z_i(D) = \sum_{j=1}^{n} \int_{q_j}^{p_j} \sigma_i. \tag{3.24}$$

Abel's theorem tells us that the kernel of the above map exactly is the principal divisors. The Jacobi inversion problem states that the map is surjective, or, in other words, the Jacobian is isomorphic to the restricted Picard group, $Jac(\Sigma) \cong \mathrm{Pic}^0(\Sigma)$.

In general, we define the Abel-Jacobi map on an integral divisor $D = \sum_i P_i$ as $\vec{z}(D) = \sum_i \vec{z}(P_i)$. Actually, what Jacobi's inversion problem tells is that the map from the integral divisors of degree g, Σ_g, is surjective. A special example is the genus one case where the Riemann surface and the Jacobian actually are isomorphic. This means that the genus one case is very special. In this case we also directly see that the number of independent components in the period matrix is the same as the number of moduli. In general, we have the Schottky problem of determining which matrices in the Siegel upper half plane actually correspond to Riemann surfaces, and further we can ask which correspond to hyperelliptic surfaces, which is of special interest to us. We will introduce these in the next section.

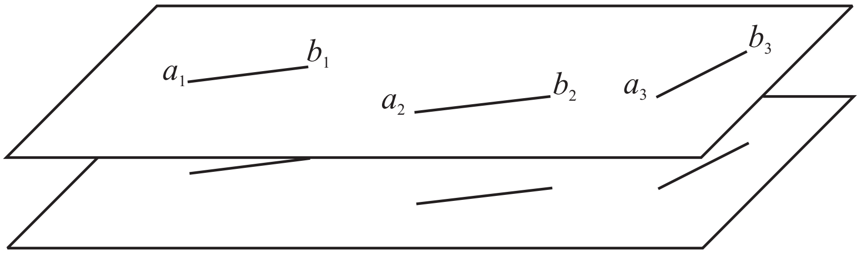

Figure 3.2: The figure shows the two sheets of the hyperelliptic curve. For each sheet one should think of adding points at infinity to obtain a compact surface.

3.4 Hyperelliptic Surfaces

We define a hyperelliptic surfaces by a set (y, x) where

$$y^2 = \prod_{i=1}^{2g+2} (x + x_i). \tag{3.25}$$

Letting x take values on $\mathbb{C}$, or rather the compact Riemann sphere $\mathbb{P}^1$, y is a multi-valued function. To make it single-valued we need to consider a two-sheeted covering space (two copies of the Riemann sphere) and we split the x_is into $g+1$ pairs $\{a_i, b_i\}$ which we connect by cuts connecting the two sheets; north bank to south bank, see figure 3.1. As should be obvious this makes up a genus g Riemann surface.

Denoting a point on the hyperelliptic curve by P we see that $x(P)$ is a meromorphic function on the curve with exactly two poles and $2g + 2$ branch points P_i with $x(P_i) = x_i$. Actually, an alternative description of a hyperelliptic curve is that it is a Riemann surface on which there exists an integral divisor D of degree 2 with $r(-D) \geq 2$. This is turn is exactly equivalent to existence of a meromorphic function with precisely two poles (i.e. it is 2-1) for which all ramification points must have branch number one (and thus we have $2g+2$ branch points by Riemann-Hurwitz). One can show that this must be x – or a Möbius transformation thereof, thus returning to the above definition. Let us also note that some only use the term hyperelliptic if the genus is greater than one. In all cases we will take $g \geq 1$. It turns out that all Riemann surfaces of genus one and two are hyperelliptic.

The uniqueness of x up to Möbius transformations is a reflection of the fact that the automorphism group of $\mathbb{P}^1$ is $\mathrm{PGL}(2, \mathbb{C})$ which exactly gives the Möbius transformations:

$$x \mapsto \frac{ax+b}{cx+d}. \tag{3.26}$$

This means that we have the freedom to choose another x with three of the branch points determined e.g. set to 0, 1 and ∞. We thus see that the number of moduli

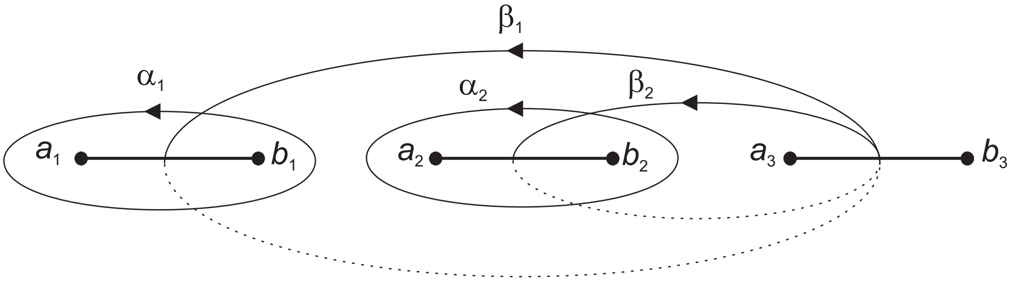

Figure 3.3: The figure shows the cycles and cuts for a hyperelliptic curve of genus 2. A dotted line means that the curve is on the lower sheet. Note that α_i and β_i only intersect once.

for a genus g hyperelliptic curve is $2g + 2 - 3 = 2g - 1$ as was shown in table 3.1.

We should here note that the Seiberg-Witten curves were exactly of this form see e.g. equation (2.25). Also remember that the PGL$(2, \mathbb{C})$ automorphism group is not directly a symmetry group on the physical side since each branch point is determined by the parameters of the vacuum moduli space u_k. This will be investigated in section 4.1.7.

Another characteristic of a hyperelliptic surface is the existence of the hyperelliptic involution. Actually, a surface is hyperelliptic if and only if there exists an involution in the group of automorphisms that fixes $2g+2$ points. In terms of (y, x) this is immediately seen as $(y, x) \mapsto (-y, x)$, i.e. it swaps the sheets.

3.4.1 Homology basis and holomorphic one-forms

On a hyperelliptic surface we can explicitly construct a canonical homology basis as shown in figure 3.3. Here the α_is encircle g of the cuts on the upper sheet. Often we will also define α_{g+1} as the curve encircling the last cut. The β_i-cycles goes between two cuts on the upper sheet and then closes on the lower sheet.

Consider now a point $\vec{z} \in Jac(\Sigma)$. This is defined to be of order n if $n\vec{z} \equiv 0$. Using the above canonical homology basis we can easily show that all branch points are of order two on a hyperelliptic surface, if we choose the base point Q_0 as one of the branch points. For a general surface we see that if $\vec{z}$ has order n then there exists a meromorphic function f with $(f) = nP - nQ_0$. Or, considering $d \log f$, there exists a meromorphic one-form with integer periods and simple poles in P and Q_0 with residues n and $-n$ respectively. This is seen directly using Abel's theorem.

We can also construct the holomorphic one-forms on a hyperelliptic surface exactly. A non-canonical basis (i.e. $\oint_{\alpha_i} \sigma_j$ is not necessarily δ_{ij}) is simply

$$\frac{x^r}{y} dx, \quad r = 0, \ldots, g-1. \tag{3.27}$$

Using this we can explicitly write the period matrix in terms of the branch points. The reverse is actually also true: The branch points can be written as a holomorphic function of the period matrix. This can be done using the theta functions that we will now introduce. Importantly, these will also allow us to construct x as a function defined on the Jacobian in the next chapter.

3.5 Theta Functions

In this section we will introduce the theta functions that allows us to write meromorphic functions and one-forms on Riemann surfaces explicitly.

Riemann's theta function, θ, is a holomorphic function $\theta : \mathbb{C}^g \times \mathscr{H}_g \mapsto \mathbb{C}$. Let $z \in \mathbb{C}^g$ and $\tau \in \mathscr{H}_g$ be a general matrix, not necessarily a period matrix, in the Siegel upper half space. Then the theta function is defined as:

$$\theta(z, \tau) = \sum_{n \in \mathbb{Z}^g} \exp 2\pi i \left(\frac{1}{2} n^T \tau n + n \cdot z \right). \tag{3.28}$$

As we saw above, we are interested in Jacobian varieties defined as $\mathbb{C}^g/L$ where $L = \mathbf{I} \cdot \mathbb{Z}^g \oplus \tau \cdot \mathbb{Z}^g$ as above, but now for a general matrix in the Siegel upper half space. However, as on Riemann surfaces, the only holomorphic functions on a Jacobian variety are the constant ones. Thus we can not expect the theta function to periodic in L, but rather it turns out to be quasi-periodic, i.e. multiplicative:

$$\theta(z + n, \tau) = \theta(z, \tau), \quad n \in \mathbb{Z}^g \tag{3.29}$$

$$\theta(z + \tau n, \tau) = e^{2\pi i(-\frac{1}{2} n^T \tau n - n \cdot z)} \theta(z, \tau), \quad n \in \mathbb{Z}^g. \tag{3.30}$$

Further, we should also note that the theta function is even in z: $\theta(-z, \tau) = \theta(z, \tau)$.

3.5.1 First order theta functions

Given a point $z \in \mathbb{C}^g$ it can be written uniquely in terms of its *characteristic* $\begin{bmatrix} \varepsilon \\ \varepsilon' \end{bmatrix}$ with $\varepsilon, \varepsilon' \in \mathbb{R}^g$ as $z = \mathbf{I}\varepsilon' + \tau\varepsilon$ (note the reversal of ε and ε'). We then define the first order theta functions with characteristic $\begin{bmatrix} 2\varepsilon \\ 2\varepsilon' \end{bmatrix}$ as:[7]

$$\theta \begin{bmatrix} 2\varepsilon \\ 2\varepsilon' \end{bmatrix} (z, \tau) = e^{2\pi i(\frac{1}{2}\varepsilon^T \tau \varepsilon + \varepsilon \cdot z + \varepsilon \cdot \varepsilon')} \theta(z + \mathbf{I}\varepsilon' + \tau\varepsilon, \tau). \tag{3.31}$$

[7] Some authors do not include the factors of 2 on the left hand side of this definition.

The multipliers under the periods are then:

$$\theta\begin{bmatrix}2\varepsilon\\2\varepsilon'\end{bmatrix}(z+e^{(k)},\tau)=e^{2\pi i\varepsilon_k}\,\theta\begin{bmatrix}2\varepsilon\\2\varepsilon'\end{bmatrix}(z,\tau) \tag{3.32}$$

$$\theta\begin{bmatrix}2\varepsilon\\2\varepsilon'\end{bmatrix}(z+\tau^{(k)},\tau)=e^{2\pi i(-z_k-\frac{1}{2}\tau_{kk}-\varepsilon'_k)}\,\theta\begin{bmatrix}2\varepsilon\\2\varepsilon'\end{bmatrix}(z,\tau), \tag{3.33}$$

where $e^{(k)}$ ($\tau^{(k)}$) is the kth column vector of the identity matrix (τ-matrix). For $\varepsilon=\varepsilon'=0$ we see that we simply get the ordinary theta function:

$$\theta\begin{bmatrix}0\\0\end{bmatrix}(z,\tau)=\theta(z,\tau). \tag{3.34}$$

It is especially the case with integer characteristic that are of interest. In this case we e.g. get

$$\theta\begin{bmatrix}\varepsilon\\\varepsilon'\end{bmatrix}(-z,\tau)=e^{\pi i\varepsilon\cdot\varepsilon'}\,\theta\begin{bmatrix}\varepsilon\\\varepsilon'\end{bmatrix}(z,\tau),\quad \text{for } \varepsilon,\varepsilon'\in\mathbb{Z}^g. \tag{3.35}$$

We thus see that a first order theta function with integer characteristic is even (odd) if $\varepsilon\cdot\varepsilon'$ is even (odd). For integer characteristic we essentially only have choices of 0 or 1 since addition of 2 to one of the ε_ks or ε'_ks gives us the same function up to a scalar factor. Thus we got one theta function for each half period in $\mathbb{C}^g/L$ (remember the factor 2 in the definition (3.31)). E.g. for the elliptic case we get the well-known Jacobi theta functions:

$$\theta_1(z,\tau)\equiv\theta\begin{bmatrix}1\\1\end{bmatrix}(z,\tau),\quad \theta_2(z,\tau)\equiv\theta\begin{bmatrix}1\\0\end{bmatrix}(z,\tau), \tag{3.36}$$

$$\theta_3(z,\tau)\equiv\theta\begin{bmatrix}0\\0\end{bmatrix}(z,\tau),\quad \theta_4(z,\tau)\equiv\theta\begin{bmatrix}0\\1\end{bmatrix}(z,\tau). \tag{3.37}$$

3.5.2 Theta functions on a Riemann surface

Since we are interested in Riemann surfaces, the idea is to consider theta functions on the corresponding Jacobian, $Jac(\Sigma)$ (section 3.3 above). The theta function can then be seen as a multiplicative holomorphic function on the surface using the Abel-Jacobi map which we denote $\varphi:\Sigma\mapsto Jac(\Sigma)$ or rather $\varphi:\Sigma\mapsto\mathbb{C}^g$, i.e. we will consider $\theta\circ\varphi:\Sigma\mapsto\mathbb{C}$. The multipliers are given above in equations (3.29) and (3.30). Even though this function is not single-valued, but multiplicative, its divisor (its zeroes) is well-defined, and likewise it zeroes on the whole Jacobian $Jac(M)$ are well-defined.

In general, we consider $\theta\begin{bmatrix}\varepsilon\\\varepsilon'\end{bmatrix}\circ\varphi$ or $\theta(\varphi(P)-e)$ where $e\in\mathbb{C}^g$. It turns out that the zeroes of the theta functions on $\mathbb{C}^g$ is a codimension one analytic set so these functions on the compact Riemann surface are either identically zero or have a finite number of zeroes, and the number can be shown to be precisely g – the genus of the surface. In the case that $\theta\begin{bmatrix}\varepsilon\\ \varepsilon'\end{bmatrix}\circ\varphi$ does not vanish identically, we can find the image of the divisor of zeroes $P_1+\ldots+P_g$ under the Abel-Jacobi map:

$$\varphi(P_1+\ldots+P_g) = -\tfrac{1}{2}\mathbf{I}\varepsilon' - \tfrac{1}{2}\tau\varepsilon - K, \tag{3.38}$$

where K is called the vector of Riemann constants and only depends on the choice of canonical homology basis and the base point of the Abel-Jacobi map. For $\theta(\varphi(P)-e)$ we then get $\varphi(P_1+\ldots+P_g) = -K+e$.

Actually, a stronger version of the theorem can be obtained. Consider the function $\theta(\varphi(P)-e)$; if D is an integral divisor of degree g fulfilling $\varphi(D) = -K+e$ then the function does not vanish identically on the surface if and only if $i(D)=0$. In that case D is the divisor of zeroes.

Again the case of hyperelliptic surfaces is special and we can actually choose the base point such that K is a half period, and further we can determine K exactly.

In the elliptic case the Jacobian was isomorphic to the Riemann surface and in accordance with the above mentioned facts, the theta function has precisely one zero (of multiplicity one)

$$\theta\left(\frac{1+\tau}{2},\tau\right) = 0. \tag{3.39}$$

In the next chapter we will use the theta functions to create the meromorphic functions and one-forms that we need in order to solve the factorization problem of the hyperelliptic Seiberg-Witten curves.

Chapter 4

Solution of the Factorization Problem

The aim in this chapter is to give a correspondence between the solutions of the factorisation problem of Seiberg-Witten curves and hyperelliptic period matrices satisfying certain constraints. Further, we will actually solve the problem in the genus one case including fundamental matter [3], and make some investigations on the implications for the vacuum structure of the $\mathcal{N} = 1$ vacua.

4.1 Factorization – General Genus

We consider the factorization of the Seiberg-Witten curve with fundamental matter (2.48) where the curve reduces to a genus g curve y_{red}

$$y^2 = P_{N_c}(x, u_k^{(fact)})^2 - 4\Lambda^{2N_c - N_f} \prod_{i=1}^{N_f} (x + m_i) = \underbrace{F_{2g+2}(x)}_{y_{red}^2} H_{N_c-1-g}(x)^2. \tag{4.1}$$

This corresponds to having $N_c - 1 - g$ mutually local massless monopoles and in the $\mathcal{N} = 1$ case the gauge group breaks into $g+1$ factors $U(N_c) \mapsto \prod_{i=1}^{g+1} U(N_i)$ as was explained in detail in section 2.3.

The factorization problem without fundamental matter in the genus zero case (complete factorization) was first solved back in 1995 by Douglas and Shenker [65] using Chebyshev polynomials. With fundamental matter the genus zero factorization problem was first solved by Demasure and Janik [68] using random matrices. We will study the complete factorization case below in section 4.4.

4.1.1 The one-form ω

The genus one factorization problem without fundamental matter was solved by Janik in [66], and with fundamental matter it was solved in [3]. The solution and its implications will be presented in section 4.5 below. The idea is here to consider the meromorphic one-form

$$\omega \equiv T(x)dx \equiv \langle \mathrm{Tr}\, \frac{dx}{x-\Phi} \rangle, \tag{4.2}$$

which was studied in details in [48, 77]. In this section we will extend the analysis of [3, 66] to general genus and show that the factorization problem is equivalent to certain constraint equations on hyperelliptic period matrices.

Note that ω is a very useful one-form since we immediately see that it determines the parameters of the vacuum moduli space:

$$u_k = \frac{1}{k}\langle \mathrm{Tr}\, \Phi^k \rangle = -\frac{1}{k}\, \mathrm{res}_{x=\infty}\; x^k \omega. \tag{4.3}$$

This equation is, actually, true for all k not just for the parameters of the vacuum moduli space where $k = 1, \ldots, N_c$. The minus sign on the right hand side is due to

$$\mathrm{res}_{x=\infty}\, \frac{1}{x} dx = -1, \tag{4.4}$$

which follows from going to a local coordinate $z = 1/x$ or remembering that the sum of the residues should be zero.

In the classical limit, $\Lambda \to 0$, Φ has $g+1$ *different* eigenvalues $\phi_1, \ldots, \phi_{g+1}$, which are the zeroes of W'_{tree}, corresponding to the breaking $U(N_c) \mapsto \prod_{i=1}^{g+1} U(N_i)$. From the definition of ω (4.2) we see that it classically has simple poles in the ϕ_is with residues $N_i \in \mathbb{N}$:

$$\omega_{cl.} = \sum_{i=1}^{g+1} \frac{N_i}{x-\phi_i} dx. \tag{4.5}$$

In the quantum case, when Λ is finite, each of these eigenvalues opens up to a cut as we see from the Seiberg-Witten curve in (4.1).[1] The cuts mean that we have two sheets. The first (upper) sheet is the one we see in the classical limit while the second (lower) is invisible classically. Quantum mechanically it is therefore natural to see ω as a meromorphic one-form on the Seiberg-Witten curve. Defining the homology basis as in figure 3.3 we see that the α-cycles encircle the cuts. We think of the cuts as replacing the poles ϕ_i and hence the α-periods are:

$$\frac{1}{2\pi i} \oint_{\alpha_i} \omega = N_i, \quad i = 1, \ldots, g, \tag{4.6}$$

[1] Generically, we get one cut for each of the N_c eigenvalues. But we here consider the factorization case (4.1) where we keep the number of double roots constant.

where we could also include α_{g+1}, the cycle encircling the $(g+1)$st cut and which is not part of the homology basis. We expect ω to be regular on the rest of the first sheet (since the poles became the cuts), except at infinity where it by (4.2) must have a simple pole with residue $-N_c$. In reference [77] the chiral ring relations were further used to obtain the exact form of ω on the hyperelliptic surface. As an example one of the other one-forms that we can define is

$$R(x)dx = -\frac{1}{32\pi^2}\,\mathrm{Tr}\,\frac{\mathcal{W}_\alpha \mathcal{W}^\alpha}{x-\Phi}dx, \tag{4.7}$$

which we also met in (2.53) (with a minor redefinition) and it turns out to be $\frac{1}{2}(W'_{tree} - y)dx$. Thus the chiral ring relations give us expressions for ω in terms of x and y and hence on the whole Seiberg-Witten curve. The result is that ω only contains simple poles on the second sheet. These are located at the zeroes of $B(x) = \prod_{i=1}^{N_f}(x+m_i)$ from (2.4) i.e. at the N_f points $-m_i$, but on the lower sheet. Let us generally denote the hyperelliptic involution by tilde such that $\tilde{x}$ is the point on the lower sheet below x with $y(\tilde{x}) = -y(x)$. Also, let us denote the zeroes of $B(x)$ by $x_i = -m_i$ i.e. ω has poles in $\tilde{x}_i$. It further turns out that the residue of these poles are one. Finally, we have a pole in the infinity on the lower sheet with residue $N_c - N_f$.

4.1.2 Higgs branch roots

These poles at $\tilde{x}_i$ might be surprising at first sight since they are on the lower sheet, which is invisible classically. But they make good sense as we will now see [77]. Actually, when solving the chiral ring relations one chooses that ω is regular on the first sheet (except at the cuts). However, there is a possibility to choose to have simple poles in $x_i = -m_i$ on the upper sheet with residues one. The point is that when we consider the root of the Higgs branch, then ω classically has the form

$$\omega_{cl.} = \sum_{i=1}^{g+1} \frac{N_i}{x-\phi_i}dx + \sum_{i=1}^{N_f} \frac{r_i}{x+m_i}dx, \tag{4.8}$$

where $r_i \in \{0,1\}$ are the integers labelling the Higgs branch. Remember from section 2.1 that on the Higgs branch root some of the eigenvalues (exactly $\sum r_i$ of them such that $\sum N_i + \sum r_i = N_c$) have to be equal to $-m_i$. The solutions allowed by the chiral ring relations are exactly solutions where ω in the quantum case has poles in x_i with residues r_i (these residues are not changed quantum mechanically since they count a number of eigenvalues of Φ). Now, take a solution in the non-Higgs case where ω has a pole at $\tilde{x}_i$. Then change $B(x)$ continuously such that $\tilde{x}_i$ is moved to the jth cut, up through the cut, and all the way to x_i on the first sheet. ω then has a pole in x_i with residue one (and no pole at $\tilde{x}_i$). The only discontinuity that we encounter in this process is when the pole crosses α_j (and maybe the β_ks). This will change $N_j \mapsto N_j - 1$ and thus we precisely end up in the Higgs branch root with $r_i = 1$. Here we have not taken into consideration that the Seiberg-Witten curve changes with $B(z)$ and when we, by several applications of this procedure, take $N_j \mapsto 0$ the cut ought to close. Please note that here and henceforth we assume that the α-cycles do not encircle any of the points x_i.

4.1.3 Expression for ω

The meromorphic one-form ω reduces to a one-form on the reduced curve y_{red}. We can think of the double roots as having N_is that have been set to zero. This also means that ω does not have any poles at those points and thus reduces to a one-form with the above described poles and residues. Further the α-periods are integral, and since these mix with the β-periods under the modular transformations arising from the changes of the homology basis, we might guess that the β-periods are also integral. Indeed it was shown in [77] (see also [63, 64]) using the field equations for the effective superpotential that this is indeed the case (actually two long proofs are given).

Since ω has integral periods it can be written as a logarithmic derivative of a meromorphic function. To get the right poles and residues we see that ω must take the form:

$$\omega = d\log(P_{N_c}(x) + y(x)) = \left(\frac{P'_{N_c}(x)}{y(x)} + \frac{B'(x)}{2B(x)} - \frac{P_{N_c}(x)B'(x)}{2y(x)B(x)} \right) dx, \tag{4.9}$$

again with $B(x) = \prod_{i=1}^{N_f}(x+m_i)$ and $B = 1$ in the flavourless case, and we have used the definition of the Seiberg-Witten curve (4.1) to write out the expression for ω. Actually, (4.9) does not tell us the values of the periods only that they are integral. We might worry if the α-periods are indeed N_i. Once we know this (4.9) must describe ω since a meromorphic one-form is given uniquely by its poles, residues and α-periods, see theorem at equation (3.14). However, the difference between ω and the expression (4.9) must be a holomorphic one-form with integral periods which must be zero. This is because it would have the form $\sum_i l_i \sigma_i$ with l_i being the α-periods and σ the basis of one-forms dual to the homology basis. The β-periods l'_i must fulfill $l'_i = \sum_j l_j \tau_{ji}$. But this is in contradiction with $\operatorname{Im}\tau > 0$ and thus the l_is must be zero.

Using (4.9) and the form of y in (4.1) we also see that not only can we retrieve the u_ks from ω, but also Λ [77, 3]:

$$\int_{\widetilde{\Lambda}_0}^{\Lambda_0} \omega = -\log(\Lambda^{2N_c - N_f}) + \log(\Lambda_0^{2N_c-N_f}) + \mathcal{O}\left(\frac{1}{\Lambda_0}\right), \tag{4.10}$$

where Λ_0 is seen as a large cut-off for the integration from infinity on the lower sheet, $\widetilde{\infty}$, to infinity on the upper sheet, ∞. $\widetilde{\Lambda}_0$ is then the point corresponding to Λ_0 on the lower sheet.

4.1.4 The case $N_f = 2N_c$

The case where $N_f = 2N_c$ is special since the Seiberg-Witten curve has a different form (2.37). This especially means that if the highest degree coefficient in y^2 is 1 then this can not be true for P_{N_c} as we usually have. Let $P_{N_c}(x) \sim cx^{N_c}$. Then by (2.37) $c - h(h+2) = 1$. We still have (4.9), but this means that (4.10) becomes

$$\int_{\widetilde{\Lambda_0}}^{\Lambda_0} \omega = \log\left(\frac{c+1}{c-1}\right) + \mathcal{O}\left(\frac{1}{\Lambda_0}\right), \tag{4.11}$$

So in this case the integral is finite, but again determines the factor in front of $B(x)$ in the Seiberg-Witten curve.

4.1.5 Factorization and integral periods

In appendix A (which is a revised version of appendix A in [3]) we actually show that a genus g surface corresponds to the reduced curve of a factorized Seiberg-Witten curve if and only if there exist a meromorphic one-form with simple poles in ∞ (with residue $-N_c$), infinity at the lower sheet $\widetilde{\infty}$ (residue $N_c - N_f$) and minus the mass-points on the lower sheets $\tilde{x}_i$ (residues 1), and with integral periods (and fulfills (4.10)). This one-form is exactly (4.9) and, as shown in the appendix, it reduces to a one-form on the reduced surface y_{red} with the above mentioned poles since $y = y_{red} H_{N_c-1-g}(x)$ and the zeroes of $H_{N_c-1-g}(x)$ cancel with zeroes in the numerator. Given such a Riemann surface and one-form with some α-periods N_i, the one-form has to be the ω from (4.2) (uniqueness of meromorphic one-forms with given poles and residues) with these N_i as we see e.g. by going to the classical limit $\Lambda \mapsto 0$ (which does not change the integers N_i) where (4.9) reduces to the classical form for ω. This gives another proof that ω has integral periods.

In the appendix it is also shown that:

$$P_{N_c}(x) = 2\Lambda^{\frac{2N_c - N_f}{2}} \sqrt{B(a)} \left(\frac{1}{2} e^{\int_a^x \omega} + \frac{1}{2} \frac{B(x)}{B(a)} e^{-\int_a^x \omega} \right), \tag{4.12}$$

where a is a branch point. Here the integral periods of ω are essential since the integrals of ω are only well-defined up to the periods. Similarly, we can get y from ω as in equation (A.23).

4.1.6 Quantum corrected Newton relation

Using (4.12) we can also show the relationship between P_{N_c} and the u_ks. Equation (4.3) allows us to write

$$\omega = \frac{N_c}{x}dx + \sum_{k=1}^{\infty} k\frac{u_k}{x^{k+1}}dx. \tag{4.13}$$

Using (2.28) we see that

$$\langle \det(x\mathbf{I} - \Phi)\rangle = \left[x^{N_c}\exp\left(-\sum_{n=1}^{\infty}\frac{u_n}{x^n}\right)\right]_+ = \frac{P_{N_c}(a)}{2}\left[\exp\left(\int_a^x \omega\right)\right]_+, \tag{4.14}$$

where the index + means taking the polynomial part. The constant of proportionality in the last equation have been found using (4.9) and taking $x \to \infty$. We thus see that the relation between the coefficients of P_{N_c}, which in the classical limit simply is given by the Newton relation $P_{N_c}(x) = \det(x\mathbf{I} - \Phi)$, is changed quantum mechanically by (4.12) into

$$P_{N_c}(x, u_k) = \langle \det(x\mathbf{I} - \Phi)\rangle + \left[\Lambda^{2N_c - N_f}\frac{B(x)}{x^{N_c}}\exp\left(\sum_{i=1}^{\infty}\frac{u_i}{x^i}\right)\right]_+, \tag{4.15}$$

hence deriving (2.36).

Please note that the non-polynomial part of (4.12) tells us how u_k with $k > N_c$ are related to the u_ks with $k = 1, \ldots, N_c$.

4.1.7 The action of $\mathbf{PGL}(2, \mathbb{C})$

Before continuing on to solve the factorization problem let us just remember from section 3.4 that Möbius transformations of x on a Riemann surface determined by $(y(x), x)$ gave isomorphic Riemann surfaces – and hence e.g. the same period matrices. However, this $\mathrm{PGL}(2, \mathbb{C})$ symmetry is not a symmetry of the Seiberg-Witten curve (4.1). We now want to examine what these transformations mean.

$\mathrm{PGL}(2, \mathbb{C})$ is generated by translations $x' = x + x_0$, scalings $x' = \lambda x$ and the inversion $x' = 1/x$. Lets us now consider each of these in order.

In the case without flavours the factorization problem is (2.47)

$$y^2 = P_{N_c}(x)^2 - 4\Lambda^{2N_c} = F_{2g+2}(x)H_{N_c-1-g}(x)^2. \tag{4.16}$$

Here translations $x = x' - x_0$ simply maps solutions to solutions and x_0 can be taken as one of the parameters of the theory. In the case with flavours (4.1) such a translation will, however, translate the masses:

$$y'^2 = P'_{N_c}(x')^2 - 4\Lambda^{2N_c - N_f}\prod_{i=1}^{N_f}(x' + m_i - x_0) = F'_{2g+2}(x')H'_{N_c-1-g}(x')^2, \tag{4.17}$$

where the prime on the functions simply are defined by $P'_{N_c}(x') = P_{N_c}(x)$. We thus have a simple one-to-one map between solutions with masses m_i and solutions with masses $m_i - x_0$, and one could e.g. choose to solve the problem with at least one of the masses equal to zero.

In the case of scalings, $x = x'/\lambda$, we change the holomorphic scale Λ since considering $P_{N_c}(x'/\lambda)$, we have to multiply with λ^{N_c} to get a polynomial with one as the highest degree coefficient. Equation (4.1) then becomes

$$y'^2 = P'_{N_c}(x')^2 - 4(\lambda\Lambda)^{2N_c-N_f}\prod_{i=1}^{N_f}(x' + \lambda m_i) = F'_{2g+2}(x')H'_{N_c-1-g}(x')^2, \tag{4.18}$$

where $P'_{N_c}(x') = P_{N_c}(x)\lambda^{N_c}$ etc. Also note that the masses have been scaled. So we map solutions with scale Λ to solutions with scale $\lambda\Lambda$ (and scaled masses). Note here that $N_f = 2N_c$ is special, since the factor in front of $B(x)$ is not changed. Thus the scalings here simply give a one-to-one map between solutions with masses m_i and masses λm_i, and we could choose one of the masses to be 1.

A special case is obtained when $\lambda^{2N_c-N_f} = 1$ then $\Lambda^{2N_c-N_f}$ is not changed and we can think of Λ as changed by the $2N_c - N_f$ root of unity which is merely a change of ϑ-vacua corresponding to the breaking of $\mathbb{Z}_{2(2N_c-N_f)}$ to $\mathbb{Z}_2$ – see section 2.1. We thus expect a discrete parameter in our solutions parameterising these vacua. In the case with flavours this parameter should not simply be a scaling, but also ensure that the masses are not changed as in (4.18).

Finally, we consider the inversion $x = 1/x'$. In order to have polynomials we see that we have to multiply with x'^{2N_c}. Further, looking at

$$F_{2g+2}(x)H_{N_c-1-g}(x)^2 \equiv \prod_{k=1}^{2N_c}(x - e_k) = \frac{1}{x'^{2N_c}}\prod_{k=1}^{2N_c}(1 - e_k x') = \frac{\prod_k e_k}{x'^{2N_c}}\prod_{k=1}^{2N_c}\left(x' - \frac{1}{e_k}\right), \tag{4.19}$$

we see that we should not only multiply with x'^{2N_c} but also divide by $\prod_k e_k$ to keep the normalisation of y^2. We thus see that (4.1) is transformed into:

$$y'^2 = P'_{N_c}(x')^2 - 4\Lambda^{2N_c-N_f}\frac{\prod_{i=1}^{N_f} m_i}{\prod_{k=1}^{2N_c} e_k}x'^{2N_c-N_f}\prod_{i=1}^{N_f}\left(x' + \frac{1}{m_i}\right) = F'_{2g+2}(x')H'_{N_c-1-g}(x')^2. \tag{4.20}$$

We have thus mapped the solution with N_f flavours into a solution with $N'_f = 2N_c$ flavours, but where $2N_c - N_f$ of the masses are zero, and the rest are the inverse of the original masses. Here P'_{N_c} is no longer normalised, but this is not expected in the $N_f = 2N_c$ case. Comparing with (2.37) we see that $h(h+2) = 4\Lambda^{2N_c-N_f}\prod_{i=1}^{N_f} m_i/\prod_{k=1}^{2N_c} e_k$. This is actually an invertible form of the integrating out of flavours discussed in section 2.2. This is because the inverse of the zero masses are infinite masses.

Note that we should be careful in the above procedure if some of the masses are equal to zero. For example, if we start with k of the masses equal to zero we will end up in a theory with $N_f' = 2N_c - k$. E.g. the factorization solutions with N_f flavours and all masses equal to zero are in one-to-one correspondence with the theory with $2N_c - N_f$ flavours all with zero masses.

In the case of $N_f = 2N_c$ and none of the masses zero, the inversion transformation maps solutions to solutions inside the $N_f = 2N_c$ theory, but gives the inverse masses, however, also the factor in front of $B(x)$ is changed.

Combining inversion and translation we can also see that the solutions with $N_f = 2N_c - 1$ generically are in one-to-one correspondence with the solutions of $N_f = 2N_c$ for any choice of masses. In general one can play with the whole $\mathrm{PGL}(2, \mathbb{C})$ to find equivalent solutions.

Also note that ω gets mapped to new one-forms under these transformations. E.g. the flavourless case corresponds to $N_f = 2N_c$ with all masses equal to zero. In this case we have a ω' which has integer periods, poles in ∞ on the upper sheet and the lower sheet both with residue $-N_c$, and a pole in zero on the lower sheet with residue $2N_c$. Back in the flavourless case this means that we have a one-form with the same integral periods as ω, but poles in zero on both sheets with residues $-N_c$ and pole in infinity on the lower sheet with residue $2N_c$, and which generates the $N_f = 2N_c$ solution. This can be checked directly.

4.2 Solution using the Jacobian

We have seen above that the factorization problem is solved once we have determined ω. The $u_k^{(fact)}$s parameterising the submanifold of the vacuum moduli space corresponding to the factorization are then determined by (4.3)

$$u_k^{(fact)} = -\frac{1}{k}\,\mathrm{res}_{x=\infty}\; x^k \omega. \tag{4.21}$$

$P_{N_c}(x)$ can be found using (4.15) or equivalently directly from ω using (4.12).

4.2.1 Strategy

To be more precise, and to sum up the knowledge from above, we should find a genus g hyperelliptic surface with a one-form fulfilling (remembering $x_a = -m_a$ for

$a = 1, \ldots, N_f$)

$$\mathrm{res}_{x=\infty}\,\omega = -N_c,\ \ \mathrm{res}_{x=\widetilde{\infty}}\,\omega = N_c - N_f,\ \ \mathrm{res}_{\tilde{x}_a}\,\omega = 1 \tag{4.22}$$

$$\frac{1}{2\pi i}\oint_{\alpha_i}\omega = N_i, \quad \frac{1}{2\pi i}\oint_{\beta_i}\omega = \Delta k_i \tag{4.23}$$

$$\int_{\widetilde{\Lambda_0}}^{\Lambda_0}\omega = -\log(\Lambda^{2N_c-N_f}) + \log(\Lambda_0^{2N_c-N_f}) + \mathcal{O}\left(\frac{1}{\Lambda_0}\right) \tag{4.24}$$

Here Δk_i are integers since ω has integral periods.[2] The last equation should be changed into (4.11) in the case of $N_f = 2N_c$. Note that the canonical homology basis (α_i, β_i) should here be thought of as definite curves so that the integers N_i and Δk_i are well-defined.

The overall strategy will here be to try to solve the problem on the Jacobian introduced in section 3.3. Consider figure 4.1 showing the Riemann surface corresponding to the factorized Seiberg-Witten curve, the Jacobian of the curve $Jac(\Sigma)$ and finally $\mathbb{C}$ seen as the upper sheet of the two-sheeted covering. $x : \Sigma \mapsto \mathbb{C}$ is the 2-1 map giving the x-value on the (upper) sheet, φ is the Abel-Jacobi map $\varphi : \Sigma \mapsto Jac(\Sigma)$. Finally, we define (abusing the notation) $x : Jac(\Sigma) \mapsto \mathbb{C}$ as giving $x : \Sigma \mapsto \mathbb{C}$ by composing with φ thus giving us a commutative diagram.

The point is that we, in principle, can construct x and ω on the Jacobian and thus should be able to solve the problem using (4.21) – if we can determine the period matrix τ_{ij} (defining the Jacobian) and the point corresponding to infinity.

4.2.2 Calculation of the β-periods

To proceed, we know that ω is given uniquely by its poles, residues and α-periods (section 3.2):

$$\omega = -N_c\omega_{\infty,\widetilde{\infty}} + \sum_{a=1}^{N_f}\omega_{\tilde{x}_a,\widetilde{\infty}} + \sum_{i=1}^{g}2\pi i N_i\sigma_i. \tag{4.25}$$

Here ω_{PQ} is the unique one-form with zero α-periods and simple poles in P (with residue 1) and Q (with residue -1). $\{\sigma_i\}$ is the basis of one-forms dual to the canonical homology basis from equation (3.6) and equation (3.7), and the last term in (4.25) simply determines ω to have α-periods N_i.

Equation (4.25) fulfills (4.22) and first equation in (4.23). But we can find such a one-form on any Riemann surface. The non-trivial constraint is the last part of (4.23) saying that the β-periods should be integer. To calculate these let us

[2] The reason for writing Δk_i is that, as explained below equation (2.56), we have $g+1$ non-compact curves along which ω integrates to, what has been denoted, k_i. The β_i-curves here are the differences between two such curves and hence a difference of k_is. Actually, the k_is are theta angles [62].

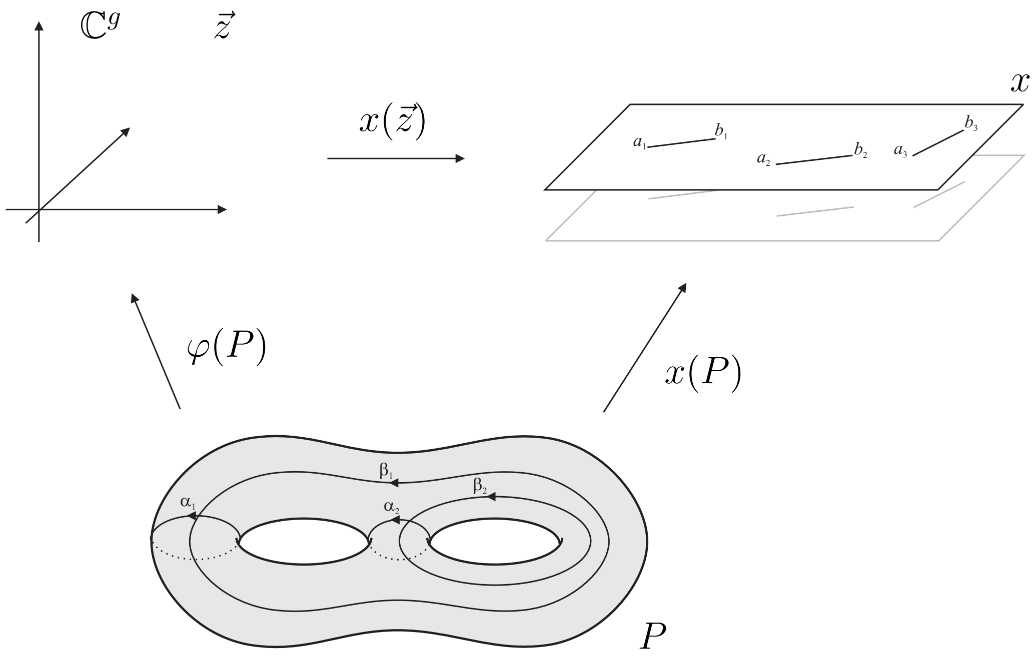

Figure 4.1: The figure shows the Riemann surface, the Jacobian and $\mathbb{C}$. Also the function x and the Abel-Jacobi map, φ, are indicated.

use (3.15)

$$\int_{\beta_i} \omega_{PQ} = 2\pi i \int_Q^P \sigma_i, \tag{4.26}$$

where the curve from P to Q should not cross any of the α- and β-cycles. Applied on (4.25) we obtain

$$\Delta k_i = -N_c \int_{\widetilde{\infty}}^{\infty} \sigma_i + \sum_{a=1}^{N_f} \int_{\widetilde{\infty}}^{\tilde{x}_a} \sigma_i + \sum_{j=1}^{g} N_j \tau_{ji}, \tag{4.27}$$

where we have used (3.7). These g equations together with equation (4.24) are exactly the ones obtained in reference [77] by the equations of motion of f_i, the coefficients of f in (2.52). Note, that since the path of integration in (4.27) should not cross the cycles, the integral will actually depend on the choice of curves for our homology basis. This will be important for the understanding of the global structure of the vacuum moduli space, but let us first see how to solve these equations.

4.2.3 Mapping to the Jacobian

The point is that (4.27) has direct interpretation on the Jacobian. The integrals over the holomorphic one-forms exactly give points on the Jacobian. Let us define the Abel-Jacobi map φ into $\mathbb{C}^g$ instead of $Jac(\Sigma)$ by requiring that for $\varphi_i(P) = \int_{Q_0}^P \sigma_i$

the integration path should not cross any of the α- and β-cycles, hence making the definition unique. Equation (4.27) then becomes

$$\begin{aligned}\Delta k_i &= -N_c(\varphi_i(\infty) - \varphi_i(\widetilde{\infty})) + \sum_{a=1}^{N_f}(\varphi_i(\tilde{x}_a) - \varphi_i(\widetilde{\infty})) + \sum_{j=1}^{g} N_j\tau_{ji} \\ &= -N_c\varphi_i(\infty) + (N_c - N_f)\varphi_i(\widetilde{\infty}) + \sum_{a=1}^{N_f}\varphi_i(\tilde{x}_a) + \sum_{j=1}^{g} N_j\tau_{ji}, \quad (4.28)\end{aligned}$$

where $\varphi_i(P)$ denotes the ith coordinate of $\varphi(P)$. Note that this equation is independent of the choice of base point Q_0.

Let the branch points on the surface be denoted P_i, Q_i for $i = 1, \ldots, g+1$ such that the ith cut is between P_i and Q_i. With the notation in figure 3.3 we have $x(P_i) = a_i$ and $x(Q_i) = b_i$. We choose the canonical homology basis as in the figure. It is then natural to take the base point of the Abel-Jacobi map to be $Q_0 = Q_{g+1}$. Let us, as before, denote hyperelliptic involution by tilde. If we do not care about crossing homology cycles, the path from Q_{g+1} to some $\tilde{x}$ on the lower sheet can be taken to be the hyperelliptic involution of the path to x, $\int_{Q_0}^{\tilde{x}} \sigma_i = \int_{Q_0}^{x} \tilde{\sigma}_i = -\int_{Q_0}^{x} \sigma_i$ since σ_i changes sign under the hyperelliptic involution. But since we have to care about not crossing homology cycles, the path might have to be changed, but only up to a homology curve. We then have with this choice of base point

$$\varphi(\tilde{x}) \equiv_L -\varphi(x), \tag{4.29}$$

where we, as usual on the Jacobian, have to calculate modulo the lattice $L = \mathbf{I} \cdot \mathbb{Z}^g \oplus \tau \cdot \mathbb{Z}^g$. Note that this tells us that the branch points are of order 2.

Using (4.29) taking $\varphi_i(\widetilde{\infty}) = n'_i + \sum_j n_j\tau_{ji} - \varphi_i(\infty)$ for n_i and n'_i integers, we can write equation (4.28) as:

$$\varphi_i(\infty) = \frac{-\Delta k_i + (N_c - N_f)n'_i + (N_c - N_f)\sum_{j=1}^{g} n_j\tau_{ji} + \sum_{a=1}^{N_f}\varphi_i(\tilde{x}_a) + \sum_{j=1}^{g} N_j\tau_{ji}}{2N_c - N_f}. \tag{4.30}$$

Another choice of base point would be to set $Q_0 = \widetilde{\infty}$. Then (4.28) takes the form

$$\varphi_i^{\widetilde{\infty}}(\infty) = \frac{-\Delta k_i + \sum_{a=1}^{N_f}\varphi_i^{\widetilde{\infty}}(\tilde{x}_a) + \sum_{j=1}^{g} N_j\tau_{ji}}{N_c}. \tag{4.31}$$

Where $\varphi^{\widetilde{\infty}}$ is the Abel-Jacobi map with $\widetilde{\infty}$ as the base point. In the flavourless case this equation tells us that we have a point of order N_c on our Riemann surface. By the note in section 3.4 this is exactly equivalent to the existence of our meromorphic function with simple poles in ∞ and $\widetilde{\infty}$ with residues $-N_c$ and N_c and integral periods.

4.2.4 Counting of parameters

Equations (4.30) are our basic equations that we would like to solve. Remember that the ingredients needed to solve the problem are: The period matrix τ, the meromorphic map x, the holomorphic one-form ω and, finally, the point on the Jacobian corresponding to ∞. Then the solution is given by equation (4.21).

On the other hand, we expect to have $g+1$ continuous parameters in our solution of the factorization problem, as we saw in section 2.3. Let us make a counting to see that this fits.

Firstly, counting without minding the Jacobian structure, we could think of constructing the solution on the sheets. y_{red} is defined by its $2g+2$ branch points. Given these we can construct a basis of holomorphic one-forms using (3.27). By making the integrations of this basis over the α-cycles we obtain a matrix, whose inverse gives us the linear combinations turning this basis into the basis dual to the canonical homology basis, like above equation (3.11). Having obtained the σ_is we can integrate this from the last branch point to infinity and obtain $\varphi(\infty)$ as a complicated function of the branch points, and also $\varphi(x_a)$ can be obtained. Similarly, we can obtain τ_{ij} by integrating over the β-cycles. (4.30) then gives g constraints leaving us with $g+2$ continuous parameters. Finally, (4.24) gives one more constraint (ω can be determined by (A.19) and thus the integration can be performed) and thus leaves us with $g+1$ continuous parameters.

Let us now do the counting on the Jacobian. A general genus g hyperelliptic curve has a period matrix τ_{ij} with $2g-1$ parameters (see section 3.4). Given the period matrix one can in principle calculate $\varphi(P)$ as a function of τ, as above. On the Jacobian we can also construct x. However, as explained in section 3.4 we can only determine this up to Möbius transformations. We thus have three free parameters in determining x. Especially, we can choose any point on the surface to correspond to ∞. Thus (4.30) only needs to hold for some point on the curve ($\varphi(\tilde{x}_a)$ should be kept unspecified and in the end determined by $x(\varphi(\tilde{x}_a)) = -m_a$). The point is that the image of the Riemann surface, $\varphi(\Sigma)$, is a complex dimension one submanifold in the g-dimensional Jacobian. Thus (4.30), which can be written as equations in τ_{ij}, constitutes $g-1$ constraints to ensure that the right hand side is a point on $\varphi(\Sigma)$. We are thus left with g continuous parameters in τ. x now has two constraints: $x(\varphi(\infty)) = \infty$ and (4.24) which turns out to determine the scale of x, as we will see below where we will also see how to construct ω. Thus we only have one continuous parameter in determining x and in all we have $g+1$ continuous parameters.

In this way we have seen that we in principle can obtain τ in terms of g parameters. This is the on-shell τ restricted by the equations of motion.

However, all of this is very inexplicit. Even though we have obtained equations (4.30), which in principle solves the problem, the point $\varphi(\infty)$ is a very complicated function of τ and can not be hoped to be solved for analytically. Even worse, we have not even written the functions explicitly. In principle, one would have to construct the σ_is on the sheets, as we saw above, giving very complicated expressions. Fortunately, we will in the next section be able to suggest $g-1$ explicit equations that give the wanted constraints, and which for sure works for the genus two case.

4.2.5 Explicit form of equations of motion

Let us now take a bit different view on (4.30). Notice that for the full $g \times g$ matrix τ only the vector $\sum_i N_i \tau^{(i)}$ ($\tau^{(i)}$ being the ith column of τ) appears explicitly. By the counting above we know that we should expect g free parameters in the period matrix. Let us take these to exactly be $\sum_i N_i \tau^{(i)}$. Actually, these can not take any values. E.g. $\sum_{i,j} N_i \tau_j^{(i)} N_j$ has to have a positive imaginary part. Further, we do not have an explicit expression for τ_{ij} in terms of its $2g-1$ parameters. This is like a Schottky problem for the hyperelliptic matrices: The Schottky problem is how to give equations for τ as being a period matrix for a Riemann surface, i.e. how to express τ in its $3g-3$ moduli. However, for hyperelliptic surfaces we can at least make complicated expressions for τ as mentioned in section 3.4. So which constrains there are on $\sum_i N_i \tau^{(i)}$ is complicated, but let us assume that we have g continuous parameters with some constraints.

Let us first consider the case without flavours since these complicate things by the presence of the mass poles in (4.30). Without the flavours we have

$$\varphi_i(\infty) = \frac{-\Delta k_i + \sum_{j=1}^{g} N_j \tau_{ji}}{2N_c} + \tfrac{1}{2} n_i' + \tfrac{1}{2} \sum_{j=1}^{g} n_j \tau_{ji}. \tag{4.32}$$

To proceed, let us first note that we can find the images of the branch points in the Jacobian. We put the base point at Q_{g+1} where we, as explained above, denote the branch points by P_i and Q_i. We can now find the $\varphi(P_i)$ and $\varphi(Q_i)$ by integrating along deformed version of the α- and β-cycles (see figure 3.3) that pass through the branch points and such that their path on the lower sheet is the hyperelliptic involution of the path on the upper sheet, but of course in the opposite direction. Since we have a sign change in σ_i under the hyperelliptic involution, integrating from one branch point to the other along one of the curves gives half of integrating all the way around the cycle. However, we should remember not to cross any of the original cycles on the path of integration. As an example $\varphi(P_1) = \int_{Q_{g+1}}^{P_1}$ is obtained by integrating along the lower half of β_1 from Q_{g+1} to P_1, thus giving

$\varphi(P_1) = -\tau^{(1)}/2$. Similarly we get:

$$
\begin{aligned}
\varphi(P_1) &= -\tfrac{1}{2}\tau^{(1)}, \\
\varphi(Q_1) &= \tfrac{1}{2}e^{(1)} - \tfrac{1}{2}\tau^{(1)}, \\
&\vdots \\
\varphi(P_k) &= \tfrac{1}{2}\sum_{i=1}^{k-1} e^{(i)} - \tfrac{1}{2}\tau^{(k)}, \\
\varphi(Q_k) &= \tfrac{1}{2}\sum_{i=1}^{k} e^{(i)} - \tfrac{1}{2}\tau^{(k)}, \\
&\vdots \\
\varphi(P_{g+1}) &= \tfrac{1}{2}\sum_{i=1}^{g} e^{(i)}, \\
\varphi(Q_{g+1}) &= 0,
\end{aligned}
\tag{4.33}
$$

where $e^{(i)}$ is the ith row of the identity matrix.

We can now use this to investigate zeroes of theta functions. Remember from section 3.5 that a theta function with integer characteristic $\begin{bmatrix} \varepsilon \\ \varepsilon' \end{bmatrix}$ (which up to a non-zero factor is $\theta(z + \mathbf{I}\varepsilon'/2 + \tau\varepsilon/2))$ is even (odd) if $\varepsilon \cdot \varepsilon'$ is even (odd). Likewise we call the point $z = \mathbf{I}\varepsilon' + \tau\varepsilon$ even or odd depending on this. We thus see that $2Q_i$ for $i = 1, \ldots, g$ are all odd while the rest of the branch points (multiplied by two) are even. As shown in [127] the vector of Riemann constants, K, is then:

$$K \equiv_L \sum_{i=1}^{g} \varphi(Q_i) = \tfrac{1}{2}(ge^1 + (g-1)e^2 + \ldots + e^g) - \tfrac{1}{2}\sum_{i=1}^{g} \tau^{(i)}. \tag{4.34}$$

This follows by the theorem for zeroes of theta functions in section 3.5 that says if we consider $\theta(\varphi(P) - e)$, and $D = P_1' + \ldots + P_g'$ fulfills $\varphi(P_1') + \ldots + \varphi(P_g') = -K + e$, then, if the function does not vanish identically (and this happens if and only if $i(D) = 0$), D is the divisor of zeroes. And on the other hand if D is the divisor of zeroes then $\varphi(D) = -K + e$. This combined with the fact that $\theta(0) \neq 0$ and $\theta(\varphi(Q_i)) = 0$ for $i = 1, \ldots, g$ (since these were odd) gives (4.34).

It can also be shown that if the divisor D is the sum of g distinct branch points, then $i(D) = 0$ and thus $\theta(\varphi(P) - e)$ with $e = K + \varphi(D)$ does not vanish identically. Using this on $D = Q_2 + \ldots + Q_{g+1}$ we get that $\theta(\varphi(P) - e)$ with

$$e = K + \varphi(D) \equiv_L \varphi(Q_1) = \tfrac{1}{2}e^{(1)} - \tfrac{1}{2}\tau^{(1)}, \tag{4.35}$$

has divisor of zeroes equal to $Q_2 + \ldots + Q_{g+1}$. Especially

$$0 \neq \theta(\varphi(\widetilde{\infty}) - \tfrac{1}{2}e^{(1)} + \tfrac{1}{2}\tau^{(1)}) \propto \theta(-\varphi(\infty) - \tfrac{1}{2}e^{(1)} + \tfrac{1}{2}\tau^{(1)}). \tag{4.36}$$

Now consider $D = \infty + Q_2 + \ldots + Q_g$ (as before we denote the point on the Riemann surface corresponding to ∞ on the upper sheet by ∞). We calculate e:

$$e = K + \varphi(D) \equiv_L \varphi(Q_1) + \varphi(\infty) = \varphi(\infty) + \tfrac{1}{2}e^{(1)} - \tfrac{1}{2}\tau^{(1)}. \tag{4.37}$$

Considering $\theta(\varphi(P) - e)$, this is non-vanishing on the Riemann surface as we see by (4.36) for $P = Q_{g+1}$. Thus we conclude that the divisor of zeroes is $\infty + Q_2 + \ldots + Q_g$. Especially, it must vanish in $Q_2, \ldots, Q_g$ giving the $g-1$ equations:

$$\theta(\varphi(Q_i) - e, \tau) = \theta(\tfrac{1}{2}\sum_{k=2}^{g} e^{(k)} - \tfrac{1}{2}\tau^{(i)} + \tfrac{1}{2}\tau^{(1)} - \varphi(\infty), \tau) = 0, \quad i = 2, \ldots, g. \tag{4.38}$$

We could obtain other equations starting from divisors being other combinations of g different branch points. Let $P'_1, \ldots P'_{g-1}$ be $g-1$ different branch points and consider the divisor $D = \infty + \sum_i P'_i$. Then in the same way as above, D is the divisor of $\theta(\varphi(P) - e)$ where

$$e = K + \varphi(D) = K + \varphi(\infty) + \sum_{i=1}^{g-1} \varphi(P'_i). \tag{4.39}$$

Inserting P'_{g-1} gives (θ is even)

$$\theta(\varphi(\infty) + \sum_{i=1}^{g-2} \varphi(P'_i) + K, \tau) = 0, \tag{4.40}$$

where P'_i can be arbitrary, but different, branch points and their value under ϕ is given in (4.33). Only $g-1$ of these equations can really be thought of as inequivalent. We will suggest how to choose them below.

As we did above, we can think of $\varphi(\infty)$ as being determined completely by our g continuous parameters $\sum_j N_j \tau_{ji}$ leaving us with $g-1$ undetermined parameters in τ_{ij}. Our point is that we by (4.40) have obtained $g-1$ explicit equations which have to hold if $\varphi(\infty)$ really is a point on the surface. Thus we can see the equations as $g-1$ constraints on the $g-1$ continuous parameters. We can visualise this by considering the codimension one analytical set of zeroes for $\theta(z, \tau)$. We have to vary the $g-1$ parameters in τ such that the $g-1$ points in (4.38) are on the zero-set, or rather such that $g-1$ carefully chosen points in (4.40) are on the zero-set.

Note that we have not proven that a τ that solves (4.40) really corresponds to a solution of the factorization problem, but only the converse. However, the counting for continuous parameters fits nicely. Since ∞ is an arbitrary point (except for some choices of branch points) in the derivation of (4.40) we can use it for all points on the Riemann surface, that are not branch points. I.e.

$$\theta(\varphi(P) + \sum_{i=1}^{g-2} \varphi(P^a_i) + K, \tau) = 0, \quad a = 1, \ldots, g-1, \tag{4.41}$$

where a indexes the choice of independent sets of branch points. Firstly considering (4.33), $2g$ of the branch points are linearly independent on the Jacobian. Now, choose the sets $\{P_i^a\}_{i=1,\ldots,g-2}$ such that any two sets has at least two points that are not in common. This can e.g. be done by setting $P_i^a = \hat{P}_{i+a-1}$ where $\hat{P}_j$ denotes the $2g$ linearly independent branch points (this only uses $2g-4$ of the branch points).

Denoting the $g-1$ dimensional analytical set of zeroes for the theta function by Θ^0 we have thus shown that $\phi(\Sigma) \subseteq \bigcap_{a=1}^{g-1}(\Theta^0 - \sum_{i=1}^{g-2}\varphi(P_i^a) - K)$. In general the intersection of a $g-1$ dimensional analytical (curved) set with itself translated ($g-2$ times) is a dimension one set. Here it contains the embedding of the Riemann surface, and thus we can hope it actually is $\varphi(\Sigma)$. That would mean that the equations

$$\theta(z + \sum_{i=1}^{g-2}\varphi(P_i^a) + K, \tau) = 0, \quad a = 1, \ldots, g-1, \tag{4.42}$$

would hold if and only if z corresponds to a point on the curve.

Actually, it can be shown [127] that the zero set of the theta function is $\Theta^0 = \varphi(\Sigma_{g-1}) + K$, where Σ_{g-1} is the set of integral divisors of degree $g-1$, and we can write $\varphi(\Sigma_{g-1}) = \sum_{i=1}^{g-1}\varphi(\Sigma)$. This means that in the case $g=2$ this really holds true. In the case $g=3$ we should look at

$$\big(\varphi(\Sigma) + \varphi(\Sigma) - \varphi(P_1^1)\big) \cap \big(\varphi(\Sigma) + \varphi(\Sigma) - \varphi(P_1^2)\big). \tag{4.43}$$

This set will, besides $\varphi(\Sigma)$, at least also contain $\varphi(\Sigma) - \varphi(P_1^1) - \varphi(P_1^2)$. However, this discrete extra possibility could perhaps be ruled out by checking (4.43) for an extra independent set of P_i^as. But whether equations (4.42) really are enough to give the necessary constraints that the point is on the curve is not determined directly by (4.43), and this should be investigated further. The higher genus cases are similar. But at least we can say that in the genus two case we can give a constraint on the period matrix that ensures it solves the problem.

Note that all fails if $\varphi(\infty)$ is equal to one of the branch points, but this case would fail anyway since ∞ can not be a branch point, because ω has poles of different order at ∞ and $\widetilde{\infty}$ which then would be the same point.

In the case with flavours we also have to take into account the N_f vectors $\varphi(\tilde{x}_a)$ which are unknown, but have the constraint that $x(\varphi(\tilde{x}_a)) = -m_a$. For each of these vectors we also make constraints as in (4.42). One then has to solve all $(N_f+1)(g-1)$ equations for τ in terms of the remaining N_f parameters which has to be determined by the mapping to $-m_a$, or one can take the masses as parameters of the solution, and see them as extra continuous parameters.

We have thus obtained an explicit, albeit complicated, suggestion for the $g-1$ equations of motion (or more in the case of flavours). We now go on to construct ω.

4.2.6 Construction of ω

By now we think of having determined τ, which depends on the g free parameters. However, to solve the problem in total we still need x on the Jacobian. But here we need to remember the constraint (4.24) and thus we need to know ω on the Jacobian.

For simplicity we consider the flavourless case, but the case with flavours is solved analogously. Below we will do this explicitly in the $g = 0, 1$ cases.

The point is that $\omega_{\infty,\widetilde{\infty}}$ (and in general $\omega_{P,Q}$) can be constructed using theta functions [135]. Simply take

$$\omega_{\infty,\widetilde{\infty}} = d\log\frac{\theta(\varphi(P) - \varphi(\infty) - \frac{1}{2}e^{(1)} + \frac{1}{2}\tau^{(1)})}{\theta(\varphi(P) - \varphi(\widetilde{\infty}) - \frac{1}{2}e^{(1)} + \frac{1}{2}\tau^{(1)})}. \tag{4.44}$$

Even though this is a logarithmic derivative it does not necessarily have integer β-periods since the argument is a multiplicative function. The theta function in the numerator has divisor of zeroes $\infty + Q_2 + \ldots + Q_g$ as we saw in (4.37) while the theta function in the denominator in the same way has divisor of zeroes $\widetilde{\infty} + Q_2 + \ldots + Q_g$. Thus the argument is a function with zero in ∞ and pole in $\widetilde{\infty}$ and hence we got a function with the right poles and residues. We also need to show that it is well-defined on the Jacobian, i.e. that it is not multiplicative as we add $e^{(k)}$ or $\tau^{(k)}$ to $\varphi(P)$. But this follows directly from the periods of the theta function (3.29) and (3.30). Using these we can also check that

$$\oint_{\alpha_i} \omega_{\infty,\widetilde{\infty}} = \int_{\varphi(P)}^{\varphi(P)+e^{(i)}} \omega_{\infty,\widetilde{\infty}} = 0. \tag{4.45}$$

We can then use (4.25) to get ω:

$$\omega = -N_c d\log\frac{\theta(\varphi(P) - \varphi(\infty) - \frac{1}{2}e^{(1)} + \frac{1}{2}\tau^{(1)})}{\theta(\varphi(P) - \varphi(\widetilde{\infty}) - \frac{1}{2}e^{(1)} + \frac{1}{2}\tau^{(1)})} + 2\pi i\sum_i N_i dz_i, \tag{4.46}$$

where the coordinates on the Jacobian are denoted z_i and hence σ_i maps to dz_i on the Jacobian by the definition of the Abel-Jacobi map. We can use the periods in (3.30) to check formula (4.28).

4.2.7 Construction of x

We now want to find $x : \Sigma \mapsto \mathbb{C}$. x is defined to be a 2-1 meromorphic map with exactly two poles and hence two zeroes. As we saw in section 3.4 x is defined up to Möbius transformations, or in other words, has three unconstrained parameters. But in our case we actually have a chosen x, and we saw that the factorization was not invariant under the action of $\mathrm{PGL}(2, \mathbb{C})$, but rather gave dualities between the theories. In our case we have one immediate constraint: That x is infinite in the point corresponding to infinity i.e. in $\varphi(\infty)$ on the Jacobian. Further assuming that x takes the value x_0 at Q_{g+1}, x can be written as:

$$x = \alpha \frac{\theta^2(\varphi(P) - \frac{1}{2}e^{(1)} + \frac{1}{2}\tau^{(1)})}{\theta(\varphi(P) - \varphi(\infty) - \frac{1}{2}e^{(1)} + \frac{1}{2}\tau^{(1)})\,\theta(\varphi(P) - \varphi(\widetilde{\infty}) - \frac{1}{2}e^{(1)} + \frac{1}{2}\tau^{(1)})} + x_0. \quad (4.47)$$

Firstly, this is a well-defined function on the Jacobian, i.e. it is independent under changes by the periods using (3.29) and (3.30). Here we have for simplicity assumed $\varphi(\widetilde{\infty}) = -\varphi(\infty)$. Consider now $x - x_0$, by our assumptions this should have divisor $2Q_{g+1} - \infty - \widetilde{\infty}$. But by the divisors of the involved theta functions that were determined above this is exactly the case. Now there is only an overall scaling left since two meromorphic functions with the same poles and residues can only differ by a scalar factor, because their quotient is a holomorphic function.

In the flavourless case, x_0 is actually the last of our continuous parameters since, as we saw in section 4.1, we have an overall translational symmetry. In the case with flavour this is not the case. Rather, we can take one of the $\varphi(\tilde{x}_a)$s as a parameter of the solution (remember this is only one degree of freedom). Then x_0 is determined in this free parameter by using $x(\varphi(\tilde{x}_a)) = -m_a$.

Let us now move on to determine α. We know from the analysis in section 4.1 that scalings are related to Λ and by dimensional analysis we immediately have that $\alpha \propto \Lambda$. To determine α we use (4.24). Let P_{Λ_0} be the point corresponding to Λ_0 i.e. $x(P_{\Lambda_0})$. As usual $\tilde{P}_{\Lambda_0}$ denotes its hyperelliptic involution. We think of Λ_0 close to infinity thus P_{Λ_0} is close to P_∞, the point corresponding to infinity which we above have simply denoted ∞. Let v be a local coordinate on the manifold around P_∞ such that $v(P_\infty) = 0$. Denote by $z : \mathbb{C} \mapsto \mathbb{C}^g$ the map $z(v) = \varphi(P(v))$ and let $\Lambda_0 = P(v_{\Lambda_0})$. Also note that by the definition we have $z(0) = \varphi(\infty)$. Then

$$\varphi(P_{\Lambda_0}) = z(v_{\Lambda_0}) = \varphi(\infty) + \frac{\partial z}{\partial v}(0)v_{\Lambda_0} + \mathcal{O}(v_{\Lambda_0}^2). \quad (4.48)$$

This gives us

$$\theta(\varphi(P_{\Lambda_0}) - \varphi(\infty) - \tfrac{1}{2}e^{(1)} + \tfrac{1}{2}\tau^{(1)}) = 0 + (\partial_{z_i}\theta)(-\hat{\tau})\frac{\partial z_i}{\partial v}(0)v_{\Lambda_0} + \mathcal{O}(v_{\Lambda_0}^2), \quad (4.49)$$

where we for simplicity have defined

$$\hat{\tau} = \tfrac{1}{2}e^{(1)} - \tfrac{1}{2}\tau^{(1)}. \quad (4.50)$$

In the same way we get using (4.29):

$$\varphi(\tilde{P}_{\Lambda_0}) = \varphi(\widetilde{\infty}) - \frac{\partial z}{\partial v}(0)v_{\Lambda_0} + \mathcal{O}(v_{\Lambda_0}^2), \quad (4.51)$$

and

$$\theta(\varphi(\tilde{P}_{\Lambda_0}) - \varphi(\widetilde{\infty}) - \tfrac{1}{2}e^{(1)} + \tfrac{1}{2}\tau^{(1)}) = -(\partial_{z_i}\theta)(-\hat{\tau})\frac{\partial z_i}{\partial v}(0)v_{\Lambda_0} + \mathcal{O}(v_{\Lambda_0}^2), \quad (4.52)$$

Now we can perform the integration in (4.24) using ω from (4.46):

$$\begin{aligned}\int_{\widetilde{\Lambda_0}}^{\Lambda_0} \omega = &\int_{\varphi(\tilde{P}_{\Lambda_0})}^{\varphi(P_{\Lambda_0})} \Big(- N_c d \log \frac{\theta(z - \varphi(\infty) - \hat{\tau})}{\theta(z - \varphi(\widetilde{\infty}) - \hat{\tau})} + 2\pi i \sum_i N_i dz_i \Big) \\ = &- 2N_c \log v_{\Lambda_0} - N_c i\pi - 2N_c \log \partial_{z_i} \theta(-\hat{\tau}) \frac{\partial z_i}{\partial v}(0) \\ &+ N_c \log \theta(\varphi(\widetilde{\infty}) - \varphi(\infty) - \hat{\tau})\, \theta(\varphi(\infty) - \varphi(\widetilde{\infty}) - \hat{\tau}) \\ &+ 2\pi i \sum_i N_i(\varphi_i(\infty) - \varphi_i(\widetilde{\infty})) + \mathcal{O}(v_{\Lambda_0}). \end{aligned} \tag{4.53}$$

To compare with the original calculation in (4.24) we use the expression for x in (4.47) to get:

$$\Lambda_0 = x(\varphi(P_{\Lambda_0})) = \alpha \frac{\theta^2(\varphi(\infty) - \hat{\tau})}{(\partial_{z_i} \theta)(-\hat{\tau}) \frac{\partial z_i}{\partial v}(0) v_{\Lambda_0}\, \theta(\varphi(\infty) - \varphi(\widetilde{\infty}) - \hat{\tau})} + \mathcal{O}(v_{\Lambda_0}^0). \tag{4.54}$$

Finally, we can compare the two expressions for the integral. Solving for α we get:

$$\begin{aligned}\alpha = \Lambda e^{2\pi i \frac{k}{2N_c}} &\left(\frac{\theta(\varphi(\widetilde{\infty}) - \varphi(\infty) - \hat{\tau})\, \theta^3(\varphi(\infty) - \varphi(\widetilde{\infty}) - \hat{\tau})}{\theta^4(\varphi(\infty) - \hat{\tau})} \right)^{1/2} \\ &\times e^{-\frac{i\pi}{2}} e^{2\pi i \sum_i N_i \frac{\varphi_i(\infty) - \varphi_i(\widetilde{\infty})}{2N_c}}, \end{aligned} \tag{4.55}$$

where $k = 1, \ldots, 2N_c$ is a new discrete parameter of the solution that arises since we have to take the $2N_c$-root of α. This is the expected parameter from our analysis of the scalings of the factorized Seiberg-Witten curves that parameterises the $2N_c$ vacua. In the case with matter we see that $k = 1, \ldots, 2N_c - N_f$ as we would expect. Note that we could use $\varphi(\widetilde{\infty}) \equiv_L -\varphi(\infty)$ to remove the square root of the right hand side simply giving the quotient $\theta^2(\varphi(\infty) - \varphi(\widetilde{\infty}) - \hat{\tau}) / \theta^2(\varphi(\infty) - \hat{\tau})$, however this will give an extra exponential factor in the formula.

4.2.8 The solution

We have thus finally obtained x and we have in principle solved the problem: We can obtain the value of all the branch points $x(P_i)$, $x(Q_1)$ and $x(Q_{g+1})$ by insertion of the values of these on the Jacobian (equations (4.33)) in the formula for x. We can, however, not use (4.47) for the branch points corresponding to Q_i with $i = 2, \ldots, g$ since we have zero in numerator and denominator. What we should do is to write an expression of x as in equation (4.47), but now based on divisors built of P_i, ∞ and $\widetilde{\infty}$ in exactly the same way. The two undetermined parameters are found by equating with the x-function already obtained in Q_1 and Q_g. We can now use the new function to obtain $x(Q_i)$. This means that y_{red} is determined in our specified $g+1$ continuous parameters (together with the discrete parameters). ω can then be constructed directly as in (A.19) and the u_ks can be found.

The technical problem in obtaining the u_ks by (4.3) using our obtained ω, x and $\varphi(\infty)$ is that we do not directly know the one-dimensional curve of our Riemann surface in the g-dimensional Jacobian. This is, of course, not a problem for $g = 1$ where we do not have any further constraints on τ as in the higher genus cases. We will examine this solution below in section 4.5.

There might, however, be a way round this problem. To construct the u_ks by (4.3) or P_{N_c} by (4.12) we need to know the derivatives of $\varphi(P)$. Let us now remember (4.41) could be used for any point, P:

$$\theta(\varphi(P) + \sum_{i=1}^{g-2} \varphi(P_i^a) + K, \tau) = 0, \quad a = 1, \dots, g-1, . \tag{4.56}$$

Letting v be a local coordinate around some point P_0 we thus get by differentiation:

$$\sum_{j=1}^{g} \frac{\partial\, \theta(z + \sum_{i=1}^{g-2} \varphi(P_i^a) + K)}{\partial z_j}\Big|_{z=\varphi(P_0)} \frac{d\varphi_j(P(v))}{dv}\Big|_{v=0} = 0, \quad a = 1, \dots, g-1. \tag{4.57}$$

As above, we hope that these are really independent equations, and we have thus obtained $g-1$ equations in $d\varphi_i(P)$ giving os the wanted derivatives. In the case $g = 2$ we know it works, and we have obtained a relation between dz_1 and dz_2 for the curve where z_1 and z_2 are the coordinates on the Jacobian. As soon as equation (4.40) has been solved, e.g. numerically, we can get the u_ks directly.

Let us note that the method for the case of $N_f = 2N_c$ is somewhat different, but we can use that the solutions with $N_f = 2N_c$ can always be found using the solutions of $N_f = 2N_c - 1$ (or less flavours) as we saw in the study of $\mathrm{PGL}(2, \mathbb{C})$.

4.3 Global structure of the vacuum moduli space

We have seen how to obtain solutions of the factorization problem that depends on g continuous parameters in τ and one extra continuous parameter which is an overall translation in the flavourless case, and the position of a mass point in the case with matter. Further, we have discrete parameters N_i, Δk_i and k. However, different specifications of these parameters may give rise to the same solution. Examining when this happens tells us about the global structure of the vacuum moduli space. Importantly, one of the reasons for this can be that we have physically dual description of the same physics. E.g. it turns out that classical solutions with different specifications of N_i can be continuously related to each other. The structure of vacua has been studied extensively in the literature [62, 63, 64, 77, 78, 79, 80, 81, 66, 67]. We will here give a crude overview of the structure using the knowledge we have obtained above. Since the Seiberg-Witten curve should be the same for the two sets of parameters, the period matrix must be related by a modular transformation. We can then split into two cases: Those where τ is unchanged and those where the τs are related by a modular transformation.

4.3.1 Equivalences with identical τ

We will first examine equivalences that have identical τ. Let us start by considering the case without flavour. We expect N_i and Δk_i to be defined only modulo N_c because of the poles with residue $\pm N_c$ for ω. Indeed, considering a solution of the problem with given α- and β-curves, we can think of stretching α_i or β_i such that it crosses ∞ or $\widetilde{\infty}$ (this is most easily visualised on the torus in figure 3.1) one or more times, but we still have a canonical homology basis. Since what we have done is homologically equivalent this does not change τ, but crossing the pole change the α_i or β_i integration of ω by $\pm 2\pi i N_c$, i.e. changing N_i or Δk_i by $\pm N_c$. This shows that N_i and Δk_i are only defined modulo N_c. However, when keeping track of the discrete parameters $[N, \Delta k, k]$ where N and Δk are vectors, we should be careful since k is also changing. The reason is that the points $\varphi(\infty)$ and $\varphi(\widetilde{\infty})$ changes by periods when we move the homology curve, since the path of integration defining the points must not cross any of the basis curves. Now, k was defined as a comparison between the integral (4.53), that changes by periods of ω i.e. by N_is or Δk_is, and (4.24), which does not take the positions of the curves into consideration. This means that k will change by the N_is or Δk_is. We then e.g. get $[N, \Delta k, k] \equiv [N, \Delta k - N_c e^{(i)}, k - N_i]$.

Finally, k is by definition periodic with $2N_c$ or in the case with flavours by $2N_c - N_f$.

For the case with flavour we also have the poles at minus the masses on the lower sheets, and the poles at the infinities have residues $-N_c$ and $N_c - N_f$. We thus have a much larger group of equivalences. If we have a single mass point we can actually change the N_i and Δk_is by one at a time. In principle they can then all be set to zero. But the information is not gone, it has merely been exchanged by the position of $\varphi(\tilde{x}_a)$ on $\mathbb{C}^g$ rather than on the Jacobian $\mathbb{C}^g/L$, and remember that in this case the position of (one of the mass points) is one of the continuous parameters. In principle it should lie in $\mathbb{C}^g/L$, but defining it on $\mathbb{C}^g$ have actually put the information of the N_i and Δk_i into the position of the continuous parameter. If the masses are all the same we can not simply change N_i and Δk_i by 1, but only by N_f at the time. However, we still have the periodicity with both N_c and $N_c - N_f$.

Finally, which should also remember that we have the transition of moving the mass pole from the lower sheet to the upper sheet changing to the Higgs branch root and we no longer have $\sum_i N_i = N_c$.

Below we will also discuss the structure in the case of the explicit construction of the genus one and zero curves.

4.3.2 Equivalences with different τ

Physically more interesting are the equivalences that involve a change of τ. In this case we consider a change in canonical homology basis to another canonical basis as in (3.9):

$$\begin{pmatrix} \alpha' \\ \beta' \end{pmatrix} = M \begin{pmatrix} \alpha \\ \beta \end{pmatrix} \equiv \begin{pmatrix} A & B \\ C & D \end{pmatrix} \begin{pmatrix} \alpha \\ \beta \end{pmatrix}, \quad M \in \mathrm{Sp}(2g, \mathbb{Z}). \tag{4.58}$$

We will now get a modular transformed period matrix of the form (3.11)

$$\tau' = (C + D\tau)(A + B\tau)^{-1}. \tag{4.59}$$

In the genus one case the transformations are simply $\tau \mapsto \tau + 1$ and $\tau \mapsto -1/\tau$. The Seiberg-Witten curve stays the same since we have merely changed to other basis curves. But the new N_i' and $\Delta k_i'$ are now linear combination of the old ones by (4.58):

$$\begin{pmatrix} N' \\ \Delta k' \end{pmatrix} = \begin{pmatrix} A & B \\ C & D \end{pmatrix} \begin{pmatrix} N \\ \Delta k \end{pmatrix}, \quad \begin{pmatrix} A & B \\ C & D \end{pmatrix} \in \mathrm{Sp}(2g, \mathbb{Z}). \tag{4.60}$$

where N and Δk are again vectors. We thus see that all of the N_is and Δk_is can mix, but under the constraint of the symplectic group. We should also remember that we can have a change of k under the transformations.

Physically this is important since it means that solutions with different N_is can really correspond to the same solution. We can now think of a process where we take the classical limit $\Lambda \mapsto 0$ thereby shrinking the cuts to poles of $\omega_{cl.}$ with the given N_is. We demand that the number of cuts is unchanged in the process, thus considering the same genus factorization problem for all Λ. Notably, this shrinking of the cuts happens between the branch points in the α-cycles. If we now again consider the quantum case, but make a transformation to different cycles (4.58) we have new N_i's and Δk_is. We then go to the classical solution, but this time it happens along the new α' cycles (it is thus other branch points that now move close to each other in the semi-classical limit) and we end up in another classical solution where the cuts shrink to poles of $\omega_{cl.}'$ with the N_i's. As promised, we see that we can interpolate continuously between vacua with different N_is, and (4.60) gives the possibilities. Importantly, we can also have solutions with some $N_i = 0$ in the quantum case. If we can find a transformation such that all $N_i' \neq 0$ we can take the classical limit for these without having to go to lower genus factorization. We have simply put the cuts "wrongly".

We now move on to give the solution of factorization problems in the simplest cases, namely genus 0 and 1, where we can solve the problem exactly.

4.4 Factorization – Genus Zero Case

This section is a revised version of section 5 in [3].

The genus zero case without fundamental matter was solved in 1995 by Douglas and Shenker using Chebyshev polynomials [65]. We will here study the case with fundamental matter which was first solved by Demasure and Janik [68] using random matrices. We will here give an easy way of solving the problem in the spirit of the above higher genus solutions where we solve the problem using the meromorphic one-form ω.

In the genus zero case (complete factorization) we expect a single continuous parameter in the solution.[3]

Let us start from the reduced curve which in this case is given by the equation

$$y^2 = F_2(x) \equiv (x-a)(x-b) \ . \tag{4.61}$$

As explained in section 4.1, we have to construct a meromorphic one-form ω on the curve with residues $-N_c$ at infinity on the physical sheet, $N_c - N_f$ at infinity on the second sheet and with residue 1 at $x = -m_i$.

It turns out to be much easier to use an unconstrained parametrization of the reduced curve, i.e. to pass to the universal covering space.

4.4.1 Parametrization and $\mathbb{Z}_2$ map

Since the curve (4.61) has genus zero, it can be parameterized by functions on a sphere, which is represented as a compactified complex plane. This can be done very easily. Let us first rewrite the equation (4.61) in the form

$$y^2 = (x-T)^2 - 4R \ , \tag{4.62}$$

where we used the notation of [68]

$$T = \frac{a+b}{2} \quad , \quad R = \frac{(a-b)^2}{16} \ . \tag{4.63}$$

Then a rational parameterisation is

$$x = T + 2\sqrt{R}\frac{1+z^2}{1-z^2} \quad , \quad y = 2\sqrt{R}\frac{2z}{1-z^2} \ . \tag{4.64}$$

For our application we have to keep track of some additional structure on the curve. Firstly, we have to single out points on the sphere ∞_+, ∞_- which correspond to points at infinity in the (x, y) plane. Here these are $z = \pm 1$. Secondly, it is

[3] For the complete factorization of the Seiberg-Witten curve with fundamental matter see Ref. [68] and Refs. [53, 69].

convenient to exhibit the $\mathbb{Z}_2$ covering transformation which exchanges the sheets $(x, y) \to (x, -y)$ corresponding to the hyperelliptic involution in the higher genus cases. In terms of the z coordinate it is represented as $z \to -z$. Its fixed points are exactly the branch points of the curve (4.61). These are $z = 0$ and $z = \infty$ and correspond to $x = T + 2\sqrt{R}$ and $x = T - 2\sqrt{R}$ respectively.

4.4.2 The meromorphic one-form

Using the z coordinate we can at once write the unique meromorphic one-form with the prescribed poles and residues

$$\omega = \left(\frac{-N_c}{z-1} + \frac{N_c - N_f}{z+1} + \sum_{i=1}^{N_f} \frac{1}{z + z_{m_i}} \right) dz \ , \tag{4.65}$$

where the location of the pole corresponding to $x = -m$ can be found to be

$$z_m = \pm \frac{\sqrt{(m+T)^2 - 4R}}{m + T - 2\sqrt{R}} \ . \tag{4.66}$$

The two choices of sign correspond to putting the pole on either of the two sheets. Since all parameters are complex we can always analytically continue the answer from one sheet to the other one. As mentioned above, this has the interpretation of interpolating between Coulomb and Higgs vacua.

4.4.3 Factorization solution

We can now calculate the u_k's using (4.3). Remarkably enough all the formulas from [68] (compare e.g. formulas (38)-(40) in [136]) now follow from the simple formula

$$u_k = -\frac{1}{k} \mathrm{res}_{x=\infty}\, x^k \omega = -\frac{1}{k} \mathrm{res}_{z=1} \left(T + 2\sqrt{R} \frac{1+z^2}{1-z^2} \right)^k \cdot \omega \ . \tag{4.67}$$

The final ingredient is the calculation of Λ. We use formula (4.24) in the form:

$$\log \Lambda^{2N_c - N_f} = -\lim_{\varepsilon \to 0} \left\{ \int_{-1+\varepsilon}^{1-\varepsilon} \omega - N_c \log x(1-\varepsilon) - (N_c - N_f) \log x(-1+\varepsilon) \right\} \ . \tag{4.68}$$

Taking for simplicity all masses $m_i = m$ equal, a brief calculation gives

$$\begin{aligned} \Lambda^{2N_c - N_f} &= R^{N_c - \frac{N_f}{2}} \left(\frac{\sqrt{(m+T)^2 - 4R} - m - T + 2\sqrt{R}}{\sqrt{(m+T)^2 - 4R} + m + T - 2\sqrt{R}} \right)^{N_f} \\ &= \frac{R^{N_c}}{\prod_{i=1}^{N_f} \frac{1}{2} \left(m + T + \sqrt{(m+T)^2 - 4R} \right)} \ , \end{aligned} \tag{4.69}$$

which is exactly the formula obtained from matrix models in [68]. Plugging these parameters into the SW-curve will lead to a complete factorization regardless of whether the flavour poles are on a single or on different sheets (which amounts to a choice of the signs of the relevant square-roots). Equation (4.69) exactly gives one constraint so we end up with one continuous parameter as expected.

4.4.4 Number of vacua

Finally, let us discuss the number of such vacua. From the above construction one can obtain a discrete set of $2N_c - N_f$ vacua in the following manner. Let us rescale the parameters by

$$T \to e^{i\alpha} T \quad , \quad R \to e^{2i\alpha} R \quad , \quad m \to e^{i\alpha} m \; . \tag{4.70}$$

Then x is effectively rescaled as $x \to e^{i\alpha} x$. In order for the resulting factorization to be related to the same theory, $\Lambda^{2N_c - N_f}$ should be unchanged hence

$$\alpha = 2\pi \frac{k}{2N_c - N_f} \quad , \quad k = 0, \ldots, 2N_c - N_f - 1 \; , \tag{4.71}$$

which proves the claim.

However, the rescaling above did not keep the mass invariant. What we should really do is to translate to the theory with zero mass which, as we saw in the study of $\mathrm{PGL}(2, \mathbb{C})$ is in one-to-one correspondence with this case. For $m = 0$ the scalings does not change the mass, showing that we have $2N_c - N_f$ vacua.

Also note that in the flavourless case we only have N_c vacua, since $R \mapsto \alpha R$ should keep R^{N_c} constant. This makes the genus zero case special compared to the higher genus case [65].

Let us now continue to the case of genus one factorization.

4.5 Factorization – Genus One Case

This is a modified version of section 6 in [3].

We now solve the genus one case corresponding to gauge group breaking $U(N_c) \mapsto U(N_1) \times U(N_2)$, but in the case with fundamental matter. The method is the same as for the general genus cases above. Since $g - 1 = 0$ we do not have any equations of motions for the period matrix – it is itself one of the continuous parameters. The reason is that the Riemann surface and the Jacobian are in fact equivalent in the genus one case as mentioned in section 3.4. Since the covering of the Jacobian is simply $\mathbb{C}$, the determined value of $\varphi(\infty)$ will always be a point on the curve.

This case is interesting as, in contrast to the genus zero case described above, there is gauge symmetry breaking, one has additional discrete parameters labelling the vacua (inequivalent factorizations), new types of Coulomb vacua appear with increasing N_c which cannot be induced from those with smaller N_c. Even more interestingly, differing discrete labels like $(N_1, N_2, \Delta k, k) \neq (N_1', N_2', \Delta k', k')$ may lead to *the same* factorized SW-curves thus allowing for *dual* descriptions of the same physics, as we discussed above.

Here we start from the reduced curve which in this case is given by the quartic equation

$$y^2 = F_4(x) \equiv (x-a)(x-b)(x-c)(x-d) \ . \tag{4.72}$$

Note that for cubic superpotentials $W(x)$ relevant to this case the right hand side can be written as $F_4(x) = W'(x)^2 - f(x)$ with $f(x)$ a linear polynomial, as we saw in (2.58).

4.5.1 Parametrization and $\mathbb{Z}_2$ map.

Since the above curve is quartic, it has genus one and hence can be parameterized by a torus i.e. the complex plane modulo $(1, \tau)$, where τ is a complex parameter (the modulus) with positive imaginary part.

Again we would like to exhibit the $\mathbb{Z}_2$ covering map (the hyperelliptic involution) moving between the two branches of (4.72). As we saw in (4.29) a convenient choice of base point allow us to set

$$z \to 1 + \tau - z \ . \tag{4.73}$$

Note that we here, unlike what we did above, will stay on the fundamental region, equivalent to the Jacobian rather than the covering $\mathbb{C}$. This means that the modular addition in (4.29) is fixed to be $1+\tau$.

There are *four* fixed points on the torus: 0, $1/2$, $\tau/2$ and $1/2+\tau/2$ which under the embedding $x(z)$, which we will soon give explicitly, go over to the branch points of (4.72). This is as we saw it in (4.33), but moved to the fundamental region.

Next we need to mark the two points corresponding to the infinities on the upper and lower sheet – these will be denoted ∞_+ and ∞_- respectively. In figure 4.2 the torus is illustrated with the two marked points.

The points at infinity are here denoted by ∞_+ for the point corresponding infinity on the upper sheet and ∞_- for the lower sheet. These should go to each other under the $\mathbb{Z}_2$ covering map thus giving the relation

$$\infty_+ = 1 + \tau - \infty_- \ . \tag{4.74}$$

We will find that then ∞_- will be fixed completely when constructing the meromorphic one-form.

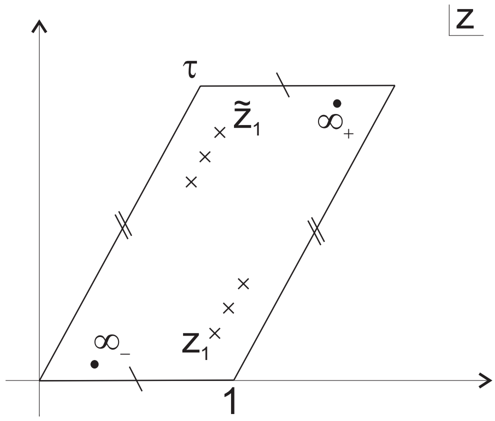

Figure 4.2: The figure shows the torus with modular parameter τ and the two points ∞_+ and ∞_- corresponding to the infinities, denoted by dots, on the upper and lower sheet. Also shown are the points z_i, denoted by crosses, corresponding to the masses m_i. $\tilde{z}_i$ are the corresponding points on the lower sheet.

4.5.2 The meromorphic one-form

Let us now construct the meromorphic one-form with the appropriate properties this time explicitly in the case with matter. The form has to have poles at $z = \infty_\pm$ and z_i such that $x(z_i) = -m_i$ (see figure 4.2) with the prescribed residues and integral periods (4.22)

$$\mathrm{res}_{z=\infty_+}\,\omega = -N_c, \quad \mathrm{res}_{z=\infty_-}\,\omega = N_c - N_f, \quad \mathrm{res}_{z=\tilde{z}_i}\,\omega = 1, \tag{4.75}$$

$$\frac{1}{2\pi i}\int_0^1 \omega = N_1, \quad \frac{1}{2\pi i}\int_0^\tau \omega = \Delta k \ , \tag{4.76}$$

where we have used that the α-cycle integration corresponds to integrating from 0 to 1 on the torus, and the β-cycle from 0 to τ. We again have to think of definite curves for the integration not encircling the poles of ω.

As we saw in (4.25) we can write ω uniquely as

$$\omega = N_c\omega_{\infty_-\infty_+} + \sum_i \omega_{\tilde{z}_i\infty_-} + 2\pi i N_1 \mathrm{d}z \ , \tag{4.77}$$

where we have used that the holomorphic one-forms on the torus has the simple form of a constant times dz. The constant is then determined by the α-period in (4.76). The remaining β-period gives the important constraint determining ∞_+ (which is equal to $-\infty_-$ modulo $(1,\tau)$). Thus it seems like no continuous parameter is undetermined on the torus except the modular parameter τ. However, for the embedding we have a scalar factor and a translation. We will see, as above, that we determine the scale factor using (4.24) thus leaving us with two continuous parameters.

Now, the main point is that on the torus we have a formula for ω_{PQ} using the elliptic theta function:

$$\theta(z,\tau) = \sum_{n=-\infty}^{\infty} e^{i\pi\tau n^2 + i2\pi z n} \ . \tag{4.78}$$

We will often suppress the τ dependence and just write $\theta(z)$. The theta function is a multiplicative holomorphic function with periods (3.29) and (3.30):

$$\theta(z+1,\tau) = \theta(z,\tau), \quad \theta(z+\tau,\tau) = e^{-i\pi\tau - i2\pi z}\theta(z,\tau) \ . \tag{4.79}$$

Importantly, $\theta(z)$ is only zero in $(1+\tau)/2$ and the multiplicity is one (3.39). Using (4.79) this gives us the formula for ω_{PQ} (see e.g. [137])

$$\omega_{PQ} = \mathrm{d}\log\frac{\theta(z-P+\frac{1+\tau}{2})}{\theta(z-Q+\frac{1+\tau}{2})} = \frac{\theta'(z-P+\frac{1+\tau}{2})}{\theta(z-P+\frac{1+\tau}{2})}\mathrm{d}z - \frac{\theta'(z-Q+\frac{1+\tau}{2})}{\theta(z-Q+\frac{1+\tau}{2})}\mathrm{d}z \ . \tag{4.80}$$

Using (4.77) we thus get an explicit expression for ω:

$$\omega = N_c \mathrm{d}\log\frac{\theta(z-\infty_-+\frac{1+\tau}{2})}{\theta(z-\infty_++\frac{1+\tau}{2})} + \sum_i \mathrm{d}\log\frac{\theta(z-\tilde{z}_i+\frac{1+\tau}{2})}{\theta(z-\infty_-+\frac{1+\tau}{2})} + 2\pi i N_1 \mathrm{d}z \ . \tag{4.81}$$

We should now perform the β-cycle integration in (4.76). Using (4.79) this gives

$$-N_c\infty_+ + (N_c - N_f)\infty_- + \sum_i \tilde{z}_i + N_1\tau = \Delta k \ , \tag{4.82}$$

which also directly follows from (3.15) that takes the form $\int_\beta \omega_{PQ} = 2\pi i(P-Q)$. We may now use the relation (4.74) between ∞_+ and ∞_- derived earlier to obtain

$$\infty_- = \frac{(N_1 - N_c)\tau - \Delta k - N_c + \sum_i \tilde{z}_i}{N_f - 2N_c} \ , \tag{4.83}$$

where we think modulo $(1,\tau)$ on the torus. Note that, as is suggested by this equation and mentioned above, we could trade in N_1 and Δk for the location of the flavour poles in appropriate copies of the fundamental domain.

At this stage we have uniquely fixed the meromorphic one-form ω and hence we may now extract the factorization solution.

4.5.3 Factorization solution

The u_k's are given by calculating the residues of $x(z)^k\omega$ at $z=\infty_+$ using (4.3):

$$u_k^{(\mathrm{fact})} = -\frac{1}{k}\mathrm{res}_{z=\infty_+}\, x^k\omega \ . \tag{4.84}$$

We thus have to construct the embedding map $x(z)$. It has to be a meromorphic map with single poles at ∞_+, ∞_-. Then necessarily it will have two zeroes z_0 and, since it should be invariant under the $\mathbb{Z}_2$ map, $\tilde{z}_0 = 1+\tau-z_0$. It is thus fixed uniquely up to a multiplicative constant B and the embedding map takes the form

$$x(z) = B\frac{\theta(z-z_0+\frac{1+\tau}{2})\theta(z-1-\tau+z_0+\frac{1+\tau}{2})}{\theta(z-\infty_+ +\frac{1+\tau}{2})\theta(z-\infty_- +\frac{1+\tau}{2})} , \tag{4.85}$$

In order to compute the complete solutions it remains to determine Λ. To this end let us perform the integral in (4.24): We take z_{Λ_0} as the point corresponding to Λ_0 on the upper sheet, i.e. we think of z_{Λ_0} as being close to ∞_+. Then $\widetilde{z_{\Lambda_0}} = 1+\tau-z_{\Lambda_0}$. Using (4.81) we get (in close similarity with (4.53))

$$\begin{aligned}\int_{1+\tau-z_{\Lambda_0}}^{z_{\Lambda_0}} \omega = &-\log(z_{\Lambda_0}-\infty_+)^{2N_c-N_f} + \log\theta(\infty_+ - \infty_- + \tfrac{1+\tau}{2})^{2N_c-N_f} \\ &+ \sum_i \log\frac{\theta(\infty_+ - \tilde{z}_i + \frac{1+\tau}{2})}{\theta(\infty_- - \tilde{z}_i + \frac{1+\tau}{2})} + \log\theta'(\tfrac{1+\tau}{2})^{N_f-2N_c} \\ &+ (N_c+N_1)2\pi i(\infty_+ - \infty_-) - N_f\pi i + \mathcal{O}(z_{\Lambda_0}-\infty_+) ,\end{aligned} \tag{4.86}$$

where we have used $\theta(-z+\frac{1+\tau}{2}) = \exp(i\pi + i2\pi z)\theta(z+\frac{1+\tau}{2})$ which can be proven using (4.79) and that $\theta(z)$ is an even function. Since $x(z)$ has a pole of order one at ∞_+ we can write

$$\Lambda_0 = x(z_{\Lambda_0}) = A\frac{1}{z_{\Lambda_0}-\infty_+} + \mathcal{O}((z_{\Lambda_0}-\infty_+)^0) , \tag{4.87}$$

where A is a constant. Thus

$$\Lambda_0(z_{\Lambda_0}-\infty_+) = A + \mathcal{O}(z_{\Lambda_0}-\infty_+) . \tag{4.88}$$

Hence we get the relation

$$\log\Lambda_0^{2N_c-N_f} + \log(z_{\Lambda_0}-\infty_+)^{2N_c-N_f} = \log A^{2N_c-N_f} + \mathcal{O}(z_{\Lambda_0}-\infty_+) . \tag{4.89}$$

Using this to equate (4.24) and (4.86), we finally see that (4.24) determines the scale A of $x(z)$:

$$\begin{aligned}\log A^{2N_c-N_f} = &\log\Lambda^{2N_c-N_f} + \log\theta(\infty_+ - \infty_- + \tfrac{1+\tau}{2})^{2N_c-N_f} \\ &+ \sum_i \log\frac{\theta(\infty_+ - \tilde{z}_i + \frac{1+\tau}{2})}{\theta(\infty_- - \tilde{z}_i + \frac{1+\tau}{2})} + \log\theta'(\tfrac{1+\tau}{2})^{-2N_c+N_f} \\ &+ (N_c+N_1)2\pi i(\infty_+ - \infty_-) - N_f\pi i .\end{aligned} \tag{4.90}$$

This is solved as

$$\begin{aligned}A = \Lambda e^{\frac{i2\pi k}{2N_c-N_f}} \frac{\theta(\infty_+ - \infty_- + \frac{1+\tau}{2})}{\theta'(\frac{1+\tau}{2})} &\Big(\prod_i \frac{\theta(\infty_+ - \tilde{z}_i + \frac{1+\tau}{2})}{\theta(\infty_- - \tilde{z}_i + \frac{1+\tau}{2})}\Big)^{\frac{1}{2N_c-N_f}} \\ &\times e^{2\pi i(\infty_+ - \infty_-)\frac{N_c+N_1}{2N_c-N_f}} e^{-\pi i\frac{N_f}{2N_c-N_f}} ,\end{aligned} \tag{4.91}$$

where k is an integer, $k = 0, \ldots, 2N_c - N_f - 1$, which is a discrete parameter of our solution.

Let us now relate A to the scalar factor B appearing in the expression (4.85) for the embedding $x(z)$ using $\lim_{z\to\infty_+} x(z)(z - \infty_+) = A$. The resulting expression for B is

$$B = \Lambda e^{\frac{i2\pi k}{2N_c - N_f}} \frac{\theta(\infty_+ - \infty_- + \frac{1+\tau}{2})^2}{\theta(\infty_+ - z_0 + \frac{1+\tau}{2})\theta(\infty_+ - 1 - \tau + z_0 + \frac{1+\tau}{2})} \times \Big(\prod_i \frac{\theta(\infty_+ - \tilde{z}_i + \frac{1+\tau}{2})}{\theta(\infty_- - \tilde{z}_i + \frac{1+\tau}{2})}\Big)^{\frac{1}{2N_c - N_f}} e^{2\pi i(\infty_+ - \infty_-)\frac{N_c + N_1}{2N_c - N_f}} e^{-\pi i \frac{N_f}{2N_c - N_f}} . \quad (4.92)$$

Thus we have solved the problem and the solution is summarized by Eqs. (4.81), (4.84), (4.85) and (4.92). As expected, the construction depends on the two continuous parameters τ and z_0 (modulo $(1,\tau)$) and the discrete parameters $N_1, \Delta k$ and k. The physical given parameters are N_c, N_f, Λ and the masses m_i. In principle we should determine the $\tilde{z}_i$s, $i = 1, \ldots, N_f$, using

$$x(\tilde{z}_i) = -m_i, \quad i = 1, \ldots, N_f . \quad (4.93)$$

However, the dependence on $\tilde{z}_i$ is extremely complicated since also $x(z)$ in (4.85) depends on the $\tilde{z}_i$s through B (see (4.92)). There is, however, one exception: If all the masses are the same, $m_i = m$, and correspondingly $\tilde{z}_i = \tilde{z}_1$. Then we can consider $x'(z) = x(z) + m$. This is zero in $\tilde{z}_1$ and has the same poles as x. Thus x' is given by (4.85) and (4.92) with $\tilde{z}_1 = z_0$, and (4.84) is replaced by

$$u_k^{(\text{fact})} = -\frac{1}{k}\text{res}_{z=\infty_+} (x' - m)^k \omega . \quad (4.94)$$

Of course, in the case of different masses we can in the same way trade z_0 for an arbitrary $\tilde{z}_i$ leaving only $N_f - 1$ points to be determined by (4.93).

We have checked our solution explicitly (using algebraic computer programs) for various specific values of N_c, N_f, including the range $N_c \leq N_f < 2N_c$ for which we have the quantum corrected Newton relation (4.15). Alternatively, one may find P_{N_c} directly using (A.14) which is equivalent to (4.15). As a consistency check of our solution we have also considered the decoupling of (infinitely) massive flavours and checked that our formulas reduce to the case of pure $\mathcal{N} = 2$ theory without flavours. We present some details of the computation in Appendix B.

We note that the solution satisfies a multiplication map. This map was found in Ref. [37, 62] for the case without flavours and further generalized to the case with flavours in Ref. [78]. For any solution, with given N_c, N_1, Δk, it follows from (4.82), (4.83), (4.92) that we also have a solution for tN_c, tN_1, $t\Delta k$ with t an integer, while at the same time each $\tilde{z}_i$ is mapped onto t copies of the same $\tilde{z}_i$. This holds similarly in the higher genus cases.

We finally remark that not all of the above discrete and continuous parameters in the set $(N_1, \Delta k, k, \tau, z_0)$ give rise to different solutions. E.g. the periodicity in k is manifest and hence we have

$$(N_1, \Delta k, k) \equiv (N_1, \Delta k, k + 2N_c - N_f) \ . \tag{4.95}$$

Also periodicities of N_1 and Δk can be found. E.g. we have

$$(N_1, \Delta k - (N_f - 2N_c), k) \equiv (N_1, \Delta k, k - 2N_c - 2N_1) \ , \tag{4.96}$$

$$(N_1 + N_f - 2N_c, \Delta k, k) \equiv (N_1, \Delta k, k - 2N_c - 2\Delta k) \ . \tag{4.97}$$

Equation (4.96) is easily seen noting that ∞_- from equation (4.83) changes by one. However, this do not change the theta functions in the formula for x. Thus the relation follows directly from equation (4.92). On the other hand, the periodicity in N_1 changes ∞_- by τ and this means that x and the scale B changes non-trivially and the relation requires a calculation to check. We note that (4.97) depends on the choice of the $(2N_c - N_f)$-root for the part depending on the mass-points $\tilde{z}_i$ in (4.92). This shows the complexity in studying the vacuum structure when we have fundamental flavour in the theory compared to the flavourless case [66], see also the discussion above. Similarly, we also expect modular transformations that change τ to $\tau + 1$ or $-1/\tau$.

Finally, let us mention that this method does not work for $N_f = 2N_c$ since ∞_+ diverges. However, as mentioned above in the analysis of the $\mathrm{PGL}(2, \mathbb{C})$ structure we can actually obtain the solutions of this case directly from the case $N_f = 2N_c$. The cases $N_f > 2N_c$ are actually straightforwardly obtained by what we have found.

4.6 Conclusions and Outlook

In this chapter we have studied the factorization of the $U(N_c)$ Seiberg-Witten curve to a reduced general genus g curve. In the case where we softly break the $\mathcal{N} = 2$ supersymmetry to $\mathcal{N} = 1$ by a tree-level superpotential, this corresponds to the breaking of the gauge group as $U(N_c) \mapsto U(N_1) \times \cdots \times U(N_{g+1})$ for the Coulomb vacua that we are studying. We have also taken into account the cases where we include N_f fundamental matter multiplets into the theory.

By examining the $\mathrm{PGL}(2, \mathbb{C})$ group acting on the Seiberg-Witten curve we have found that the same genus factorizations of curves with (N_c, N_f) are equivalent to $(N_c, 2N_c)$, but with $2N_c - N_f$ of the masses being equal. Especially, the vacua solutions for the case $N_f = 2N_c$ are equivalent to the solutions of $N_f = 2N_c - 1$ (or less flavours). So, in principle, we can always consider $N_f < 2N_c$. However, one can also perform the analysis for $N_f = 2N_c$ in much the same way as above, but with some important modifications. The non-asymptotically free cases of $N_f > 2N_c$ can actually also be solved by our methods.

The method of solving the problem has been to study the one-form ω with prescribed poles and integral periods (the existence of which was shown in appendix A). The important new step here was to map the problem to the Jacobian of the reduced curve. This allows us to obtain the one-form ω and the meromorphic function x that is needed to solve the factorization problem. In the case without matter, we have further given a suggestion for $g-1$ equations of motions for the on-shell period matrix using hyperelliptic theta functions. Indeed, in the genus two case the equation gives the right constraint. Still, however, there remains the Schottky-like problem of solving the equations within the space of hyperelliptic period matrices, which only is a $2g-1$ dimensional subset of the Siegel upper half space of symmetric matrices with positive imaginary part.

The $g-1$ equations of motion has the interpretation of demanding that the point on the Jacobian determined by the integral periods of ω, i.e. N_i and Δk_i, really is a point on the hyperelliptic one-dimensional curve. The period matrix is then determined in g parameters, the last continuous parameter of the solution being an overall translation that the period matrix does not depend on.

Note here the reduction in the number of equations of motion: We start by $g+1$ equations of motion obtained by e.g. varying in terms of the glueball superfields S_i with $i = 1, \ldots, g+1$.

The case with fundamental matter is more complicated, and here we actually get $(N_f+1)(g-1)$ equations in $g-1+gN_f$ parameters with further N_f constraints that the mass points on the Jacobian should really correspond to the given masses. One of these last equations can further be traded for the extra continuous parameter in the solution.

But this still means a simplification. In the genus one-case we have no equations of motion to solve for the period matrix, and we have given the complete solution (taken from [3]). The solution for the genus zero case was also obtained in an easy way. For the higher genus cases we have described exactly how to construct the solution of the problem, e.g. by obtaining all u_ks, once the on-shell period matrix has been found. The genus two case could be solved by specifying the continuous parameters and then solve for the remaining component of the period matrix numerically using the new equation of motion. The solution with the given parameters can then be constructed.

Using the solution we have also seen the action of the multiplication map that embeds solutions with gauge group $U(N_c)$ into solutions with gauge group $U(tN_c)$, t being integer but, as in the $\mathrm{PGL}(2,\mathbb{C})$ case, without changing the genus. It would be nice to investigate these mappings of solutions even further for instance considering genus changing transformations like $x \mapsto x^t$ in the Seiberg-Witten curve.

Finally, we have also given a crude investigation of the global structure of $\mathcal{N} = 1$ vacua. We have seen that we have a discrete parameter $k = 1, \ldots, 2N_c - N_f$ labelling the equivalent vacua. We also found that the structure is directly related to the choice of explicit curves in the canonical homology basis, and we have given the allowed transformations between the N_is, Δk_is and τ. Further, we have seen that also k changes with the transformations and what the meaning of these changes is on the Jacobian. For the case with flavours, the Jacobian also plays an important role and we saw that the N_is and Δk_is could be exchanged by the position of the flavour points in the covering of the Jacobian, $\mathbb{C}^g$.

It would be interesting to pursue a better understanding of the global structure of the vacuum moduli space by a more detailed analysis along the lines of [62, 77, 63, 64]. There might be new discrete parameters when solving the $g - 1$ equations of motion for the period matrix, but we got a good understanding of how to obtain the relations between $N_i, \Delta k_i$ and k. The analysis of the connected components of vacua and the dual descriptions of the same physics is dependent on these relations between the discrete parameters.

Further, it would be nice to extend the analysis to other classical gauge groups and more complicated matter. As we saw in chapter 2, the Seiberg-Witten curves for e.g. the $SO(N)$ gauge groups are rather similar, and an extension to these groups seems natural (see also [59, 53] for the genus zero cases). Also quiver gauge theories would be interesting to consider since we here are faced with non-hyperelliptic curves, and the integrality of the periods also plays an important role here [138]. Actually, our considerations above might be useful in these cases too. The places were we really depended on the curve being hyperelliptic was in the determination of the branch points. It might be possible to find these for the non-hyperelliptic curves in question as well.

Another interesting line of investigation is the implications for the low energy potential (on-shell effective superpotential). The couplings in the tree-level superpotential g_k and the coefficients, f_i, of $f_{n-1}(x)$ can be obtained directly using (2.58) both in terms of our $g + 1$ continuous parameters (this is, for simplicity, the case where the degree of the tree-level superpotential is $g + 2$). Notice that this comparison is particularly easy to do since the roots of y_{red} simply is given by the constructed meromorphic function x used on the derived values of the branch points on the Jacobian. The effective potential itself can be obtained by (2.51). It would be important to get the expectation values of the glueball superfields $\langle S_i \rangle (g_k)$. Naturally, this should be examined in more detail, especially for the two-cut case where we have found the exact solution with matter (see also [139]).

At last, let us mention that it would be interesting to investigate more special points of the moduli space where we have e.g. higher order roots, etc. (see e.g. [140]). The investigation of such points are especially important in light of the connection that was found between rigid factorizations of Seiberg-Witten curves and Grothendieck's "dessins d'enfants" [141]. Here rigid factorization means that the factorization problem should leave only an overall translation parameter free. Grothendieck's programme of classifying these "dessins d'enfants" into orbits of the Galois groups is conjectured to be related to the classification of special phases of the $\mathcal{N} = 1$ vacua.

Chapter 5

Black Holes on a Circle

In this chapter we will very briefly outline the knowledge of static and neutral Kaluza-Klein black holes on a circle. Even though we only need the results for the five-dimensional case to study the three-charge black holes on a circle in the next chapter, we will state the results in general dimensions here.

The review is based on [8] and [142], but see also [9].

5.1 Mass and Tension

The objects of our interest in this chapter are black holes on a circle. Hereby we mean a (physically reasonable) object in gravity with at least one horizon that asymptotes to Minkowski space times a circle (Kaluza-Klein space). Further, we make the important restriction in our study to only consider static metrics (especially no angular momentum) and in this chapter we will also assume the solutions to be neutral.

5.1.1 Asymptotics

Denoting the total dimension D, the solutions should asymptote to $\mathcal{M}^d \times S^1$ with $D = d + 1$. Here $\mathcal{M}^d$ denotes d-dimensional Minkowski space. We write the asymptotic metric of $\mathcal{M}^d \times S^1$ as

$$ds^2 = -dt^2 + dr^2 + r^2 d\Omega_{d-2}^2 + dz^2, \tag{5.1}$$

where t is the time coordinate of $\mathcal{M}^d$, and r is its radial coordinate, while $d\Omega_{d-2}$ describes the angular coordinates. The coordinate of S_1 is denoted z which we assume to have period L, i.e. the radius of the circle is $L/2\pi$.

As shown in [104] the leading behaviour of the metric $g_{\mu\nu}$ is determined by the two quantities c_t and c_z defined by (for a localised object)

$$g_{tt} \simeq -1 + \frac{c_t}{r^{d-3}}, \quad g_{zz} = 1 + \frac{c_z}{r^{d-3}}, \tag{5.2}$$

and the rest of the leading behavior of the metric can be written in these two variables by gauge choice.

We then expect that we will have two physical quantities that we can measure. Indeed, these two quantities turn out to be the mass and the tension along the circle, and these are all the long-range quantities that we can measure. The latter arises because of the self-interaction of the black hole over the circle. It can be seen as measuring the binding energy of the configuration when we use the covering space of the circle.

5.1.2 Calculation of mass and tension

To calculate the mass, M, and tension, $\mathcal{T}_z$, in terms of c_t and c_z let us use the method of equivalent sources (following [143]): Replace the black hole with an everywhere weakly gravitating (and hence horizonless) object that has the same asymptotics. Let us abuse the notation and also denote its metric by $g_{\mu\nu}$. We split the metric as

$$g_{\mu\nu} = \eta_{\mu\nu} + h_{\mu\nu}, \tag{5.3}$$

where we consider $h_{\mu\nu}$ to be small. In the linear approximation to gravity we consider $h_{\mu\nu}$ to leading order and can therefore raise and lower by the Minkowski metric. The linearised equations of motion are then

$$-\frac{1}{2}\left(\Box h_{\mu\nu} + {h_\lambda}^{\lambda}{}_{,\mu\nu} - {h_\mu}^{\lambda}{}_{,\nu\lambda} - {h_\nu}^{\lambda}{}_{,\mu\lambda}\right) = 8\pi G_D S_{\mu\nu}, \tag{5.4}$$

where G_D is the D-dimensional Newton's constant. $S_{\mu\nu}$ is related to the energy-momentum tensor $T_{\mu\nu}$ (containing both the gravitational and the matter part) as $S_{\mu\nu} \equiv T_{\mu\nu} - \frac{1}{D-2} g_{\mu\nu} T$. This can be reversed as

$$T_{\mu\nu} \simeq S_{\mu\nu} - \frac{1}{2}\eta_{\mu\nu} S. \tag{5.5}$$

Let us assume that the equivalent metric only depends on r (the real metric will also depend on z (see next section), but we assume an asymptotic ∂_z Killing vector). Further, we assume it has a diagonal form (remember we assumed static metrics). What we are interested in are the physical parameters which are integrals of T_{ij} over all of space. By (5.4) we see that the energy-momentum tensor is diagonal and thus the non-zero components are T_{tt}, T_{zz} and T_{ii}, where i indexes the spatial directions of Minkowski space. However, the integral over T_{ii} is zero by the energy-momentum conservation $\partial_i T_{ij} = 0$. This follows from $T_{ii} = \partial_i(x^j T_{ij})$ and Gauss' law. All that remains is thus the integrals over T_{tt} and T_{zz} which we define to be the mass (as usual) and (minus) L times the tension:

$$M = \int d^{D-1}x\, T_{tt}, \quad L\mathcal{T}_z = -\int d^{D-1}x\, T_{zz}. \tag{5.6}$$

Since T_{ii} integrates to zero, we get from (5.5) that under integration we can use $S = 2(S_{tt} - S_{zz})/(D-2)$. Thus we get

$$
\begin{aligned}
M &= \frac{1}{D-4} \int d^{D-1}x \; ((D-3)S_{tt} - S_{zz}) = \frac{\Omega_{d-2} L}{16\pi G_D} [(d-2)c_t - c_z], \\
L\mathcal{T}_z &= \frac{1}{D-4} \int d^{D-1}x \; (-(D-3)S_{zz} + S_{tt}) = \frac{\Omega_{d-2} L}{16\pi G_D} [c_t - (d-2)c_z],
\end{aligned} \tag{5.7}
$$

where we have used (5.4) to write S_{tt} and S_{zz} as a total derivative of the metric, and then performed the integration using Gauss' law and the asymptotics of the metric.

Note, however, that we could have a constant $dtdz$ term in the metric. This would not violate the metric being static. But we can simply boost such a term away, since boosts are in the symmetry group of the background. On the other hand, starting from a solution as in (5.2) we can boost it. This means that the mass and tension defined above will change (the energy momentum tensor transforms as a special relativistic covariant tensor), but the formulae still hold.

These formulae can be generalised to branes [4], and in the case of non-flat asymptotics a more involved definition of the tension has been given in [143], see in general [144, 145, 146]. As an example consider the case where the asymptotic flat space is instead $\mathcal{M}^{D-k} \times \mathbb{T}^k$. Here $\mathbb{T}^k$ is the rectangular k-torus which has the coordinates z_a with $a = 1, \ldots, k$ and their periods are L_a. The asymptotics of the metric is in this case given by:

$$
g_{tt} \simeq -1 + \frac{c_t}{r^{D-k-3}}, \quad g_{z_a z_a} = 1 + \frac{c_a}{r^{D-k-3}}, \tag{5.8}
$$

where r is again the radial coordinate of the Minkowski space. In the same way as above, and with the same assumptions, the mass and tensions $\mathcal{T}_a$ in the z_a directions are:

$$
\begin{aligned}
M &= \frac{\left(\prod_{a=1}^k L_a\right) \Omega_{D-k-2}}{16\pi G_D} [(D-k-2)c_t - \sum_a c_a], \\
L_a \mathcal{T}_a &= \frac{\left(\prod_{a=1}^k L_a\right) \Omega_{D-k-2}}{16\pi G_D} [c_t - (D-k-2)c_a - \sum_{b \neq a} c_b], \quad a = 1, \ldots, k.
\end{aligned} \tag{5.9}
$$

5.1.3 Dimensionless quantities

In order to be able to compare the Kaluza-Klein solutions that we will discuss below, we need to define dimensionless quantities for the mass and tension. General relativity does not contain a scale in itself, but the Kaluza-Klein space contains the length scale L that it is natural to rescale our quantities with. It turns out that the equations takes the most simple form if we define the rescaled mass μ and the relative tension n as (here in the case with one circle):

$$\mu = \frac{16\pi G_D}{L^{d-2}} M = \frac{\Omega_{d-2}}{L^{d-3}}[(d-2)c_t - c_z],$$
$$n = \frac{L\mathcal{T}_z}{M} = \frac{c_t - (d-2)c_z}{(d-2)c_t - c_z}. \tag{5.10}$$

Importantly, these dimensionless quantities are bounded. Of course, the mass has the lower bound $\mu \geq 0$, but it turns out that the relative tension is actually bounded both from above and below:

$$0 \leq n \leq d-2. \tag{5.11}$$

Here the lower bound of positive tension was found in [147, 148]. The proof is similar to the proof of the Positive Energy Theorem [104]. The upper bound is due to the Strong Energy Condition and basically ensures that gravity is not repulsive in the asymptotic region [104].

5.2 The Ansatz

Let us now consider what happens if we assume that the solutions have a local $SO(d-1)$ symmetry. Actually, all known solutions with $0 \leq n \leq 1/(d-2)$ have such a symmetry. Let us consider objects with a single connected horizon. The $SO(d-1)$ symmetry means that the topology of their horizon is either S^{d-1} or $S^{d-2} \times S^1$. The first case corresponds to localised black holes on the cylinder $R^{d-1} \times S^1$. When the radius of the circle is large (i.e. L large) these are like ordinary Schwarzschild-Tangherlini black holes, but they receive corrections due to the presence of the circle. In the case of $S^{d-2} \times S^1$ horizon topology we speak of black strings that wind around the circle. If the solution does not depend on z we speak of a uniform black string, otherwise we have a non-uniform string.

These solutions – and the copied versions thereof – are all captured by the following ansatz for the metric derived by the local $SO(d-1)$ symmetry [84],

$$ds^2 = -f dt^2 + \frac{L^2}{(2\pi^2)}\left[\frac{A}{f} dR^2 + \frac{A}{K^2} dv^2 + K R^2 d\Omega_{d-2}^2\right], \qquad f = 1 - \frac{R_0^{d-3}}{R^{d-3}}. \tag{5.12}$$

In this ansatz the metric is specified by the two functions $A(R,v)$ and $K(R,v)$ where R and v are dimensionless parameters, and v is periodic with 2π. One has furthermore that $A(R,v)$ can be found explicitly in terms of $K(R,v)$ [84]. The horizon is located at $R = R_0$. See [84, 85, 86, 149] for more on this ansatz.

To refer back to the asymptotic metric written in the parameters r and z, we note that in the asymptotic region (R large) we have $r \simeq LR/2\pi$ and $z \simeq Lv/2\pi$.

Thus $A, K \to 1$ as $R \to \infty$. Further, we can determine the mass and tension by the asymptotics of K:

$$K(R, v) = 1 - \chi \frac{R_0^{d-3}}{R^{d-3}} + \mathcal{O}\left(R^{-2(d-3)}\right). \tag{5.13}$$

The asymptotics of $A(R, v)$ is, as noted, related to this and actually it turns out that asymptotically $A(R, v) \simeq K(R, v)$. Thus the rescaled mass and relative tension becomes by (5.10)

$$\mu = \frac{(d-3)\Omega_{d-2}}{(2\pi)^{d-3}} R_0^{d-3} \left(\frac{d-2}{d-3} - \chi\right), \quad n = \frac{1-(d-2)(d-3)\chi}{d-2-(d-3)\chi}. \tag{5.14}$$

5.3 Thermodynamics

In this section we consider black holes on a circle with a single connected horizon. As we know, black holes can be seen as thermodynamic objects obeying the four (classical) black hole mechanics laws [150]. These are in complete analogy with the laws of thermodynamics. The (Hawking) temperature of the black hole is (Boltzmann's constant and the speed of light are taken to one)

$$T = \frac{\hbar\kappa}{2\pi}, \tag{5.15}$$

where κ is the surface gravity on the horizon which by the laws of black hole mechanics is constant on the horizon. This is thus the same as the 0th law of thermodynamics saying that the temperature is constant throughout an object in thermal equilibrium. Often it is much easier to calculate the temperature by performing a Wick rotation and demanding that the Wick rotated time has a period, the inverse of which is the temperature, such that we avoid a conical singularity.

The (Bekenstein-Hawking) entropy was identified by Bekenstein [151, 152] as being proportional to the area, A, of the horizon. The precise relation is

$$S = \frac{A}{4\hbar G_D}. \tag{5.16}$$

This means that the first law of thermodynamics is of the form $\delta M = T\delta S$ plus work terms involving the long-range quantities. In our case we have seen that the only other asymptotic quantity that we have is the tension. The first law then takes the form [105, 86, 146]

$$\delta M = T\delta S + \mathcal{T}_z\, \delta L. \tag{5.17}$$

In the next chapter we will also have a term for the charges of the black holes. Further, the second law states that the area of the horizon (the entropy) always increases in a (classical) physical process, and the third law that we can not achieve zero surface gravity (zero temperature) by such a process.

Also very useful is the Smarr formula (the integrated form of the first law) which in the case with tension takes the form [104, 105]

$$(d-1)TS = (d-2)M - L\mathcal{T}_z. \tag{5.18}$$

This can be proven using Hamiltonian methods [153]. Note that the Smarr formula provides a nice check of the quantities that we can obtain by other means.

5.3.1 Rescaled entropy and temperature

Again it useful to introduce dimensionless versions of the thermodynamical quantities. The rescaled temperature, $\mathfrak{t}$, and rescaled entropy, $\mathfrak{s}$, are defined as:

$$\mathfrak{t} = LT, \quad \mathfrak{s} = \frac{16\pi G_D}{L^{d-1}} S. \tag{5.19}$$

The first law written in terms of dimensionless quantities takes the simple form (using the Smarr formula)

$$\delta\mu = \mathfrak{t}\delta\mathfrak{s}, \tag{5.20}$$

while the Smarr formula becomes

$$(d-1)\mathfrak{t}\mathfrak{s} = (d-2-n)\mu. \tag{5.21}$$

5.3.2 Thermodynamics of the ansatz

Using the ansatz introduced in the last section, we can write the entropy and temperature in terms of A_h which is the value of $A(R,v)$ on the horizon, which is at $R = R_0$. Actually, by the equations of motion it turns out that $A(R,v)$ does not depend on v on the horizon, so A_h is well-defined. We get

$$\mathfrak{t} = \frac{d-3}{2\sqrt{A_h}R_0}, \quad \mathfrak{s} = \frac{4\pi\Omega_{d-2}}{(2\pi)^{d-2}}\sqrt{A_h}R_0^{d-2}. \tag{5.22}$$

5.4 Phases of Kaluza-Klein Black Holes

An important tool in investigating the Kaluza-Klein black holes on a circle is the (μ, n) phase diagram. We have already seen that the diagram is restricted by $\mu > 0$ and $0 \le n \le d-2$. What we really want to know is the plot of all solutions in this diagram. In this section we will review the present knowledge of this.

Importantly, we can also obtain the thermodynamics from the (μ, n) phase diagram. Suppose that we for a phase know the relative tension in terms of μ, $n(\mu)$, then we can obtain the entropy, $\mathfrak{s}(\mu)$, as a function of μ using

$$\frac{\delta \log \mathfrak{s}}{\delta \log \mu} = \frac{d-1}{d-2-n}, \tag{5.23}$$

which is obtained using the Smarr formula (5.21) and the first law of thermodynamics (5.20).

This also gives the intersection rule presented in [104]: Suppose that two branches intersect at a point (μ_0, n_0). Then for masses above μ_0 the branch with the highest entropy also has the highest relative tension n and oppositely for masses lower than μ_0.

5.4.1 Phases with Kaluza-Klein bubbles

As mentioned in last section, no solutions have been found without local $SO(d-1)$ symmetry for $0 \leq n \leq 1/(d-2)$. However, for $1/(d-2) < n < d-2$ we have solutions without this symmetry, but they involve Kaluza-Klein bubbles.

The simplest case is where we have a single static Kaluza-Klein bubble, which simply is the Euclidean rotation of the d-dimensional Schwarzschild black hole where we add a trivial time direction:

$$ds^2 = -dt^2 + \left(1 - \frac{R^{d-3}}{r^{d-3}}\right) dz^2 + \left(1 - \frac{R^{d-3}}{r^{d-3}}\right)^{-1} dr^2 + r^2 d\Omega_{d-2}. \tag{5.24}$$

Here z has to be periodic with $L = 4\pi R/(d-3)$ to avoid a conical singularity. We can then calculate the rescaled mass and relative tension using (5.10) giving us

$$\mu = \Omega_{d-2} \left(\frac{d-3}{4\pi}\right)^{d-3}, \quad n = d-2. \tag{5.25}$$

Thus we see that the bubble satisfies the bound $n \leq d-2$.

For $d = 4$ and $d = 5$ exact solutions with a black hole attached to a Kaluza-Klein bubble were constructed by Emparan and Reall [87] using a generalised Weyl ansatz. This was developed further in [88, 89] to more general sequences of bubbles and black holes where the bubbles balance the gravitational attraction between the black holes. One then obtains a very rich phase structure for the range $1/(d-2) < n \leq d-2$. We will, however, not go into further details of this part of the phase diagram, but focus on the part with $n \leq 1/(d-2)$. As we discussed above all known solutions in this part of the diagram has $SO(d-1)$ symmetry and thus fall into three categories: The localised black holes, the uniform and the non-uniform black strings.

5.4.2 The localised black hole branch

As mentioned above, the localised black holes have horizon topology S^{d-1} and correspond to black holes that are localised on the circle S^1. For $\mu \to 0$ these are the higher dimensional Schwarzschild black holes, especially, $n \to 0$ as $\mu \to 0$. But for μ finite we get corrections due to the circle. The localised black hole can be written in the ansatz (5.12), see [84, 86, 85]. The ansatz was used to find the metric to first order in μ in [90], see also [91, 92]. This allows one to find the relative tension to first order in μ. Actually, using the results of [93, 94] we can give the result to second order

$$n = \frac{(d-2)\zeta(d-2)}{2(d-1)\Omega_{d-1}}\mu - \left(\frac{(d-2)\zeta(d-2)}{2(d-1)\Omega_{d-1}}\mu\right)^2 + \mathcal{O}(\mu^3), \tag{5.26}$$

where $\zeta(p)$ is Riemann's zeta function.

The thermodynamics of this branch can be obtained to the next-to-leading order in μ using (5.26) in (5.23)

$$\mathfrak{s}(\mu) = C_1^{(d)}\mu^{\frac{d-1}{d-2}}\left(1 + \frac{\zeta(d-2)}{2(d-2)\Omega_{d-1}}\mu - \frac{d^2-6d+7}{2(d-1)}\left(\frac{\zeta(d-2)}{2(d-2)\Omega_{d-1}}\mu\right)^2 + \mathcal{O}(\mu^3)\right), \tag{5.27}$$

where $C_1^{(d)}$ is a constant of integration that can be fixed by comparing with the Schwarzschild black hole in the limit $\mu \to 0$

$$C_1^{(d)} = 4\pi(\Omega_{d-1})^{-\frac{1}{d-2}}(d-1)^{-\frac{d-1}{d-2}}. \tag{5.28}$$

5.4.3 The uniform black string phase

The uniform black string with horizon topology $S^{d-2}\times S^1$ is simply the Schwarzschild-Tangherlini black hole with the circle added [154]

$$ds^2 = -\left(1 - \frac{r_0^{d-3}}{r^{d-3}}\right)dt^2 + \left(1 - \frac{r_0^{d-3}}{r^{d-3}}\right)^{-1}dr^2 + r^2 d\Omega_{d-2}^2 + dz^2. \tag{5.29}$$

Since $c_z = 0$ we directly get from (5.10) that

$$n = \frac{1}{d-2}. \tag{5.30}$$

And the mass is simply

$$\mu = \frac{(d-2)\Omega_{d-2}}{L^{d-3}}r_0^{d-3}. \tag{5.31}$$

Thus the phase is simply a horizontal line in our phase diagram. To get the thermodynamics note that metric is the trivial solution in the ansatz (5.12) with $A(R,v) = 1$ and $K(R,v) = 1$ with the identifications $R = 2\pi r/L$ and $v = 2\pi z/L$ and thus $R_0 = 2\pi r_0/L$. Then by (5.22)

$$\mathfrak{t} = \frac{d-3}{4\pi r_0}L, \quad \mathfrak{s} = 4\pi\Omega_{d-2}\left(\frac{r_0}{L}\right)^{d-2}. \tag{5.32}$$

Solving for $\mathfrak{s}(\mu)$ we get

$$\mathfrak{s}(\mu) = C_1^{(d-1)}\mu^{\frac{d-2}{d-3}}, \tag{5.33}$$

where C_1^{d-1} was defined in (5.28).

Gregory and Laflamme found in [98, 99] that the uniform black string is classically unstable for $\mu < \mu_{\rm GL}$ where μ_{GL} is the Gregory-Laflamme mass. This mass depends on the dimension. It can be determined numerically, and for the five-dimensional black string that we will use in the next chapter one has $\mu_{\rm GL} \simeq 3.52$. At $\mu = \mu_{\rm GL}$ we have a marginal mode [100] and this means that we have a new static branch which emanates from this point. This is the non-uniform black string. See also review in [142].

5.4.4 The non-uniform black string phase

The non-uniform black string has the same horizon topology, $S^{d-2} \times S^1$, as the uniform string, but it is non-uniformly distributed over the circle.

This branch has only been determined numerically (except for large d) and the results can be found in [100, 101, 102, 103]. It emanates from the uniform black hole branch at $(\mu, n) = (\mu_{\rm GL}, 1/(d-2))$ and has $n \leq 1/(d-2)$. An important parameter is the slope γ where it meets the uniform branch

$$n(\mu) = \frac{1}{d-2} - \gamma(\mu - \mu_{\rm GL}) + \mathcal{O}((\mu - \mu_{\rm GL})^2). \tag{5.34}$$

γ can be found numerically and in the five-dimensional case ($d = 4$) we have $\gamma \simeq 0.14$. Importantly, γ is positive for $d < 13$, but is negative for $d \geq 13$ meaning that the branch starts off in the negative μ direction. Using the intersection rule explained in the beginning of this section this means that the non-uniform black string for $d \geq 13$ has a higher entropy than the unstable uniform string for the range it exists at $\mu < \mu_{\rm GL}$. In this range it is possible that the unstable uniform string can decay to a non-uniform string. For $d < 13$ this is not possible, but it is possible that it decays to a localised black hole since this has higher entropy comparing (5.33) and (5.27) for small μ. For $d = 4, 5$ this holds for all $\mu < \mu_{\rm GL}$.

5.4.5 The $d = 4$ phase diagram

Also the localised face has been investigated numerically and the results are found in [97] (see also [95, 96]). In the case of $d = 4$ the results for the (μ, n) phase diagram with $0 \leq n \leq 1/2$ are plotted in figure 5.1.

As we see from this diagram, and which is even more clear in the six-dimensional case, it seems like the localised and non-uniform branch meet in some merger point. This is in support of the suggestion by Kol [155] that the branches meet in a merger point where the topology changes.

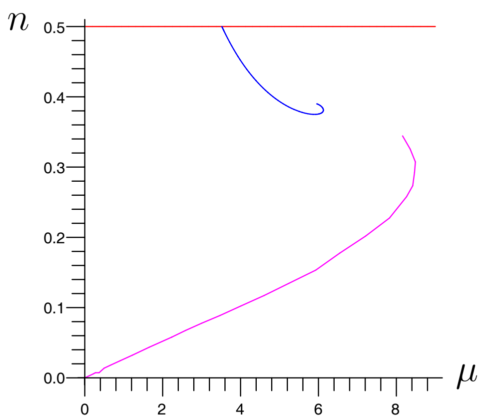

Figure 5.1: Diagram with μ versus n for the uniform black string (red), non-uniform black string (blue) and localized black hole phase (magenta) for five-dimensional Kaluza-Klein black holes, using numerical results of [97, 103]. The diagram is taken from [1].

5.4.6 Multi-black hole solutions

The diagram in figure 5.1 is, however, not the full story.

Firstly, we have copies: Given a solution in the non-uniform or localised phase we can simply copy it k times on the circle [156, 86, 4]. This produces an infinite number of phases that are copies of the two phases that are non-uniform on the circle.

Referring to the ansatz (5.12) we obtain for any $k = 2, 3, ...$ a new solution with $A'(R, v) = A(kR, kv)$, $K'(R, v) = K(kR, kv)$ and $R_0' = R_0/k$. In terms of μ, n and the thermodynamical quantities $\mathfrak{s}$ and $\mathfrak{t}$ this means using (5.14) and (5.22)

$$\mu' = \frac{\mu}{k^{d-3}}, \quad n' = n, \quad \mathfrak{s}' = \frac{\mathfrak{s}}{k^{d-2}}, \quad \mathfrak{t}' = k\mathfrak{t}. \tag{5.35}$$

Further, it was recently shown in [157] that there exist more general multi-black solutions. E.g. consider two small black holes on the circle placed oppositely to each other. For the copy solutions these two black holes have the same mass, but also solutions with different mass are possible. These more general solutions are in mechanical equilibrium, but it is not stable since a small perturbation will cause the system to collapse into a single black hole. For small masses it also turns out that they are neither in thermal equilibrium, except for the copies, since the temperatures for each of the black holes are different. It is, however, conceivable that the temperatures converge in the non-perturbative regime.

The existence of several dimensionless continuous parameters (the relative masses) for these multi-black hole solutions means that we have a continuity of non-uniqueness

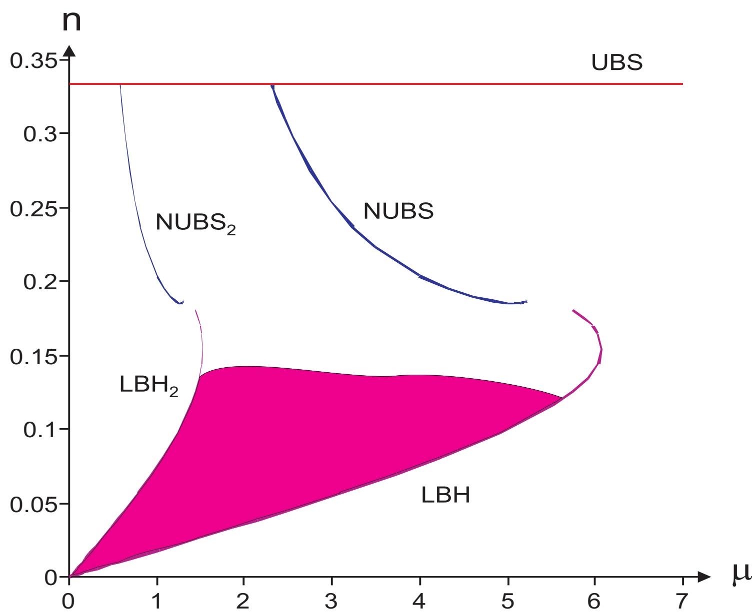

Figure 5.2: The (μ, n) phase diagram for $d = 5$ showing the phase with two-black hole configurations which fills the region between the localised black hole phase (LBH) and its copy with two equal size black holes (LBH_2). Also shown in the figure are the uniform black string phase (UBS), the non-uniform phase (NUBS) and its two copied phase (NUBS_2). The diagram taken from [157].

in the phase diagram (as also happens for the Kaluza-Klein bubbles and black holes sequences for $n > 1/(d-2)$). The phase with k black holes will, for small masses, lie between the localised black hole phase and the phase where it is copied k times. In figure 5.2 we show this for the solution with two black holes. Also note that for larger masses the phases may fan out and cross the phases of the single black hole and its copy.

Finally, the results on the multi-black hole phases points to the existence of new non-uniform black strings, new equilibrium phases, and also the possibility of a class of new "lumpy" black holes.

Also note the interesting recent work [158] where the phase structure of Kaluza-Klein black holes is mapped to phases of stationary black rings and black holes in asymptotically flat non-compact space.

In the next chapter we will show how to create three-charge solutions given one of the five-dimensional neutral and static black holes on a circle that we have examined in this chapter.

Chapter 6

Three-Charge Black Holes on a Circle

This chapter is a modified version of [1], for a review see [2].

As mentioned in the introduction, three-charge black holes play a prominent role in the understanding of the Bekenstein-Hawking entropy. In this chapter we will examine five-dimensional versions of these on a circle.

6.1 Generating Three-Charge Solutions from Kaluza-Klein Black Holes

In this section we will present the non-extremal three-charge solution generated from a neutral Kaluza-Klein black hole in 4+1 dimensions (reviewed in last chapter). The neutral solution is referred to as the *seeding solution*. Further, we will see how to calculate the physical quantities of the new three-charge solution given the seeding solution.

6.1.1 Three-charge configuration on a circle

The system that we are interested in is a three-charge solution of Type IIA Supergravity that describes a thermal excitation of the 1/8-BPS configuration with an F1-string, D4-brane and a D0-brane. The configuration is a solution to the equations of motion of the action

$$I = \frac{1}{16\pi G_{10}} \int d^{10}x\sqrt{-g}\Big(R - \frac{1}{2}\partial_\mu\phi\partial^\mu\phi - \frac{1}{12}e^{-\phi}(dB)^2 - \frac{1}{2\cdot 6!}e^{-\frac{1}{2}\phi}(dA_{(5)})^2 - \frac{1}{4}e^{\frac{3}{2}\phi}(dA_{(1)})^2\Big) \quad (6.1)$$

where ϕ is the dilaton field, B is the Kalb-Ramond two-form field and the $A_{(i)}, i = 5, 1$ are the gauge fields that couple to the D4-brane and the D0-brane, respectively. This is the low energy action of Type IIA String Theory when the only gauge fields present are the ones that correspond to the three extended objects that we are interested in. Note that the action is written in Einstein frame which we will use throughout.

The extremal 1/8-BPS solution of the action (6.1) is well known and can be found *e.g.* by using the harmonic rule [20, 159, 160]. The metric for such a solution consists of a world-volume part for the extended objects times a transverse space which will be four-dimensional if the extended objects do not intersect. It is important that the non-compact part of the transverse space has at least three dimensions in order to be able to measure asymptotic quantities. We are interested in solutions where the transverse space asymptotes to $\mathbb{R}^3 \times S^1$. The compact transverse circle gives rise to some interesting physics that we wish to explore.

The solution can be compactified on T^5 which is spanned by the spatial world-volume directions of the D4-brane and the F1-string. This gives a five-dimensional black hole with three charges that can be compared to the extremal solution of Strominger and Vafa [16]. We choose to consider the F1-D0-D4 configuration instead of the more traditional P-D1-D5 configuration because the background turns out to be simpler, it has diagonal metric and the objects do not share spatial world-volume directions. The systems are, however, T-dual.

6.1.2 Generating F1-D4-D0 solutions

The main idea of the present chapter is that we can generate charged solutions of the type described above, starting from a neutral 4+1 dimensional Kaluza-Klein black hole. A $d+1$ dimensional static and neutral Kaluza-Klein black hole is, as mentioned in last chapter, defined here as a pure gravity solution that has at least one event horizon and asymptotes to d-dimensional Minkowski-space times a circle at infinity. As we have reviewed, the thermodynamics of these kinds of Kaluza-Klein black holes has been studied extensively and there are both numerical and analytical results available about their different phases. The key observation is that we can translate information about the thermodynamics of the well-studied seeding solutions into information about the thermal three-charge configuration in ten-dimensional supergravity with a transverse circle where little or nothing was known before.

Let us start with a static and neutral five-dimensional Kaluza-Klein black hole as a seeding solution. There is no dilaton and no gauge fields and we assume that the metric can be written in the form

$$ds_5^2 = -Udt^2 + \frac{L^2}{(2\pi)^2} V_{ab} dx^a dx^b \tag{6.2}$$

where U is a non-constant function that vanishes at the horizon(s) and asymptotes to one, and $V_{ab}dx^a dx^b$ describes a cylinder of circumference 2π in the asymptotic region. The metric should in other words asymptote to (5.1)

$$ds^2 = -dt^2 + dr^2 + r^2 d\Omega_2^2 + dz^2 \tag{6.3}$$

where z is periodic with period L. We will refer to the dimensionful coordinates r and z when discussing the asymptotic behavior of the full metric.

By adding five flat dimensions x and u_i, $i = 1, ..., 4$, to the neutral solution (6.2), and performing a series of boosts and U-dualities, we can construct a ten-dimensional solution of Type IIA Supergravity with three charges. Each boost adds one charge which depends on the rapidity parameter α of the boost. The derivation is sketched in Appendix C. The new solution has metric

$$\begin{aligned} ds_{10}^2 = H_1^{-\frac{3}{4}} H_4^{-\frac{3}{8}} H_0^{-\frac{7}{8}} \Bigg(& -Udt^2 + H_4 H_0 dx^2 + H_1 H_0 \sum_{i=1}^{4} (du^i)^2 \\ & + H_1 H_4 H_0 \frac{L^2}{(2\pi)^2} V_{ab} dx^a dx^b \Bigg), \end{aligned} \tag{6.4}$$

a dilaton ϕ given by

$$e^{2\phi} = H_1^{-1} H_4^{-\frac{1}{2}} H_0^{\frac{3}{2}}, \tag{6.5}$$

a Kalb-Ramond field given by

$$B = \coth\alpha_1 (H_1^{-1} - 1) dt \wedge dx, \tag{6.6}$$

and gauge fields

$$A_{(5)} = \coth\alpha_4 (H_4^{-1} - 1) dt \wedge du^1 \wedge du^2 \wedge du^3 \wedge du^4, \tag{6.7}$$

$$A_{(1)} = \coth\alpha_0 (H_0^{-1} - 1) dt. \tag{6.8}$$

The H_a are harmonic functions of the transverse space, given by

$$H_a = 1 + (1 - U)\sinh^2\alpha_a, \quad \text{for } a = 1, 4, 0. \tag{6.9}$$

This three-charge solution describes a non-extremal configuration with an F1-string, D4-brane and D0-brane. The label $a = 1, 4, 0$ refers to the type of object. In the following we will refer to the fields B, $A_{(5)}$ and $A_{(1)}$ collectively as A_a.

We can perform one more U-duality and map this solution into a configuration with three non-extremal M2-branes which is an excitation of a known 1/8-BPS state.

6.1.3 Measuring asymptotic quantities

The physical quantities of the configuration that can be measured asymptotically far away in the transverse space are the mass, the three different kind of charges, and, since we have a compact circle in the transverse space, the tension in the direction of the circle. The tension measures how hard the black hole pulls itself across the circle and has an interpretation as the binding energy of the black holes in the covering space of the circle. For extremal BPS black holes there is no net force between the black holes in the covering space because the electric force exactly cancels the gravitational force and the tension therefore is zero. For non-extremal black holes this is not the case and more interesting physics appears. We now show how information about all these quantities can be mapped from the neutral seeding solution to the new three-charge solution.

It is useful to assume that each spatial world-volume direction x and u^i is compactified on a circle of length L_x and L_{u^i} respectively. This gives us two rectangular tori with volumes V_1 and $V_4 = \prod_i L_{u^i}$. In the asymptotic region of the transverse space the components of the metric can be expanded to leading order[1] in r

$$g_{tt} \simeq -1 + \frac{\bar{c}_t}{r}, \quad g_{zz} \simeq 1 + \frac{\bar{c}_z}{r} \tag{6.10}$$

$$g_{xx} \simeq 1 + \frac{\bar{c}_x}{r}, \qquad g_{ii} \simeq 1 + \frac{\bar{c}_u}{r}, \quad \text{for } i = 1, ..., 4, \tag{6.11}$$

and the dilaton and the non-vanishing components of the gauge fields are to leading order

$$\phi \simeq \frac{\bar{c}_\phi}{r}, \qquad (A_a)_{t\ldots} \simeq \frac{\bar{c}_{A_a}}{r}, \quad \text{for } a = 1, 4, 0. \tag{6.12}$$

The non-vanishing gauge field components are the same as in equations (6.6)–(6.8).

The total mass and the total tension along any compact direction can be found from the asymptotic behavior of the metric using the general formulae of [143] (see also [145, 146]). Following [4, 143] we find the mass and charge via (see eq. (5.9))

$$\bar{M} = \frac{\Omega_2}{gL} \left(2\bar{c}_t - \bar{c}_z - \bar{c}_x - 4\bar{c}_u\right) \tag{6.13}$$

$$Q_a = -\frac{\Omega_2}{gL} \bar{c}_{A_a} \tag{6.14}$$

where we have defined

$$g \equiv \frac{16\pi G_{10}}{V_1 V_4 L^2}. \tag{6.15}$$

The dimensionful parameter g is useful to define dimensionless mass and charge as

$$\bar{\mu} \equiv g\bar{M}, \qquad q_a \equiv gQ_a. \tag{6.16}$$

[1]Note that the dependence on r really is in terms of $r^{(d-3)}$ where d is the number of transverse dimensions which in this case is 4.

The tensions in the compactified directions are also found via (5.9)

$$L\bar{\mathcal{T}}_z = \frac{\Omega_2}{gL}\left(\bar{c}_t - 2\bar{c}_z - \bar{c}_x - 4\bar{c}_u\right) \tag{6.17}$$

$$L_x\bar{\mathcal{T}}_x = \frac{\Omega_2}{gL}\left(\bar{c}_t - \bar{c}_z - 2\bar{c}_x - 4\bar{c}_u\right) \tag{6.18}$$

$$L_{u^i}\bar{\mathcal{T}}_{u^i} = \frac{\Omega_2}{gL}\left(\bar{c}_t - \bar{c}_z - \bar{c}_x - 5\bar{c}_u\right). \tag{6.19}$$

The world-volume of the D0-brane has no spatial direction, but for calculational purposes we can still pretend that there is a "phantom" u^0 direction compactified on a circle of length L_0. The tension in that direction would then be given by

$$L_0\bar{\mathcal{T}}_0 = \frac{\Omega_2}{gL}\left(\bar{c}_t - \bar{c}_z - \bar{c}_x - 4\bar{c}_u - \bar{c}_0\right). \tag{6.20}$$

This is useful when we discuss the contribution of the D0-brane to the electric mass in the next subsection.

6.1.4 Mapping of physical quantities

To find how the physical quantities of the charged solution are related to the original seeding solution we write the asymptotics of the metric of the seeding solution as

$$-g_{tt}^{\text{seed}} = U \simeq 1 - \frac{c_t}{r}, \qquad g_{zz}^{\text{seed}} \simeq 1 + \frac{c_z}{r}. \tag{6.21}$$

Expressed in c_t and c_z the mass and tension of the seeding solution is given by (5.7)

$$M = \frac{\Omega_2 L}{16\pi G_5}(2c_t - c_z), \quad \mathcal{T}_z = \frac{\Omega_2 L}{16\pi G_5}(c_t - 2c_z). \tag{6.22}$$

Correspondingly we have the dimensionless mass, μ, and tension, n, given by (5.10)

$$\mu = \frac{16\pi G_5}{L^2}M = \frac{\Omega_2}{L}(2c_t - c_z), \quad n = \frac{\mathcal{T}L}{M} = \frac{c_t - 2c_z}{2c_t - c_z}. \tag{6.23}$$

By plugging the asymptotics (6.21) into the solution (6.4)–(6.9) and expanding to first order, we find a relation between the expansion coefficients of the new solution and the seeding solution. This relation is spelled out in Appendix D. Plugging into the equations for mass, charge and tension we get

$$\bar{M} = \frac{\Omega_2}{gL}\left(-c_z + c_t(2 + \sinh^2\alpha_1 + \sinh^2\alpha_4 + \sinh^2\alpha_0)\right), \tag{6.24}$$

$$Q_a = \frac{\Omega_2}{gL} c_t \sinh\alpha_a \cosh\alpha_a, \tag{6.25}$$

$$L\bar{\mathcal{T}}_z = \frac{\Omega_2}{gL}\left(c_t - 2c_z\right), \tag{6.26}$$

$$L_x\bar{\mathcal{T}}_x = \frac{\Omega_2}{gL}\left(-c_z + c_t(1 + \sinh^2\alpha_1)\right), \tag{6.27}$$

$$L_{u^i}\bar{\mathcal{T}}_{u^i} = \frac{\Omega_2}{gL}\left(-c_z + c_t(1 + \sinh^2\alpha_4)\right), \tag{6.28}$$

$$L_0\bar{\mathcal{T}}_0 = \frac{\Omega_2}{gL}\left(-c_z + c_t(1 + \sinh^2\alpha_0)\right). \tag{6.29}$$

Thus we have found how the physical quantities of the charged solution are given in terms of the boost parameters α_a and the two independent quantities c_t and c_z of the neutral solution.

The electric mass and tensions

The electric part of the mass and tensions are simply defined as the parts that go to zero when the charges Q_a vanish. We can directly read from equations (6.24) and (6.25) that

$$M^{\text{el}} = \sum_a \frac{\Omega_2}{gL} c_t \sinh^2\alpha_a. \tag{6.30}$$

We see that the electric mass consists of a three parts – one for each of the charged objects. Thus it is natural to define the electric mass M_a^{el} corresponding to the charge Q_a as

$$M_a^{\text{el}} = L_a(\bar{\mathcal{T}}_a)^{\text{el}} = \frac{\Omega_2}{gL} c_t \sinh^2\alpha_a, \tag{6.31}$$

for $a = 1, 4, 0$ $(x, u^i, 0)$. In this notation a can either label the type of object or one of the spatial world-volume directions of the corresponding object.

Note that the electric mass can be written as

$$M_a^{\text{el}} = \nu_a Q_a \tag{6.32}$$

where

$$\nu_a = \tanh\alpha_a \tag{6.33}$$

is the chemical potential. The chemical potential can also be measured as $\nu_a = -A_a|_{\text{Horizon}}$ which by setting $U = 0$ in (6.6)–(6.8) gives the same result.

We also note that the electric part of the tension $\mathcal{T}_z$ is zero. To see how all of this follows from the harmonic function rule in generality see Appendix E where the electric masses and tensions are calculated in detail.

The mapping of dimensionless quantities

In the Kaluza-Klein black hole literature it is customary to define a relative tension n as the total tension divided by the total mass. Branches of different types of static solutions are then plotted on a (μ, n) phase diagram, where μ is the dimensionless mass. This kind of phase diagrams will be discussed further in section 6.2.

For the charged black holes under consideration here, we define the relative tension along the z direction as [4]

$$\bar{n} \equiv \frac{L\bar{\mathcal{T}}_z}{\bar{M} - M^{\text{el}}} = \frac{c_t - 2c_z}{2c_t - c_z} \tag{6.34}$$

and the relative tension along each of the world-volume directions as

$$\bar{n}_a \equiv \frac{L_a(\bar{\mathcal{T}}_a - \bar{\mathcal{T}}_a^{\text{el}})}{\bar{M} - M^{\text{el}}} = \frac{c_t - c_z}{2c_t - c_z}. \tag{6.35}$$

Note that we have chosen to subtract the electrical contribution in these definitions. In equations (6.34)–(6.35) we have also written the relative tensions in terms of the seeding parameters c_t and c_z.

Writing the physical parameters $\bar{\mu}$, $\bar{n}$ and q_a in terms of the original quantities μ, n of the seeding solution and the boost parameters α_a gives

$$\bar{\mu} = \mu\left(1 + \frac{2-n}{3}(\sinh^2\alpha_1 + \sinh^2\alpha_4 + \sinh^2\alpha_0)\right), \tag{6.36}$$

$$q_a = \mu\frac{2-n}{3}\sinh\alpha_a\cosh\alpha_a, \quad \text{for } a = 1, 4, 0 \tag{6.37}$$

and finally

$$\bar{n} = n, \qquad \bar{n}_a = \frac{1+n}{3}. \tag{6.38}$$

We can solve equation (6.37) for $\cosh\alpha_a$ and get

$$\cosh\alpha_a = \sqrt{\frac{1}{2}\left(1 + \frac{1}{b_a}\sqrt{1+b_a^2}\right)} \tag{6.39}$$

with

$$b_a \equiv \frac{2-n}{6}\frac{\mu}{q_a}. \tag{6.40}$$

Given the values of the three charges, the map between the mass and relative tension of the neutral and charged solutions can therefore be written as

$$\bar{n} = n, \tag{6.41}$$

$$\bar{\mu} = \sum_a q_a + \frac{1}{2}\mu n + \frac{(2-n)\mu}{6}\sum_a \frac{b_a}{1+\sqrt{1+b_a^2}}. \tag{6.42}$$

This map from neutral to three-charge Kaluza-Klein black holes is one of our main results.

There are a few things to notice here. The neutral seeding solutions always have $\mu \geq 0$ and $0 \leq n \leq 2$ and therefore we see that for fixed q_a the mass $\bar{\mu}$ is bounded from below by $\sum_a q_a$. This is to be expected for a charged black hole. An object with mass smaller than its charge results in a naked singularity rather than a black hole. We therefore define the *energy above extremality* to be the mass minus the sum of the charges. Later we will see that $b_a \to 0$ in the near-extremal limit, and therefore

$$\epsilon \equiv \bar{\mu} - \sum_a q_a \to \frac{1}{2}\mu n \tag{6.43}$$

in that limit. The mass of the charged black hole can also be written as $\bar{\mu} = \mu + \sum_a \nu_a q_a$, where $\nu_a = \tanh \alpha_a$ is the chemical potential from equation (6.32).

If the seeding solution has a single connected horizon we can find its temperature T and entropy S from the metric. We will mostly work with rescaled temperature and entropy which are defined for the seeding solution as [8] (see (5.19))

$$\mathfrak{t} = LT, \quad \mathfrak{s} = \frac{16\pi G_5}{L^3} S. \tag{6.44}$$

For the three-charge solution we define the rescaled temperature and entropy analogously by

$$\bar{\mathfrak{t}} = L\bar{T}, \quad \bar{\mathfrak{s}} = \frac{g}{L}\bar{S}, \tag{6.45}$$

where g is given in equation (6.15). These quantities are calculated at the horizon where $U = 0$ and thus $H_a = \cosh^2 \alpha_a$. It is easy to see from the metric (6.4) that the three-charge solution therefore has temperature and entropy given by

$$\bar{\mathfrak{t}} = \mathfrak{t} / \cosh \alpha_1 \cosh \alpha_4 \cosh \alpha_0, \tag{6.46}$$

$$\bar{\mathfrak{s}} = \mathfrak{s} \cosh \alpha_1 \cosh \alpha_4 \cosh \alpha_0. \tag{6.47}$$

The factors of $\cosh \alpha_a$ cancel when we multiply the temperature and entropy and therefore the product

$$\bar{\mathfrak{t}}\bar{\mathfrak{s}} = \mathfrak{t}\mathfrak{s} \tag{6.48}$$

remains fixed. The generalized Smarr formula from [143] gives a relation between the temperature, entropy, and the gravitational mass for our three-charge solution in terms of the relative tension (can be seen directly from (5.21))

$$\bar{\mathfrak{t}}\bar{\mathfrak{s}} = \frac{2 - \bar{n}}{3} \left(\bar{\mu} - \mu^{\mathrm{el}} \right). \tag{6.49}$$

6.2 Non-Extremal Three-Charge Black Holes on a Circle

In this section we apply the map, that was found in section 6.1, to obtain three-charge black holes on a circle from neutral Kaluza-Klein black holes. We restrict ourselves to neutral black holes without Kaluza-Klein bubbles. We describe the three different phases that we obtain for three-charge black holes on a circle, using the map.

6.2.1 The neutral seeding solutions

We have seen in section 6.1 that we can transform five-dimensional static and neutral black hole solutions to three-charge solutions via boosts and U-dualities. The static and neutral black holes on a circle were reviewed in chapter 5. The classes of solutions that we consider as seeding solutions here, i.e. what solutions we will map to three-charge solutions, are essentially all solutions obeying the ansatz (5.12), which for $d = 4$ takes the form

$$ds^2 = -fdt^2 + \frac{L^2}{(2\pi^2)} \left[\frac{A}{f} dR^2 + \frac{A}{K^2} dv^2 + KR^2 d\Omega_2^2 \right] \quad , \quad f = 1 - \frac{R_0}{R}. \tag{6.50}$$

This means that we consider solutions without Kaluza-Klein bubbles and thus with the relative tension in the range $0 \leq n \leq 1/2$. We will focus on the three branches: The uniform black string, the non-uniform black string and the localized black holes (see section 5.4).

We have displayed the (μ, n) phase diagram for $0 \leq n \leq 1/2$ with the three types of solutions[2] in figure 5.1. We will review these three phases further as needed for describing the three-charge phases.

6.2.2 The ansatz for three-charge black holes on a circle

Using the map described in section 6.1.2, we map the ansatz (6.50) for neutral Kaluza-Klein black holes to the following ansatz for three-charge black holes:

$$\begin{aligned} ds_{10}^2 = H_1^{-\frac{3}{4}} H_4^{-\frac{3}{8}} H_0^{-\frac{7}{8}} \Bigg[& -fdt^2 + H_4 H_0 dx^2 + H_1 H_0 \sum_{i=1}^{4} (du^i)^2 \\ & + H_1 H_4 H_0 \frac{L^2}{(2\pi)^2} \left(\frac{A}{f} dR^2 + \frac{A}{K^2} dv^2 + KR^2 d\Omega_2^2 \right) \Bigg] , \end{aligned} \tag{6.51}$$

with

$$f = 1 - \frac{R_0}{R} \quad , \quad H_a = 1 + \frac{R_0 \sinh^2 \alpha_a}{R}, \quad \text{for } a = 1, 4, 0, \tag{6.52}$$

[2]Note that we also have the copied phases described in subsection 5.4.6.

and with the dilaton and the gauge fields still given by (6.5)–(6.8).

Using the ansatz for three-charge black holes on a circle (6.51), (6.52), (6.5)–(6.8), we can work out the following explicit physical parameters (assuming a single connected horizon)

$$\bar{\mu} = 2R_0\Big(2 - \chi + \sum_a \sinh^2\alpha_a\Big) \quad , \quad \bar{n} = \frac{1-2\chi}{2-\chi} \quad ,$$
$$\bar{\mathfrak{t}} = \frac{1}{2\sqrt{A_h}R_0\prod_a \cosh\alpha_a} \quad , \quad \bar{\mathfrak{s}} = 4\sqrt{A_h}R_0^2\prod_a \cosh\alpha_a \quad ,$$
$$q_a = 2R_0 \sinh\alpha_a \cosh\alpha_a \quad , \quad \nu_a = \tanh\alpha_a \quad , \quad \bar{n}_a = \frac{1-\chi}{2-\chi} \quad , \quad a = 1,4,0 \quad , \tag{6.53}$$

where χ is defined from the asymptotic behavior of $K(R,v)$ as (5.13)

$$K(R,v) = 1 - \chi\frac{R_0}{R} + \mathcal{O}(R^{-2}) \tag{6.54}$$

for $R \gg 1$, and where

$$A_h \equiv A(R,v)\big|_{R=R_0} \ . \tag{6.55}$$

Note that one can show that $\partial_v A(R,v) = 0$ on the horizon $R = R_0$ [84]. It is straightforward to see from the thermodynamics (6.53) along with the relation $\mu^{\mathrm{el}} = \sum_a \nu_a q_a$ that we get the Smarr formula (6.49).

6.2.3 The uniform and non-uniform phases

The uniform phase corresponds to the F1-D0-D4 system smeared uniformly on a transverse circle. The supergravity solution for this is easily obtained by putting $A = K = 1$ in the ansatz (6.51), (6.52), (6.5)–(6.8). The thermodynamics is obtained from (6.53) setting $\chi = 0$ and $A_h = 1$, giving

$$\bar{\mu} = 2R_0\Big(2+\sum_a \sinh^2\alpha_a\Big) \quad , \quad \bar{\mathfrak{t}} = \frac{1}{2R_0\prod_a \cosh\alpha_a} \quad , \quad \bar{\mathfrak{s}} = 4R_0^2\prod_a \cosh\alpha_a \tag{6.56}$$

with q_a and ν_a as given in (6.53). We have furthermore that the relative tension is $\bar{n} = 1/2$. The uniform phase is mapped from the neutral uniform black string in five dimensions. The horizon topology for our non-extremal F1-D0-D4 system in the uniform phase is $T^5 \times S^2 \times S^1$, where the T^5 is along the charged directions.

The non-uniform phase of our F1-D0-D4 system is a phase in which the F1-D0-D4 is still distributed on the transverse circle without gaps, but with the distribution being non-uniform along the circle direction. The horizon topology is therefore the same as for the uniform phase: $T^5 \times S^2 \times S^1$. The non-uniform phase is mapped by (6.4)–(6.9) from the neutral non-uniform black string phase. From this fact it is easy to see using equation (6.42) that the non-uniform phase emanates from the uniform phase in a critical point corresponding to the mass

$$\bar{\mu}_c = \sum_a q_a + x + x^2 \sum_a (q_a + \sqrt{x^2 + q_a^2})^{-1} \quad , \quad x \simeq 0.88 \tag{6.57}$$

which is mapped from the Gregory-Laflamme mass $\mu_{\rm GL} = 3.52$ of the five-dimensional neutral uniform black string [100, 102, 8] using that $x = \mu_{\rm GL}/4$. We expect that the uniform phase is unstable to linear perturbations for masses $\bar{\mu} < \bar{\mu}_c$. Indeed, one should be able to find the explicit unstable mode using the methods of [6, 161] where the unstable mode of one-charge smeared branes were constructed by transforming the unstable mode for the neutral black string.

As reviewed in chapter 5, the neutral non-uniform black string solution is obtained numerically in [103]. This numerical solution can then be mapped to a numerical solution for the non-uniform phase of the F1-D0-D4 system, using either the map (6.4)–(6.9), or the ansatz (6.51), (6.52), (6.5)–(6.8). Similarly we can map the physical quantities using the results of section 6.1.4. We do not go into details with this, since the qualitative features of the mapped solution are highly similar to that of the neutral seeding solution. Only in the near-extremal limits that we consider in sections 6.3 and 6.4, one sees significant differences in the qualitative behavior. However, it is interesting to find the slope of the non-uniform phase in the $(\bar{\mu}, \bar{n})$ diagram near the critical point $(\bar{\mu}_c, 1/2)$ since this in a simple way can tell us about some of the features of the non-uniform phase as we change the charges. Using that the neutral non-uniform black string has the slope $n \simeq 1/2 - \gamma(\mu - \mu_{\rm GL})$ ($\gamma \simeq 0.14$) near the Gregory-Laflamme point $(\mu, n) = (\mu_{\rm GL}, 1/2)$ [100, 102, 8], we get the slope

$$\bar{n} \simeq \frac{1}{2} - \eta(\bar{\mu} - \bar{\mu}_c), \quad \eta = \gamma \left[\frac{1}{4} - 2\gamma x + x \left(\frac{1}{4} + \frac{2}{3}\gamma x \right) \sum_a \frac{2q_a\sqrt{x^2 + q_a^2} + x^2 + 2q_a^2}{\sqrt{x^2 + q_a^2}(q_a + \sqrt{x^2 + q_a^2})} \right]^{-1} \tag{6.58}$$

for $0 \leq \bar{\mu} - \bar{\mu}_c \ll 1$, when considering fixed charges q_a.

6.2.4 The localized phase

The localized phase of the F1-D0-D4 system corresponds to having the horizon of F1-D0-D4 localized on the transverse circle, such that the horizon is not connected across the circle. The horizon topology is therefore $S^3 \times T^5$, where T^5 is along the charged directions.

If we consider the case in which the size of the horizon is very small compared to the circumference of the transverse circle, we can write down an analytic expression for the metric using [90] (see [91, 93, 94] for more analytical results for such black holes). To this end, we should slightly modify the ansatz (6.51), (6.52), (6.5)–(6.8) by expressing it instead in the new coordinates $\tilde{\rho}$ and $\tilde{\theta}$ defined by

$$2R = \tilde{\rho}^2 \quad , \quad v = \pi - 2\tilde{\theta} + 2\sin\tilde{\theta}\cos\tilde{\theta} \ . \tag{6.59}$$

We thus have the relation $\rho_0^2 = 2R_0$ for the horizon radius. With this, we can rewrite the ansatz (6.51), (6.52), (6.5)–(6.8) as

$$\begin{aligned} ds_{10}^2 = H_1^{-\frac{3}{4}} H_4^{-\frac{3}{8}} H_0^{-\frac{7}{8}} \Bigg[& -f dt^2 + H_4 H_0 dx^2 + H_1 H_0 \sum_{i=1}^{4} (du^i)^2 \\ & + H_1 H_4 H_0 \frac{L^2}{(2\pi)^2} \left(\frac{\tilde{A}}{f} d\tilde{\rho}^2 + \frac{\tilde{A}}{\tilde{K}^2} \tilde{\rho}^2 d\tilde{\theta}^2 + \tilde{K} \tilde{\rho}^2 \sin^2 \tilde{\theta} d\Omega_2^2 \right) \Bigg] , \end{aligned} \tag{6.60}$$

with

$$f = 1 - \frac{\rho_0^2}{\tilde{\rho}^2} \quad , \quad H_a = 1 + \frac{\rho_0^2 \sinh^2 \alpha_a}{\tilde{\rho}^2}, \quad \text{for } a = 1, 4, 0. \tag{6.61}$$

Using the results of [90] one can now write down the full solution for the case in which the horizon is very small, i.e. for $\rho_0 \ll 1$. For simplicity, we discuss here only the part concerning the solution near the horizon, but it is straightforward to use the map to find the full solution. From [90] we get for $\rho_0 \leq \tilde{\rho} \ll 1$ that

$$\tilde{A}^{-\frac{1}{3}} = \tilde{K}^{-1} = \frac{1 - w^2}{w} \frac{\tilde{\rho}^2}{\rho_0^2} + w \quad , \quad w = 1 + \frac{1}{24}\rho_0^2 + \mathcal{O}(\rho_0^4). \tag{6.62}$$

From [90] we have furthermore that $\chi = \frac{1}{2} - \frac{1}{32}\rho_0^2 + \mathcal{O}(\rho_0^4)$ and $\tilde{A}_h = 1 + \frac{1}{8}\rho_0^2 + \mathcal{O}(\rho_0^4)$, with $\tilde{A}_h = \tilde{A}|_{\tilde{\rho}=\rho_0}$. Using then that $A = \tilde{A}/\tilde{\rho}^2$ together with the thermodynamics (6.53), we can get the thermodynamics for $\rho_0 \ll 1$. However, before writing down this thermodynamics, we note that the second order correction has been obtained in [93, 94] which we can translate to our notation as[3]

$$\chi = \frac{1}{2} - \frac{1}{32}\rho_0^2 + \mathcal{O}(\rho_0^6) \quad , \quad \sqrt{\tilde{A}_h} = 1 + \frac{1}{16}\rho_0^2 + \frac{1}{512}\rho_0^4 + \mathcal{O}(\rho_0^6). \tag{6.63}$$

This now gives the thermodynamics

$$\begin{aligned} &\bar{\mu} = \rho_0^2 \left(\frac{3}{2} + \frac{1}{32}\rho_0^2 + \mathcal{O}(\rho_0^6) + \sum_a \sinh^2 \alpha_a \right) , \quad \bar{n} = \frac{1}{24}\rho_0^2 - \frac{1}{1152}\rho_0^4 + \mathcal{O}(\rho_0^6), \\ &\bar{\mathfrak{t}} = \frac{1 - \frac{1}{16}\rho_0^2 + \frac{1}{512}\rho_0^4 + \mathcal{O}(\rho_0^6)}{\rho_0 \prod_a \cosh \alpha_a}, \quad \bar{\mathfrak{s}} = \rho_0^3 \left(1 + \frac{1}{16}\rho_0^2 + \frac{1}{512}\rho_0^4 + \mathcal{O}(\rho_0^6) \right) \prod_a \cosh \alpha_a, \\ &q_a = \rho_0^2 \cosh \alpha_a \sinh \alpha_a, \quad \nu_a = \tanh \alpha_a, \quad \bar{n}_a = \frac{1}{3} + \frac{1}{72}\rho_0^2 - \frac{1}{3456}\rho_0^4 + \mathcal{O}(\rho_0^6). \end{aligned} \tag{6.64}$$

This is thus the thermodynamics of a small three-charge black hole localized on a circle.

[3]Note that this follows from the slope of $n(\mu) = \mu/6^2 - \mu^2/6^4 + \mathcal{O}(\mu^3)$ for the neutral seeding solution, as one can see from the fact that $\mu = (2-\chi)\rho_0^2$ and $n = (1-2\chi)/(2-\chi)$.

6.3 Near-Extremal Three-Charge Black Holes on a Circle

We now consider the near-extremal limit of our three-charge black holes on a circle. This is an interesting limit in view of the microscopic counting of entropy and, more generally, in the context of the dual CFT. In this section we will see how to define this limit and its consequences for the physical quantities.

6.3.1 The near-extremal limit

There are two ways to take the near-extremal limit. One can either keep the charges fixed and send the temperature to zero or keep the temperature fixed and send the charges to infinity. Since we are interested in the thermodynamics of the near-extremal black hole, it is natural for us to take the second option.

In order to retain the non-trivial physics related to the presence of the circle we want to take the limit in such a way that the size of the circle has the same scale as the energy above extremality. This means that the metric components multiplying dt^2 and $V_{ab}dx^a dx^b$ should scale in the same way. From the metric in equation (6.4) we therefore require

$$\lim_{L\to 0} H_1 H_4 H_0 \left(\frac{L}{2\pi}\right)^2 = \text{finite}. \tag{6.65}$$

A natural way to achieve (6.65) is to demand

$$\lim_{L\to 0} H_a \left(\frac{L}{2\pi}\right)^{2\gamma_a} = \text{finite}, \quad a = 1, 4, 0, \tag{6.66}$$

where $\gamma_a \geq 0$ and $\gamma_1 + \gamma_4 + \gamma_0 = 1$. In this section we consider only the case when all γ_a are non-vanishing, postponing other limits to the next section. For $\gamma_a > 0$ the requirement of equation (6.66) means that

$$H_a = 1 + (1 - U)\sinh^2 \alpha_a \to \infty \tag{6.67}$$

so that the boost parameters α_a must go to infinity (for simplicity we will take α_a to be positive). In order to see what this means for the charges, it is convenient to introduce rescaled coordinates on the transverse space[4]

$$\hat{r} \equiv \frac{2\pi}{L} r, \qquad \hat{z} \equiv \frac{2\pi}{L} z, \tag{6.68}$$

and corresponding rescaled expansion coefficients for the seeding metric (6.21)

$$-g_{tt}^{\text{seed}} \simeq 1 - \frac{\hat{c}_t}{\hat{r}}, \qquad g_{zz}^{\text{seed}} \simeq 1 + \frac{\hat{c}_z}{\hat{r}}. \tag{6.69}$$

[4]Note that the coordinates of the ansatz (6.50) approach these dimensionless coordinates in the asymptotic region, $R \to \hat{r}$ and $v \to \hat{z}$.

These coefficients are more appropriate in the near-extremal limit since they remain finite. We can now write the dimensionless charges (6.16) as

$$q_a = \frac{\Omega_2}{2\pi} \hat{c}_t \sinh \alpha_a \cosh \alpha_a \tag{6.70}$$

and from this expression it is apparent how the charges diverge. Notice that in order to satisfy the condition (6.65), we should keep fixed the parameters

$$\ell_a \equiv L^{\gamma_a} \sqrt{q_a} = \left(\frac{\Omega_2 \hat{c}_t}{2\pi} \right)^{1/2} L^{\gamma_a} \sqrt{\sinh \alpha_a \cosh \alpha_a}. \tag{6.71}$$

To get a finite solution for the metric, the gauge fields and the dilaton in the near-extremal limit, we must rescale the fields with appropriate powers of $L/2\pi$ and the powers will depend on γ_a. This rescaling should be a symmetry of the action (6.1). It is fairly easy to check that the following scaling works

$$e^{2\phi^{\text{new}}} = \left(\frac{L}{2\pi} \right)^{-2\gamma_1 - \gamma_4 + 3\gamma_0} e^{2\phi^{\text{old}}}, \tag{6.72}$$

$$g_{tt}^{\text{new}} = \left(\frac{L}{2\pi} \right)^{-\frac{3}{2}\gamma_1 - \frac{3}{4}\gamma_4 - \frac{7}{4}\gamma_0} g_{tt}^{\text{old}}, \qquad g_{xx}^{\text{new}} = \left(\frac{L}{2\pi} \right)^{-\frac{3}{2}\gamma_1 - \frac{3}{2}\gamma_4 + \frac{1}{4}\gamma_0} g_{xx}^{\text{old}}, \tag{6.73}$$

$$g_{u_i u_i}^{\text{new}} = \left(\frac{L}{2\pi} \right)^{\frac{1}{2}\gamma_1 - \frac{3}{4}\gamma_4 + \frac{1}{4}\gamma_0} g_{u_i u_i}^{\text{old}}, \qquad g_{rr}^{\text{new}} = \left(\frac{L}{2\pi} \right)^{\frac{1}{2}\gamma_1 + \frac{5}{4}\gamma_4 + \frac{1}{4}\gamma_0 + 2} g_{rr}^{\text{old}}, \tag{6.74}$$

$$A_a^{\text{new}} = \left(\frac{L}{2\pi} \right)^{-2\gamma_a} A_a^{\text{old}}, \qquad G_{10}^{\text{new}} = \left(\frac{L}{2\pi} \right)^{2} G_{10}^{\text{old}}. \tag{6.75}$$

The components of the metric for the other transverse directions are rescaled in the same way as g_{rr}. The choice of powers of $L/2\pi$ is unique and can be found by first requiring the gauge fields, B field, and dilaton to be finite in the limit. Next the scalings of the metric is found by requiring all the terms in the action to scale in the same way. Finally, the scaling of Newton's constant is found by requiring the scaling to be a symmetry of the action.

The choice of gauge in equations (6.6)–(6.8) is not convenient in the near-extremal limit because the constant term will be dominant. But we are free to change the gauge by adding the constant $\coth \alpha_a$ to our old A_a^{old} before taking the limit. This gives

$$A_a^{\text{old}} = \coth \alpha_a H_a^{-1} = \left(\frac{L}{2\pi} \right)^{2\gamma_a} \coth \alpha_a \hat{H}_a^{-1} \tag{6.76}$$

where we have defined

$$\hat{H}_a \equiv \lim_{L \to 0} \left(\frac{L}{2\pi} \right)^{2\gamma_a} H_a. \tag{6.77}$$

By construction, $\hat{H}_a$ is finite in the near-extremal limit and from equation (6.75) we see that after rescaling A_a^{new} will be finite as well.

To summarize, the particular near-extremal limit that we are interested in can be defined as

$$L \to 0, \quad \alpha_a \to \infty, \quad \ell_a \equiv L^{\gamma_a} \sqrt{q_a} = \text{fixed}, \quad g \equiv \frac{16\pi G_{10}}{V_1 V_4 L^2} = \text{fixed}. \tag{6.78}$$

The near-extremal limit of the three-charge solution (6.4)–(6.8) can now be written down. The metric and the dilaton are given by

$$ds^2 = \hat{H}_1^{-\frac{3}{4}} \hat{H}_4^{-\frac{3}{8}} \hat{H}_0^{-\frac{7}{8}} \left(-U dt^2 + \hat{H}_4 \hat{H}_0 dx^2 + \hat{H}_1 \hat{H}_0 \sum_{i=1}^{4} (du^i)^2 + \hat{H}_1 \hat{H}_4 \hat{H}_0 V_{ab} dx^a dx^b \right), \tag{6.79}$$

$$e^{2\phi} = \hat{H}_1^{-1} \hat{H}_4^{-\frac{1}{2}} \hat{H}_0^{\frac{3}{2}}, \tag{6.80}$$

where from (6.77)

$$\hat{H}_a = \begin{cases} \hat{h}_a \frac{1-U}{\hat{c}_t} & \text{for } \gamma_a > 0 \\ H_a & \text{for } \gamma_a = 0 \end{cases}, \qquad \hat{h}_a \equiv \frac{(2\pi)^{1-2\gamma_a} \ell_a^2}{\Omega_2}. \tag{6.81}$$

In the case that all $\gamma_a > 0$ the dilaton is constant

$$e^{2\phi} = \hat{h}_1^{-1} \hat{h}_4^{-\frac{1}{2}} \hat{h}_0^{\frac{3}{2}}. \tag{6.82}$$

The non-vanishing components of the gauge fields are given by

$$(A_a)_{t\ldots} = \begin{cases} \hat{H}_a^{-1} & \text{for } \gamma_a > 0, \\ \coth \alpha_a (H_a^{-1} - 1) & \text{for } \gamma_a = 0. \end{cases} \tag{6.83}$$

Note that the near-horizon limit of the extremal three-charge metric is $AdS_2 \times S^3 \times T^5$ for the localized phase of F1-D0-D4. For the uniformly smeared phase there is not such a simple description.

Relation to string scale units

Before discussing the physical quantities of the new near-extremal solution, it is useful to see how the parameters that are kept fixed in near-extremal limit, namely g and ℓ_a, are related to the string coupling g_s and the string length ℓ_s. By comparing the parameters $\hat{h}_a$ in equation (6.81) to the usual harmonic functions of smeared extremal branes, we find

$$\ell_1^2 = L^{2\gamma_1} \frac{(2\pi \ell_s)^6 g_s^2 N_1}{L^2 V_4}, \tag{6.84}$$

$$\ell_4^2 = L^{2\gamma_4} \frac{(2\pi \ell_s)^3 g_s N_4}{L^2 V_1}, \tag{6.85}$$

$$\ell_0^2 = L^{2\gamma_0} \frac{(2\pi \ell_s)^7 g_s N_0}{L^2 V_1 V_4}, \tag{6.86}$$

and

$$g = \frac{(2\pi)^7 \ell_s^8 g_s^2}{L^2 V_1 V_4} \tag{6.87}$$

where N_1 is the number of $F1$-strings, N_4 is the number of D4-branes and N_0 is the number of D0-branes.

From the fixed parameters in equations (6.84)–(6.87) we can form the dimensionless combination

$$\frac{\ell_1 \ell_4 \ell_0}{g} = 2\pi \sqrt{N_1 N_4 N_0} \tag{6.88}$$

which will be useful to reinstate the units in the rescaled entropy that we obtain below.

6.3.2 Physical quantities

In the near-extremal limit we define the energy above extremality and the tensions in the compact directions as[5]

$$E = \lim_{L\to 0} \left(\bar{M} - \sum_a Q_a \right), \quad \hat{\mathcal{T}}_z = \lim_{L\to 0} \frac{L}{2\pi} \bar{\mathcal{T}}_z, \quad L_a \hat{\mathcal{T}}_a = \lim_{L\to 0} \left(L_a \bar{\mathcal{T}}_a - Q_a \right). \tag{6.89}$$

The general definitions for the energy and tensions in backgrounds that are not asymptotically flat can be found in [143] (see also [144]). In reference [4] it was actually shown that for one-charge solutions written in the ansatz (6.50) the general definition is equivalent to (6.89). We have checked that the same is true for the three-charge case.

The dimensionless versions of these quantities are defined as

$$\epsilon = gE, \qquad r = \frac{2\pi \hat{\mathcal{T}}_z}{E}, \qquad r_a = \frac{L_a \hat{\mathcal{T}}_a}{E}. \tag{6.90}$$

These variables are the possible independent physical parameters analogous to μ and n in the neutral case and $\bar{\mu}$, $\bar{n}$ and $\bar{n}_a$ in the non-extremal case.

Using equations (6.24) and (6.25) and the fact that

$$\lim_{\alpha\to\infty} \left(\sinh^2\alpha - \sinh\alpha \cosh\alpha \right) = -\frac{1}{2} \tag{6.91}$$

we find the energy above extremality in terms of $\hat{c}_t$ and $\hat{c}_z$ as

$$E = \frac{\Omega_2}{2\pi g} \left(\frac{1}{2} \hat{c}_t - \hat{c}_z \right) \tag{6.92}$$

[5] We will always assume the Q_as to be positive.

while the tension of the transverse circle and the tensions in the spatial world-volume directions are given by

$$2\pi\hat{\mathcal{T}}_z = \frac{\Omega_2}{2\pi g}(\hat{c}_t - 2\hat{c}_z), \quad L_a\hat{\mathcal{T}}_a = \frac{\Omega_2}{2\pi g}\left(\frac{1}{2}\hat{c}_t - \hat{c}_z\right). \tag{6.93}$$

Rewriting the dimensionless energy ϵ and the relative tensions, r and r_a, in terms of the seeding μ and n we get the remarkable result

$$\epsilon = \frac{1}{2}\mu n, \qquad r = 2, \qquad r_a = 1 \quad , \quad a = 1,4,0\ . \tag{6.94}$$

Note that the relative tensions are constant. That means that the tensions are proportional to the energy above extremality. This is a very special result that depends on the fact that we have exactly three charges and four spatial transverse dimensions. In section 6.3.3 we will see that r being a constant is a necessary condition in order for the localized five-dimensional black hole to have a finite non-vanishing entropy in the extremal limit. But first we look at the near-extremal thermodynamics.

The near-extremal temperature and entropy are given by

$$\hat{T} = \lim_{L\to 0}\bar{T}, \qquad \hat{S} = \lim_{L\to 0}\bar{S} \tag{6.95}$$

where $\bar{T}$ and $\bar{S}$ are the non-extremal temperature and entropy. To get rescaled temperature and entropy we need a new length scale and it turns out to be useful to define

$$\ell \equiv \ell_1\ell_4\ell_0 \tag{6.96}$$

with ℓ_a given in equation (6.71). Note that ℓ has the dimension of length since the γ_a sum to one. Dimensionless versions of the temperature and entropy in the near-extremal limit can now be defined by[6]

$$\hat{\mathfrak{t}} = \ell\hat{T}, \qquad \hat{\mathfrak{s}} = \frac{g}{\ell}\hat{S}. \tag{6.97}$$

These quantities can be related to the non-extremal temperature and entropy via

$$\bar{\mathfrak{t}}\sqrt{q_1q_4q_0} = L\bar{T}\sqrt{q_1q_4q_0} \to \ell\hat{T} = \hat{\mathfrak{t}}, \tag{6.98}$$

$$\bar{\mathfrak{s}}/\sqrt{q_1q_4q_0} = \frac{g}{L\sqrt{q_1q_4q_0}}\bar{S} \to \frac{g}{\ell}\hat{S} = \hat{\mathfrak{s}}, \tag{6.99}$$

and this implies the map

$$\hat{\mathfrak{t}}\hat{\mathfrak{s}} = \bar{\mathfrak{t}}\bar{\mathfrak{s}} = \mathfrak{t}\mathfrak{s}. \tag{6.100}$$

[6] This is assuming that all the charges are non-zero. If one or two of the charges are zero then the corresponding ℓ_a should be left out of the definition of ℓ. We will come back to this in section 6.5.

Given the temperature and entropy of the neutral seeding solution, we find the rescaled temperature and entropy of the near-extremal three-charge solution as

$$\hat{\mathfrak{t}} = \mathfrak{t}(\mathfrak{t}\mathfrak{s})^{3/2}, \quad \hat{\mathfrak{s}} = \mathfrak{s}(\mathfrak{t}\mathfrak{s})^{-3/2} \tag{6.101}$$

This can be derived from

$$\hat{\mathfrak{t}} = \bar{\mathfrak{t}}\sqrt{q_1 q_4 q_0} = \frac{\sqrt{q_1 q_4 q_0}}{\cosh\alpha_1 \cosh\alpha_4 \cosh\alpha_0}\mathfrak{t} \tag{6.102}$$

by noticing that from the neutral Smarr formula $\mathfrak{t}\mathfrak{s} = (2-n)\mu/3$ and equation (6.37) we have

$$\lim_{\alpha_a \to \infty} \frac{\sqrt{q_a}}{\cosh\alpha_a} = \sqrt{\mathfrak{t}\mathfrak{s}}. \tag{6.103}$$

In the near-extremal three-charge case we do not have a Smarr relation in the traditional sense since the relative tensions are constant. However, we can write a Smarr relation in a 'mixed' notation where we use the relative tension n of the seeding solution

$$\hat{\mathfrak{t}}\hat{\mathfrak{s}} = \frac{2(2-n)}{3n}\epsilon. \tag{6.104}$$

From this and the first law of thermodynamics we obtain

$$\frac{\delta \log \hat{\mathfrak{s}}}{\delta \log \hat{\epsilon}} = \frac{3n}{2(2-n)} \tag{6.105}$$

so that given the curve $n(\epsilon)$ we can find the entire thermodynamics.

The Helmholtz free energy is

$$\hat{\mathfrak{f}} = \epsilon - \hat{\mathfrak{t}}\hat{\mathfrak{s}}, \quad \delta\hat{\mathfrak{f}} = -\hat{\mathfrak{s}}\delta\hat{\mathfrak{t}} \tag{6.106}$$

and using the Smarr relation (6.104) we can rewrite this for near-extremal black holes on a circle as

$$\hat{\mathfrak{f}} = \frac{5n-4}{3n}\epsilon. \tag{6.107}$$

This is the near-extremal free energy written in mixed notation, using the neutral tension n instead of r which is a constant in this case.

Note that the free energy is negative for $n \leq 4/5$. This is important for the dual field theory which is only thermodynamically stable if the free energy is negative. The region $n \leq 4/5$ contains all the usual phases with $SO(3)$ symmetry (which have $n \leq 1/2$), and also some of the Kaluza-Klein bubbles [8].

From the first law of thermodynamics we get

$$\frac{\delta \log \hat{\mathfrak{f}}}{\delta \log \hat{\mathfrak{t}}} = -\frac{\hat{\mathfrak{s}}\hat{\mathfrak{t}}}{\hat{\mathfrak{f}}} = \frac{4-2n}{4-5n}. \tag{6.108}$$

Given $n(\hat{\mathfrak{t}})$ we can integrate the above equation and get $\hat{\mathfrak{f}}$ as a function of $\hat{\mathfrak{t}}$. Note that we again have to use the relative tension of the seeding solution.

The world-volume pressure is

$$\hat{\mathfrak{p}}_a = -r_a \epsilon = -\epsilon \tag{6.109}$$

where we used (6.94). This not proportional to the free energy (6.107), contrary to the one-charge solutions [4] for which the world-volume pressure is always equal to minus the free energy.

6.3.3 Finite entropy from the first law of thermodynamics

In this section we try to understand why the relative tension is a constant for the near-extremal three-charge solution. Let us start with an ansatz for the energy above extremality in terms of the seeding μ and n

$$\epsilon = (a + bn)\mu \tag{6.110}$$

where a and b depend on the number of charges and the number of transverse dimensions. We can argue for this ansatz using only the expression for the gauge fields (6.6)–(6.8). Since μ and μn are linear combinations of the seeding c_t and c_z it is enough to show that the same is true for the energy above extremality. To see that, we write

$$\epsilon = \mu + \sum_a (\nu_a - 1) q_a \tag{6.111}$$

where the chemical potential $\nu_a = -A_a|_{\text{Horizon}}$ is independent of c_t and c_z. Since q_a is proportional to c_t we immediately see that ε is indeed a linear combination of c_t and c_z.

In the next section we will see that ϵ takes the form (6.110) for the one- and two-charge cases with non-zero a and b [cf. equation (6.154) and (6.158) for the near-extremal map in the one- and two-charge case respectively] but for the three-charge case we have seen that $a = 0$ [cf. (6.94)]. We will ignore this knowledge for now, and first examine what the first law of thermodynamics implies.

From the non-extremal Smarr formula (6.49) and the map (6.100) we know that the product of the rescaled entropy and temperature is given by

$$\hat{\mathfrak{t}}\hat{\mathfrak{s}} = \frac{2-n}{3}\mu = \frac{2-n}{3(a+bn)}\epsilon \tag{6.112}$$

where in the last equation we used the ansatz (6.110). Plugging this into the first law of thermodynamics, $\delta\epsilon = \hat{\mathfrak{t}}\delta\hat{\mathfrak{s}}$, we therefore find

$$\frac{\delta \log \hat{\mathfrak{s}}}{\delta \log \epsilon} = \frac{3(a+bn)}{2-n}. \tag{6.113}$$

For small black holes in the localized phase, $n \to 0$ as $\epsilon \to 0$, since the tension should vanish in the extremal (BPS) limit. Therefore it follows that for small black holes close to extremality

$$\frac{\delta \log \hat{\mathfrak{s}}}{\delta \log \epsilon} \simeq \frac{3a}{2}. \tag{6.114}$$

Integrating this equation for small ϵ gives

$$\hat{\mathfrak{s}} \simeq A\epsilon^{3a/2} \tag{6.115}$$

where A is a constant of integration. But for this type of a localized black hole with three-charges in five spacetime dimensions, we expect to find [16]

$$\hat{\mathfrak{s}} \to \text{constant} \neq 0 \tag{6.116}$$

as $\epsilon \to 0$. This can only be true if $a = 0$. We have therefore seen that in order for the entropy of the small three-charge black hole to be non-vanishing in the extremal limit, the number a in the ansatz (6.110) should be zero. This is what makes the three-charge case special compared to the one- and two-charge case. The fact that a vanishes has an immediate consequence for the relative tension

$$r = \frac{L\bar{\mathcal{T}}_z}{E} = \frac{\mu n}{\epsilon} = \frac{n}{a+bn} = \frac{1}{b}. \tag{6.117}$$

From equation (6.94) we see that the five-dimensional near-extremal three-charge black hole indeed has $a = 0$ and $b = 1/2$ which gives the correct value $r = 2$.

Let us finally note that we can quickly see how r depends on the number of transverse dimensions and charges.[7] Firstly, in this general case we still have that $L\bar{\mathcal{T}}_z = L\mathcal{T}_z = \mu n$ (see Appendix E). Thus we only have to see how a and b depends on d, the number of transverse spatial dimensions, and N_{ch}, the number of charges. We assume that (6.32) applies and that the form of the gauge fields is the same in the general case such that $\nu_a = \tanh\alpha_a$ and

$$M^{\text{el}} = \sum_{a=1}^{N_{\text{ch}}} \tanh\alpha_a Q_a. \tag{6.118}$$

Further, from [4] we get $c_t \propto \frac{(d-2)M - L\mathcal{T}}{(d-2)^2-1}$. Using this and the form of the gauge fields, we see that $Q_a = (d-3)\sinh\alpha_a\cosh\alpha_a \frac{(d-2)M-L\mathcal{T}}{(d-2)^2-1}$ thus giving

$$\varepsilon = \left(1 - \frac{N_{\text{ch}}(d-2)}{2(d-1)}\right)\mu + \frac{N_{\text{ch}}}{2(d-1)}\mu n \tag{6.119}$$

where we have used that $(\tanh\alpha_a - 1)\sinh\alpha_a\cosh\alpha_a \to -1/2$ as $\alpha_a \to \infty$. This, of course, agrees with our case where $N_{\text{ch}} = 3$ and $d = 4$. The only other case with $a = 0$ is for $N_{\text{ch}} = 4$ and $d = 3$. For the latter case it is actually known that one can have configurations with finite entropy (see e.g. [162]). However, our derivation does not hold in this case since the asymptotic c_t and c_z do not make sense for $d = 3$.

[7] We choose a short derivation here. One can also obtain the result by calculating $\bar{c}_t$, $\bar{c}_z$, etc.

6.4 Phase Diagrams for the Near-Extremal Case

In this section we discuss consequences of the near-extremal map for the different phases of the seeding solution that we also considered for the non-extremal case in section 6.2 and display the phase diagrams.

6.4.1 Energy versus relative tension

In normal situations it would be appropriate to draw the different phases of near-extremal solutions on an (ϵ, r) phase diagram. But in the special case of a five-dimensional three-charge black holes on a circle the relative tension r is a constant independent of the seeding solution. The phase diagram is therefore just a straight line $r(\epsilon) = 2$ which does not contain much information about the different phases.

We can, however, see how the relative tension approaches this constant as the charges are sent to infinity. In this discussion we define, with a slight abuse of notation, the *non-extremal* energy above extremality for finite charges as $\epsilon = \bar{\mu} - \sum_a q_a$. From the definition of the relative tension, we then have that

$$r = \frac{L\bar{\mathcal{T}}_z}{E} = \frac{\mu n}{\epsilon}. \tag{6.120}$$

We can plug in our equations for the tension and energy above extremality (6.42) and get

$$\frac{\mu n}{\bar{\mu} - \sum_a q_a} = \left(\frac{1}{2} + \frac{(2-n)}{6n} \sum_a \frac{b_a}{1 + \sqrt{1 + b_a^2}} \right)^{-1}. \tag{6.121}$$

This quantity clearly goes to $r = 2$ in the near-extremal limit, since by equation (6.40) the b_a vanish when the charges go to infinity. We do not have analytic expressions for the full localized phase nor for the non-uniform phase, but from the numerical data [97, 103] we can plot a non-extremal (ϵ, r) phase diagram and see how it evolves as the charges go to infinity. Figure 6.1 depicts this phase diagram for four increasing values of the charges and we clearly see how all the phases collapse to the degenerate line $r = 2$ as the charges go to infinity.

6.4.2 Thermodynamics of the uniform and non-uniform phases

The thermodynamics of the uniform phase in the near-extremal limit follows directly from the general map (6.94), (6.101) and the known thermodynamics ($\mathfrak{s}_\mathrm{u}(\mu) = \mu^2/4$) of the uniform black string in five dimension, and we find

$$\hat{\mathfrak{s}}_\mathrm{u}(\epsilon) = \sqrt{2\epsilon}, \qquad \hat{\mathfrak{f}}_\mathrm{u}(\hat{\mathfrak{t}}) = -\frac{1}{2}\hat{\mathfrak{t}}^2. \tag{6.122}$$

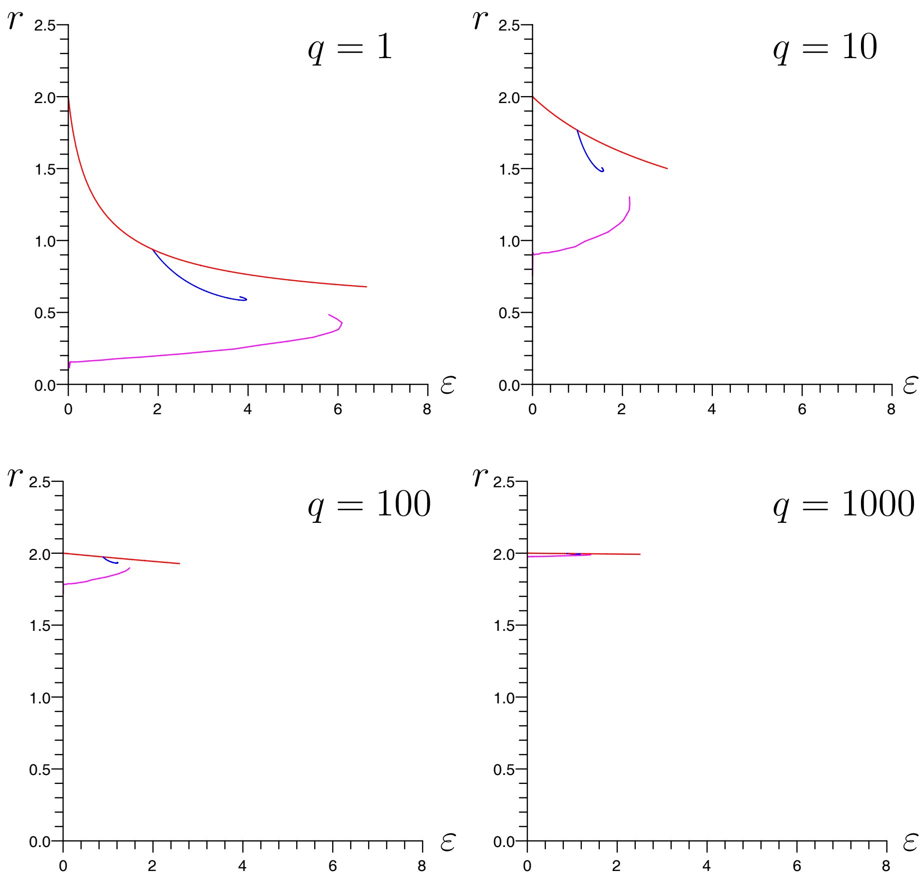

Figure 6.1: The non-extremal (ϵ, r) phase diagram for four different values of the charges. The three charges are all taken to be equal and have the value $q = 1$, $q = 10$, $q = 100$, and $q = 1000$. Notice how all the phases collapse to the line $r = 2$ as the charges go to infinity. The curves were found from equation (6.121) using $n = 1/2$ for the uniform phase (red curve), numerical data from [97] for the localized phase (magenta curve) and numerical data from [103] for the non-uniform phase (blue curve).

If we apply the general map (6.94) to the neutral non-uniform branch that was reviewed in section 5.4.4 we get a new non-uniform phase of near-extremal three-charge black holes on a circle. The Gregory-Laflamme point $(\mu_{\rm GL}, 1/2)$ where the non-uniform phase branches off the uniform phase is mapped to a critical point with energy above extremality $\epsilon_{\rm c} = \mu_{\rm GL}/4$. The relative tension at this point is $r = 2$ as for all other points and therefore we cannot describe the non-uniform phase as a curve on the (ϵ, r) diagram like in the non-extremal case. We can, however, express the neutral tension n in terms of $\epsilon - \epsilon_{\rm c}$ near the critical point. The expression is

$$n(\epsilon) = \frac{1}{2} - \hat{\gamma}(\epsilon - \epsilon_{\rm c}) + \mathcal{O}((\epsilon - \epsilon_{\rm c})^2) \tag{6.123}$$

with $\hat{\gamma}$ given by

$$\hat{\gamma} = \frac{4\gamma}{1 - 2\gamma\mu_{\rm GL}} = 38.89 \tag{6.124}$$

where $\gamma = 0.14$ is the slope of the neutral non-uniform branch and $\mu_{\rm GL} = 3.52$ is the Gregory-Laflamme critical mass. It is useful to have the neutral tension in terms of the energy above extremality because we can integrate (6.105) to find the entropy for the non-uniform branch to leading order

$$\hat{\mathfrak{s}}_{\rm nu}(\epsilon) = \hat{\mathfrak{s}}_{\rm c}\left(1 + \frac{\epsilon - \epsilon_{\rm c}}{2\epsilon_{\rm c}} - \big(\frac{1}{8} + \frac{2}{3}\hat{\gamma}\epsilon_{\rm c}\big)\frac{(\epsilon - \epsilon_{\rm c})^2}{\epsilon_{\rm c}^2}\right) + \mathcal{O}((\epsilon - \epsilon_{\rm c})^3) \tag{6.125}$$

where $\hat{\mathfrak{s}}_{\rm c} = \sqrt{2\epsilon_{\rm c}}$ is the critical entropy.

We can recover the entropy of the uniform branch by replacing $\hat{\gamma}$ with zero in the expression (6.125) above. Notice that the entropy of the non-uniform phase deviates from that of the uniform phase only to second order. These two phases [8] are depicted in figure 6.2 together with the localized phase which will be discussed in section 6.4.3.

In the canonical ensemble we can get the free energy of the non-uniform phase as an expansion around the critical temperature $\hat{\mathfrak{t}}_{\rm c} = \sqrt{2\epsilon_{\rm c}}$. Using the Smarr formula to relate temperature to energy above extremality, we get from (6.125)

$$\hat{\mathfrak{f}}_{\rm nu} = -\epsilon_{\rm c} - \hat{\mathfrak{s}}_{\rm c}(\hat{\mathfrak{t}} - \hat{\mathfrak{t}}_{\rm c}) - \frac{c}{2\hat{\mathfrak{t}}_{\rm c}}(\hat{\mathfrak{t}} - \hat{\mathfrak{t}}_{\rm c})^2 + \mathcal{O}((\hat{\mathfrak{t}} - \hat{\mathfrak{t}}_{\rm c})^3) \tag{6.126}$$

where

$$c = \frac{3\hat{\mathfrak{s}}_{\rm c}}{3 + 16\hat{\gamma}\epsilon_{\rm c}} = 0.0072 \tag{6.127}$$

[8] Note that for each of these two phases we also have copies, which are mapped from the copies [156, 86, 4] of the non-uniform and localized phase of the seeding solution. The thermodynamic quantities of the copies of the near-extremal three-charge solutions are given by $\tilde{\epsilon} = \epsilon/k$, $\tilde{\hat{\mathfrak{t}}} = \hat{\mathfrak{t}}/\sqrt{k}$, $\tilde{\hat{\mathfrak{s}}} = \hat{\mathfrak{s}}/\sqrt{k}$ where $k = 2, 3, \ldots$.

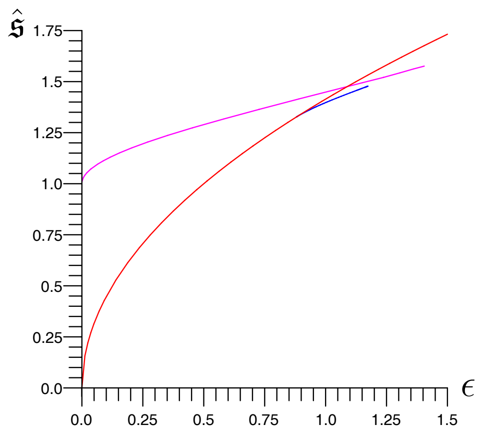

Figure 6.2: The entropy $\hat{\mathfrak{s}}$ as a function of the energy above extremality ϵ for the localized phase (magenta), the uniform phase (red) and the non-uniform phase (blue). The curves are based on numerical data from [97, 103].

is the heat capacity of the non-uniform phase at $\hat{\mathfrak{t}} = \hat{\mathfrak{t}}_c$. The free energy of the uniform branch around $\hat{\mathfrak{t}} = \hat{\mathfrak{t}}_c$ is also given by (6.126) but with heat capacity $c = \hat{\mathfrak{s}}_c$ as can be easily derived from (6.122). These phases are depicted in figure 6.3 together with the localized branch which will be discussed in section 6.4.3.

6.4.3 Thermodynamics of small three-charge black holes on a circle

We now consider the case of a small localized black hole. In the neutral case we have (see section 6.2.4)

$$\mu = \frac{3}{2}\rho_0^2 + \frac{1}{32}\rho_0^4 + \mathcal{O}(\rho_0^8), \quad n = \frac{1}{24}\rho_0^2 - \frac{1}{1152}\rho_0^4 + \mathcal{O}(\rho_0^6) \tag{6.128}$$

which gets mapped by (6.94) to the energy above extremality

$$\epsilon = \frac{1}{32}\rho_0^4 + \mathcal{O}(\rho_0^8). \tag{6.129}$$

Note that not only is the ρ_0^2 term missing but the ρ_0^6 term cancels as well. The rescaled entropy and temperature are by (6.101) mapped into

$$\hat{\mathfrak{s}} = 1 + \frac{\rho_0^2}{16} + \frac{\rho_0^4}{512} + \mathcal{O}(\rho_0^6), \tag{6.130}$$

$$\hat{\mathfrak{t}} = \rho_0^2 - \frac{\rho_0^4}{16} + \frac{\rho_0^6}{512} + \mathcal{O}(\rho_0^8). \tag{6.131}$$

Using (6.129) we can also write the entropy in terms of ε

$$\hat{\mathfrak{s}}_{\rm loc}(\epsilon) = 1 + \sqrt{\frac{\epsilon}{8}} + \frac{\epsilon}{16} + \mathcal{O}(\epsilon^{3/2}). \tag{6.132}$$

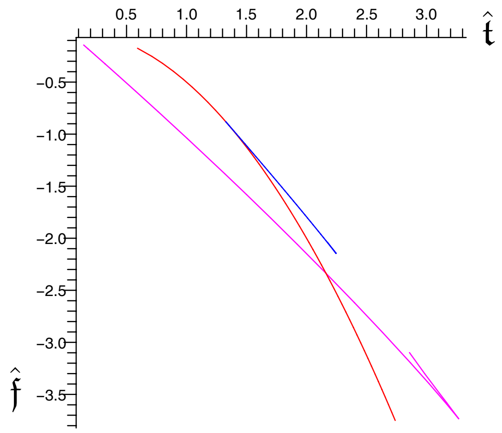

Figure 6.3: The free energy $\hat{\mathfrak{f}}$ as a function of the temperature $\hat{\mathfrak{t}}$ for the localized phase (magenta), the uniform phase (red) and the non-uniform phase (blue). The curves are based on numerical data from [97, 103].

showing the first two corrections to the extremal entropy for a thermal black hole localized on a circle. We correctly see that the entropy (6.132) goes to a non-vanishing constant in the extremal limit $\epsilon \to 0$. It is not surprising that the first correction comes with a power of ϵ smaller than one, otherwise the temperature would not go to zero in the extremal limit.

Restoring the normalization of the entropy using (6.88) we find

$$\hat{S}_{\text{loc}} = \frac{\ell \hat{\mathfrak{s}}}{g} = 2\pi \sqrt{N_1 N_4 N_0} \left(1 + \sqrt{\frac{\epsilon}{8}} + \frac{\epsilon}{16} + \mathcal{O}(\epsilon^{3/2}) \right) . \tag{6.133}$$

The entropy in the extremal limit is the constant $\hat{S}_0 = 2\pi\sqrt{N_1 N_4 N_0}$ in agreement with the well-known result of [16]. Eq. (6.133) is one of the central results of this thesis and gives, as a function of the energy above extremality, the first two corrections to the finite entropy due to the interactions of the black hole. We will come back to this in section 6.6, where we will present a microscopic counting of the corrected entropy in case of the partial extremal limit described in section 6.5.1.

The Helmholtz free energy of small localized black holes in the canonical ensemble (6.106) is given by

$$\hat{\mathfrak{f}}_{\text{loc}}(\hat{\mathfrak{t}}) = -\hat{\mathfrak{t}} - \frac{1}{32}\hat{\mathfrak{t}}^2 - \frac{1}{512}\hat{\mathfrak{t}}^3 + \mathcal{O}(\hat{\mathfrak{t}}^4). \tag{6.134}$$

The fact that the leading term in the free energy is linear in $\hat{\mathfrak{t}}$ is in accord with the localized black hole background being asymptotically $AdS_2 \times S^3 \times T^5$. One expects the dual gauge theory to be quantum mechanical and hence the free energy to be proportional to the temperature. The higher order terms are then due to the presence of the circle.

It is also interesting to see how the thermodynamics changes if only one or two of the charges are sent to infinity with the others kept finite. These cases are studied in the next section.

6.5 Other Near-Extremal Limits

In this section we discuss some other limiting cases for the near-extremal three-charge background, involving one or two finite charges. We also present the special case of non-extremal solutions with two charges only and present the corresponding near-extremal limit.

6.5.1 Near-extremal limit with finite charges

We start by considering near-extremal limits where one or two of the three charges stay finite. This corresponds to having one or more of the γ_a in (6.78) vanishing.

One finite charge

Without loss of generality we can choose any of the three charges finite. We choose here to take $q_4, q_0 \to \infty$ with q_1 finite. The presence of this finite charge corresponds to choosing $\gamma_1 = 0$ with $\gamma_4, \gamma_0 > 0$ in the near-extremal limit (6.78). The explicit form of the resulting background is easily obtained using the general expressions in (6.79)–(6.83). This limit is also called the dilute gas limit in the literature [18] and after a T-duality in the x-direction where the F1-string lies, corresponds to the near-extremal D1-D5 brane system with finite KK momentum in the direction of the D-string.

In close analogy to (6.89), the energy and tensions in this partial limit are defined as

$$
\begin{aligned}
E &= \lim_{L\to 0}\left(\bar{M} - \sum_{a=0,4} Q_a\right), \quad \hat{\mathcal{T}}_z = \lim_{L\to 0}\frac{L}{2\pi}\bar{\mathcal{T}}_z, \\
\hat{\mathcal{T}}_1 &= \lim_{L\to 0}(L_1\bar{\mathcal{T}}_1 - L_1\bar{\mathcal{T}}_1^{\rm el}), \quad L_a\hat{\mathcal{T}}_a = \lim_{L\to 0}\left(L_a\bar{\mathcal{T}}_a - Q_a\right) \text{ for } a = 0,4. \quad (6.135)
\end{aligned}
$$

The dimensionless versions of these quantities are taken to be

$$
\epsilon = gE, \qquad r = \frac{2\pi\hat{\mathcal{T}}_z}{E - M_1^{\rm el}}, \qquad r_a = \frac{L_a\hat{\mathcal{T}}_a}{E - M_1^{\rm el}} \quad , \quad \hat{\mathfrak{t}} = \ell\hat{T} \quad , \quad \hat{\mathfrak{s}} = \frac{g}{\ell}\hat{S} \quad (6.136)
$$

where $M_1^{\rm el}$ is the electric mass defined in (6.31), g is defined in (6.15) and $\ell = \ell_0\ell_4$.

Using the definitions (6.135), (6.136) and the results in (6.24)–(6.29) for the physical quantities of the general three-charge background, one finds after some algebra

$$\epsilon = \frac{1+n}{3}\mu + \mu_1^{\mathrm{el}} \quad , \quad r = \frac{3n}{1+n} \quad , \quad r_1 = 1 \quad , \quad r_a = \frac{3n}{2(1+n)}, \quad \text{for } a = 4, 0, \tag{6.137}$$

where we used equations (6.23) to write the final result in terms of the physical parameters μ and n of the original seeding black hole. This provides for this partial near-extremal case the map from the neutral solution to the charged one. In this case, the only relative tension that is constant is the one in the spatial world-volume direction corresponding to the charge that is finite.

For temperature and entropy one easily finds the mapping

$$\hat{\mathfrak{t}} = \frac{\mathfrak{t}^2 \mathfrak{s}}{\cosh \alpha_1} \quad , \quad \hat{\mathfrak{s}} = \mathfrak{t}^{-1} \cosh \alpha_1 . \tag{6.138}$$

We also recall that $\mu_1^{\mathrm{el}} = \nu_1 q_1$, with the chemical potential ν_1 and charge q_1 given by (6.33), (6.37) in terms of α_1. Finally, the Smarr relation in this case takes the form

$$\hat{\mathfrak{t}}\hat{\mathfrak{s}} = (2 - r)\left(\epsilon - \mu_1^{\mathrm{el}}\right) . \tag{6.139}$$

The above map can of course be applied in particular to the neutral solutions that fall into the black hole/string ansatz (6.51), as was done in section 6.4 for the full near-extremal limit. For later use, we present here the result for the localized phase, obtained by applying the map (6.137) to the localized black hole on a circle. The corrected background for the near-extremal two-charge localized black hole follows by taking the near-extremal limit (6.78) of the non-extremal background (6.60) with the appropriate choice of γ_a. In particular, this amounts to $H_a \to \hat{H}_a$ where $\hat{H}_a$ are given in (6.81).

The thermodynamic quantities of the resulting near-extremal localized phase, carrying one finite charge q_1 are then given by

$$\epsilon = \rho_0^2 \sinh^2 \alpha_1 + \frac{1}{2}\rho_0^2 \left(1 + \frac{1}{16}\rho_0^2\right) + \mathcal{O}(\rho_0^6), \tag{6.140}$$

$$r = \frac{1}{8}\rho_0^2 - \frac{1}{128}\rho_0^4 + \mathcal{O}(\rho_0^6), \tag{6.141}$$

$$\hat{\mathfrak{s}} = \rho_0 \cosh \alpha_1 \left(1 + \frac{1}{16}\rho_0^2 + \frac{1}{512}\rho_0^4\right) + \mathcal{O}(\rho_0^7), \tag{6.142}$$

$$\hat{\mathfrak{t}} = \frac{\rho_0}{\cosh \alpha_1}\left(1 - \frac{1}{16}\rho_0^2 + \frac{1}{512}\rho_0^4\right) + \mathcal{O}(\rho_0^7). \tag{6.143}$$

In section 6.6 we will provide a microscopic derivation of the entropy found in the case of one finite charge. However, we will consider a permutated version of the above limit, namely with the D0-brane charge kept finite and F1 and D4-brane charge sent to infinity. It is not difficult to see that this case is completely analogous to the one discussed above.

In these expressions, we can send $\alpha_1 \to 0$ (and hence $q_1 \to 0$) and obtain the entropy and temperature of a small localized two-charge black hole on a circle (see section 6.5.2). The entropy clearly vanishes in the extremal limit $\rho_0 \to 0$.

Two finite charges

We now choose $q_4 \to \infty$ with q_1 and q_0 finite, corresponding to taking $\gamma_4 = 1$ with $\gamma_1 = \gamma_0 = 0$ in the expressions (6.78). Again, the explicit form of the resulting background is easily obtained using the general expressions in (6.79)–(6.83).

The energy and tensions in this partial limit are defined by the obvious generalizations of (6.135) and the dimensionless quantities are similar to those in (6.136), where we now divide by $E - M_1^{\mathrm{el}} - M_0^{\mathrm{el}}$.

We then find after some algebra the map

$$\epsilon = \frac{4+n}{6}\mu + \mu_1^{\mathrm{el}} + \mu_0^{\mathrm{el}}, \tag{6.144}$$

$$r = \frac{6n}{4+n} \quad , \quad r_a = \frac{2(1+n)}{4+n}, \quad \text{for } a = 1,0 \quad , \quad r_4 = \frac{3n}{4+n}, \tag{6.145}$$

where we recall that $\mu_a^{\mathrm{el}} = \nu_a q_a$, with the chemical potential ν_a and charge q_a given by (6.33), (6.37) in terms of α_a. For vanishing q_1 and q_0 the above results agree with the one-charge $d = 4$ case considered in [4].

For temperature and entropy one easily finds the mapping

$$\hat{\mathfrak{t}} = \frac{\mathfrak{t}^{3/2}\mathfrak{s}^{1/2}}{\cosh\alpha_1 \cosh\alpha_0} \quad , \quad \hat{\mathfrak{s}} = \mathfrak{t}^{-1/2}\mathfrak{s}^{1/2}\cosh\alpha_1\cosh\alpha_0 \tag{6.146}$$

Finally, the Smarr relation in this case takes the form

$$\hat{\mathfrak{t}}\hat{\mathfrak{s}} = \frac{1}{2}(2-r)\left(\epsilon - \mu_1^{\mathrm{el}} - \mu_0^{\mathrm{el}}\right). \tag{6.147}$$

As before, all of this can be applied to the ansatz, and in particular for the localized phase we now get

$$\epsilon = \rho_0^2(\sinh^2\alpha_1 + \sinh^2\alpha_0) + \rho_0^2\left(1 + \frac{1}{32}\rho_0^2\right) + \mathcal{O}(\rho_0^6), \tag{6.148}$$

$$r = \frac{1}{16}\rho_0^2 - \frac{1}{512}\rho_0^4 + \mathcal{O}(\rho_0^6), \tag{6.149}$$

$$\hat{\mathfrak{s}} = \rho_0^2\cosh\alpha_1\cosh\alpha_0\left(1 + \frac{1}{16}\rho_0^2 + \frac{1}{512}\rho_0^4\right) + \mathcal{O}(\rho_0^8), \tag{6.150}$$

$$\hat{\mathfrak{t}} = \frac{1}{\cosh\alpha_1\cosh\alpha_0}\left(1 - \frac{1}{16}\rho_0^2 + \frac{1}{512}\rho_0^4\right) + \mathcal{O}(\rho_0^6). \tag{6.151}$$

The entropy vanishes in the extremal limit, as we expect, but one finds finite extremal temperature. This is in accord with the fact that we know that for $d = 4$ (see e.g. [4]) the localized phase corresponds to the near-extremal Type II NS5-brane, which has a Hagedorn temperature.

6.5.2 Two-charge black holes on a circle

Starting with the general three-charge non-extremal case one may also consider the situation with a smaller number of non-zero charges. In this section, we present some further details for the case with two non-zero charges, which was not studied before.

Brief review of one-charge case

As remarked earlier, when we set two of the three charges equal to zero, we should recover the one-charge case which was extensively studied in Ref. [4, 106]. In particular, by sending say $q_1, q_0 \to 0$, equation (6.42) becomes

$$\bar{\mu} - q_4 = \frac{(4+n)\mu}{6} + \frac{(2-n)\mu}{6} \frac{b_4}{1+\sqrt{1+b_4^2}} \tag{6.152}$$

which agrees with equation (4.18) of [4] for $d = 4$. Recall that b_a was defined in equation (6.40). As an example, for the localized phase discussed in section 6.2.4 we can eliminate μ and n to arrive at [4]

$$\bar{n}(\bar{\mu}; q_4) = \frac{1}{24}(\bar{\mu} - q_4) + \mathcal{O}\left((\bar{\mu} - q_4)^2\right) . \tag{6.153}$$

For comparison below, we also give here the map from the neutral five-dimensional Kaluza-Klein black holes to the near-extremal one-charge physical quantities

$$\epsilon = \frac{4+n}{6}\mu \quad , \quad r = \frac{6n}{4+n} \quad , \quad r_4 = \frac{3n}{4+n} \quad , \quad \hat{\mathfrak{t}} = \mathfrak{t}^{3/2}\mathfrak{s}^{1/2} \quad , \quad \hat{\mathfrak{s}} = \mathfrak{t}^{-1/2}\mathfrak{s}^{1/2} . \tag{6.154}$$

Non-extremal two-charge case

Turning to the two-charge case, we keep q_0, q_4 finite and take $q_1 \to 0$. The non-extremal background can simply be obtained by setting $\alpha_1 = 0$ in the general form in (6.4)–(6.9). For the thermodynamic quantities, we can use for example (6.42) to compute the non-extremal map

$$\bar{\mu} - \sum_{a=0,4} q_a = \frac{(1+n)\mu}{3} + \frac{(2-n)\mu}{6} \sum_{a=0,4} \frac{b_a}{1+\sqrt{1+b_a^2}} \tag{6.155}$$

and for the temperature and entropy we simply have (6.46), (6.47) with $\alpha_1 = 0$.

As an application of (6.155), it follows using the results of section 6.2.4 that for the localized phase

$$\bar{n}(\bar{\mu}; q_4, q_0) = \frac{1}{12}(\bar{\mu} - q_4 - q_0) + \mathcal{O}\left((\bar{\mu} - q_4 - q_0)^2\right). \tag{6.156}$$

We observe from (6.153) and (6.156) that in both the two-charge and the one-charge case, the relative tension for a small black hole is linear in the energy above extremality. For the three-charge case, which is special in many respects, this is not the case (see equation (6.42)).

Near-extremal limit

We consider here the near-extremal limit of the two-charge black hole solution, in which we send both of the charges to infinity. Before discussing these results we briefly review the near-horizon limit of the corresponding extremal two-charge background.

For the localized phase, corresponding to D0-D4 smeared in the x-direction, we find after a T-duality in that direction the D1-D5 brane system, which has near-horizon geometry $AdS_3 \times S^3 \times T^4$. As a consequence we expect that the leading behavior of the thermodynamics of the localized phase in the near-extremal two-charge system with a transverse circle corresponds to that of a two-dimensional CFT. As we will see below this is indeed the case. For the uniform phase we find that the extremal background is described by a doubly-smeared configuration of D0-D4 branes, which after a double T-duality (in the x and z-direction) corresponds to the D2-D6 brane system. The dual description of this is less clear and presumably gravity is not decoupled, due to the presence of the D6-brane. However, as we will see below the system exhibits a Hagedorn behavior, in close analogy to the near-extremal NS5-brane system [163, 164].

The definition of the near-extremal two-charge limit follows the same route as discussed in section 6.3 for the three-charge case, where now the harmonic function H_1 is set to one. The corresponding background follows likewise from (6.79)–(6.81) by taking $\gamma_0 > 0$, $\gamma_4 > 0$ and setting $\hat{H}_1 = 1$. In this case the quantity ℓ (of dimension length) that enters the dimensionful physical quantities is given by

$$\ell = \ell_0 \ell_4 = \frac{(2\pi l_s)^5 g_s}{L V_1 \sqrt{V_4}} \sqrt{N_0 N_4} \tag{6.157}$$

where we used (6.85), (6.86). The quantity g is still given by (6.87).

The physical quantities are defined as in (6.89) with $\alpha_1 = 0$ (and hence $M_1^{\rm el} = Q_1 = 0$) and the dimensionless quantities are as in (6.90) (in this case there is no $\mathcal{T}_1$). The map follows easily by setting $q_1 = 0$ in the map (6.137), (6.138) so that the map from neutral Kaluza-Klein black holes to near-extremal two-charge physical quantities is

$$\epsilon = \frac{1+n}{3}\mu \quad , \quad r = \frac{3n}{1+n} \quad , \quad r_a = \frac{3n}{2(1+n)} \text{ for } a = 4, 0\,, \tag{6.158}$$

$$\hat{\mathfrak{t}} = \mathfrak{t}^2 \mathfrak{s} \quad , \quad \hat{\mathfrak{s}} = \mathfrak{t}^{-1}. \tag{6.159}$$

Like the one-charge map in (6.154), this is a one-to-one map that maps from the neutral two-dimensional (μ, n) phase diagram to the two-dimensional (ϵ, r) phase diagram of near-extremal two-charge solutions.

The Smarr relation is

$$\hat{\mathfrak{t}}\hat{\mathfrak{s}} = (2-r)\epsilon. \tag{6.160}$$

It is useful to recall that for a given curve in the (ϵ, r) phase diagram we can find the entire thermodynamics from this Smarr relation and the first law of thermodynamics $\delta\epsilon = \hat{\mathfrak{t}}\delta\hat{\mathfrak{s}}$, by integrating the equation

$$\frac{\delta \log \hat{\mathfrak{s}}(\epsilon)}{\delta \log \epsilon} = \frac{1}{2 - r(\epsilon)}\,. \tag{6.161}$$

In particular, for the solutions that are generated from the ansatz (6.50) the metric takes the form of (6.79)–(6.83) with $\hat{H}_1 = 1$. For the three known phases of black holes/strings on a cylinder discussed in section 5.4 we can then map to the corresponding phases of two-charge black holes with a circle in the transverse space.

For this we can use, as in section 6.2, the known data for the phases of five-dimensional Kaluza-Klein black holes along with the analytically known results for the uniform phase, the non-uniform phase near the GL point and localized phase in the small mass limit.[9]

The results can be summarized are as follows. For the uniform phase we have

$$r_{\rm u}(\epsilon) = 1 \quad , \quad \hat{\mathfrak{s}}_{\rm u}(\epsilon) = \epsilon \quad , \quad \hat{\mathfrak{f}}_{\rm u}(\hat{\mathfrak{t}}) = 0 \tag{6.162}$$

showing that this phase has Hagedorn thermodynamics with Hagedorn temperature $\hat{\mathfrak{t}}_{\rm c} = 1$ found e.g. from $t^{-1} = \partial s/\partial\epsilon$. For the non-uniform phase we have

$$r_{\rm nu}(\epsilon) = 1 - \hat{\gamma}\cdot(\epsilon - \epsilon_{\rm c}) + \mathcal{O}\left((\epsilon - \epsilon_{\rm c})^2\right), \tag{6.163}$$

$$\hat{\mathfrak{s}}_{\rm nu}(\epsilon) = \hat{\mathfrak{s}}_{\rm u}(\epsilon)\left(1 - \frac{\hat{\gamma}}{2\epsilon_{\rm c}}(\epsilon - \epsilon_{\rm c})^2 + \mathcal{O}\left((\epsilon - \epsilon_{\rm c})^3\right)\right), \tag{6.164}$$

[9]Note that the non-uniform and localized phases also have copies, which are mapped from the copies [156, 86, 4] of the non-uniform and localized phase of the seeding solution. The thermodynamic quantities of the copies of the near-extremal two-charge solutions are given by $\tilde{\epsilon} = \epsilon/k$, $\tilde{\hat{\mathfrak{t}}} = \hat{\mathfrak{t}}$, $\tilde{\hat{\mathfrak{s}}} = \hat{\mathfrak{s}}/k$ where $k = 2, 3, \ldots$.

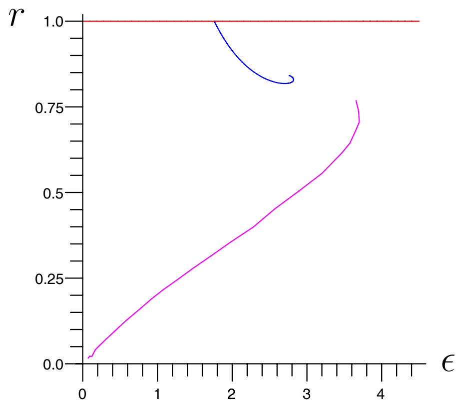

Figure 6.4: (ϵ, r) phase diagram for near-extremal two-charge black holes on a circle. Shown are the localized phase (magenta), the uniform phase (red) and the non-uniform phase (blue). The curves are based on numerical data from [97, 103].

$$\hat{\mathfrak{f}}_{\rm nu}(\hat{\mathfrak{t}}) = -\epsilon_{\rm c}(\hat{\mathfrak{t}} - 1) - \frac{1}{2\hat{\gamma}}(\hat{\mathfrak{t}} - 1)^2 + \mathcal{O}\left((\hat{\mathfrak{t}} - 1)^3\right) \tag{6.165}$$

$$\epsilon_{\rm c} = \frac{\mu_{\rm GL}}{2} = 1.76 \quad , \quad \hat{\gamma} = \frac{8\gamma}{3 - 2\mu_{\rm GL}\gamma} = 0.56, \tag{6.166}$$

exhibiting the departure at the critical point from the Hagedorn thermodynamics. Finally, for the localized phase

$$r_{\rm loc}(\epsilon) = \frac{1}{4}\epsilon - \frac{1}{16}\epsilon^2 + \mathcal{O}(\epsilon^3), \tag{6.167}$$

$$\hat{\mathfrak{s}}_{\rm loc}(\epsilon) = \sqrt{2}\epsilon^{1/2}\left(1 + \frac{1}{16}\epsilon - \frac{1}{512}\epsilon^2 + \mathcal{O}(\epsilon^3)\right), \tag{6.168}$$

$$\hat{\mathfrak{f}}_{\rm loc}(\hat{\mathfrak{t}}) = -\frac{1}{2}\hat{\mathfrak{t}}^2 - \frac{1}{32}\hat{\mathfrak{t}}^4 - \frac{1}{256}\hat{\mathfrak{t}}^6 + \mathcal{O}(\hat{\mathfrak{t}}^8). \tag{6.169}$$

The numerically obtained plots for all of these quantities are shown in figures 6.4 and 6.5.

We first observe that the leading order thermodynamics (for small temperatures) of the localized phase of the near-extremal D1-D5 brane system on a transverse circle correctly exhibits a free energy that is proportional to $\hat{\mathfrak{t}}^2$, as expected for a two-dimensional conformal field theory at finite temperature. The results in (6.168), (6.169) then describe the departure of this behavior due to higher order temperature corrections in the presence of the circle.

On the other hand, note that the near-extremal uniformly smeared D1-D5 brane phase exhibits a Hagedorn temperature $T_{\rm hg} = 1/\ell$ (since $\hat{\mathfrak{t}}_{\rm c} = 1$) with ℓ given in

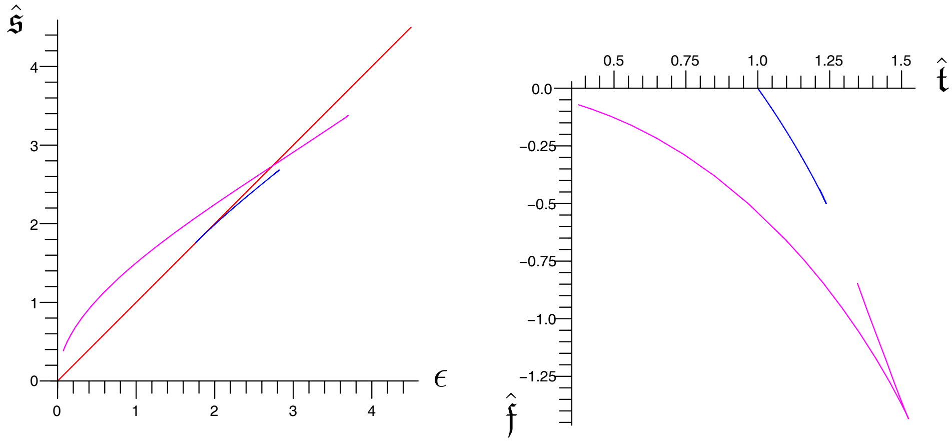

Figure 6.5: $(\epsilon, \hat{\mathfrak{s}})$ and $(\hat{\mathfrak{t}}, \mathfrak{f})$ diagrams for near-extremal two-charge black holes on a circle. Shown are the localized phase (magenta), the uniform phase (red) and the non-uniform phase (blue). The curves are based on numerical data from [97, 103].

(6.157), with the non-uniformly smeared phase emerging at the Hagedorn temperature. The picture that emerges in this system is in many respects analogous to the one considered in Ref. [107] where the thermodynamics of near-extremal NS5-branes was studied, and applied to Little String Theory. In particular, we see from the above that also here, the localized phase provides a new stable phase in the canonical ensemble, extending to a maximum temperature that lies above the Hagedorn temperature. It would be interesting to see if there is a dual interpretation of this, which would require a further examination of the near-extremal D2-D6 brane system.

6.6 Microscopic Entropy

In this section we use the microstate counting technique of [16, 20] to recalculate the entropy of our three-charge black holes on a circle. The non-extremal branes will interact across the transverse circle and this interaction effectively shifts the number of branes [33]. In the case of a small localized near-extremal black hole with one finite charge, we find agreement between the first correction obtained via microstate counting and the macroscopic corrected entropy in equation (6.140).

6.6.1 Review of non-extremal black hole microstate counting

Horowitz, Maldacena and Strominger [20] showed how to count the microstates for a special class of five-dimensional non-extremal black holes with three charges. In their case the metric asymptotes to Minkowski space with no circle in the transverse space.

In the weak string coupling limit the extremal black hole can be described as a configuration with N_4 D4-branes, N_1 fundamental strings and N_0 D0-branes. Non-extremal black holes can be generated, for example, by adding a small number $N_{\bar{0}}$ of anti-D0-branes. In a thermal system one would of course expect the non-extremality also to excite the D4-branes and the F1-strings, but we assume that the anti-D0-brane excitation is much lighter than the other two. The mass of the black hole is then given by the sum of the masses of each type of object

$$M = V_1\tau_1 N_1 + V_4\tau_4 N_4 + V_0\tau_0\left(N_0 + N_{\bar{0}}\right) \tag{6.170}$$

where V_a is the world-volume of each object, $\tau_1 = (2\pi\ell_s^2)^{-1}$ is the tension of the string, $\tau_4 = (g_s(2\pi)^4\ell_s^5)^{-1}$ is the tension of the D4-brane and $\tau_0 = (g_s\ell_s)^{-1}$ is the tension of the D0-brane. The charge associated to the D0-branes is given by

$$Q_0 = V_0\tau_0\left(N_0 - N_{\bar{0}}\right) \tag{6.171}$$

while the other charges are extremal and therefore given by $Q_a = V_a\tau_a N_a$ for $a = 1, 4$.

The D4-branes are separated in the spatial world-volume direction of the F1-string. There are therefore effectively N_4N_1 strings between neighboring D4-branes. The D0-branes are like beads threaded on any one of these strings and in the dilute gas limit the strings are far apart and the beads can therefore only be threaded by one string at a time. In the extremal case with $N_{\bar{0}} = 0$, this gives rise to an entropy [20]

$$S = 2\pi\sqrt{N_1N_4N_0}. \tag{6.172}$$

In the non-extremal case the anti-D0-branes are like beads with opposite charge. In the dilute gas limit the forces between the beads are small and so interactions can be ignored. The entropy is additive in this case and given by [20]

$$S = 2\pi\sqrt{N_1N_4}\left(\sqrt{N_0} + \sqrt{N_{\bar{0}}}\right). \tag{6.173}$$

This is the equation that we want to generalize for our near-extremal three-charge black hole with one finite charge on a circle.

6.6.2 Microstate counting on a circle

In the previous subsection the beads were far apart and did not interact, but with the small transverse circle present that is no longer a safe assumption to make. In our near-extremal limit, the size of the transverse circle was taken to be at the same scale as the energy above extremality and the interaction energy is therefore not negligible compared to the excitation energy. That means that interactions across the transverse circle between beads of opposite charge must be taken into account. The effect of the interaction is to shift the number of beads for a given total energy [33]. We now examine this for the localized phase of three-charge black holes on a circle.[10]

The non-extremal mass of the three-charge black hole (6.24) can be rewritten as

$$\bar{M} = \frac{\Omega_2 c_t}{2gL}\left[\left(1 - 2\frac{c_z}{c_t}\right) + \cosh 2\alpha_1 + \cosh 2\alpha_4 + \cosh 2\alpha_0\right]. \tag{6.174}$$

The first term is equal to

$$\tilde{E} \equiv \frac{\Omega_2 c_t}{2gL}\left(1 - 2\frac{c_z}{c_t}\right) \tag{6.175}$$

and we notice that $\tilde{E}$ is proportional to the tension along the transverse circle. This term is absent in the case where there is no transverse circle. The terms involving $\cosh 2\alpha_a$ are recognized as the contribution of each type of extended object to the total mass of five-dimensional three-charge black hole without the circle [20]. It is therefore natural to write

$$\bar{M} = \tilde{E} + \bar{M}_1 + \bar{M}_4 + \bar{M}_0 \tag{6.176}$$

with

$$\bar{M}_a = \frac{\Omega_2 c_t}{2gL}\cosh 2\alpha_a. \tag{6.177}$$

The charges (6.70) can also be rewritten as

$$Q_a = \frac{\Omega_2 c_t}{2gL}\sinh 2\alpha_a. \tag{6.178}$$

It is now easy to see that in the full near-extremal limit we have $\bar{M}_a - Q_a \to 0$ and $\bar{M} - \sum_a Q_a \to \tilde{E}$.

Partial extremal limit

Let us now consider the case where two of the charges are taken to be extremal, say Q_1 and Q_4, while Q_0 has some small non-extremality. The total mass of the black hole is then

$$\bar{M} = Q_1 + Q_4 + \bar{M}_0 + \tilde{E}. \tag{6.179}$$

Following Costa and Perry [33][11], we want to write the total mass in the form

$$\bar{M} = Q_1 + Q_4 + \delta E + V_{\rm int} \tag{6.180}$$

[10] We thank Roberto Emparan for suggesting this computation to us.

[11] The same idea has been applied in [165].

where δE is the energy carried by the D0-branes and the anti-D0-branes, and $V_{\rm int}$ is the interaction energy related to the presence of the transverse circle. As we start adding anti-D0-branes to the extremal system, they will interact with the D0-branes across the circle, reducing their energy by $V_{\rm int}$.

The force between the beads across the circle gives rise to the tension $\mathcal{T}$ and the interaction energy is the "energy stored in the tension". In $d = 4$ the tension is proportional[12] to L and therefore

$$V_{\rm int} = -\int \mathcal{T} dL = -\frac{1}{2}\mathcal{T} L. \tag{6.181}$$

Notice that from the near-extremal map (6.94) we have $\frac{1}{2}\mathcal{T} L = \tilde{E}$ and hence $V_{\rm int} = -\tilde{E}$.

Equation (6.179) can now be written as

$$\bar{M} = Q_1 + Q_4 + (\bar{M}_0 + 2\tilde{E}) + V_{\rm int} \tag{6.182}$$

so we can identify

$$\delta E = \bar{M}_0 + 2\tilde{E}. \tag{6.183}$$

We find the effective number of D0- and anti-D0-branes from requiring

$$\delta E = V_0 \tau_0 (N_0' + N_{\bar{0}}'), \tag{6.184}$$

$$Q_0 = V_0 \tau_0 (N_0' - N_{\bar{0}}'). \tag{6.185}$$

This gives

$$\tau_0 N_0' = \frac{1}{2}\left(\bar{M}_0 + Q_0\right) + \tilde{E} = \frac{1}{2}\frac{\Omega_2 c_t}{2gL}\exp(2\alpha_0) + \tilde{E}, \tag{6.186}$$

$$\tau_0 N_{\bar{0}}' = \frac{1}{2}\left(\bar{M}_0 - Q_0\right) + \tilde{E} = \frac{1}{2}\frac{\Omega_2 c_t}{2gL}\exp(-2\alpha_0) + \tilde{E} \tag{6.187}$$

where we used the expression (6.178) for Q_0. We thus see that there is a shift of $\tilde{E}$ in the effective number of zero-branes compared to the black hole without the transverse circle [20, 33]. Recall that $\tau_0 = 1/g_s \ell_s$ and $V_0 = 1$.

The microstate entropy for our interacting system on a circle is then given by

$$S = 2\pi\sqrt{N_1 N_4}\left(\sqrt{N_0'} + \sqrt{N_{\bar{0}}'}\right) \tag{6.188}$$

where N_0' and $N_{\bar{0}}'$ are the effective number of D0- and anti-D0-branes given in equations (6.186)–(6.187).

[12]Since $\mathcal{T} = nM/L$ and $M \propto L^{d-2}$ by the definition of the dimensionless quantities (5.10) we have $\mathcal{T} \propto L^{d-3}$.

Application to small localized three-charge black holes

For small (neutral) localized black holes we have $c_t = \rho_0^2 L/(4\pi)$ and recall from equation (6.63) that $c_z/c_t = \chi = 1/2 - \rho_0^2/32 + \mathcal{O}(\rho_0^6)$. We therefore get that

$$\frac{\Omega_2 c_t}{2L} = \frac{1}{2}\rho_0^2, \qquad g\tilde{E} = \frac{1}{32}\rho_0^4 + \mathcal{O}(\rho_0^6) \tag{6.189}$$

where we used the definition of $\tilde{E}$ in (6.175). We thus compute from (6.186), (6.187) the expressions

$$g\tau_0 N_0' = \frac{1}{4}\rho_0^2 \exp(2\alpha_0) + \frac{1}{32}\rho_0^4 + \mathcal{O}(\rho_0^6), \tag{6.190}$$

$$g\tau_0 N_{\bar{0}}' = \frac{1}{4}\rho_0^2 \exp(-2\alpha_0) + \frac{1}{32}\rho_0^4 + \mathcal{O}(\rho_0^6). \tag{6.191}$$

To this order we therefore get

$$\sqrt{N_0'} + \sqrt{N_{\bar{0}}'} = \frac{\sqrt{N_0}}{\ell_0}\rho_0 \cosh\alpha_0 \left(1 + \frac{\rho_0^2}{16} + \mathcal{O}(\rho_0^4)\right) \tag{6.192}$$

where we have used equation (6.86) to rewrite $g\tau_0 = \ell_0^2/N_0$. The microstate entropy in equation (6.188) then becomes

$$S = \frac{2\pi\sqrt{N_1 N_4 N_0}}{\ell_0}\rho_0 \cosh\alpha_0 \left(1 + \frac{\rho_0^2}{16} + \mathcal{O}(\rho_0^4)\right) \tag{6.193}$$

$$= \frac{\ell_1 \ell_4}{g}\rho_0 \cosh\alpha_0 \left(1 + \frac{\rho_0^2}{16} + \mathcal{O}(\rho_0^4)\right). \tag{6.194}$$

This agrees with our previous result for the partial near-extremal entropy obtained from the black hole side (6.140), up to the order ρ_0^4 term.

We could in principle include higher order terms in equations (6.189) and hope to find agreement in the entropy to higher order, but it is not clear to which degree the method of shifting the effective number of branes is accurate. We do not expect the microstate picture to hold for the uniform or the non-uniform phase so it is clear that somewhere on the way it must break down.

From equation (6.129) we know that the ρ_0^6 order term in $\tilde{E}$ is vanishing and this information would yield $(1 - 2\cosh\alpha_0)\rho_0^4/512$ as the next order term in the parenthesis of equation (6.193). This is to be compared to $\rho_0^4/512$ from the Bekenstein-Hawking entropy on the black hole side. It is not too surprising to find a minor discrepancy at such an high order.

6.7 Conclusions and Outlook

In this chapter we have seen how the solution generating technique can be used to create an explicit map from the static and neutral Kaluza-Klein black holes on a circle in five space-time dimensions, that we reviewed in the chapter 5, to three-charge black holes also on a circle. The three-charge solutions can either be seen as ten-dimensional solutions of low-energy string theory or be compactified on their world-volume to five-dimensional solutions. The construction of the map involved taking a series of boosts and U-dualities where each of the boosts gave a new charge, thus extending the mapping to one-charge black holes found in [4].

We restricted ourselves to considering seeding solutions without Kaluza-Klein bubbles i.e. with relative tension less than one half. Using the very general ansatz for Kaluza-Klein black holes with $SO(3)$ symmetry found in [84] we have obtained, via the map, an ansatz for three-charge black holes on a circle with this symmetry. Especially, this ansatz includes the three main studied phases: A localised phase, where the three-charge black holes are located on the transverse circle, a uniform phase, where the three-charge solution is uniformly smeared around the transverse circle, and, finally, a new type of non-uniform phase, where the three-charge black hole is also smeared on the transverse circle without gaps, but in a non-uniform way. Further, we have also given explicit formulas for how to obtain the copied versions of these phases.

Given these non-extremal three-charge solutions that are thermal excitations of the F1-D4-D0 1/8-BPS extremal brane system, we have shown how to take a new near-extremal limit of these where (some of) the charges are sent to infinity, but the radius of the circle is taken to zero in such a way that we retain the interesting physics. Importantly, we have seen how new physics appear which we have shown to be special for the case of three charges and four transverse space directions (except possibly three transverse space directions and four charges). The most important result is that the relative tension, for any seeding solution, is always constant equal to two i.e. the tension along the circle is proportional to the energy above extremality with fixed constant of proportionality. We have explained how this is a consequence of the finite entropy, $S = 2\pi\sqrt{N_1 N_4 N_0}$, of the solution in the extremal limit. Also, we have seen in an appendix how this follows from how the tensions depend on the boosts.

Further, we examined the physical properties of the constructed three-charge solutions, especially for each of the three phases: We examined the thermodynamic stability both in the microcanonical and canonical ensemble. We have given a formula for the entropy as a function of the energy above extremality for the small three-charge black holes localised on the circle, giving the corrections to the finite extremal entropy due to the interaction of the black hole. For the new non-uniform phase the corrections to the entropy are found in the vicinity of the critical point where it departs from the uniform branch. It was, finally, visualised how the constant relative tension is approached as we take the charges to infinity.

We also considered other near-extremal limits where one or two of the charges were kept finite. Especially, the case with one finite charge for the small black holes turned out to be important since we obtained an expression for the entropy to next-to-leading order which we later could compare to the microscopic counting.

The two-charge solutions were also considered in detail since the solutions were not known before. The uniform branch exhibits Hagedorn behaviour, whereas the localised phase is stable and extends up to a temperature that lies above the Hagedorn temperature. This is the same behaviour that was found in the thermodynamics of the near-extremal NS5-brane [107]. The near-extremal small black holes correspond to a D1-D5 brane system with the usual near-horizon geometry $AdS_3 \times S^3 \times T^4$. In the light of the AdS/CFT conjecture it is therefore interesting that there are deformations of the dual CFT_2 that are counterparts of our deformations of the usual two-charge solution without a circle in the transverse space.

Finally, we extended the microstate counting of the entropy performed in [20] to our case of small three-charge black holes localized on the transverse circle where two of the charges are sent to infinity and one is kept constant. This was done following an analysis similar to that of [33]. We found that, in fact, the first correction to the entropy due to the presence of the transverse circle is in perfect agreement with the microstate counting of the entropy, thus giving a non-trivial check of the microscopic picture.

In [166] the microscopic calculations were taken even further. They use that tension is invariant under the boosting (note this was the same we used to get the constant relative tension) to get the energy, which we determined to second order in the number of D0- and anti-D0-branes, to third order. This means that they can go to one higher order in the small black hole expansion and explain the vanishing of the sixth order term in the energy above extremality (6.129). It would be interesting to pursue this further. Actually, reference [166] also presents a simple microscopic model (using "fractionation") that reproduces most of the features of the three new phases. This would, naturally, be very interesting to pursue as well.

Another interesting research direction is the non-uniform phase and the stability of the uniform phase. Both with two and three charges we found a new non-uniform phase emerging from the uniform phase where the black hole is smeared along the transverse circle. In the one-charge case the existence of this mapped non-uniform phase has been shown to be connected with a map from the Gregory-Laflamme mode of the neutral black string to an unstable mode of the singly-charged uniform phase [6, 161]. The construction of such a map for the two- and three-charge cases would, in addition to boosts and U-dualities, also include complex rotations as in [6, 161]. The question of the existence of such unstable modes is highly interesting in view of the Correlated Stability Conjecture of [167, 168, 169, 170], which is examined in

[161] for the one-charge case, also in view of recent work on the conjecture for other brane bound states [171, 172, 173]. See also review in [142].

Finally, the study of the three-charge map should be completed by examining the mappings of the seeding solutions that we have not considered in this chapter. Especially, we should consider the five-dimensional bubble-black hole sequences of [89]. These will map to new three-charge solutions with regular event horizons which could be very interesting to examine, since the free energy of the near-extremal limit of such solutions can be negative, as one can see from (6.107), and the fact that there exist plenty of bubble-black hole configurations with $n \leq 4/5$. This could very well hint at the existence of new stable phases of the three-charge system. We intend to report on this in the future [174]. But also the multi-black hole configurations found in [157] could be interesting to consider. Maybe adding charge and taking the near-extremal limit would give new insight on the microscopic side.

Appendix A

Factorization and Integral Periods

This is a revised version of appendix A in [3].

In this appendix we will prove that *the SW-curve with fundamental matter factorizes as in* (2.48) *if and only if there exist a meromorphic one-form with only simple poles on a hyperelliptic curve, $y_{\rm red}^2 = F_{2(N_c-l)}(x)$, which has residue $-N_c$ at infinity on the upper sheet, residue $N_c - N_f$ at infinity on the lower sheet, residue* 1 *at $-m_i$, fulfills* (4.10)*, and, finally, has integral α- and β-periods.*[1] Note that N_c, N_f, m_i and Λ are thought of as given.

This was proven in the case without fundamental matter in [66]. The ideas here are much the same. The proof is independent of the genus and is thus not confined to the genus one curves.

Let us first, for completeness, consider the easy part of the proof and show that factorization of the SW-curve implies the existence of the meromorphic one-form on the reduced curve with the prescribed properties.

A.1 Factorization Implies Integral One-Form

In the first part of the proof we consider the factorized SW-curve (2.48) as given. Let us define

$$\omega \equiv \left(\frac{P'_{N_c}(x)}{y(x)} + \frac{B'(x)}{2B(x)} - \frac{P_{N_c}(x)B'(x)}{2y(x)B(x)} \right) \mathrm{d}x \ . \tag{A.1}$$

This is nicely a meromorphic one-form on the SW-curve (2.35):

$$y^2 = P_{N_c}(x)^2 - 4\Lambda^{2N_c - N_f} B(x) \ , \tag{A.2}$$

where $B(x) = \prod_{i=1}^{N_f}(x + m_i)$. In fact, using (A.2) we get:

$$\omega = \mathrm{d}\log(P_{N_c}(x) + y(x)) \ , \tag{A.3}$$

[1]That a meromorphic one-form with the given poles, residues, and integral α-periods exists is, of course, always true.

which tells us that ω has integral periods. From (A.1) we can also see that ω has the right poles and residues. However, since the curve is now factorized according to (2.48):

$$y^2 = P_{N_c}(x)^2 - 4\Lambda^{2N_c-N_f}B(x) = F_{2(N_c-l)}(x)H_l(x)^2 = y_{\rm red}^2 H_l(x)^2 \ , \tag{A.4}$$

we should check that we do not have poles at the zeroes of H_l. Therefore let x_0 be a root in H_l. Then by (A.4) x_0 is a double root in y^2 and hence a root in both y^2 and dy^2/dx. This gives

$$P_{N_c}(x_0)^2 - 4\Lambda^{2N_c-N_f}B(x_0) = 0 \ , \tag{A.5}$$

$$2P_{N_c}(x_0)P'_{N_c}(x_0) - 4\Lambda^{2N_c-N_f}B'(x_0) = 0 \ . \tag{A.6}$$

We assume $B(x_0) \neq 0$ and hence $P_{N_c}(x_0) \neq 0$. Thus we get from (A.5) and (A.6)

$$P'_{N_c}(x_0) - \frac{1}{2}P_{N_c}(x_0)\frac{B'(x_0)}{B(x_0)} = 0 \ . \tag{A.7}$$

Thus rewriting ω from (A.1) as

$$\omega = \left(\frac{P'_{N_c}(x) - \frac{1}{2}P_{N_c}(x)\frac{B'(x)}{B(x)}}{H_l(x)}\frac{1}{y_{\rm red}(x)} + \frac{B'(x)}{2B(x)}\right)\mathrm{d}x \ , \tag{A.8}$$

we see by (A.7) that the zeroes of H_l are cancelled and we do not get any poles from H_l. Thus we have proven that we have a meromorphic one-form on the reduced curve, $y_{\rm red}$, with the right poles and residues and with integral periods.[2] That ω fulfills (4.10) follows directly from (A.3) given that P_{N_c} is normalized.

Before going to the second part of the proof let us get a little inspiration from this case where we assume that the SW-curve factorizes. In the following, if x is a point in the upper sheet then (with obvious abuse of notation) $\tilde{x}$ is the corresponding point on the lower sheet. By (A.1) we then get (since $y(\tilde{x}) = -y(x)$):

$$\omega(x) + \omega(\tilde{x}) = \frac{B'}{B} \ . \tag{A.9}$$

Now, let a denote a branch point of $y_{\rm red}$. Then integrating (A.3) gives

$$P_{N_c}(a)e^{\int_a^x \omega} = P_{N_c}(x) + y(x) \ , \tag{A.10}$$

$$P_{N_c}(a)e^{\int_a^{\tilde{x}} \omega} = P_{N_c}(x) - y(x) \ . \tag{A.11}$$

Performing the integrations entirely on the upper/lower sheet we get from (A.9):

$$\int_a^{\tilde{x}} \omega = -\int_a^x \omega + \log\frac{B(x)}{B(a)} \ . \tag{A.12}$$

[2]By uniqueness (given the α-periods) this must be $T(x)\mathrm{d}x$ from (4.2).

Using this and choosing[3] $P_{N_c}(a) = 2\Lambda^{\frac{2N_c-N_f}{2}}\sqrt{B(a)}$ we find by addition of (A.10) and (A.11) that

$$P_{N_c}(x) = 2\Lambda^{\frac{2N_c-N_f}{2}}\sqrt{B(a)}\left(\frac{1}{2}e^{\int_a^x \omega} + \frac{1}{2}\frac{B(x)}{B(a)}e^{-\int_a^x \omega}\right) \ . \tag{A.13}$$

This is independent of the chosen path of integration since ω has integral periods. (A.13) is the generalization for the formula for the case without fundamental matter found in [66]. There the generalization of the Chebyshev polynomials from the one-cut case was found to be $P(x) \propto \cosh(\int_a^x \omega)$ which we get from (A.13) by taking $B(x)$ to be constant.

Let us now use the above considerations to complete the proof of the theorem.

A.2 Integral One-Form on the Reduced Curve Implies Factorization

For the second part of the proof we take as given a hyperelliptic curve y_{red} and a meromorphic one-form ω on y_{red} with the prescribed poles, residues, integral periods, and fulfilling (4.10). In this case we simply define (a is again a branch point and we will, as above, assume that B and y_{red}^2 do not share roots)

$$P_{N_c}(x) \equiv 2\Lambda^{\frac{2N_c-N_f}{2}}\sqrt{B(a)}\left(\frac{1}{2}e^{\int_a^x \omega} + \frac{1}{2}\frac{B(x)}{B(a)}e^{-\int_a^x \omega}\right) \ , \tag{A.14}$$

where we of course do not know if this is a polynomial. However, we do know P_{N_c} is well-defined in the sense that it is independent of the choice of integration since ω has integral periods. To show that P_{N_c} is indeed polynomial we will first have to see that ω fulfills (A.9). We know that we can express ω in the unique meromorphic one-forms ω_{PQ} with simple poles in P and Q with residues $+1$ and -1, respectively, and zero α-periods. In this way we can write

$$\omega = -N_c\omega_{\infty_+\infty_-} + \sum_i \omega_{\widetilde{-m_i}\infty_-} + \text{holo. one-forms} \ , \tag{A.15}$$

We can now use that

$$\omega_{\infty_+\infty_-}(x) = -\frac{x^g}{y_{\mathrm{red}}(x)}\mathrm{d}x + \text{holo. one-forms} \ , \tag{A.16}$$

$$\begin{aligned}\omega_{\tilde{P}\infty_-}(x) = & \frac{1}{2}\frac{1}{x-P}\mathrm{d}x - \frac{1}{2}\frac{1}{x-P}\frac{x^{g+1}}{y_{\mathrm{red}}(x)}\frac{y_{\mathrm{red}}(P)}{P^{g+1}}\mathrm{d}x \\ & -\frac{1}{2}\left(1-\frac{y(P)}{P^{g+1}}\right)\frac{x^g}{y_{\mathrm{red}}(x)}\mathrm{d}x + \text{holo. one-forms} \ .\end{aligned} \tag{A.17}$$

[3] There is really no sign choice in P_{N_c} since the coefficient of x^{N_c} should be 1.

Here g is the genus of the reduced curve, i.e. if $y_{\rm red}^2 = F_{2(N_c-l)}(x)$ then $g = N_c - l - 1$. Further a basis for the holomorphic one-forms takes the form (3.27)

$$\frac{x^i}{y_{\rm red}(x)}{\rm d}x, \quad i = 0, \ldots, g-1 \ . \tag{A.18}$$

Thus we can write ω in (A.15) as

$$\omega(x) = \frac{1}{y_{\rm red}(x)}\left(R_g(x) - \frac{1}{2}\sum_i \frac{x^{g+1}}{x+m_i}\frac{y_{\rm red}(-m_i)}{(-m_i)^{g+1}}\right){\rm d}x + \frac{1}{2}\sum_i \frac{1}{x+m_i}{\rm d}x \ , \tag{A.19}$$

where $R_g(x)$ is some polynomial of degree g and we recognize the last term as the expression $\frac{1}{2}B'(x)/B(x){\rm d}x$. From this (A.9) is immediate. (A.9) then tells us that P_{N_c} is continuous across the cuts (it is of course by definition continuous *through* the cuts) since using (A.12):

$$\begin{aligned} P_{N_c}(\tilde{x}) &= 2\Lambda^{\frac{2N_c-N_f}{2}}\sqrt{B(a)}\left(\frac{1}{2}e^{-\int_a^x \omega + \log\frac{B(x)}{B(a)}} + \frac{1}{2}\frac{B(x)}{B(a)}e^{\int_a^x \omega - \log\frac{B(x)}{B(a)}}\right) \\ &= P_{N_c}(x) \ . \end{aligned} \tag{A.20}$$

This means that P_{N_c} can be continued to a holomorphic function in the (non-compact) complex plane with the possible exception of the poles of ω i.e. $\widetilde{-m_i}$. However, the value of P_{N_c} here is the same value as in $-m_i$ by (A.20) and the are no poles in $-m_i$ at the upper sheet. Thus we only have to care about the behavior of P_{N_c} at infinity. Since $\int_a^x \omega \sim N_c \log x$ for x going to infinity we get

$$\log P_{N_c}(x) \sim \log\left(e^{N_c \log x} + \frac{x^{N_f}}{B(a)}e^{-N_c\log x}\right) = \log\left(x^{N_c} + \frac{x^{N_f - N_c}}{B(a)}\right) \sim N_c \log x \ , \tag{A.21}$$

since $N_f \leq 2N_c$. We can thus conclude that $P_{N_c}(x)$ is a polynomial of degree N_c as wanted. That P_{N_c} is correctly normalized follows by redoing the calculation in (A.21) also including the x^0-order and this time using the assumption (4.10) and the derived equation (A.12).[4]

Having established that P_{N_c} is a polynomial it follows that

$$y^2 \equiv P_{N_c}(x)^2 - 4\Lambda^{2N_c - N_f}B(x) \ , \tag{A.22}$$

must also be polynomial. Now, all we need to prove is that $y^2 = y_{\rm red}^2 H_l(x)^2$ for some polynomial H_l. Using equation (A.14) we get

$$y^2 = 4\Lambda^{2N_c-N_f}B(a)\left(\frac{1}{4}e^{2\int_a^x \omega} + \frac{1}{4}\frac{B(x)^2}{B(a)^2}e^{-2\int_a^x \omega} - \frac{1}{2}\frac{B(x)}{B(a)}\right) \ . \tag{A.23}$$

[4]It is unclear if one really has to assume (4.10). In the case without fundamental matter we simply rescale x to get the correct value of Λ. However, in this case the rescaling also affects the masses thus giving poles in the wrong places.

To see that y^2 contains y_{red}^2 as a factor we first realize that a, which was a root in y_{red}, is also trivially a root in y^2 by inserting a in (A.23). Let now b be any other root in y_{red}^2. We want to know the value of $\exp(\pm 2\int_a^b \omega)$. To find these values we first note that the α- and β-cycles on y_{red} can all be seen as curves from one branch point to another on the upper sheet and then back again (i.e. in the reverse direction) on the lower sheet (think of continuous deformations of the curves in figure 3.3). The curve in the integral $\int_a^b \omega$ can then be seen as being put together of the upper sheet parts of the α- and β-curves. We can then write (using (A.12) and explicitly writing whether the integral is taken on the upper or the lower sheet):

$$\begin{aligned}\int_a^b \omega\Big|_{upper} &= \frac{1}{2}\int_a^b \omega\Big|_{upper} - \frac{1}{2}\int_a^b \omega\Big|_{lower} + \frac{1}{2}\log\frac{B(b)}{B(a)} \\ &= \frac{1}{2}\int_{\sum_i c_i\alpha_i + c_i'\beta_i} \omega + \frac{1}{2}\log\frac{B(b)}{B(a)} \ ,\end{aligned} \tag{A.24}$$

where the first integral in the last line simply is the half of a sum of α- and β-periods of ω (c_i and c_i' are ± 1 or zero). However, since we know that the periods are integral (this is the crucial dependence on the integrality of the periods) the first integral in the last line simply is an integer times $i\pi$. Thus inserting in (A.23) gives

$$y^2(b) = 4\Lambda^{2N_c-N_f}B(a)\left(\frac{1}{4}\frac{B(b)}{B(a)} + \frac{1}{4}\frac{B(b)}{B(a)} - \frac{1}{2}\frac{B(b)}{B(a)}\right) = 0 \ . \tag{A.25}$$

Thus the integrality of ω gives us that y^2 contains y_{red}^2 as a factor, so that

$$y^2(x) = y_{\text{red}}^2(x)Q(x) \ . \tag{A.26}$$

To complete the proof we simply have to show that $Q(x)$ is the square of a polynomial. First we note that

$$y(x) = 2\Lambda^{\frac{2N_c-N_f}{2}}\sqrt{B(a)}\left(\frac{1}{2}e^{\int_a^x \omega} - \frac{1}{2}\frac{B(x)}{B(a)}e^{-\int_a^x \omega}\right) \ , \tag{A.27}$$

since this nicely fulfills (A.23) (we ignore the sign choice). We can then calculate

$$\begin{aligned}\frac{1}{\sqrt{Q}}\frac{dy^2}{dx} &= \frac{y_{\text{red}}}{y}\frac{dy^2}{dx} = \frac{y_{\text{red}}}{y}\left(2P_{N_c}P_{N_c}' - 4\Lambda^{2N_c-N_f}B'\right) \\ &\overset{(A.14),(A.27)}{=} \frac{y_{\text{red}}}{y}\left(2P_{N_c}\left(y\frac{\omega}{\mathrm{d}x} + 2\Lambda^{\frac{2N_c-N_f}{2}}\sqrt{B(a)}\frac{1}{2}\frac{B'}{B(a)}e^{-\int_a^x \omega}\right) - 4\Lambda^{2N_c-N_f}B'\right) \\ &\overset{(A.14),(A.27)}{=} \frac{y_{\text{red}}}{y}\left(2P_{N_c}\left(y\frac{\omega}{\mathrm{d}x} + \frac{1}{2}\frac{B'}{B}(P-y)\right) - 4\Lambda^{2N_c-N_f}B'\right) \\ &\overset{(A.19),(A.22)}{=} \frac{y_{\text{red}}}{y}\left(2P_{N_c}y\frac{1}{y_{\text{red}}}\left(R_g - \frac{1}{2}\sum_i \frac{x^{g+1}}{x+m_i}\frac{y_{\text{red}}(-m_i)}{(-m_i)^{g+1}}\right) + y^2\frac{B'}{B}\right) \\ &\overset{(A.26)}{=} \tilde{R} + y_{red}^2\sqrt{Q}\frac{B'}{B} \ ,\end{aligned} \tag{A.28}$$

where $\tilde{R}$ is some rational function. Solving this for $\sqrt{Q}$ gives

$$\sqrt{Q(x)} = \frac{1}{\tilde{R}(x)} \left(\frac{dy^2}{dx} - y_{red}^2 \frac{B'}{B} Q \right) . \tag{A.29}$$

Since $\sqrt{Q}$ is the square-root of a polynomial and the right hand side is a rational function we can finally conclude that $\sqrt{Q}$ is a polynomial, thus finishing the proof.

The given one-form ω must then – by uniqueness given the α-periods – be $T(x)\mathrm{d}x$ from equation (4.2) and thus (4.3) applies.

Appendix B

Flavour Decoupling

This is a revised version of appendix B in [3].

We can obtain the case without fundamental flavours by taking the limits described after equation (2.37). This means that we should take $\Lambda \to 0$ and $m_i \to \infty$ for all i while keeping constant:

$$\Lambda^{2N_c-N_f} \prod_i m_i \equiv \Lambda_{\text{new}}^{2N_c} \, , \tag{B.1}$$

where Λ_{new} is the new scale for the theory without flavours. The limit means that for all i we have $\tilde{z}_i \to \infty_-$. However, ∞_- is itself changed by changing the $\tilde{z}_i$s so from (4.83) we get the consistency equation

$$\infty_- = \frac{(N_1 - N_c)\tau - \Delta k - N_c + N_f \infty_-}{N_f - 2N_c} \, , \tag{B.2}$$

which, as could be expected, is solved as

$$\infty_- = \frac{(N_1 - N_c)\tau - \Delta k - N_c}{-2N_c} \, . \tag{B.3}$$

For $x(z)$ in (4.85) all we should do then is to find the formula for B after the limit has been taken. Using (4.85) in $m_i = -x(\tilde{z}_i)$ we can rewrite equation (B.1) as

$$\lim \frac{\Lambda^{2N_c-N_f}}{\prod_i \theta(\tilde{z}_i - \infty_- + \frac{1+\tau}{2})} \left(- B \frac{\theta(\infty_- - z_0 + \frac{1+\tau}{2})\theta(\infty_- - 1 - \tau + z_0 + \frac{1+\tau}{2})}{\theta(\infty_- - \infty_+ + \frac{1+\tau}{2})} \right)^{N_f} = \Lambda_{\text{new}}^{2N_c} \, . \tag{B.4}$$

This means we can solve for $\lim \Lambda^{2N_c-N_f} / \prod_i \theta(\tilde{z}_i - \infty_- + \frac{1+\tau}{2})$ and the result can be used in (4.92) to obtain:

$$\begin{aligned} B = e^{\frac{i2\pi k}{2N_c-N_f}} & \frac{\theta(\infty_+ - \infty_- + \frac{1+\tau}{2})^2}{\theta(\infty_+ - z_0 + \frac{1+\tau}{2})\theta(\infty_+ - 1 - \tau + z_0 + \frac{1+\tau}{2})} \\ & \times \theta(\infty_+ - \infty_- + \tfrac{1+\tau}{2})^{\frac{N_f}{2N_c-N_f}} e^{2\pi i(\infty_+ - \infty_-)\frac{N_c+N_1}{2N_c-N_f}} e^{-\pi i \frac{N_f}{2N_c-N_f}} \\ \times \Lambda_{\text{new}}^{\frac{2N_c}{2N_c-N_f}} & \left(- \frac{\theta(\infty_- - \infty_+ + \frac{1+\tau}{2})}{B\theta(\infty_- - z_0 + \frac{1+\tau}{2})\theta(\infty_- - 1 - \tau + z_0 + \frac{1+\tau}{2})} \right)^{\frac{N_f}{2N_c-N_f}} \, . \end{aligned} \tag{B.5}$$

We can then solve for B to obtain

$$B = \Lambda_{\rm new} e^{\frac{i2\pi k}{2N_c}} \frac{\theta(\infty_+ - \infty_- + \frac{1+\tau}{2})^2}{\theta(\infty_+ - z_0 + \frac{1+\tau}{2})\theta(\infty_+ - 1 - \tau + z_0 + \frac{1+\tau}{2})} \times e^{2\pi i(\infty_+ - \infty_-)\frac{N_c+N_1}{2N_c}} \ . \quad \text{(B.6)}$$

This gives the solution together with (4.85):

$$x(z) = B\frac{\theta(z - z_0 + \frac{1+\tau}{2})\theta(z - 1 - \tau + z_0 + \frac{1+\tau}{2})}{\theta(z - \infty_+ + \frac{1+\tau}{2})\theta(z - \infty_- + \frac{1+\tau}{2})} \ , \quad \text{(B.7)}$$

and the limit of (4.81):

$$\omega = N_c \mathrm{d} \log \frac{\theta(z - \infty_- + \frac{1+\tau}{2})}{\theta(z - \infty_+ + \frac{1+\tau}{2})} + 2\pi i N_1 \mathrm{d}z \ . \quad \text{(B.8)}$$

This is exactly what we would get if we solved the factorization problem without fundamental matter directly.

Appendix C

The Boosts and U-dualities

This is a revised version of appendix A in [1].

In this appendix we show how the neutral solution is charged up via boosts and U-dualities. Let us start with a static and neutral five-dimensional Kaluza-Klein black hole as a seeding solution. The metric of such a solution can be written in the form

$$ds_5^2 = -U dt^2 + \frac{L^2}{(2\pi)^2} V_{ab} dx^a dx^b \tag{C.1}$$

where $V_{ab}dx^a dx^b$ describes a cylinder in the asymptotic region of circumference L. There is no dilaton and no gauge fields. By adding flat dimensions x and u_i, $i = 1, ..., 4$, and performing a series of boosts and U-dualities we can construct the ten-dimensional solution of Type IIA Supergravity given in section 6.1.2.

C.1 The Route

Before going through the calculation, let us first schematically sketch the route that we will take. First we make a boost in t and x direction with boost-parameter α_1:

	t	x	u_1	u_2	u_3	u_4
(α_1) P	$\times$	$\times$				

Type IIB

T-dualize in x direction:

	t	x	u_1	u_2	u_3	u_4
(α_1) F1	$\times$	$\times$				

Type IIA

Boost in t and x direction with boost-parameter α_4:

	t	x	u_1	u_2	u_3	u_4
(α_1) F1	$\times$	$\times$				
(α_4) P	$\times$	$\times$				

Type IIA

Lift to M-theory by adding the 11th dimension y:

	t	y	x	u_1	u_2	u_3	u_4	
(α_1) M2	×	×	×					M-theory
(α_4) P	×		×					

Go back to Type IIA by reducing on x:

	t	y	u_1	u_2	u_3	u_4	
(α_1) F1	×	×					Type IIA
(α_4) D0	×						

T-dualize in u_1, u_2, u_3, u_4:

	t	y	u_1	u_2	u_3	u_4	
(α_1) F1	×	×					Type IIA
(α_4) D4	×		×	×	×	×	

Lift to M-theory again by adding an 11th dimension x:

	t	x	y	u_1	u_2	u_3	u_4	
(α_1) M2	×	×	×					M-theory
(α_4) M5	×	×		×	×	×	×	

Boost in t and x with boost parameter α_0:

	t	x	y	u_1	u_2	u_3	u_4	
(α_1) M2	×	×	×					
(α_4) M5	×	×		×	×	×	×	M-theory
(α_0) W	×	×						

Go back to IIA by reducing on x:

	t	y	u_1	u_2	u_3	u_4	
(α_1) F1	×	×					
(α_4) D4	×		×	×	×	×	Type IIA
(α_0) D0	×						

We stop here with a configuration that is a thermal excitation of an F1-string, D4-brane and a D0-brane, but we could T-dualize in directions u_3 and u_4 and lift to M-theory once more to get the configuration:

	t	x	y	u_1	u_2	u_3	u_4	
(α_1) M2	×	×	×					
(α_4) M2	×			×	×			M-theory
(α_0) M2	×					×	×	

This is a thermal excitation of a configuration that is known to be 1/8-BPS.

C.2 Transformation of the Solution

We now examine how the solution transforms under the boosts and U-dualities described in the previous subsection. We start with the metric

$$ds_{10}^2 = -U dt^2 + dx^2 + \sum_{i=1}^{4} (du^i)^2 + ds_4^2 \tag{C.2}$$

where we have introduced the shorthand $ds_4^2 \equiv \frac{L^2}{(2\pi)^2} V_{ab} dx^a dx^b$. This is considered to be a solution of Type IIB Supergravity with vanishing dilaton and no gauge fields present.

Under a Lorentz-boost along the x-axis with rapidity α_1, the coordinates transform as

$$\begin{pmatrix} t_{\text{new}} \\ x_{\text{new}} \end{pmatrix} = \begin{pmatrix} \cosh\alpha_1 & \sinh\alpha_1 \\ \sinh\alpha_1 & \cosh\alpha_1 \end{pmatrix} \begin{pmatrix} t_{\text{old}} \\ x_{\text{old}} \end{pmatrix} \tag{C.3}$$

and the metric becomes

$$\begin{aligned} ds_{10}^2 &= \left(-U\cosh^2\alpha_1 + \sinh^2\alpha_1\right) dt^2 - 2(1-U)\cosh\alpha_1 \sinh\alpha_1 dt dx \\ &\quad + \left(-U\sinh^2\alpha_1 + \cosh^2\alpha_1\right) dx^2 + \sum_{i=1}^{4}(du^i)^2 + ds_4^2. \end{aligned} \tag{C.4}$$

There is an isometry in the x direction and we can therefore use equations (2.54) in [175] to T-dualize in that direction and get a solution of Type IIA Supergravity. The dilaton becomes (fields with/without a tilde are new/old)

$$e^{2\tilde{\phi}} = \frac{e^{\phi}}{g_{xx}} = \frac{1}{\left(-U\sinh^2\alpha_1 + \cosh^2\alpha_1\right)} = H_1^{-1} \tag{C.5}$$

where we have defined

$$H_1 \equiv \left(-U\sinh^2\alpha_1 + \cosh^2\alpha_1\right) = 1 + (1-U)\sinh^2\alpha_1. \tag{C.6}$$

The components of the metric that change under the duality are

$$\tilde{g}_{xx} = \frac{1}{g_{xx}} = H_1^{-1} \tag{C.7}$$

$$\tilde{g}_{tx} = 0 \tag{C.8}$$

$$\tilde{g}_{tt} = g_{tt} - (g_{tx})^2/g_{xx} = -U H_1^{-1} \tag{C.9}$$

and we get a Kalb-Ramond field with component

$$\tilde{B}_{tx} = \frac{g_{tx}}{g_{xx}} = \coth\alpha_1 \left(H_1^{-1} - 1\right). \tag{C.10}$$

Therefore the solution has become

$$ds_{10}^2 = H_1^{-1}\left(-Udt^2 + dx^2\right) + \sum_{i=1}^{4}(du^i)^2 + ds_4^2 \tag{C.11}$$

$$e^{2\phi} = H_1^{-1} \tag{C.12}$$

$$B = \coth\alpha_1 \left(H_1^{-1} - 1\right) dt \wedge dx \tag{C.13}$$

and we see that we have already picked up one charge. Two to go.

To produce the second charge we make another Lorentz boost in the x direction, now with boost parameter α_4. The effect on the metric is analogous to the one above, except now all terms with dt and dx are multiplied with H_1^{-1}. The dilaton is a scalar and does therefore not transform and it turns out that B is also invariant because

$$dt_{\text{new}} \wedge dx_{\text{new}} = dt_{\text{old}} \wedge dx_{\text{old}}. \tag{C.14}$$

We lift the boosted solution to M-theory by adding an eleventh dimension y in the following S-duality fashion

$$ds_{11}^2 = e^{-2\phi/3} ds_{10}^2 + e^{4\phi/3}\left(dy + A_\mu dx^\mu\right)^2. \tag{C.15}$$

There is no gauge field A_μ in our solution and we therefore have, using $e^{2\phi} = H_1^{-1}$,

$$ds_{11}^2 = H_1^{1/3} ds_{10}^2 + H_1^{-2/3} dy^2. \tag{C.16}$$

The B field gives rise to a three-form with non-vanishing components

$$C_{txy} = \coth\alpha_1 \left(H_1^{-1} - 1\right). \tag{C.17}$$

There is no dilaton in 11 dimensions and this is therefore the full solution.

Let us rewrite the boosted part of the metric (the dt and dx components) before reducing on x. Defining $H_4 \equiv 1 + (1-U)\sinh^2\alpha_4$, we find

$$\begin{aligned}\big(-U\cosh^2\alpha_4 + \sinh^2\alpha_4\big)dt^2 - 2(1-U)\cosh\alpha_4 \sinh\alpha_4 dt dx \\ + \left(-U\sinh^2\alpha_4 + \cosh^2\alpha_4\right)dx^2 \\ = -H_4^{-1}Udt^2 + H_4\left(dx + \coth\alpha_4\left(H_4^{-1} - 1\right)dt\right)^2.\end{aligned} \tag{C.18}$$

The total metric can therefore be written as

$$\begin{aligned}ds_{11}^2 &= H_1^{1/3}\left\{H_1^{-1}\left[-H_4^{-1}Udt^2 + H_4\left(dx + A_t dt\right)^2\right] + \sum_{i=1}^{4}(du^i)^2 + ds_4^2\right\} + H_1^{-2/3}dy^2 \\ &= H_1^{-2/3}H_4\left(dx + A_t dt\right)^2 + H_1^{-2/3}\left(-H_4^{-1}Udt^2 + dy^2\right) + H_1^{1/3}\left(\sum_{i=1}^{4}(du^i)^2 + ds_4^2\right)\end{aligned} \tag{C.19}$$

with $A_t \equiv \coth\alpha_4 \left(H_4^{-1} - 1\right)$.

We can now reduce on x by reading the S-duality transformation (C.15) backwards. From the factor multiplying the first term we see that

$$e^{2\phi} = H_1^{-1} H_4^{3/2} \tag{C.20}$$

and therefore

$$ds_{10}^2 = H_1^{-1} H_4^{-1/2} \left[-U dt^2 + H_4 dy^2 + H_1 H_4 \left(\sum_{i=1}^{4} (du^i)^2 + ds_4^2 \right) \right]. \tag{C.21}$$

The three-form gives back our B field and we also have a new one-form

$$B_{ty} = \coth\alpha_1 \left(H_1^{-1} - 1\right), \tag{C.22}$$

$$A_t = \coth\alpha_4 \left(H_4^{-1} - 1\right). \tag{C.23}$$

This is a two-charge solution and we only need one more.

Before boosting again, let us transform the D0-brane into a D4-brane by T-dualizing in u_1, u_2, u_3, u_4. The dilaton becomes

$$e^{\phi} = \frac{H_1^{-1} H_4^{3/2}}{(H_4^{1/2})^4} = H_1^{-1} H_4^{-1/2}, \tag{C.24}$$

the B-field is unchanged and the gauge field is simply

$$A_{(5)} = \coth\alpha_4 (H_4^{-1} - 1) dt \wedge du^1 \wedge du^2 \wedge du^3 \wedge du^4. \tag{C.25}$$

The only part of the metric that changes is in the u-directions and we find

$$ds_{10}^2 = H_1^{-1} H_4^{-1/2} \left(-U dt^2 + H_4 dy^2 + H_1 \sum_{i=1}^{4} (du^i)^2 + H_1 H_4 ds_4^2 \right). \tag{C.26}$$

To add the third charge we lift once more to M-theory, boost and reduce. The procedure is analogous to what has been done before and the end result is as given in section (6.1.2).

These U-duality transformations of the solution take place in the string frame, but in the main text we always use the Einstein frame. Going to ten-dimensional Einstein frame the metric transforms as

$$g_{\mu\nu}^{\mathrm{E}} = e^{-\phi/2} g_{\mu\nu}^{\mathrm{string}} \tag{C.27}$$

and we get

$$\begin{aligned} ds_{\mathrm{E}}^2 = H_1^{-\frac{3}{4}} H_4^{-\frac{3}{8}} H_0^{-\frac{7}{8}} \bigg(& - U dt^2 + H_4 H_0 dx^2 + H_1 H_0 \sum_{i=1}^{4} (du^i)^2 \\ & + H_1 H_4 H_0 \frac{L^2}{(2\pi)^2} V_{ab} dx^a dx^b \bigg). \end{aligned} \tag{C.28}$$

Appendix D

Relating the c's and $\bar{c}$'s

This is a revised version of appendix B in [1].

To find how the expansion coefficients of the non-extremal metric (the $\bar{c}$'s) are related to the original seeding solution we recall that the seeding solution has

$$-g_{tt}^{\text{seed}} \simeq U = 1 - \frac{c_t}{r}, \qquad g_{zz}^{\text{seed}} \simeq 1 + \frac{c_z}{r}. \tag{D.1}$$

The harmonic functions can then be written as

$$H_a \simeq 1 + \frac{c_t}{r} \sinh^2 \alpha_a \tag{D.2}$$

and we can read the asymptotics off the new metric

$$\begin{aligned} -g_{tt} &= H_1^{-\frac{3}{4}} H_4^{-\frac{3}{8}} H_0^{-\frac{7}{8}} U & \text{(D.3)} \\ &= 1 - \frac{c_t}{r} \left(1 + \frac{3}{4} \sinh^2 \alpha_1 + \frac{3}{8} \sinh^2 \alpha_4 + \frac{7}{8} \sinh^2 \alpha_0 \right) + \cdots & \text{(D.4)} \end{aligned}$$

This shows that

$$\bar{c}_t = c_t \left(1 + \frac{3}{4} \sinh^2 \alpha_1 + \frac{3}{8} \sinh^2 \alpha_4 + \frac{7}{8} \sinh^2 \alpha_0 \right). \tag{D.5}$$

Similarly we find

$$\bar{c}_x = c_t \left(-\frac{3}{4} \sinh^2 \alpha_1 + \frac{5}{8} \sinh^2 \alpha_4 + \frac{1}{8} \sinh^2 \alpha_0 \right), \tag{D.6}$$

$$\bar{c}_u = c_t \left(\frac{1}{4} \sinh^2 \alpha_1 - \frac{3}{8} \sinh^2 \alpha_4 + \frac{1}{8} \sinh^2 \alpha_0 \right), \tag{D.7}$$

$$\bar{c}_z = c_z + c_t \left(\frac{1}{4} \sinh^2 \alpha_1 + \frac{5}{8} \sinh^2 \alpha_4 + \frac{1}{8} \sinh^2 \alpha_0 \right), \tag{D.8}$$

and

$$\bar{c}_{A_a} = -c_t \sinh \alpha_a \cosh \alpha_a. \tag{D.9}$$

For the phantom direction u^0 the factor in front of $(du^0)^2$ inside the parenthesis in equation (C.28) would be $H_1 H_4$ (from the harmonic rule of [175]) and we find

$$\bar{c}_0 = c_t \left(\frac{1}{4} \sinh^2 \alpha_1 + \frac{5}{8} \sinh^2 \alpha_4 - \frac{7}{8} \sinh^2 \alpha_0 \right). \tag{D.10}$$

Appendix E

Electric Masses and Tensions

This is a revised version of appendix C in [1].

In this appendix we examine the electric mass and tensions in greater detail.

E.1 Direct Calculation

In this subsection we will show how to calculate the electric mass and tensions in 10 and 11 dimensions for general objects composed of transverse branes, F1-strings etc. obeying the harmonic function rule, and based on a seeding solution of dimension $d+1$. This will be done using the method of equivalent sources.

The matter part of the energy momentum tensor, T^{mat}, consists of a dilatonic part, $T^{\mathrm{dil}}_{\mu\nu}$, and parts from the gauge field strengths F_a, $T^{(F_a)}_{\mu\nu}$:

$$T^{\mathrm{mat}}_{\mu\nu} = T^{\mathrm{dil}}_{\mu\nu} + \sum_{a=1}^{N_{\mathrm{ch}}} T^{(F_a)}_{\mu\nu}, \tag{E.1}$$

where N_{ch} is the number of different charges. The explicit expressions for the energy-momentum tensors are:

$$8\pi G_D T^{\mathrm{dil}}_{\mu\nu} = -\frac{1}{4} g_{\mu\nu} \partial^\rho \phi \partial_\rho \phi + \frac{1}{2} \partial_\mu \phi \partial_\nu \phi \tag{E.2}$$

$$8\pi G_D T^{(F_a)}_{\mu\nu} = -\frac{1}{2} g_{\mu\nu} \frac{1}{2(p_a+2)!} e^{\kappa_a \phi} (F_a)^2 + \frac{1}{2(p_a+1)!} e^{\kappa_a \phi} (F_a)_\mu{}^{\rho_1 \cdots \rho_{p_a+1}} (F_a)_{\nu \rho_1 \cdots \rho_{p_a+1}}, \tag{E.3}$$

where D is the total number of dimensions, p_a is the number of world-volume directions for object a, and κ_a is a number depending on p_a.

To calculate the mass and tension we use the method of equivalent sources. This means that instead of studying the real metric we will study a metric with the same asymptotics as our solution, but which is everywhere Newtonian, i.e. we can split the metric as:

$$g_{\mu\nu} = \eta_{\mu\nu} + h_{\mu\nu}, \tag{E.4}$$

where $\eta_{\mu\nu}$ is the Minkowski metric and $h_{\mu\nu}$ is small so we can ignore second order contributions in h.

We now define:

$$S_{\mu\nu} \equiv T_{\mu\nu} - \frac{1}{D-2} g_{\mu\nu} T \simeq T_{\mu\nu} - \frac{1}{D-2} \eta_{\mu\nu} T, \tag{E.5}$$

where D is the total number of dimensions and $T = T^{\mu}{}_{\mu} \simeq \eta^{\mu\nu} T_{\nu\mu}$. We can inverse this as:

$$T_{\mu\nu} \simeq S_{\mu\nu} - \frac{1}{2} \eta_{\mu\nu} S. \tag{E.6}$$

Then Einstein's equation takes the form

$$S^{\text{mat}}_{\mu\nu} = \frac{1}{8\pi G_D} R_{\mu\nu} \tag{E.7}$$

The linearized Ricci tensor is

$$R^{(1)}_{\mu\nu} = -\frac{1}{2} \left(\Box h_{\mu\nu} + h_{\lambda}{}^{\lambda}{}_{,\mu\nu} - h_{\mu}{}^{\lambda}{}_{,\nu\lambda} - h_{\nu}{}^{\lambda}{}_{,\mu\lambda} \right) \tag{E.8}$$

The gravitational part of the energy-momentum tensor is then defined from:

$$S^{\text{gr}}_{\mu\nu} \equiv \frac{1}{8\pi G_D} \left(R^{(1)}_{\mu\nu} - R_{\mu\nu} \right) \tag{E.9}$$

Summing the contributions from both the gravitational part and the matter part gives:

$$S_{\mu\nu} = S^{\text{gr}}_{\mu\nu} + S^{\text{dil}}_{\mu\nu} + \sum_{a=1}^{N_{\text{ch}}} S^{(F_a)}_{\mu\nu} = \frac{1}{8\pi G_D} R^{(1)}_{\mu\nu} \tag{E.10}$$

The electric part of the energy momentum tensor will simply be defined as the part of the tensor that goes to zero when we set the charges to zero, i.e.:

$$S^{\text{el}}_{\mu\nu} \equiv S_{\mu\nu} - S_{\mu\nu}|_{Q_a=0} \tag{E.11}$$

We note that we a priori have contributions from all the parts of the energy momentum tensor in (E.10), especially, we see that both the terms from the gauge fields and the dilatonic term (the dilaton is constant in the case where the charges are zero) are completely electric.

Using that all raisings and lowerings can be done with $\eta_{\mu\nu}$, that the covariant derivatives can be replaced with ordinary, and that $h_{\mu\nu}$ only depends on r and is diagonal, we get from (E.6):

$$\begin{aligned} T_{\mu\mu} &= \frac{1}{16\pi G_D} \partial_r^2 \left(-h_{\mu\mu} - \eta_{\mu\mu} (h_{rr} - \eta^{\alpha\beta} h_{\beta\alpha}) \right) \\ &= \partial_r^2 \left(-h_{\mu\mu} - \eta_{\mu\mu} \left(h_{tt} - \frac{(d-2)}{r^2} h_{\Omega\Omega} - h_{zz} - \sum_a p_a h_{u_{(a)} u_{(a)}} \right) \right), \end{aligned} \tag{E.12}$$

where $\mu \neq r$, Ω refers to the angular directions, and $u^i_{(a)}$ are the coordinates for the world-volume for object a which will have a volume denoted by V_{p_a}. We see that this is a boundary term so that we easily can get the masses and tensions (since $h_{xx} \sim \bar{c}_x/r^{d-3}$):

$$\bar{M} = \int d^{D-1}x T_{tt} = \frac{(\prod V_{p_a})L\Omega_{(d-2)}}{16\pi G_D}(d-3)\Big((d-2)\bar{c}_\Omega + \bar{c}_z + \sum_a p_a \bar{c}_{u_{(a)}}\Big), \quad \text{(E.13)}$$

$$L\bar{\mathcal{T}}_z = -\int d^{D-1}x T_{zz} = \frac{(\prod V_{p_a})L\Omega_{(d-2)}}{16\pi G_D}(d-3)\Big((d-2)\bar{c}_\Omega + \sum_a p_a \bar{c}_{u_{(a)}} - \bar{c}_t\Big), \quad \text{(E.14)}$$

$$L_{u_{(a)}}\bar{\mathcal{T}}_a = \frac{(\prod V_{p_a})L\Omega_{(d-2)}}{16\pi G_D}(d-3)\Big((d-2)\bar{c}_\Omega + \bar{c}_z + \sum_{a'\neq a} p_{a'}\bar{c}_{u_{(a')}} + (p_a-1)\bar{c}_{u_{(a)}} - \bar{c}_t\Big). \quad \text{(E.15)}$$

The asymptotic quantities are determined by the real physical metric which by the harmonic function rule has components:

$$\begin{aligned} g_{tt} &= -H\Big(\prod_a H_{(a)}^{-1}\Big)U, \quad g_{u^i_{(a)}u^i_{(a)}} = H_{(a)}^{-1}H, \\ g_{zz} &= Hf_z, \quad g_{\Omega\Omega} = Hf_\Omega, \end{aligned} \quad \text{(E.16)}$$

where $U \sim 1$, $f_z \sim 1$, and $f_\Omega \sim r^2$ are functions from the seeding solution, and:

$$H \equiv \prod_a H_{(a)}^{\beta_a}, \quad \beta_a = \frac{p_a+1}{D-2}, \quad \text{(E.17)}$$

which holds for Dp-branes, F1-strings and NS5-branes in $D = 10$ dimensions, and M2- and M5-branes in $D = 11$ dimensions. The harmonic function is assumed to be given by:

$$H_{(a)} = 1 + (1-U)\sinh^2\alpha_a. \quad \text{(E.18)}$$

The electric part of the mass and tensions are defined by (E.11) as the part that goes to zero when we set the charges to zero. We can now use the metric to find the electric parts of $\bar{c}_t$, $\bar{c}_z$, etc. in terms of the seeding c_t:

$$\begin{aligned} \bar{c}_t^{\text{el}} &= \sum_a \frac{D-2-p_a-1}{D-2}\sinh^2\alpha_a c_t \\ \bar{c}_{u_{(a)}}^{\text{el}} &= \sum_{a'} \frac{p_{a'}+1}{D-2}\sinh^2\alpha_{a'}c_t - \sinh^2\alpha_a c_t \\ \bar{c}_z^{\text{el}} &= \sum_a \frac{p_a+1}{D-2}\sinh^2\alpha_a c_t \\ \bar{c}_\Omega^{\text{el}} &= \bar{c}_z^{\text{el}} \end{aligned} \quad \text{(E.19)}$$

Inserting this in (E.13)–(E.15) finally gives:

$$\bar{M}^{\mathrm{el}} = \frac{(\prod V_{p_a})L\Omega_{(d-2)}}{16\pi G_D}(d-3)c_t \sum_a \sinh^2 \alpha_a \tag{E.20}$$

$$L\bar{\mathcal{T}}_z^{\mathrm{el}} = 0 \tag{E.21}$$

$$L_{u_{(a)}}\bar{\mathcal{T}}_a^{\mathrm{el}} = \frac{(\prod V_{p_a})L\Omega_{(d-2)}}{16\pi G_D}(d-3)c_t \sinh^2 \alpha_a \tag{E.22}$$

which, of course, is the same result as (6.30). We note that since we should look at the asymptotic behavior of our metric, then by the form of $H_{(a)}$ in (E.18) our electric masses and tensions split in a sum of contributions from each object a. We also observe that there is no contribution to the electric parts of the tension in some given direction from objects transverse to this direction. Especially, the electric part of the tension in the z-direction is zero. We will use this as one of the basic principle in the next section.

E.2 Symmetry Considerations

In this section we will investigate the electric masses and tensions, but this time based on some simple symmetry consideration and some physical principles that have been confirmed in the last subsection. We will follow the analysis in [4, section 3.2], but with our definition of the electric mass and tension.

First, we assume that the electric parts of the energy-momentum tensor split up into contributions from each of the objects a, as was confirmed in last section, i.e.:

$$T_{\mu\nu}^{\mathrm{el}(a)} = T_{\mu\nu}|_{\forall a' \neq a : Q^{a'}=0} - T_{\mu\nu}|_{\forall a' : Q^{a'}=0}. \tag{E.23}$$

This gives rise to the electric parts of the mass and tensions.

We will still use the method of equivalent sources, so that we can neglect second order contributions in $h_{\mu\nu}$. We then require boost-invariance for object a, i.e. $T_{tt}^{\mathrm{el}(a)} = -T_{u_{(a)}^j u_{(a)}^j}^{\mathrm{el}(a)}$. This can be seen to be fulfilled by the dilatonic and gauge part of the energy-momentum tensor in (E.2) and (E.3) (using that ϕ only depends on r) and, actually, also for $R_{\mu\nu}^{(1)}$ using (E.16) (assuming the symmetry holds for the equivalent metric also) and (E.8), and hence for the whole energy-momentum tensor. After integrating, the boost-invariance implies:

$$M^{\mathrm{el}(a)} = L_{u_{(a)}}\bar{\mathcal{T}}_a^{\mathrm{el}(a)}. \tag{E.24}$$

We further require that for ν a transverse direction to object a we have (i.e. after integrating the electromagnetic part of the energy-momentum tensor):

$$L_\nu \bar{\mathcal{T}}_\nu^{\mathrm{el}(a)} = -\int T_{\nu\nu}^{\mathrm{el}(a)} = 0, \quad \nu \text{ transverse to object } a. \tag{E.25}$$

This means that we in (E.24) can replace the tension on the right hand side with the total electric tension in the $u_{(a)}$-direction:

$$M^{\mathrm{el}(a)} = L_{u_{(a)}} \bar{\mathcal{T}}_a^{\mathrm{el}}. \tag{E.26}$$

Assuming a diagonal energy-momentum tensor and using the method of equivalent sources we get from [143] that

$$\nabla^2 g_{u^i_{(a)} u^i_{(a)}} = -16\pi G_D \left(T_{u^i_{(a)} u^i_{(a)}} - \frac{1}{D-2} T^\rho{}_\rho \right). \tag{E.27}$$

Taking the non-electric part of this we should set all the charges to zero. In that case the directions $u^i_{(a)}$ should be completely flat, and hence the left hand side should be zero, i.e.:

$$T^{\text{non-el}}_{u^i_{(a)} u^i_{(a)}} = \frac{1}{D-2} \sum_\rho \eta^{\rho\rho} T^{\text{non-el}}_{\rho\rho}, \tag{E.28}$$

or:

$$(D-2) T^{\text{non-el}}_{u_{(a)} u_{(a)}} = -T^{\text{non-el}}_{tt} + T^{\text{non-el}}_{zz} + \sum_a p_a T^{\text{non-el}}_{u_{(a)} u_{(a)}} + \text{overall transverse terms.} \tag{E.29}$$

Integrating, using (E.25) and (E.26), and solving we get:

$$(d-1)(L_{u_{(a)}} \mathcal{T}_a - M^{\mathrm{el}(a)}) = \bar{M} - M^{\mathrm{el}} + L \bar{\mathcal{T}}_z. \tag{E.30}$$

In general these N_{ch} equations can be solved for the unknowns $M^{\mathrm{el}(a)}$. However, precisely in our three-charge case with $d-1=3$ the equations have determinant zero. Adding the three equations gives:

$$L_x \bar{\mathcal{T}}_x + L_{u^i} \bar{\mathcal{T}}_{u^i} + L_0 \bar{\mathcal{T}}_0 = \bar{M} + L \bar{\mathcal{T}}, \tag{E.31}$$

which exactly is independent of M^{el}. From this equation we, however, obtain the two nice relations:

$$\bar{n}_x + \bar{n}_0 + \bar{n}_u = 1 + \bar{n}, \tag{E.32}$$

$$r_x + r_0 + r_u = 1 + r \tag{E.33}$$

which are indeed obeyed by (6.34) and (6.35), and (6.94).

For general dimensions and charges we instead get:

$$\sum_a \bar{n}_a = \frac{N_{\mathrm{ch}}}{d-1} + \frac{N_{\mathrm{ch}}}{d-1} \bar{n}, \tag{E.34}$$

$$\sum_a r_a = \left(1 - \frac{d-2}{2}\right) \frac{N_{\mathrm{ch}} \mu}{(d-1)\varepsilon} + \frac{3N_{\mathrm{ch}}}{2(d-1)} r, \tag{E.35}$$

where in the last equation the limit $\alpha_a \to \infty$ had to be taken in the same way as in the end of section 6.3.3. We see that for $d = 4$ the last relation reduces to:

$$\sum_a r_a = \frac{N_{\mathrm{ch}}}{2} r. \tag{E.36}$$

If we use this for the three-charge case we exactly get $r = 2$.

Finally, if we use this on near-extremal two-charge case we get:

$$r_0 + r_4 = r \tag{E.37}$$

in agreement with (6.137) (we set the last charge to zero). Using (E.33) we also conclude that the last relative tension should be once again in agreement with (6.137).

Bibliography

[1] T. Harmark, K. R. Kristjansson, N. A. Obers, and P. B. Ronne, "Three-charge black holes on a circle," *JHEP* **01** (2007) 023, hep-th/0606246.

[2] T. Harmark, K. R. Kristjansson, N. A. Obers, and P. B. Ronne, "Entropy of three-charge black holes on a circle," *Fortsch. Phys.* **55** (2007) 748–753, hep-th/0701070.

[3] R. A. Janik, N. A. Obers, and P. B. Ronne, "Factorization of seiberg-witten curves with fundamental matter," *JHEP* **05** (2007) 080, hep-th/0701087.

[4] T. Harmark and N. A. Obers, "New phases of near-extremal branes on a circle," *JHEP* **09** (2004) 022, hep-th/0407094.

[5] P. Bostock and S. F. Ross, "Smeared branes and the Gubser-Mitra conjecture," *Phys. Rev.* **D70** (2004) 064014, hep-th/0405026.

[6] O. Aharony, J. Marsano, S. Minwalla, and T. Wiseman, "Black hole - black string phase transitions in thermal 1+1 dimensional supersymmetric Yang-Mills theory on a circle," *Class. Quant. Grav.* **21** (2004) 5169–5192, hep-th/0406210.

[7] S. F. Hassan and A. Sen, "Twisting classical solutions in heterotic string theory," *Nucl. Phys.* **B375** (1992) 103–118, hep-th/9109038.

[8] T. Harmark and N. A. Obers, "Phases of Kaluza-Klein black holes: A brief review," hep-th/0503020.

[9] B. Kol, "The phase transition between caged black holes and black strings: A review," hep-th/0411240.

[10] N. Seiberg and E. Witten, "Electric - magnetic duality, monopole condensation, and confinement in $\mathcal{N} = 2$ supersymmetric Yang-Mills theory," *Nucl. Phys.* **B426** (1994) 19–52 [Erratum–ibid.B430:485–486,1994], hep-th/9407087.

[11] N. Seiberg and E. Witten, "Monopoles, duality and chiral symmetry breaking in $\mathcal{N} = 2$ supersymmetric QCD," *Nucl. Phys.* **B431** (1994) 484–550, `hep-th/9408099`.

[12] J. M. Maldacena, "The large n limit of superconformal field theories and supergravity," *Adv. Theor. Math. Phys.* **2** (1998) 231–252, `hep-th/9711200`.

[13] S. S. Gubser, I. R. Klebanov, and A. M. Polyakov, "Gauge theory correlators from noncritical string theory," *Phys. Lett.* **B428** (1998) 105, `hep-th/9802109`.

[14] E. Witten, "Anti-de Sitter space and holography," *Adv. Theor. Math. Phys.* **2** (1998) 253, `hep-th/9802150`.

[15] O. Aharony, S. S. Gubser, J. Maldacena, H. Ooguri, and Y. Oz, "Large N field theories, string theory and gravity," *Phys. Rept.* **323** (2000) 183, `hep-th/9905111`.

[16] A. Strominger and C. Vafa, "Microscopic origin of the Bekenstein-Hawking entropy," *Phys. Lett.* **B379** (1996) 99–104, `hep-th/9601029`.

[17] J. Curtis G. Callan and J. M. Maldacena, "D-brane approach to black hole quantum mechanics," *Nucl. Phys.* **B472** (1996) 591–610, `hep-th/9602043`.

[18] G. T. Horowitz and A. Strominger, "Counting states of near-extremal black holes," *Phys. Rev. Lett.* **77** (1996) 2368–2371, `hep-th/9602051`.

[19] J. C. Breckenridge, R. C. Myers, A. W. Peet, and C. Vafa, "D-branes and spinning black holes," *Phys. Lett.* **B391** (1997) 93, `hep-th/9602065`.

[20] G. T. Horowitz, J. M. Maldacena, and A. Strominger, "Nonextremal black hole microstates and U duality," *Phys. Lett.* **B383** (1996) 151–159, `hep-th/9603109`.

[21] M. Cvetic and D. Youm, "Singular bps saturated states and enhanced symmetries of four-dimensional n=4 supersymmetric string vacua," *Phys. Lett.* **B359** (1995) 87–92, `hep-th/9507160`.

[22] M. Cvetic and D. Youm, "All the static spherically symmetric black holes of heterotic string on a six torus," *Nucl. Phys.* **B472** (1996) 249–267, `hep-th/9512127`.

[23] G. T. Horowitz, D. A. Lowe, and J. M. Maldacena, "Statistical entropy of nonextremal four-dimensional black holes and u-duality," *Phys. Rev. Lett.* **77** (1996) 430–433, `hep-th/9603195`.

[24] R. Emparan and G. T. Horowitz, "Microstates of a neutral black hole in m theory," *Phys. Rev. Lett.* **97** (2006) 141601, `hep-th/0607023`.

[25] R. Emparan and A. Maccarrone, "Statistical description of rotating kaluza-klein black holes," *Phys. Rev.* **D75** (2007) 084006, `hep-th/0701150`.

[26] G. T. Horowitz and M. M. Roberts, "Counting the microstates of a kerr black hole," `arXiv:0708.1346 [hep-th]`.

[27] J. M. Maldacena and L. Susskind, "D-branes and fat black holes," *Nucl. Phys.* **B475** (1996) 679–690, `hep-th/9604042`.

[28] J. M. Maldacena and A. Strominger, "Black hole greybody factors and d-brane spectroscopy," *Phys. Rev.* **D55** (1997) 861–870, `hep-th/9609026`.

[29] S. R. Das and S. D. Mathur, "Comparing decay rates for black holes and d-branes," *Nucl. Phys.* **B478** (1996) 561–576, `hep-th/9606185`.

[30] I. R. Klebanov and S. D. Mathur, "Black hole greybody factors and absorption of scalars by effective strings," *Nucl. Phys.* **B500** (1997) 115–132, `hep-th/9701187`.

[31] S. D. Mathur, "The fuzzball proposal for black holes: An elementary review," *Fortsch. Phys.* **53** (2005) 793–827, `hep-th/0502050`.

[32] S. D. Mathur, "The quantum structure of black holes," *Class. Quant. Grav.* **23** (2006) R115, `hep-th/0510180`.

[33] M. S. Costa and M. J. Perry, "Interacting black holes," *Nucl. Phys.* **B591** (2000) 469–487, `hep-th/0008106`.

[34] C. Vafa, "Superstrings and topological strings at large n," *J. Math. Phys.* **42** (2001) 2798–2817, `hep-th/0008142`.

[35] E. Witten, "Branes and the dynamics of QCD," *Nucl. Phys.* **B507** (1997) 658–690, `hep-th/9706109`.

[36] E. Witten, "Solutions of four-dimensional field theories via m-theory," *Nucl. Phys.* **B500** (1997) 3–42, `hep-th/9703166`.

[37] F. Cachazo, K. A. Intriligator, and C. Vafa, "A large N duality via a geometric transition," *Nucl. Phys.* **B603** (2001) 3–41, `hep-th/0103067`.

[38] F. Ferrari, "Planar diagrams and calabi-yau spaces," *Adv. Theor. Math. Phys.* **7** (2004) 619–665, `hep-th/0309151`.

[39] M. Atiyah, J. M. Maldacena, and C. Vafa, "An m-theory flop as a large n duality," *J. Math. Phys.* **42** (2001) 3209–3220, `hep-th/0011256`.

[40] M. Atiyah and E. Witten, "M-theory dynamics on a manifold of g(2) holonomy," *Adv. Theor. Math. Phys.* **6** (2003) 1–106, `hep-th/0107177`.

[41] R. Gopakumar and C. Vafa, "On the gauge theory/geometry correspondence," *Adv. Theor. Math. Phys.* **3** (1999) 1415–1443, `hep-th/9811131`.

[42] R. Gopakumar and C. Vafa, "Topological gravity as large n topological gauge theory," *Adv. Theor. Math. Phys.* **2** (1998) 413–442, `hep-th/9802016`.

[43] R. Dijkgraaf and C. Vafa, "Matrix models, topological strings, and supersymmetric gauge theories," *Nucl. Phys.* **B644** (2002) 3–20, `hep-th/0206255`.

[44] R. Dijkgraaf and C. Vafa, "On geometry and matrix models," *Nucl. Phys.* **B644** (2002) 21–39, `hep-th/0207106`.

[45] R. Dijkgraaf and C. Vafa, "A perturbative window into non-perturbative physics," `hep-th/0208048`.

[46] F. Ferrari, "On exact superpotentials in confining vacua," *Nucl. Phys.* **B648** (2003) 161–173, `hep-th/0210135`.

[47] R. Dijkgraaf, M. T. Grisaru, C. S. Lam, C. Vafa, and D. Zanon, "Perturbative computation of glueball superpotentials," *Phys. Lett.* **B573** (2003) 138–146, `hep-th/0211017`.

[48] F. Cachazo, M. R. Douglas, N. Seiberg, and E. Witten, "Chiral rings and anomalies in supersymmetric gauge theory," *JHEP* **12** (2002) 071, `hep-th/0211170`.

[49] F. Ferrari, "The proof of the dijkgraaf-vafa conjecture and application to the mass gap and confinement problems," *JHEP* **06** (2006) 039, `hep-th/0602249`.

[50] R. Argurio, G. Ferretti, and R. Heise, "An introduction to supersymmetric gauge theories and matrix models," *Int. J. Mod. Phys.* **A19** (2004) 2015–2078, `hep-th/0311066`.

[51] P. B. Ronne, "On the Dijkgraaf-Vafa conjecture," `hep-th/0408103`.

[52] M. Marino, "Les Houches lectures on matrix models and topological strings," `hep-th/0410165`.

[53] K. D. Kennaway, "String theory and the vacuum structure of confining gauge theories," `hep-th/0409265`.

[54] M. Shigemori, "The geometry / gauge theory duality and the dijkgraaf-vafa conjecture," `hep-th/0409038`.

[55] Y. Demasure, "Connecting strings and gauge theories through matrix model geometry (ph.d. thesis 2004),".

[56] F. Cachazo and C. Vafa, "$\mathcal{N} = 1$ and $\mathcal{N} = 2$ geometry from fluxes," `hep-th/0206017`.

[57] R. Gopakumar, "$\mathcal{N} = 1$ theories and a geometric master field," *JHEP* **05** (2003) 033, `hep-th/0211100`.

[58] S. G. Naculich, H. J. Schnitzer, and N. Wyllard, "The $\mathcal{N} = 2$ $U(N)$ gauge theory prepotential and periods from a perturbative matrix model calculation," *Nucl. Phys.* **B651** (2003) 106–124, `hep-th/0211123`.

[59] R. A. Janik and N. A. Obers, "$SO(N)$ superpotential, Seiberg-Witten curves and loop equations," *Phys. Lett.* **B553** (2003) 309–316, `hep-th/0212069`.

[60] V. Balasubramanian *et al.*, "Multi-trace superpotentials vs. matrix models," *Commun. Math. Phys.* **242** (2003) 361–392, `hep-th/0212082`.

[61] R. Boels, J. de Boer, R. Duivenvoorden, and J. Wijnhout, "Factorization of Seiberg-Witten curves and compactification to three dimensions," *JHEP* **03** (2004) 010, `hep-th/0305189`.

[62] F. Cachazo, N. Seiberg, and E. Witten, "Phases of $\mathcal{N} = 1$ supersymmetric gauge theories and matrices," *JHEP* **02** (2003) 042, `hep-th/0301006`.

[63] F. Ferrari, "Quantum parameter space and double scaling limits in $\mathcal{N} = 1$ super yang-mills theory," *Phys. Rev.* **D67** (2003) 085013, `hep-th/0211069`.

[64] F. Ferrari, "Quantum parameter space in super Yang-Mills. II," *Phys. Lett.* **B557** (2003) 290–296, `hep-th/0301157`.

[65] M. R. Douglas and S. H. Shenker, "Dynamics of $SU(N)$ supersymmetric gauge theory," *Nucl. Phys.* **B447** (1995) 271–296, `hep-th/9503163`.

[66] R. A. Janik, "Exact $U(N_c) \to U(N_1) \times U(N_2)$ factorization of Seiberg-Witten curves and $\mathcal{N} = 1$ vacua," *Phys. Rev.* **D69** (2004) 085010, `hep-th/0311093`.

[67] R. A. Janik, "Phases of $\mathcal{N} = 1$ theories and factorization of Seiberg-Witten curves," hep-th/0510116.

[68] Y. Demasure and R. A. Janik, "Explicit factorization of Seiberg-Witten curves with matter from random matrix models," *Nucl. Phys.* **B661** (2003) 153–173, hep-th/0212212.

[69] R. Boels and J. de Boer, "Classical spin chains and exact three-dimensional superpotentials," *Nucl. Phys.* **B715** (2005) 234–274, hep-th/0411110.

[70] R. Argurio, V. L. Campos, G. Ferretti, and R. Heise, "Exact superpotentials for theories with flavors via a matrix integral," *Phys. Rev.* **D67** (2003) 065005, hep-th/0210291.

[71] N. Seiberg, "Adding fundamental matter to 'Chiral rings and anomalies in supersymmetric gauge theory'," *JHEP* **01** (2003) 061, hep-th/0212225.

[72] S. G. Naculich, H. J. Schnitzer, and N. Wyllard, "Matrix model approach to the $\mathcal{N} = 2$ $U(N)$ gauge theory with matter in the fundamental representation," *JHEP* **01** (2003) 015, hep-th/0211254.

[73] M. Klein and S.-J. Sin, "Matrix model, Kutasov duality and factorization of Seiberg- Witten curves," *J. Korean Phys. Soc.* **44** (2004) 1368–1376, hep-th/0310078.

[74] C.-h. Ahn, B. Feng, Y. Ookouchi, and M. Shigemori, "Supersymmetric gauge theories with flavors and matrix models," *Nucl. Phys.* **B698** (2004) 3–52, hep-th/0405101.

[75] M. Gomez-Reino, "Exact superpotentials, theories with flavor and confining vacua," *JHEP* **06** (2004) 051, hep-th/0405242.

[76] F. Elmetti, A. Santambrogio, and D. Zanon, "On $\mathcal{N} = 1$ exact superpotentials from $U(N)$ matrix models," *JHEP* **10** (2005) 104, hep-th/0506087.

[77] F. Cachazo, N. Seiberg, and E. Witten, "Chiral rings and phases of supersymmetric gauge theories," *JHEP* **04** (2003) 018, hep-th/0303207.

[78] V. Balasubramanian, B. Feng, M.-x. Huang, and A. Naqvi, "Phases of $\mathcal{N} = 1$ supersymmetric gauge theories with flavors," *Annals Phys.* **310** (2004) 375–427, hep-th/0303065.

[79] C.-h. Ahn, B. Feng, and Y. Ookouchi, "Phases of $\mathcal{N} = 1$ $USp(2N_c)$ gauge theories with flavors," *Phys. Rev.* **D69** (2004) 026006, hep-th/0307190.

[80] C.-h. Ahn, B. Feng, and Y. Ookouchi, "Phases of $\mathcal{N} = 1$ $SO(N_c)$ gauge theories with flavors," *Nucl. Phys.* **B675** (2003) 3–69, `hep-th/0306068`.

[81] P. Merlatti, "Gaugino condensate and phases of $\mathcal{N} = 1$ super Yang-Mills theories," `hep-th/0307115`.

[82] F. Ferrari, "Microscopic quantum superpotential in n=1 gauge theories," `arXiv:0707.3885 [hep-th]`.

[83] F. Ferrari, S. Kuperstein, and V. Wens, "Glueball operators and the microscopic approach to n=1 gauge theories," `arXiv:0708.1410 [hep-th]`.

[84] T. Harmark and N. A. Obers, "Black holes on cylinders," *JHEP* **05** (2002) 032, `hep-th/0204047`.

[85] T. Wiseman, "From black strings to black holes," *Class. Quant. Grav.* **20** (2003) 1177–1186, `hep-th/0211028`.

[86] T. Harmark and N. A. Obers, "Phase structure of black holes and strings on cylinders," *Nucl. Phys.* **B684** (2004) 183–208, `hep-th/0309230`.

[87] R. Emparan and H. S. Reall, "Generalized Weyl solutions," *Phys. Rev.* **D65** (2002) 084025, `hep-th/0110258`.

[88] H. Elvang and G. T. Horowitz, "When black holes meet Kaluza-Klein bubbles," *Phys. Rev.* **D67** (2003) 044015, `hep-th/0210303`.

[89] H. Elvang, T. Harmark, and N. A. Obers, "Sequences of bubbles and holes: New phases of Kaluza-Klein black holes," *JHEP* **01** (2005) 003, `hep-th/0407050`.

[90] T. Harmark, "Small black holes on cylinders," *Phys. Rev.* **D69** (2004) 104015, `hep-th/0310259`.

[91] D. Gorbonos and B. Kol, "A dialogue of multipoles: Matched asymptotic expansion for caged black holes," *JHEP* **06** (2004) 053, `hep-th/0406002`.

[92] D. Gorbonos and B. Kol, "Matched asymptotic expansion for caged black holes: Regularization of the post-Newtonian order," *Class. Quant. Grav.* **22** (2005) 3935–3960, `hep-th/0505009`.

[93] D. Karasik, C. Sahabandu, P. Suranyi, and L. C. R. Wijewardhana, "Analytic approximation to 5 dimensional black holes with one compact dimension," *Phys. Rev.* **D71** (2005) 024024, `hep-th/0410078`.

[94] Y.-Z. Chu, W. D. Goldberger, and I. Z. Rothstein, "Asymptotics of d-dimensional Kaluza-Klein black holes: Beyond the newtonian approximation," *JHEP* **03** (2006) 013, `hep-th/0602016`.

[95] E. Sorkin, B. Kol, and T. Piran, "Caged black holes: Black holes in compactified spacetimes. II: 5d numerical implementation," *Phys. Rev.* **D69** (2004) 064032, `hep-th/0310096`.

[96] H. Kudoh and T. Wiseman, "Properties of Kaluza-Klein black holes," *Prog. Theor. Phys.* **111** (2004) 475–507, `hep-th/0310104`.

[97] H. Kudoh and T. Wiseman, "Connecting black holes and black strings," *Phys. Rev. Lett.* **94** (2005) 161102, `hep-th/0409111`.

[98] R. Gregory and R. Laflamme, "Black strings and p-branes are unstable," *Phys. Rev. Lett.* **70** (1993) 2837–2840, `hep-th/9301052`.

[99] R. Gregory and R. Laflamme, "The instability of charged black strings and p-branes," *Nucl. Phys.* **B428** (1994) 399–434, `hep-th/9404071`.

[100] S. S. Gubser, "On non-uniform black branes," *Class. Quant. Grav.* **19** (2002) 4825–4844, `hep-th/0110193`.

[101] T. Wiseman, "Static axisymmetric vacuum solutions and non-uniform black strings," *Class. Quant. Grav.* **20** (2003) 1137–1176, `hep-th/0209051`.

[102] E. Sorkin, "A critical dimension in the black-string phase transition," *Phys. Rev. Lett.* **93** (2004) 031601, `hep-th/0402216`.

[103] B. Kleihaus, J. Kunz, and E. Radu, "New nonuniform black string solutions," *JHEP* **06** (2006) 016, `hep-th/0603119`.

[104] T. Harmark and N. A. Obers, "New phase diagram for black holes and strings on cylinders," *Class. Quantum Grav.* **21** (2004) 1709–1724, `hep-th/0309116`.

[105] B. Kol, E. Sorkin, and T. Piran, "Caged black holes: Black holes in compactified spacetimes. I: Theory," *Phys. Rev.* **D69** (2004) 064031, `hep-th/0309190`.

[106] T. Harmark and N. A. Obers, "New phases of thermal SYM and LST from Kaluza-Klein black holes," *Fortsch. Phys.* **53** (2005) 536–541, `hep-th/0503021`.

[107] T. Harmark and N. A. Obers, "Thermodynamics of the near-extremal ns5-brane," *Nucl. Phys.* **B742** (2006) 41–58, hep-th/0510098.

[108] L. Alvarez-Gaume and S. F. Hassan, "Introduction to S-duality in $\mathcal{N} = 2$ supersymmetric gauge theories: A pedagogical review of the work of Seiberg and Witten," *Fortsch. Phys.* **45** (1997) 159–236, hep-th/9701069.

[109] E. D'Hoker and D. H. Phong, "Lectures on supersymmetric Yang-Mills theory and integrable systems," hep-th/9912271.

[110] W. Lerche, "Introduction to seiberg-witten theory and its stringy origin," *Nucl. Phys. Proc. Suppl.* **55B** (1997) 83–117, hep-th/9611190.

[111] P. C. Argyres, M. R. Plesser, and N. Seiberg, "The moduli space of n=2 susy QCD and duality in n=1 susy QCD," *Nucl. Phys.* **B471** (1996) 159–194, hep-th/9603042.

[112] E. D'Hoker, I. M. Krichever, and D. H. Phong, "The effective prepotential of $\mathcal{N} = 2$ supersymmetric $SU(N_c)$ gauge theories," *Nucl. Phys.* **B489** (1997) 179–210, hep-th/9609041.

[113] P. C. Argyres and A. E. Faraggi, "The vacuum structure and spectrum of n=2 supersymmetric su(n) gauge theory," *Phys. Rev. Lett.* **74** (1995) 3931–3934, hep-th/9411057.

[114] A. Klemm, W. Lerche, S. Yankielowicz, and S. Theisen, "Simple singularities and n=2 supersymmetric yang-mills theory," *Phys. Lett.* **B344** (1995) 169–175, hep-th/9411048.

[115] M. R. Abolhasani, M. Alishahiha, and A. M. Ghezelbash, "The moduli space and monodromies of the n = 2 supersymmetric yang-mills theory with any lie gauge groups," *Nucl. Phys.* **B480** (1996) 279–295, hep-th/9606043.

[116] U. H. Danielsson and B. Sundborg, "The moduli space and monodromies of n=2 supersymmetric so(2r+1) yang-mills theory," *Phys. Lett.* **B358** (1995) 273–280, hep-th/9504102.

[117] A. Brandhuber and K. Landsteiner, "On the monodromies of n=2 supersymmetric yang-mills theory with gauge group so(2n)," *Phys. Lett.* **B358** (1995) 73–80, hep-th/9507008.

[118] P. C. Argyres, M. R. Plesser, and A. D. Shapere, "The Coulomb phase of $\mathcal{N} = 2$ supersymmetric QCD," *Phys. Rev. Lett.* **75** (1995) 1699–1702, hep-th/9505100.

[119] A. Hanany and Y. Oz, "On the quantum moduli space of vacua of $\mathcal{N} = 2$ supersymmetric $SU(N_c)$ gauge theories," *Nucl. Phys.* **B452** (1995) 283–312, hep-th/9505075.

[120] A. Hanany, "On the quantum moduli space of n=2 supersymmetric gauge theories," *Nucl. Phys.* **B466** (1996) 85–100, hep-th/9509176.

[121] P. C. Argyres and A. D. Shapere, "The vacuum structure of n=2 superqcd with classical gauge groups," *Nucl. Phys.* **B461** (1996) 437–459, hep-th/9509175.

[122] J. de Boer and Y. Oz, "Monopole condensation and confining phase of n = 1 gauge theories via m-theory fivebrane," *Nucl. Phys.* **B511** (1998) 155–196, hep-th/9708044.

[123] K. A. Intriligator, R. G. Leigh, and N. Seiberg, "Exact superpotentials in four-dimensions," *Phys. Rev.* **D50** (1994) 1092–1104, hep-th/9403198.

[124] J. D. Edelstein, K. Oh, and R. Tatar, "Orientifold, geometric transition and large n duality for so/sp gauge theories," *JHEP* **05** (2001) 009, hep-th/0104037.

[125] S. Elitzur, A. Forge, A. Giveon, K. A. Intriligator, and E. Rabinovici, "Massless monopoles via confining phase superpotentials," *Phys. Lett.* **B379** (1996) 121–125, hep-th/9603051.

[126] M. Schlichenmaier, "An introduction to Riemann surfaces, algebraic curves and moduli spaces,". New York, USA: Springer (1989) 216 p. (Lecture Notes in Physics; Band 322).

[127] H. M. Farkas and I. Kra, "Riemann surfaces,". New York, USA: Springer (1992) 363 p.

[128] D. Mumford, "Tata lectures on theta. vol. 1.,". Boston, USA: Birkhaeuser (1983) 235 p. (Progress in mathematics. 28).

[129] D. Mumford, "Tata lectures on theta. vol. 2.,". Boston, USA: Birkhaeuser (1984) 272 p. (Progress in mathematics. 43).

[130] P. Griffiths and J. Harris, "Principles of algebraic geometry,". New York, USA: Wiley (1978) 813 p.

[131] R. C. Gunning, "Lectures on Riemann surfaces,". Princeton, USA: Princeton Uni. Pr. (1966) 254 p. (Princeton Mathematical Notes).

[132] R. C. Gunning, "Riemann surfaces and generalized theta functions,". Berlin: Springer (1976) 165 p.

[133] E. Arbarello, M. Cornalba, P. Griffiths, and J. Harris, "Geometry of algebraic curves, volume 1,". New York, USA: Springer (1985) 386 p.

[134] J. Jost, "Compact Riemann surfaces,". Berlin: Springer (2002) 278 p.

[135] J. D. Fay, "Theta functions on riemann surfaces,". New York, USA: Springer (1989) 216 p. (Lecture Notes in Mathematics; Band 352).

[136] R. A. Janik, "The Dijkgraaf-Vafa correspondence for theories with fundamental matter fields," *Acta Phys. Polon.* **B34** (2003) 4879–4890, `hep-th/0309084`.

[137] D. Mumford, *Tata lectures on theta. I.* Progress in Mathematics 28, Birkhauser Boston, 1984.

[138] R. Casero and E. Trincherini, "Phases and geometry of the $\mathcal{N} = 1$ A_2 quiver gauge theory and matrix models," *JHEP* **09** (2003) 063, `hep-th/0307054`.

[139] J. Marsano, K. Papadodimas, and M. Shigemori, "Nonsupersymmetric brane / antibrane configurations in type iia and m theory," `arXiv:0705.0983 [hep-th]`.

[140] D. Shih, "Singularities of n = 1 supersymmetric gauge theory and matrix models," *JHEP* **11** (2003) 025, `hep-th/0308001`.

[141] S. K. Ashok, F. Cachazo, and E. Dell'Aquila, "Children's drawings from Seiberg-Witten curves," `hep-th/0611082`.

[142] T. Harmark, V. Niarchos, and N. A. Obers, "Instabilities of black strings and branes," *Class. Quant. Grav.* **24** (2007) R1–R90, `hep-th/0701022`.

[143] T. Harmark and N. A. Obers, "General definition of gravitational tension," *JHEP* **05** (2004) 043, `hep-th/0403103`.

[144] R. C. Myers, "Stress tensors and Casimir energies in the AdS/CFT correspondence," *Phys. Rev.* **D60** (1999) 046002, `hep-th/9903203`.

[145] J. H. Traschen and D. Fox, "Tension perturbations of black brane spacetimes," *Class. Quant. Grav.* **21** (2004) 289–306, `gr-qc/0103106`.

[146] P. K. Townsend and M. Zamaklar, "The first law of black brane mechanics," *Class. Quant. Grav.* **18** (2001) 5269–5286, `hep-th/0107228`.

[147] J. H. Traschen, "A positivity theorem for gravitational tension in brane spacetimes," *Class. Quant. Grav.* **21** (2004) 1343–1350, `hep-th/0308173`.

[148] T. Shiromizu, D. Ida, and S. Tomizawa, "Kinematical bound in asymptotically translationally invariant spacetimes," *Phys. Rev.* **D69** (2004) 027503, `gr-qc/0309061`.

[149] T. Harmark and N. A. Obers, "Black holes and black strings on cylinders," *Fortsch. Phys.* **51** (2003) 793–798, `hep-th/0301020`.

[150] J. M. Bardeen, B. Carter, and S. W. Hawking, "The four laws of black hole mechanics," *Commun. Math. Phys.* **31** (1973) 161–170.

[151] J. D. Bekenstein, "Black holes and entropy," *Phys. Rev.* **D7** (1973) 2333–2346.

[152] J. D. Bekenstein, "Black holes and the second law," *Nuovo Cim. Lett.* **4** (1972) 737–740.

[153] D. Kastor and J. Traschen, "Stresses and strains in the first law for kaluza-klein black holes," *JHEP* **09** (2006) 022, `hep-th/0607051`.

[154] F. R. Tangherlini, "Schwarzschild field in n dimensions and the dimensionality of space problem," *Nuovo Cimento* **27** (1963) 636.

[155] B. Kol, "Topology change in general relativity and the black-hole black-string transition," *JHEP* **10** (2005) 049, `hep-th/0206220`.

[156] G. T. Horowitz, "Playing with black strings," `hep-th/0205069`.

[157] O. J. C. Dias, T. Harmark, R. C. Myers, and N. A. Obers, "Multi-black hole configurations on the cylinder," `arXiv:0706.3645 [hep-th]`.

[158] R. Emparan, T. Harmark, V. Niarchos, N. A. Obers, and M. J. Rodriguez, "The phase structure of higher-dimensional black rings and black holes," `arXiv:0708.2181 [hep-th]`.

[159] A. A. Tseytlin, "Harmonic superpositions of M-branes," *Nucl. Phys.* **B475** (1996) 149–163, `hep-th/9604035`.

[160] J. P. Gauntlett, D. A. Kastor, and J. H. Traschen, "Overlapping branes in M-theory," *Nucl. Phys.* **B478** (1996) 544–560, `hep-th/9604179`.

[161] T. Harmark, V. Niarchos, and N. A. Obers, "Instabilities of near-extremal smeared branes and the correlated stability conjecture," *JHEP* **10** (2005) 045, `hep-th/0509011`.

[162] R. Kallosh and A. Rajaraman, "Brane-anti-brane democracy," *Phys. Rev.* **D54** (1996) 6381–6386, `hep-th/9604193`.

[163] J. M. Maldacena, "Statistical entropy of near extremal five-branes," *Nucl. Phys.* **B477** (1996) 168–174, `hep-th/9605016`.

[164] J. M. Maldacena and A. Strominger, "Semiclassical decay of near-extremal fivebranes," *JHEP* **12** (1997) 008, `hep-th/9710014`.

[165] R. Emparan and E. Teo, "Macroscopic and microscopic description of black diholes," *Nucl. Phys.* **B610** (2001) 190–214, `hep-th/0104206`.

[166] B. D. Chowdhury, S. Giusto, and S. D. Mathur, "A microscopic model for the black hole - black string phase transition," *Nucl. Phys.* **B762** (2007) 301–343, `hep-th/0610069`.

[167] S. S. Gubser and I. Mitra, "Instability of charged black holes in anti-de Sitter space," `hep-th/0009126`.

[168] S. S. Gubser and I. Mitra, "The evolution of unstable black holes in anti-de Sitter space," *JHEP* **08** (2001) 018, `hep-th/0011127`.

[169] H. S. Reall, "Classical and thermodynamic stability of black branes," *Phys. Rev.* **D64** (2001) 044005, `hep-th/0104071`.

[170] J. P. Gregory and S. F. Ross, "Stability and the negative mode for Schwarzschild in a finite cavity," *Phys. Rev.* **D64** (2001) 124006, `hep-th/0106220`.

[171] S. S. Gubser, "The Gregory-Laflamme instability for the D2-D0 bound state," *JHEP* **02** (2005) 040, `hep-th/0411257`.

[172] S. F. Ross and T. Wiseman, "Smeared D0 charge and the Gubser-Mitra conjecture," *Class. Quant. Grav.* **22** (2005) 2933–2946, `hep-th/0503152`.

[173] J. J. Friess and S. S. Gubser, "Instabilities of d-brane bound states and their related theories," *JHEP* **11** (2005) 040, `hep-th/0503193`.

[174] T. Harmark, K. R. Kristjansson, N. A. Obers, and P. B. Ronne, "Work in progress,".

[175] A. W. Peet, "TASI lectures on black holes in string theory," `hep-th/0008241`.